Diss. ETH No. 15526

The thiol-disulfide oxidoreductase ERp57 and its interaction with calreticulin

A dissertation submitted to the
Swiss Federal Institute of Technology Zürich
for the degree of
Doctor of Natural Sciences

presented by

Eva-Maria Frickel

MSc., Uppsala Universitet

born on December 6th, 1975
citizen of Germany

accepted on the recommendation of

Prof. Dr. Ari Helenius, examiner
Prof. Dr. Rudi Glockshuber, co-examiner
Prof. Dr. Yves Barral, co-examiner

2004

Seite Leer /
Blank leaf

Eva,
lerne zu fragen und frage alles,
frage mich, frage andere,
und höre niemals auf,
Dich selbst zu fragen.

Dein Papa, 28.2.1984

Seite Leer /
Blank leaf

List of Papers

This thesis is based on the following articles and review, which will be referred to in the text by their Roman numerals. It is mentioned whenever a result was a collaborative effort. The appendix includes methods used to generate unpublished results.

I. Frickel, E.-M., Riek, R., Jelasarov, I., Helenius, A., Wüthrich, K., Ellgaard, L. (2002) TROSY-NMR reveals the interaction between ERp57 and the tip of the calreticulin P-domain. *PNAS*, 99(4): 1954-1959

II. Frickel, E.-M., Frei, P., Bouvier, M., Stafford, W.F., Helenius, A., Glockshuber, R., Ellgaard, L. (2004) ERp57 is a multifunctional thiol-disulfide oxidoreductase. *J. Biol. Chem.*, 279(18): 18277-18287

III. Ellgaard, L. and Frickel, E.-M. (2003) Calnexin, calreticulin and ERp57: teammates in glycoprotein folding. *Cell Biochem. Biophys.*, 39(3): 223-248

Contents

Summary

A protein is a polymer of amino acids synthesized on a ribosome. Each protein has to acquire a distinct three-dimensional structure in order to be fully functional in the cell. In eukaryotic cells the endoplasmic reticulum (ER) plays an essential role in the synthesis and maturation of a wide variety of important secretory and membrane proteins. For glycoproteins, the ER possesses a dedicated maturation system, which assists folding and ensures the quality of final products before ER release. Important components of this system include the lectin chaperones calnexin (CNX) and calreticulin (CRT) and their associated co-chaperone ERp57, a thiol-disulfide oxidoreductase. Compared to other essential chaperone systems, the principles whereby this system works at the molecular level are relatively poorly understood.

During this thesis, the interaction between CRT and ERp57 using biochemical techniques and NMR spectroscopy was investigated. It was found that ERp57 binds to the P-domain of calreticulin, an independently folding domain comprising residues 189–288. Isothermal titration calorimetry showed that the dissociation constant of the CRT(189–288)/ERp57 complex is $(9.1 \pm 3.0) \times 10^{-6}$ M at 8°C. Transverse relaxation-optimized NMR spectroscopy (TROSY) provided data on the thermodynamics and kinetics of the complex formation, and on the structure of this 66.5 kDa complex. The NMR measurements yielded a value of $(18 \pm 5) \times 10^{-6}$ M at 20°C for the dissociation constant, and a lower limit for the first order exchange rate constant of $k_{off} > 1000\ s^{-1}$ at 20°C. Chemical shift mapping showed that interactions with ERp57 occur exclusively through amino acid residues in the polypeptide segment 225–251 of CRT(189–288), which forms the tip of the hairpin structure of this domain. These results have led us to propose a model for the cooperative interaction of CRT and ERp57 in glycoprotein folding. In this model, the globular domain and the P-domain of CRT together with ERp57 create a partially solvent-shielded environment for folding of associated glycoproteins. Additionally, the elongated P-domain positions ERp57 favorably to access cysteines in folding glycoproteins.

The thiol-disulfide oxidoreductase ERp57 is a soluble protein of the ER and the closest known homologue of protein disulfide isomerase (PDI). We have characterized several fundamental structural and functional properties of ERp57 *in vitro*, such as the domain organization, shape, redox potential and the ability to catalyze different thiol-disulfide exchange reactions. Like PDI, we find ERp57 to be

comprised of four structural domains. The protein has an elongated shape of 3.4 ± 0.1 nm in diameter and 16.8 ± 0.5 nm in length. The two redox active **a** and **a'** domains were determined to have redox potentials of -0.167 V and -0.156 V, respectively. Furthermore, ERp57 was shown to efficiently catalyze disulfide reduction, disulfide isomerization and dithiol oxidation in substrate proteins. In summary, it is likely that ERp57 functions as a glycoprotein-specific thiol-disulfide oxidoreductase.

Zusammenfassung

Proteine sind aus Aminosäuren aufgebaute Polymere, die an den zellulären Ribosomen synthetisiert werden. Jedes Protein muss eine bestimmte dreidimensionale Struktur annehmen, um seine Funktion in der Zelle korrekt ausüben zu können. In eukaryotischen Zellen spielt das Endoplasmatische Retikulum (ER) eine entscheidende Rolle für die Synthese und Reifung einer weiten Bandbreite von wichtigen sekretorischen Proteinen und Membranproteinen. Für Glykoproteine besitzt das ER ein eigenes Reifungssystem, das bei der Faltung dieser Proteine behilflich ist und die Qualität der Endprodukte vor der Freisetzung aus dem ER sichert. Zu den zentralen Komponenten dieses Systems zählen die Lektin Chaperone Calnexin (CNX) und Calreticulin (CRT) und ihr assoziertes Co-Chaperon ERp57, eine Thiol-disulfidoxidoreduktase. Verglichen mit anderen essentiellen Chaperonsystemen, ist die Funktionsweise dieses Systems auf molekularer Ebene schlecht charakterisiert.

In dieser Doktorarbeit wurde die Interaktion zwischen CRT und ERp57 mit biochemischen Techniken und mit NMR Spektroskopie untersucht. Wir fanden, dass ERp57 an die P-Domäne von CRT bindet, welche unabhängig falten kann und aus den Aminosäuren 189-288 besteht. Isothermale Titrationskalorimetrie zeigte, dass die Dissoziationskonstante des CRT(189-288)/ERp57 Komplexes bei 8°C (9.1 ± 3.0) x 10^{-6} M beträgt. Transverse relaxation-optimierte NMR Spektroskopie (TROSY) lieferte Daten zur Thermodynamik und Kinetik der Komplexbildung und zur Struktur dieses 66.5 kDa grossen Komplexes. Die NMR Messungen ergaben einen Wert von (18 ± 5) x 10^{-6} M bei 20°C für die Dissoziationskonstante und einen Mindestwert der Ratenkonstante für eine Reaktion erster Ordnung von $k_{off} > 1000\ s^{-1}$ ebenfalls bei 20°C. Eine Kartierung der chemischen Verschiebungen zeigte, dass die Interaktion mit ERp57 nur durch die Aminosäurenreste des Polypeptidsegments 225-251 von CRT(189-288) vermittelt wird. Dieses Segment formt die Spitze der Haarnadelstruktur dieser Domäne. Aufgrund dieser Resultate schlagen wir ein kooperatives Modell für das Zusammenspiel von CRT und ERp57 vor. In diesem Modell formen die globuläre Domäne und die P-Domäne von CRT zusammen mit ERp57 eine teilweise lösungsmittelgeschützte Umgebung für die Faltung assozierter Glykoproteine. Zusätzlich platziert die lange P-Domäne ERp57 günstig, um auf Cysteine in faltenden Glykoproteinen zuzugreifen.

Die Thiol-disulfidoxidoreduktase ERp57 ist ein lösliches Protein des ERs und das am nächsten bekannte Homologe von Proteindisulfidisomerase (PDI). Wir charakterisierten mehrere grundlegende strukturelle und funktionelle Eigenschaften von ERp57 *in vitro*, wie die Domänenorganisation, das Redoxpotential und die Fähigkeit, verschiedene Thiol-disulfidaustauschreaktionen zu katalysieren. Wir konnten zeigen, dass ERp57 ebenso wie PDI aus vier strukturellen Domänen aufgebaut ist. Das Protein hat eine längliche Form mit einem Durchmesser von 3.4 ± 0.1 nm und einer Länge von 16.8 ± 0.5 nm. Für die zwei redoxaktiven Domänen **a** und **a'** wurde ein Redoxpotential von –0.167 V beziehungsweise –0.156V ermittelt. Ausserdem wurde gezeigt, dass ERp57 effizient Disulfidreduktion, -isomerisierung und Dithioloxidation in Substratproteinen katalysieren kann. Zusammenfassend lässt sich sagen, dass ERp57 als eine glykoprotein-spezifische Thiol-disulfidoxidoreduktase fungieren könnte.

Abreviations

Abs	absorbance
ATP	adenosine triphosphate
AUC	analytical ultracentrifugation
BiP	immunoglobulin binding protein
CaM	calmodulin
CNX	calnexin
CRT	calreticulin
DNA	deoxyribonucleic acid
Dsb	disulfide bond isomerase
DSG	disuccinimidyl glutarate
DTT	1,4-Dithiothreitol
E. coli	Escherichia coli
EDEM	ER degradation-enhancing α-mannosidase–like protein
ELISA	enzyme linked immunosorbent assay
ER	endoplasmic reticulum
Ero1	ER oxidoreductin
FAD	flavin adenine dinucleotide
FKBP	FK506-binding protein
GSH	reduced glutathione
GSSG	oxidized glutathione
HA	hemagglutinin
Hsp	heat shock protein
HSQC	heteronuclear Single Quantum Coherence
ITC	isothermal titration calorimetry
kDa	kilodalton
LB	Luria-Bertani media
M	molar
MHC	major histocompatibility complex
nat	native
NMR	nuclear magnetic resonance
NOESY	nuclear overhauser effect spectroscopy

OD	optical density
PCR	polymerase chain reaction
PDI	protein disulfide isomerase
PLC	peptide loading complex
PPI	peptidyl-prolyl isomerase
RNase	ribonuclease
sc	scrambled
S. cerevisiae	Saccharomyces cerevisiae
SDS-PAGE	sodium dodecyl sulphate-polyacrylamide gel electrophoesis
TAP	transporter associated with antigen processing
TROSY	Transverse relaxation-optimized NMR spectroscopy
Tris	Tris(hydroxymethyl)aminoethan
UPR	unfolded protein response
wt	wild-type
X-Gal	5-bromo-4-chloro-3-indolyl-beta-D-galactopyranoside

1 Introduction

1.1 Aim of this thesis

This thesis focuses on two proteins of glycoprotein quality control in the endoplasmic reticulum (ER). These are the thiol-disulfide oxidoreductase, ERp57 and the lectin chaperone calreticulin (CRT). ERp57 has been shown to associate with CRT and form transient mixed disulfides with folding glycoproteins. Most of what is known about the so-called calnexin/calreticulin cycle originates from cell biological studies, investigating the folding of glycoproteins in pulse-chase experiments or studying the system in ER-membrane derived vesicles called microsomes. The aim of this thesis was to characterize on a molecular level the binding site in CRT for ERp57 and to specify the thermodynamic and kinetic properties of this binding. Moreover, we wanted to gain a more detailed understanding of ERp57 in terms of its structural and enzymatic properties.

1.2 Features of protein folding

1.2.1 Protein folding

Proteins are polymers of amino acids joined by peptide bonds and synthesized by ribosomes. To achieve their functional state in the cell, the linear polypeptide has to adopt a unique three-dimensional structure. Proteins perform a vast number of tasks in and for the cell, for example by acting as catalysts or molecular motors, providing structure and stability and carrying out cell-cell communication and defense.

In 1961 Christian Anfinsen showed that bovine pancreatic ribonuclease (RNase) could regenerate in the test tube to its native conformation after having been denatured and reduced and that this happens without the addition of any helper enzymes or co-factors (Anfinsen et al., 1961). Thus, he concluded "the information for the correct pairing of half-cystine residues in disulfide linkage, and for the assumption of the native secondary and tertiary structures, is contained in the amino acid sequence itself." (Anfinsen et al., 1961). Many observed protein folding rates *in vitro* were soon recognized to be slower than the probable time it takes them to fold *in vivo*, but nevertheless too fast for the protein to have sampled every possible

conformation on the way to its native structure. The latter apparent discrepancy is called the Levinthal paradox (Levinthal, 1968).

Not until the middle of the 1990s did a new view on protein folding begin to emerge. The search for the native conformation may be energetically favored – depicted, proteins fold in a so-called "folding funnel" (Onuchic et al., 1995), a construct that represents the free energy surface of a polypeptide chain. Experiment and simulation are proposing the existence of intermediate states in protein folding that are stabilized by a polypeptide chain's intrinsic tendency of forming certain secondary structures and lasting tertiary interactions. Many more studies are needed to be able to predict the path a protein takes to fold, let alone to be able to foresee its tertiary structure from its sequence (for reviews see (Daggett and Fersht, 2003; Dinner et al., 2000).

1.2.2 Chaperones

In vivo, all proteins have to fold and oligomerize under cellular conditions, and compared to the *in vitro* parameters used, they are less than ideal. Most strikingly, the temperature inside cells is high and the environment is generally very crowded with approximately 200-300 g/l of total protein, which renders the cell 20-30% volume-occupied with macromolecules (Ellis, 2001). Many proteins are non-native and expose hydrophobic patches. To alleviate the potential problems this situation causes, cells have a set of proteins called the molecular chaperones (Ellis, 1987). These folding-helpers do not induce the correct structure of their substrates, but rather inhibit unproductive interactions leading to aggregation, thereby promoting correct protein folding.

There are several families of classical molecular chaperones. Even though almost no sequence homology between chaperones from different families exist, they often exhibit shared functional features. Typically, chaperones bind to exposed hydrophobic patches in unfolded or partially folded polypeptides preventing their aggregation. This interaction is of low specificity and since the bound folding intermediates are flexible, the chaperone can associate with a large number of target proteins. An additional feature of chaperone action is the regulated release of bound polypeptides. For the Hsp70s and Hsp60s, ATP hydrolysis stimulated by a co-chaperone drives a conformational change in the chaperone, altering its state from a

low affinity to a high affinity binding conformation. Other chaperones, like the Hsp100 or Clp family can even unfold proteins in an ATP-dependent manner (Ben-Zvi and Goloubinoff, 2001; Weber-Ban et al., 1999).

Major classes of classical molecular chaperones include Hsp60/chaperonin 10 (GroEL/ES), Hsp70/Hsp40 (DnaK/DnaJ), Hsp90 (HtpG), Hsp100 (ClpA/B/X, HslU) and the small Hsps (IbpA/B), (*E. coli* chaperones in parenthesis), (for reviews see (Bukau and Horwich, 1998; Fewell et al., 2001; Hartl and Hayer-Hartl, 2002; Walter and Buchner, 2002). In the lumen of the ER, the compartment this thesis focuses on, the most abundant Hsp70 is BiP. This protein was the first ER chaperone and component of the ER quality control system to be identified (Haas and Wabl, 1983). Just like other Hsp70s, BiP has two functional domains, an N-terminal ATPase and a C-terminal substrate-binding domain (McKay, 1993). Five Hsp40 homologues that act as ATP-hydrolysis stimulating co-chaperones for BiP have been identified and are termed ERdj1-5 (Brightman et al., 1995; Cunnea et al., 2003; Shen et al., 2002; Skowronek et al., 1999; Yu et al., 2000). A protein called BAP was found to act as the nucleotide exchange factor for BiP (Chung et al., 2002). Still elusive is the exact role of the abundant ER-resident Hsp90 homologue GRP94, which has been found to assist in the folding of only a subset of proteins (for review see (Argon and Simen, 1999) and references therein).

Calreticulin (CRT), which is discussed in this thesis, and its homologue calnexin (CNX), are both ER lectin chaperones. Unlike the chaperones described above, they do not bind to their substrates via hydrophobic residues, nor do they need ATP hydrolysis for the release of the polypeptide chain. CNX and CRT associate with a trimming intermediate of the N-linked glycan on glycoproteins in the ER. Other enzymes modifying the sugar mediate release and re-binding to the two lectin chaperones. Besides the mode and nature of association to its substrates, CNX and CRT display typical features of chaperones, including preventing their substrates from aggregation. A more detailed introduction to calnexin and calreticulin is found in section 1.4.

1.2.3 Foldases

Beside molecular chaperones, there are enzymes that aid in the correct folding and assembly of proteins.

Peptidyl-prolyl isomerases (PPIs) catalyze the cis-trans isomerization of peptide bonds N-terminal to proline residues. Three different classes of these enzymes, depending on which immunosuppressant they bind, are found: the cyclophilins, the FK506-binding proteins (FKBPs) and the parvulins (Shaw, 2002). The most prominent representative of the PPIs is probably the prokaryotic trigger factor, which associates with the large subunit of ribosomes and possesses a FK506-binding domain (Hesterkamp and Bukau, 1996). Most evidence that cis-trans peptide bond isomerization is a rate limiting step in protein folding comes from *in vitro* studies (Balbach et al., 1999; Golbik et al., 1999; Thies et al., 1999) and deletions of PPIs in various organisms often does not have deleterious effects (Deuerling et al., 1999; Dolinski et al., 1997). However, there are exceptions, as FKBP12 knock-out mice were found to be embryonically and neonatally lethal (Shou et al., 1998). Direct involvement of a PPI in protein folding *in vivo* has been demonstrated for ninaA, a *Drosophila* cyclophilin homologue of the ER specific for rhodopsin folding (Stamnes et al., 1991). More strikingly, trigger factor was recently found to be involved in the maturation of a cysteine protease in the bacterium *Streptococcus pyogenes* and this was dependent on trigger factor's PPI activity catalyzing the cis-trans isomerization of a proline residue in the protease (Lyon and Caparon, 2003).

The large family of protein disulfide isomerases (PDIs) also accelerates correct protein folding by forming and reshuffling the correct disulfide bonds in proteins. This class of proteins, especially the eukaryotic PDI and ERp57 are discussed in greater detail in section 1.6.

1.3 Endoplasmic reticulum Quality Control

1.3.1 The endoplasmic reticulum

All proteins destined for the secretory pathway or the extracellular space have to start their lifetime by being translated and translocated into the lumen of the endoplasmic reticulum (ER).

The ER plays a fundamental role in the synthesis, folding and assembly of numerous important proteins such as cell-surface receptors, membrane channels, extracellular matrix components, serum proteins and antibodies. The environment in the ER is optimal for the correct folding and maturation of such proteins. For many

proteins the maturation process involves co- and posttranslational modifications such as signal-peptide cleavage, glycophosphatidylinositol (GPI)-anchor addition and N-linked glycosylation. The ER has an oxidizing milieu with a ratio of GSH/GSSG of 3:1 versus 50:1 in the cytosol, which translates into a redox potential for the compartment of –180 mV (Hwang et al., 1992). This supports the formation of disulfide bonds, a stabilization of protein conformation that is likely to help proteins maintain their structure in the extracellular environment. When altering the ER redox environment with reducing or oxidizing agents, such as DTT or diamide, incomplete and aberrant formation of disulfide bonded proteins results and their secretion is abolished (Braakman, in preparation; Braakman et al., 1992a; Braakman et al., 1992b). Another important aspect of the environment in the ER is the elevated level of calcium in the millimolar range. Many resident ER proteins are Ca^{2+}-binding proteins and depend on the ion for their function (Michalak et al., 2002). Finally, the ER is rich in chaperones and enzymes, which are crucial in assisting the process of correct protein folding (Benham and Braakman, 2000; Fewell et al., 2001).

1.3.2 General principles of ER protein maturation

Incorrectly folded or incompletely assembled proteins are common side products during protein synthesis in the ER. Such products, which could be harmful to the cell if allowed to proceed along the secretory pathway to the cell surface or another cellular location, are subject to a stringent quality control (QC) system (Ellgaard et al., 1999; Hurtley and Helenius, 1989). Many so-called ER storage diseases are known, which arise from the ER retention of mutant alleles of certain proteins. Such diseases include cystic fibrosis and emphysema (for reviews see (Aridor and Balch, 1999; Kopito and Ron, 2000; Rutishauser and Spiess, 2002; Thomas et al., 1995).

A number of general ER chaperones, including BiP and PDI, recognize and retain proteins that expose non-native features. Like this, they are given more time in the favorable environment of the ER to attain their native structures. A specialized system for glycoprotein QC is in place that encompasses repeated cycles of binding to and release from CNX and CRT, controlled by enzymes that modify the core oligosaccharide. This is discussed in further detail in section 1.4.2. Studies in tissue culture cells and ER-derived microsomes have demonstrated that the interaction with CNX and CRT protects glycoproteins from aggregation and premature degradation

(Hebert et al., 1996; Helenius et al., 1997; Jackson et al., 1994; Labriola et al., 1995; Ou et al., 1993). The QC system with all its general and specialized chaperones ensures that misfolded and incorrectly assembled proteins are kept in the ER and eventually correctly folded or degraded.

Each protein that folds in the lumen of the ER can interact with a variety of different chaperones. There seem to be some rules governing the selection of chaperones by the substrate protein: Is an N-linked glycan located within the first 50 residues from the N-terminus, a preference for CNX/CRT interaction over BiP is observed (Molinari and Helenius, 2000). Not all proteins interact equally well with CNX and CRT (see section 1.4.4), and BiP and GRP94 are also not observed to have the same substrate specificity (Argon and Simen, 1999). Nevertheless, when one chaperone is deleted, others can take over (Molinari et al., 2004), thus ensuring the fidelity of protein QC.

If permanently misfolded, defective ER-retained proteins are typically degraded by the proteasome after selective retrotranslocation to the cytosol and ubiquitination (Tsai et al., 2002). This process is referred to as ER-associated degradation (ERAD). Moreover, the cell responds to increased misfolding of proteins in the ER by the unfolded protein response (UPR), (reviewed in (Ma and Hendershot, 2001). Signaling from the ER to the nucleus leads to increased transcription of genes encoding ER chaperones to help alleviate the folding problem. In addition, another signaling pathway involving phosphorylation of the translation initiation factor eIF2α leads to attenuation of protein translation to further reduce the load on the ER folding machinery. Lastly, yet other genes involved in degradation are upregulated, as recently shown in the case of EDEM (Yoshida et al., 2003). Several investigations show that the processes of ERAD and UPR are closely coordinated (Casagrande et al., 2000; Friedlander et al., 2000; Travers et al., 2000).

1.4 Glycoprotein Quality Control

1.4.1 N-linked glycan addition

In the endoplasmic reticulum (ER) a 14-saccharide core glycan (Fig. 1.1), $Glc_3Man_9GlcNAc_2$, is added to growing nascent polypeptide chains from a dolicholpyrophosphate-linked precursor in a reaction catalyzed by the oligosaccharyl

transferase complex (Burda and Aebi, 1999; Kornfeld and Kornfeld, 1985). The modified asparagine side chain occurs within the Asn–Xxx–Ser/Thr consensus sequence, where Xxx denotes any amino acid except proline (Gavel and von Heijne, 1990). Although only relatively few of the soluble ER-resident proteins seem to be glycosylated, the majority of extracellular proteins produced in mammalian cells carry N-linked glycans (Gahmberg and Tolvanen, 1996).

The sugar itself can directly modulate protein structure and function, for instance by increasing properties such as stability and solubility (Drickamer and Taylor, 1998; Dwek, 1996; O'Connor and Imperiali, 1996; Wormald and Dwek, 1999; Wormald et al., 2002). In addition, N-linked glycans act as tags in intracellular trafficking (Helenius and Aebi, 2001), and accordingly different lectins act as sorting receptors in the secretory pathway (Hauri et al., 2000; Schrag et al., 2001; Yamashita et al., 1999). Despite the many different and widely recognized functions of N-linked glycans, the role of the N-linked glycan in protein folding in the ER has only become fully appreciated within the past 10 years.

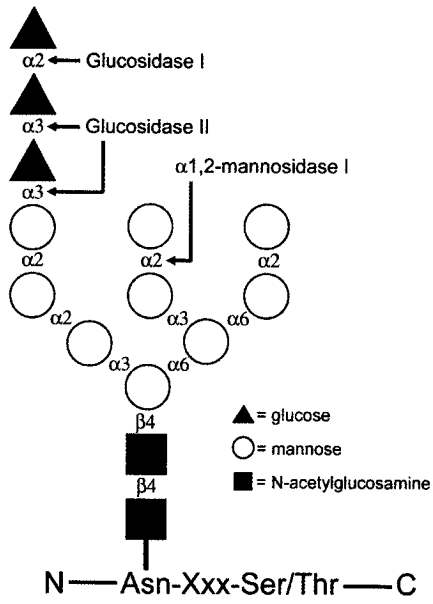

Fig. 1.1 The N-glycan. Schematic representation of the N-linked core oligosaccharide attached to an asparagine side chain in an Asn–Xxx–Ser/Thr amino acid consensus sequence. The linkage for each individual glycosyl residue is indicated along with cleavage sites for various ER enzymes that modify the sugar structure.

1.4.2 The calnexin/calreticulin cycle

The QC system described above applies to all proteins that encounter the lumen of the ER or are inserted into the ER membrane. CNX, CRT and ERp57 are important factors of this general ER QC system (High et al., 2000).

CNX and CRT cooperate with a number of enzymes in the process of assisting glycoprotein folding. The first step of this so-called CNX/CRT cycle (see Fig. 1.2) involves binding to either chaperone through the monoglucosylated glycan, $Glc_1Man_9GlcNAc_2$, present on nascent chains and on newly synthesized glycoproteins. This form of the sugar appears either as a trimmed intermediate of the triglucosylated core oligosaccharide or by re-addition of a glucose residue to the fully de-glucosylated glycan (see below). Sequential trimming of the two outermost glucose residues on the core oligosaccharide is executed by glucosidases I and II. The importance of monoglucosylation for CNX and CRT binding has been shown in living cells, in microsomes and *in vitro* for a number of different proteins (see for instance refs. (Cannon and Helenius, 1999; Hammond and Helenius, 1994b; Hebert et al., 1995; Labriola et al., 1999; Peterson et al., 1995; Radcliffe et al., 2002; Wada et al., 1997; Ware et al., 1995; Zapun et al., 1997). Many such studies have used inhibitors of glucosidase II, such as castanospermine and deoxynojirimycin, to prevent the formation of the monoglucosylated, trimmed intermediate of the original core oligosaccharide. Under these experimental conditions access to CNX and CRT is prevented and proteins are retained in the ER where they often form high molecular weight complexes and eventually are targeted for degradation. In addition to the initial binding through the monoglucosylated glycan, protein–protein interactions of CNX and CRT with their substrates could well contribute to the chaperone function of both proteins (see section 1.4.4), (Ihara et al., 1999; Saito et al., 1999).

The process of disulfide bond formation in glycoprotein substrates of CNX and CRT is assisted by the thiol-disulfide oxidoreductase ERp57, which is found non-covalently associated with both proteins *in vivo* (High et al., 2000; Oliver et al., 1999; Oliver et al., 1997). The importance of ERp57 in the CNX/CRT cycle has become apparent from studies showing that the protein interacts with soluble secretory proteins, as well as integral membrane proteins, carrying N-linked glycans (Elliott et al., 1997; Oliver et al., 1997). As observed for substrates of CNX and CRT, both the association and release of substrates from ERp57 are modulated by glucose trimming

(Elliott et al., 1997; Molinari and Helenius, 1999; Van der Wal et al., 1998). That the addition of glucosidase inhibitors can result in impaired disulfide bond formation was recently shown in the case of CD1d heavy chain, which interacts with CNX and CRT during folding (Kang and Cresswell, 2002). Furthermore, the direct involvement of ERp57 in the oxidative folding of glycoproteins is evident from the finding that the protein forms transient mixed disulfides with CNX- and CRT-associated glycoproteins during folding in living cells (Molinari and Helenius, 1999). Thus, by interacting with CNX and CRT, ERp57 functions as a specialized thiol-disulfide oxidoreductase for glycoproteins.

Glycoproteins are released from CNX and CRT by the action of glucosidase II, which removes the terminal glucose of the glycan (Cannon and Helenius, 1999; Hebert et al., 1995). This step most likely occurs irrespective of the folding state of the glycoprotein, and prevents its renewed association with CNX and CRT. If not correctly folded at this stage, the glycoprotein is recognized by UDP-glucose:glycoprotein glucosyltransferase (GT). This enzyme works as a folding sensor and only re-adds a glucose residue to the oligosaccharide on non-native glycoproteins (Parodi, 2000). In this way, the action of GT ensures that proteins in a misfolded conformation can re-associate with CNX and CRT (Cannon and Helenius, 1999; van Leeuwen and Kearse, 1996; Wada et al., 1997). GT has been shown to detect misfolding on a domain level (Ritter and Helenius, 2000), and even local folding defects in one domain can be distinguished so that only glycans in structurally destabilized regions are re-glucosylated (Ritter, in preparation). Therefore, surveillance can take place on a domain-by-domain basis and it can be hypothesized that glycosylation sites in domains with a tendency for misfolding have been maintained throughout evolution in order to optimize the folding efficiency of glycoproteins carrying such domains.

At least for certain glycoproteins, the removal of a mannose residue in the middle branch of the glycan is a signal for degradation (Liu et al., 1999). A recently discovered mannose-binding lectin, EDEM, specifically accelerates the degradation of glycoproteins and could well be directly involved in targeting $Man_8GlcNAc_2$-containing proteins for degradation (Braakman, 2001; Hosokawa et al., 2001; Jakob et al., 2001; Molinari et al., 2003; Nakatsukasa et al., 2001; Oda et al., 2003; Yoshida et al., 2003).

Overall, cycles of binding and release slow down the rate of folding but increase its efficiency for many glycoproteins by keeping them exposed to the ER QC system (Helenius et al., 1997). Like other protein QC systems in the cell, the detection of non-native glycoproteins in the ER by GT relies on features of the polypeptide chain that distinguish it from proteins in a native conformation. The benefit of using sugars as 'reporter molecules' for the protein folding status likely relates to the fact that the modifications of the core oligosaccharide that control the fate of glycoproteins in the ER are independent of the specific protein. Thereby the glycan, which is present in a large number of molecules, works as a highly versatile tag that can be modified and recognized by a relatively small number of ER-resident enzymes and lectins (Helenius and Aebi, 2001).

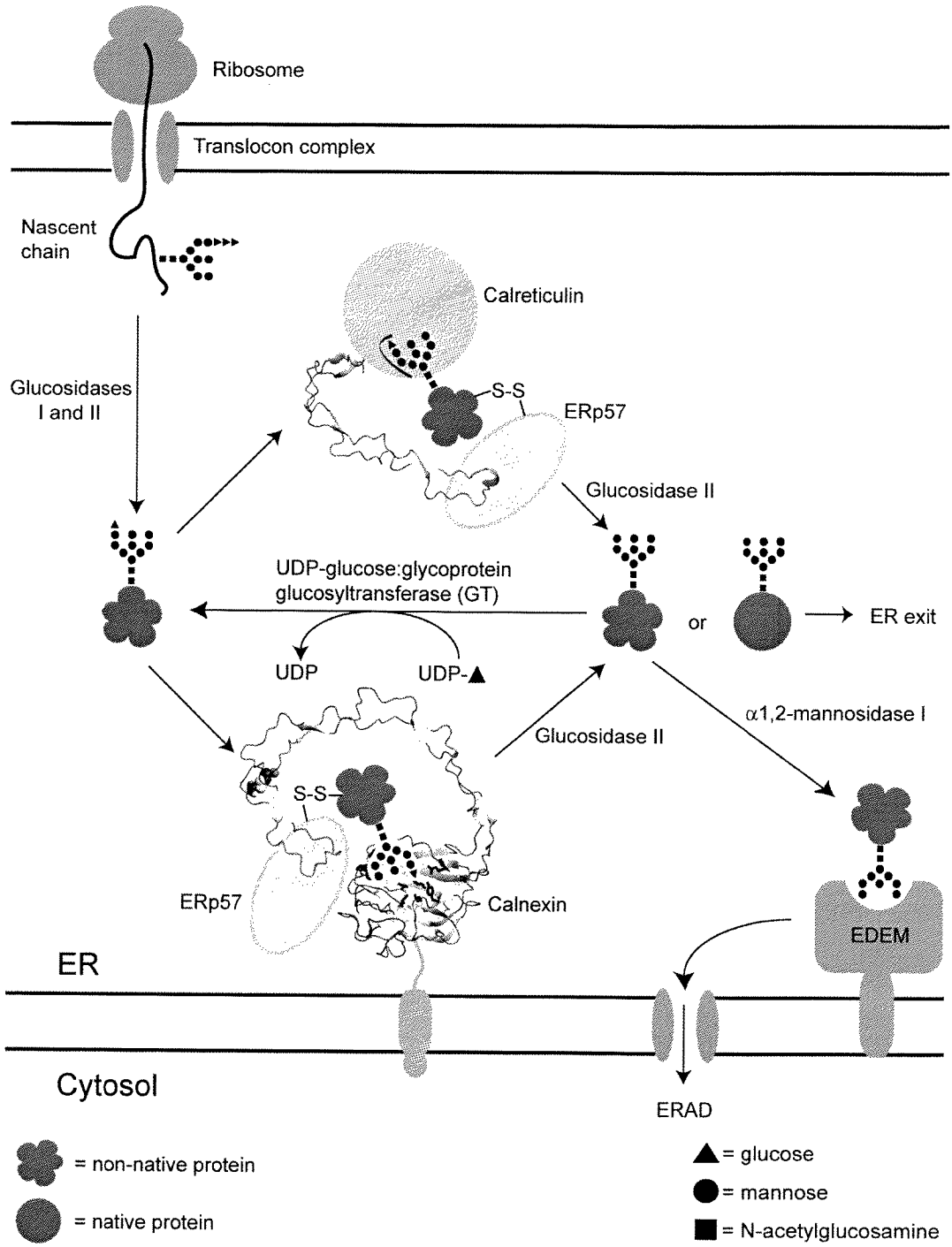

Fig. 1.2 The calnexin/calreticulin cycle. The folding of newly synthesized glycoproteins in the ER is assisted by calnexin (CNX) and calreticulin (CRT). Both proteins bind to the monoglucosylated form of the glycoprotein generated after the initial removal of two glucoses by glucosidases I and II. Here, we have used the available three-dimensional structures of CNX (the lumenal domain) and CRT (the P-domain) to depict parts of the two molecules. The glycan binds to the lectin domain of both chaperones - in CRT the glycan binding site is represented by the curved black line. Other interactions can occur through protein-protein contacts (not depicted). Disulfide bond formation in glycoprotein substrates of CNX and CRT is catalyzed by the associated thiol-disulfide oxidoreductase ERp57, with which substrates form transient mixed disulfide intermediates. In both CNX and CRT, the tip region of the P-domain mediates the interaction with ERp57. Removal of the remaining glucose, in a reaction catalyzed by glucosidase II, prevents interaction with CNX and CRT. Upon release, one of three

possible fates awaits the glycoprotein. First, if the protein has reached its native conformation it is not longer retained in the ER and is free to travel along the secretory pathway. Second, if the protein is still not correctly folded, it can be recognized by the UDP-glucose:glycoprotein glucosyltransferase (GT). This enzyme uses UDP-glucose as a sugar donor to reglucosylate non-native glycoproteins carrying high-mannose glycans. Consequently, it acts as a folding sensor in CNX/CRT cycle. The re-addition of a glucose residue to the N-linked glycan promotes re-association with CNX and CRT. An important role of CNX and CRT is to retain glycoproteins in the ER, where the conditions for folding are favorable. Finally, prolonged ER-retention increases the chances of encountering the ER α1,2-mannosidase I. This enzyme removes a mannose residue in the middle branch of the glycan to generate a form with 8 mannoses. A novel ER lectin, EDEM, is likely to recognize this form of the glycan and thereby extract the glycoprotein from the CNX/CRT cycle. Moreover, EDEM directs the glycoprotein for degradation by the ERAD pathway.

1.4.3 General features and substrate specificity of calnexin and calreticulin

A wide variety of important cellular and viral glycoproteins are known substrates of CNX and CRT (see paper III and references therein). Although many glycoproteins associate with both CNX and CRT, and despite having the same glycan specificity, these two lectins can have distinct roles in glycoprotein maturation. For instance, they can bind to the same protein at different stages of the folding process as seen for both the MHC class I heavy chain (Cresswell, 2000; Diedrich et al., 2001) and Influenza hemagglutinin (HA), (Hebert et al., 1996). For the latter, association has been shown to depend on the position of the sugar within the molecule. Whereas CRT associates preferentially with the glycans of the HA top domain, CNX associates more efficiently with those glycans present in the membrane-proximal stem domain (Hebert et al., 1997).

The set of substrates bound by the two proteins is largely, but not completely, overlapping (Peterson et al., 1995; Wada et al., 1995). Notably, there is only one substrate known to date that solely interacts with CNX – VSV G-protein (Hammond and Helenius, 1994a; Peterson et al., 1995) – but none that only associates with CRT. In line with the results obtained for HA, the difference in substrate recognition pattern has been shown to depend on the presence of the membrane anchor in CNX (Danilczyk et al., 2000; Ho et al., 1999). However, the finding that the lumenal domain of CNX cannot complement the function of CRT in MHC class I assembly when expressed in CRT-deficient cells indicates that the two proteins possess protein specific functions despite their many similarities (Gao et al., 2002).

The exact mode of interaction by CNX and CRT with their glycoprotein substrates is still a matter of debate. Studies performed *in vitro* using RNaseB as a model glycoprotein and studies of glycoprotein folding in the protozoan parasite

Trypanosoma cruzi suggest that the function of CNX and CRT as molecular chaperones can be attributed solely to their lectin activity (Labriola et al., 1999; Rodan et al., 1996; Zapun et al., 1997). However, assays of aggregation and refolding using purified proteins as substrates show that CNX and CRT could have an additional function as classical chaperones, characterized by protein–protein contacts with hydrophobic regions exposed by non-native polypeptide chains (Ihara et al., 1999; Saito et al., 1999). As observed for classical chaperones, CNX and CRT can suppress aggregation and preserve proteins in a folding competent state, independent of their glycosylation status (monoglucosylated or non-glycosylated), (Ihara et al., 1999; Saito et al., 1999). However, the efficiency of suppressing aggregation was enhanced for monoglucosylated proteins, potentially indicating an avidity effect of two binding sites, one for the glycan and one for the polypeptide chain of the substrate (Stronge et al., 2001). Whereas native conformers were shown not to interact with CNX and CRT, complexes were formed with misfolded conformers.

Complexes between CNX and proteins without a monoglucosylated glycan have also been detected *in vivo* (Danilczyk and Williams, 2001). However, these could only be observed when radiolabelling mammalian cells at 23°C and lysing them in mild conditions with 1% digitonin (Danilczyk and Williams, 2001), as opposed to radiolabelling at 37°C followed by lysis with 2% CHAPS (Ora and Helenius, 1995). The complexes in the first study were shown not to be contained in bigger protein aggregates, while complexes of CNX with nonglycosylated vesicular stomatitis virus G protein in microsomes were found to be highly aggregated (Cannon et al., 1996). The apparent discrepancy between protein/protein versus protein/sugar interaction presented in these studies might not be irreconcilable. The question remaining is do classical chaperone interactions of CNX and CRT with substrate proteins contribute to productive folding of these substrates? A first prerequisite for this is the transient association of CNX or CRT with non-glycoproteins, which could recently be demonstrated for the case of CNX and proteolipid protein (Swanton et al., 2003). Their interaction was not due to them being trapped in the same membrane micelle (Swanton et al., 2003). However, an example of CNX and CRT promoting the productive folding of a substrate via protein-protein interactions is still missing.

Besides its well-established role as a molecular chaperone, CRT is a major Ca^{2+} storage protein and plays an important role in Ca^{2+} homeostasis in the ER (Corbett and Michalak, 2000; Michalak et al., 1999). Thus, the embryonic lethal

phenotype observed in CRT-deficient mice (Mesaeli et al., 1999) is connected to the function of the protein in Ca^{2+} signaling during cardiac development (Guo et al., 2002; Li et al., 2002). Although CNX also binds Ca^{2+} (Tjoelker et al., 1994; Wada et al., 1991), the protein does not seem to play a significant role in Ca^{2+} homeostasis and its major function is that of a molecular chaperone. CNX gene-deficient mice do not show as serious defects as CRT knockout mice. However, 50% die within two days of birth, whereas the rest display severe motor disorders, a selective loss of large myelinated fibers and die within 3 months (Denzel et al., 2002).

1.4.4 Primary structure of calnexin and calreticulin

The molecular cloning of CRT (46.5 kDa, 400 residues), (Fliegel et al., 1989; Smith and Koch, 1989) and CNX (65.4 kDa, 572 residues), (Tjoelker et al., 1994; Wada et al., 1991) has revealed that the two proteins are highly similar (Fig. 1.3). The main differences are found in their carboxyl terminal regions. Whereas CRT is a soluble lumenal protein with a carboxyl terminal KDEL retrieval sequence, CNX is a type I transmembrane protein with a predicted transmembrane region spanning residues 463–485, followed by a 87 residue carboxyl terminal cytosolic tail. However, the lumenal domain of CNX is highly similar to CRT. Based on sequence analysis, both proteins have been suggested to consist of three regions, the N-, P-, and C-domains (see Appendix, Fig. 6.2), (Baksh and Michalak, 1991; Fliegel et al., 1989; Michalak et al., 1992; Smith and Koch, 1989). The N-domain (CRT residues 1–188, CNX residues 1–253) was originally predicted to comprise a β-sheet rich globular structure (Fliegel et al., 1989; Smith and Koch, 1989). The unique P-domain (CRT residues 189–283, CNX residues 254–388) constitutes the signature sequence for this family of proteins, and has obtained its name due to the many prolines present in this region. It consists in its entire length of two short sequence repeats, the type 1 and type 2 repeats. Each type of repeat is present in three or four copies in CRT and CNX, respectively. In both proteins, the arrangement of the repeat sequences is such that all type 1 repeats are clustered together, followed by a cluster of type 2 repeats (Fig. 1.3). The distinguishing feature of the CRT C-domain (residues 284–400) is the enrichment of acidic amino-acid residues in the ~60 carboxyl terminal residues. This region is known to play a role in low-affinity Ca^{2+} binding (Baksh and Michalak, 1991; Khanna et al., 1986; Ostwald and MacLennan, 1974). In contrast, the C-domain

of CNX, residues 389–462, does not display noticeable traits. Here, the membrane-proximal region of ~20 residues is likely to represent a linker sequence between the membrane anchor and a globular lectin domain.

The sequences of both CNX and CRT encode cysteine residues that form intrachain disulfide bonds. In CNX the four cysteines pair to form the Cys140–Cys174 and Cys340–Cys346 disulfides (Schrag et al., 2001). In CRT a free cysteine is present at position 146, whereas the Cys89–Cys120 disulfide is equivalent to the Cys140–Cys174 disulfide in CNX (Houen and Koch, 1994). Although certain animal CRT sequences contain a conserved N-glycosylation site at residue 326, human placental CRT has been shown not to be glycosylated (Houen and Koch, 1994). Animal CNXs do not contain potential sites for N-linked glycosylation. A unique feature of the carboxyl terminal cytosolic tail of CNX is the presence of sites for phosphorylation by casein kinase II at Ser534 and Ser 544 and by extracellular-signal regulated kinase-1 at Ser653 (Ou et al., 1992; Wong et al., 1998). Phosphorylation at these positions has been shown to regulate the association of CNX with ribosomes (Chevet et al., 1999).

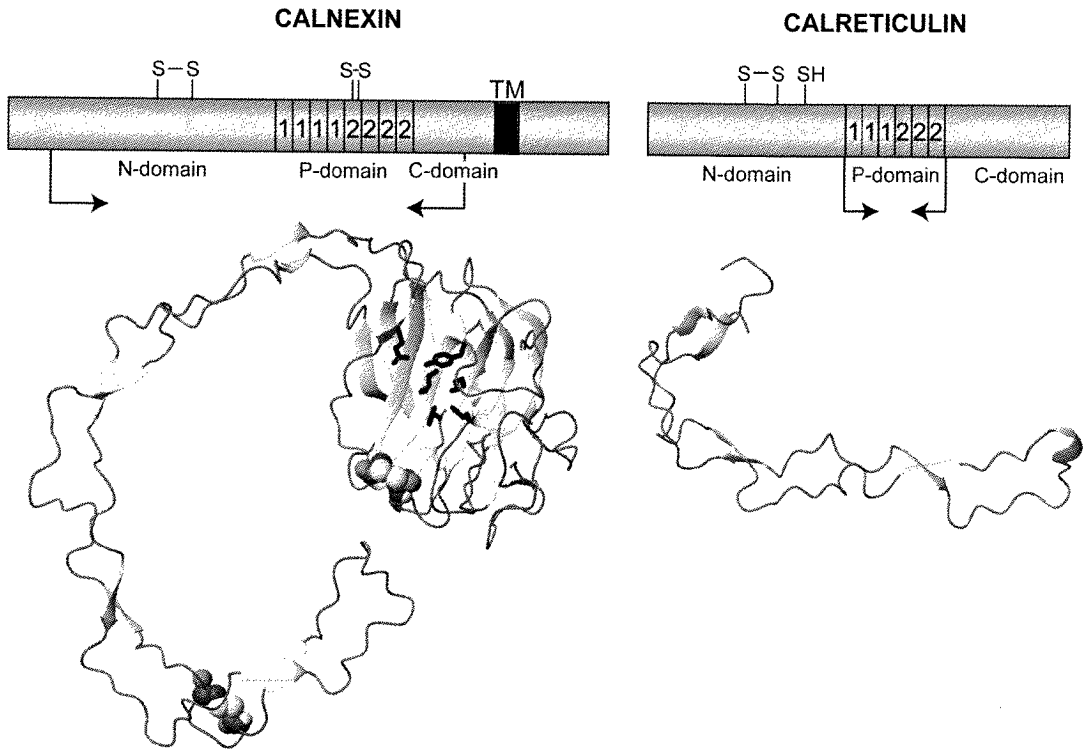

Fig. 1.3. Structures of CNX and CRT. Overview of the primary amino-acid sequence of CNX and CRT, and the three-dimensional structures solved for the two proteins. In the schematic representation, the position of type 1 and type 2 repeats of the P-domain is indicated along with the position of free

and disulfide-bonded cysteine residues. 'TM' denotes the transmembrane region in CNX. The arrows indicate the boundaries of the fragments for which the three-dimensional structures are shown below. In the representation of the three-dimensional structure of the lumenal domain of CNX, residues involved in the binding of the glucose are shown as black stick models and the cysteines forming the two disulfide bonds are shown as CPK models. This figure was prepared using the program MOLMOL (Koradi et al., 1996).

1.4.5 Glycan binding to calnexin and calreticulin

A number of studies performed *in vitro* have characterized the direct interaction of CNX and CRT with isolated glycans using biochemical methods. All support the notion that both proteins are lectins that specifically interact with the monoglucosylated form of the core glycan (Fig. 1.1 and 1.2), (Kapoor et al., 2003; Peterson and Helenius, 1999; Spiro et al., 1996; Vassilakos et al., 1998; Ware et al., 1995). These studies also show that CNX and CRT interact with glycans with increasing affinity when comparing oligosaccharides of different lengths as follows: Glc(G1) << Glcα1-3Man(G1M1) << Glcα1-3Manα1-2Man(G1M2) < Glcα1-3Manα1-2Manα1-2Man(G1M3), (Kapoor et al., 2003). Therefore, the glycan interaction is likely to involve the entire α1-3 branch of the oligosaccharide, which forms a continuous molecular surface in the NMR structure of $Glc_1Man_9GlcNAc_2$ (Petrescu et al., 1997). Direct affinity measurements have demonstrated that the G1M3 tetrasaccharide binds CRT with comparable affinity to an IgG molecule carrying the entire monoglucosylated glycan (Kapoor et al., 2003). However, glycan binding by CNX and CRT could potentially also involve contacts to the mannose residues on the α1-6 branch of the glycan (Spiro et al., 1996; Ware et al., 1995).

Detailed biophysical analysis of the binding of IgG carrying a single monoglucosylated glycan to CRT demonstrated a K_d of ~2 μM (Patil et al., 2000). Furthermore, this study showed that – at least under these experimental conditions using a native monoglucosylated protein – no contribution to the binding reaction was observed from protein–protein interactions. As proposed by Surolia and coworkers (Patil et al., 2000), the relatively low affinity of CRT for the glycan could be advantageous to allow for rounds of glycoprotein association and dissociation. This feature would permit trimming of the remaining glucose of the glycan by glucosidase II to occur on the non-bound substrate. Such a model is supported by the finding that RNaseB bound by the lumenal domain of CNX is protected effectively from glucosidase II and PNGaseF digestion (Zapun et al., 1997).

In vitro, the binding of the oligosaccharide by either CNX or CRT depends critically on the presence of Ca^{2+} (Patil et al., 2000; Vassilakos et al., 1998). Thus, it is possible that the deleterious effect of Ca^{2+} depletion from the ER, observed for the folding of glycoproteins known to interact with CNX and CRT, directly reflects structural changes in the lectin domain, which render both proteins incapable of ligand interaction (Di Jeso et al., 2003).

1.4.6 Structural studies of calnexin

The biochemically determined properties of CNX and CRT have been put into new perspective by structural studies on both molecules. For CNX, the crystal structure of a fragment encompassing most of the lumenal domain, has been reported to a resolution of 2.9 Å (Fig. 1.3), (Schrag et al., 2001). This highly unusual structure contains two separate entities: a globular β-sandwich domain homologous to legume lectins and an extended hairpin fold of ~140 Å in length, corresponding to the P-domain.

The globular domain comprises a concave and a convex β-sheet with six and seven β-strands, respectively. By soaking the crystal in glucose and determining its location in the electron density, it was found that the concave β-sheet of the globular domain harbors a monovalent glycan binding site. Modeling the binding of the G1M3 tetrasaccharide indicated that steric hindrance is likely to prevent the access of glucosidase II to its sugar substrate. This finding supports the idea that the glycoprotein must dissociate from the lectin for cleavage by glucosidase II to occur. A disulfide bond is present in the globular domain in the vicinity of the proposed glycan-binding site. This feature can account for the observed sensitivity of oligosaccharide binding by CNX towards reduction (Ou et al., 1995; Vassilakos et al., 1998). In this part of the molecule, the CNX model also shows a putative Ca^{2+} binding site, with the Ca^{2+} ion proposed to play a role in structural stabilization rather than ligand interaction.

The only regular secondary structure elements in the P-domain are four short, anti-parallel β-sheets where each β-strand contains three residues. A disulfide bond is found close to the tip of the P-domain.

Interestingly, legume lectins, galectins and neurexin 1β possess a closely related fold to the globular domain of CNX (Schrag et al., 2001). The laminin G-like

domain of neurexin 1β contains alternative splice sites in loops connecting the β-strands and the absence or presence of inserted sequences at these sites determines ligand interactions (Rudenko et al., 1999). Similarly, the P-domain of CNX is introduced at the same topological position as one of the splice sites in neurexin 1β.

1.4.7 Structural studies of calreticulin

For CRT, the NMR structure of the P-domain, residues 189–288, has been solved (Fig. 1.3), (Ellgaard et al., 2001a; Ellgaard et al., 2001b). Like the CNX P-domain it shows an extended hairpin fold, in the case of CRT with a length of ~110 Å. Three short anti-parallel β-sheets and three small hydrophobic clusters stabilize the structure. This three-fold repetition of structural elements and the four-fold repetition of similar structural features in the CNX P-domain closely reflect the repetitive nature of the P-domain sequence in the two molecules (Fig. 1.3). Roughly, each type 1 repeat sequence pairs up with a type 2 repeat sequence in the structure of both P-domains by forming interactions across the hairpin. In addition, it has recently been shown that a short fragment corresponding to one type 1 repeat and one type 2 repeat, and comprising the β-sheet and the hydrophobic cluster at the tip of CRT P-domain, constitutes an independently folding structure (Ellgaard et al., 2002). It is tempting to speculate that the unique sequence of the P-domain has evolved by the sequential insertion of such '12' units into a loop region of the globular lectin domain.

Currently, the structure corresponding to the CNX lectin domain is not known for CRT. However, the crystal structure of the lumenal domain of CNX and the sequence similarity between the two proteins (Figs. 1.3 and Appendix, Fig. 6.2) strongly indicate that the CRT N-domain and residues 284–337 of the C-domain will form a globular domain with structural similarity to the CNX lectin domain. Indeed, this is exactly what the recently modeled structure of the CRT lectin domain also suggests (Kapoor et al., 2003). Furthermore, biochemical and biophysical analysis of full-length CRT has shown that the molecule is asymmetric and elongated (Bouvier and Stafford, 2000). Based on this information, the known structural data for both proteins and the overall high conservation of sequence and function between the two proteins, it can be assumed that both CNX and CRT show a two domain structure comprising a globular lectin domain and a long protruding P-domain. In addition, the residues of CNX proposed to be involved in the binding of glucose and Ca^{2+} are

largely conserved in CRT. Likewise, residues in CRT proposed to bind the G1M3 tetrasaccharide are well conserved in CNX (Kapoor et al., 2003); Kapoor, 2004, Biochemistry), (see Appendix, Fig. 6.2).

Whereas the crystal structure of the lumenal domain of CNX revealed the lectin function of the globular domain, the function of the P-domain remained unclear despite detailed structural analysis obtained by both X-ray crystallography and NMR spectroscopy.

1.5 Oxidative protein folding

1.5.1 Disulfide bond formation

The formation of disulfide bonds is crucial for proteins of the secretory pathway, both for their folding and their stability. Thus, the ER of eukaryotes and the periplasm of prokaryotes are the places in the cell were these covalent bonds are created. Often a protein cannot fold correctly if its disulfides are not generated in the proper manner or even order (Braakman et al., 1992a; Braakman et al., 1992b). A disulfide bridge renders the native form of a protein more stable by reducing the conformational entropy of the denatured state (Fersht, 1999).

In vitro, a loss of electrons from two cysteine thiols can occur spontaneously when an adequate electron acceptor like molecular oxygen is present resulting in the generation of a disulfide bond. *In vivo*, usually a thiol-disulfide exchange reaction occurs between an already disulfide-bonded molecule and one carrying free thiols. In this reaction a thiolate anion performs a nucleophilic attack on a sulfur of a disulfide bond forming a transient mixed-disulfide (see Fig. 1.4). Next, another thiolate anion releases this new-formed bond, either yielding the transfer of a disulfide bond or restoring the original situation. This disulfide exchange reaction in proteins can happen between two proteins, a protein and a redox molecule or intramolecularly in a protein.

The catalysts for disulfide bond formation in cells are a class of proteins that are known as thiol-disulfide oxidoreductases. Their activity results from two cysteines arranged in a CXXC motif contained in a so-called thioredoxin domain. The name originates from the small cytosolic reductase thioredoxin and this globular fold is comprised of beta-sheets that form the core of the molecule surrounded by alpha-

helices (Fig. 1.5), (Katti et al., 1990). The disulfide bridge between the two active site cysteines is located at the amino terminus of the second alpha-helix. The catalytic CXXC is found in an exposed loop.

In a disulfide reduction or isomerization reaction the N-terminal cysteine is the one that perfoms the initial attack on the disulfide bridge of the substrate. The reaction rates of a thiol-disulfide oxidoreductase with a peptide substrate can vary between 10^3-10^7 $M^{-1}s^{-1}$ (Darby et al., 1998b), which is several orders of magnitude faster than disulfide exchange between alkyl thiols (10-10^3 $M^{-1}s^{-1}$), (Shaked et al., 1980; Szajewski and Whitesides, 1980). Factors that determine the reaction rates are the pK_a of the N-terminal cysteine, the effective concentration and accessibility of the thiol or disulfide groups and the chemical surroundings of the active site. The mechanism for a PDI-mediated isomerization reaction has been shown to largely be mediated by cycles of reduction and reoxidation (Schwaller et al., 2003; Walker and Gilbert, 1997), as opposed to intramolecular rearrangement while being engaged in an intermolecular disulfide bond with an oxidoreductase as depicted in Fig. 1.4.

The prototype and the first identified eukaryotic thiol-disulfide oxidoreductase is protein disulfide isomerase (PDI), (Goldberger et al., 1963). PDI is a versatile redox enzyme capable of catalyzing oxidation, reduction or isomerization of a substrate protein (see section 1.6.1). Which type of redox reaction a certain enzyme catalyzes not only depends on the equilibrium redox potential of the compartment, but also on the redox potential of the enzyme. Other factors playing an important role in determining the direction of electron flow is the enzyme's steric ability and tendency to interact with the substrate, as well as the concentration of the enzyme and the substrate.

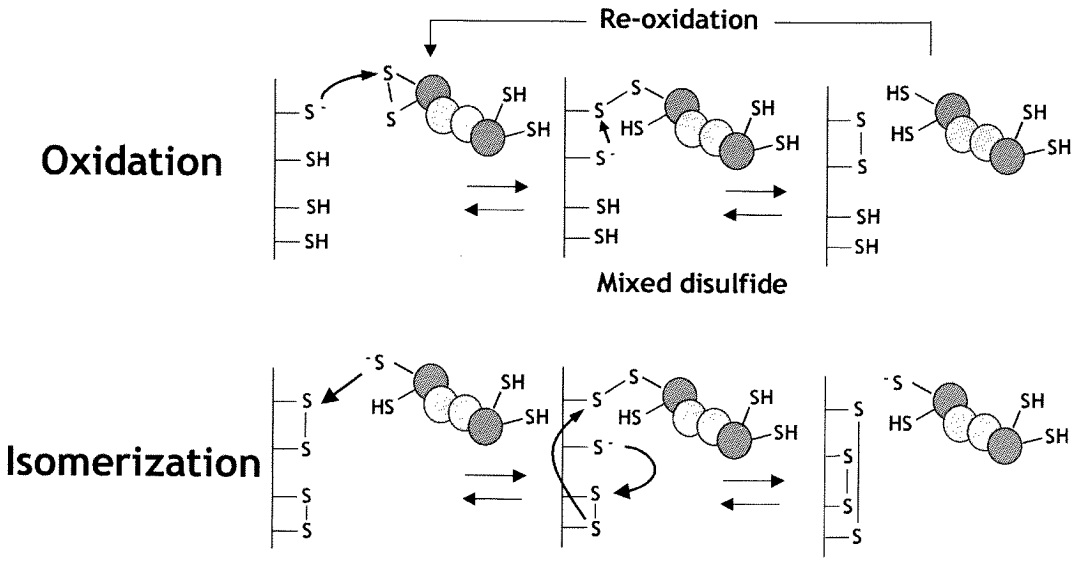

Fig. 1.4 Scheme of disulfide bond oxidation and isomerization. In an oxidation reaction the disulfide bond of an oxidase is transferred to a substrate protein. This involves the generation of a mixed disulfide between the N-terminal cysteine of the catalyst and a cysteine in the substrate. If this species is resolved through the attack of a further cysteine in the substrate, the result is an oxidized substrate protein and a reduced oxidoreductase. In order to function as an oxidase in a second round, the oxidoreductase has to be re-oxidized. The first step in a catalytically mediated isomerization reaction is the reduction of an existing disulfide in the substrate again via a mixed disulfide intermediate between the substrate and the N-terminal cysteine in the oxidoreductase. Effectively, this frees cysteines that can now arrange intramolecularly and the outcome will be a differently disulfide-bonded substrate. Rather than intramolecular rearrangement while disulfide-linked to a thiol-disulfide oxidoreductase, it seems more likely that cycles of reduction and oxidation by the catalytic oxidoreductase mediate the isomerization reaction. The thiol-disulfide oxidoreductase enters the isomerization reaction in its reduced state and also exits it in that state.

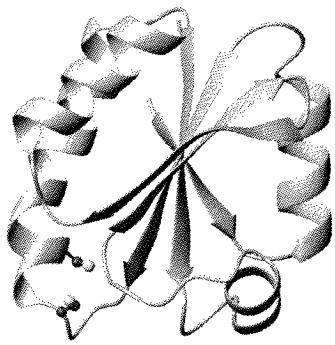

Fig. 1.5 Ribbon model of the crystal structure of reduced human thioredoxin (Weichsel et al., 1996). The two active site cysteines are shown as ball and stick representation.

1.5.2 Prokaryotic oxidative folding

In Gram-negative bacteria, the periplasm is the compartment where disulfide bonds are formed. It has been estimated that more than half of the proteins located in the

periplasm and in the membrane contain two or more cysteine residues (Hiniker and Bardwell, 2004). Separate pathways with different redox enzymes for protein oxidation and isomerization exist. DsbA and DsbB are responsible for substrate oxidation, while DsbC and DsbD drive polypeptide isomerization (see Figure 1.6).

DsbA, the bacterial oxidase, is a 21 kDa soluble periplasmic protein with a characteristic CXXC motif embedded in a thioredoxin domain (Martin et al., 1993). DsbA has a very oxidizing redox potential of −122 mV (Wunderlich and Glockshuber, 1993). This results at least in part from the unusually low pK_a of about 3.5 of the N-terminal cysteine in its active site (Grauschopf et al., 1995; Hennecke et al., 1997; Nelson and Creighton, 1994) and its unstable oxidized state (Wunderlich et al., 1993; Zapun et al., 1993). Once DsbA has oxidized a substrate, it is re-oxidized by the integral membrane protein DsbB.

DsbB is a 21 kDa four transmembrane helix protein that has two pairs of cysteines in two separate loops in the periplasmic space. The electrons in the reaction to re-oxidize DsbA flow from DsbA to the C-terminal cysteine pair in DsbB, which has a redox potential of −186 mV. The N-terminal cysteines with a redox potential of −69 mV provide the driving force of the reaction by performing a rapid intramolecular disulfide exchange and taking on the electrons (Grauschopf et al., 2003). Re-oxidation of this cysteine pair occurs through ubiquinone, which donates the electrons to cytochrome oxidases and finally to oxygen (Bader et al., 1999; Bader et al., 2000). This links aerobic bacterial disulfide bond formation to the electron transport chain. Under anaerobic conditions the electrons are passed from DsbB to menaquinone and then to fumerate reductase or nitrate reductase (Bader et al., 1999).

DsbC is the isomerase of proteins containing more than two cysteines in the periplasm. It is a soluble V-shaped dimer, with each 23 kDa monomeric unit consisting of a thioredoxin domain and a dimerization domain (McCarthy et al., 2000). The active site CXXC motifs are positioned across from each other on the top and inside of the V. The surface of the cleft between the two arms of the V is lined with hydrophobic and uncharged residues, possibly enabling substrate protein binding. *In vivo*, DsbC is found in the reduced state, which is the prerequisite for it to always be functional (Joly and Swartz, 1997; Rietsch et al., 1997).

DsbD is the reductant of DsbC in the isomerization pathway (Missiakas et al., 1995). This 59 kDa protein is comprised of three domains (Chung et al., 2000; Gordon et al., 2000): an N-terminal periplasmic Ig domain (nDsbD), (Goulding et al.,

2002; Haebel et al., 2002), an eight transmembrane spanning domain (TMD), and a C-terminal thioredoxin-like domain (cDsbD), (Kim et al., 2003). Electrons flow from cytosolic thioredoxin, which has a redox potential of –270 mV (Krause et al., 1991), to the TMD and from there to the nDsbD domain (redox potential of –241 mV), (Collet et al., 2002). Then they can be passed on to the cDsbD domain (redox potential of –229 mV), (Collet et al., 2002), which reduces DsbC that has a redox potential of –159 mV (Aslund et al., 1997; Zapun et al., 1995).

DsbA and DsbC guarantee the separation of the oxidation and isomerization pathways by only interacting with their respective partner protein in the membrane. The determinants that keep for example DsbC from productively forming a complex with DsbB are becoming increasingly clear. One reason could be the dimeric state of DsbC as opposed to the monomeric state of DsbA (Bader et al., 2001). In a comprehensive study on the kinetics of the disulfide exchange reactions between the two separate pathways, it was found that large kinetic barriers prevent nonfunctional reactions from taking place (Rozhkova et al., 2004). This seems to be the result of steric hindrance rather than specific side-chain interactions in the contact area, as the number of salt bridges and specific hydrogen bonds compared to the interface area is small for the interaction between nDsbD and cDsbD (Rozhkova et al., 2004).

Even though the molecular details of periplasmic oxidative protein folding are becoming well characterized, only relatively few endogenous substrates of DsbA and DsbC have been studied such as alkaline phosphatase (Bardwell et al., 1991; Sone et al., 1997), OmpA (Bardwell et al., 1991; Rietsch et al., 1997), and the P-ring protein of flagellar (Dailey and Berg, 1993). Recently, a more comprehensive study has begun to identify *in vivo* substrates of DsbA and DsbC (Hiniker and Bardwell, 2004). Additionally, another group was able to trap covalent intermediates of DsbA and some of its substrates *in vivo* (Kadokura et al., 2004).

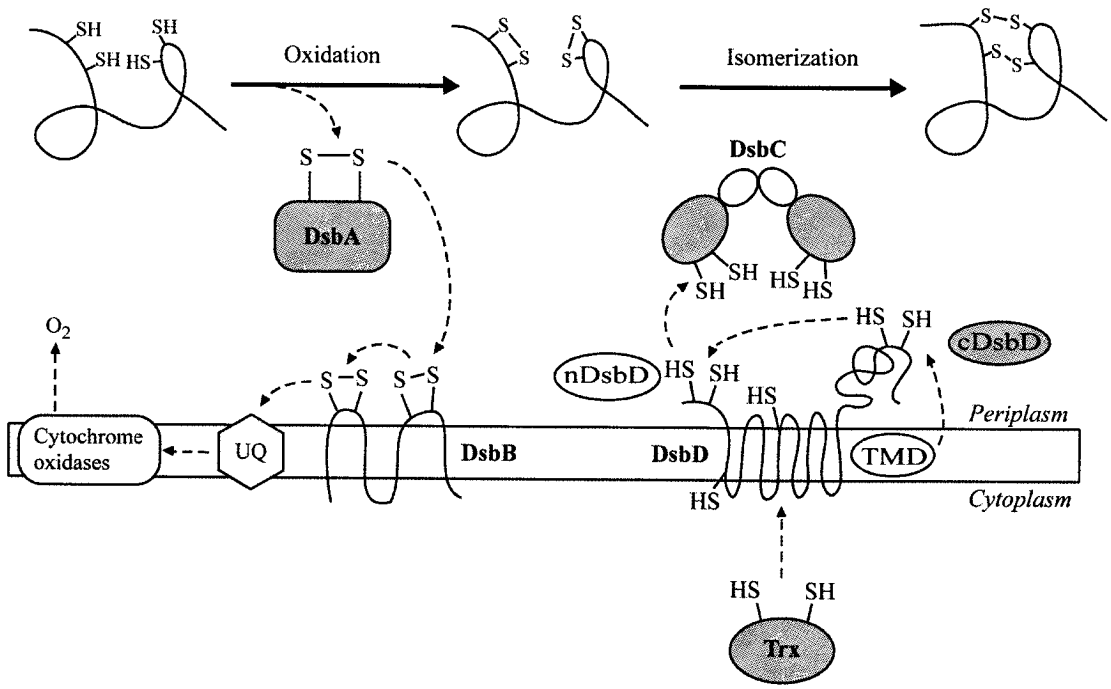

Fig. 1.6 Periplasmic protein oxidation and isomerization pathway in *E. coli*. Proteins are oxidized in the periplasmic space through the action of DsbA, which passes the electrons on to the membrane protein DsbB. The flow of electrons is shown as dotted arrows. From DsbB the electrons passage to ubiquinone (UQ) via cytochrome oxidases to oxygen under aerobic conditions and to nitrate or fumarate under anaerobic conditions (not shown). Disulfide bond isomerization is mediated by DsbC, which obtains electrons from the N-terminal domain of DsbD (nDsbD). nDsbD is maintained in the reduced state by the C-terminal domain of DsbD (cDsbD), which obtains electrons from the transmembrane domain (TMD) of DsbD. Cytoplasmic Trx keeps the TM domain of DsbD reduced. All proteins shaded in dark gray contain the Trx fold (DsbA, DsbC, cDsbD, Trx).

1.5.3 Principles of oxidative folding in eukaryotes

In order to gain a complete understanding of oxidative folding, it is crucial to determine where the oxidizing equivalents for disulfide bond formation come from. For a long time it was thought that glutathione was the thiol oxidant of the ER (Hwang et al., 1992). This was the only small-molecule redox component that was detected within the ER that could form mixed disulfides with cysteines in polypeptide chains. Furthermore, in the oxidative folding of proteins *in vitro*, GSH/GSSG mixtures were effective buffers (Creighton et al., 1993; Walker and Gilbert, 1997). This view was revised with the discovery of Ero1p (for ER oxidoreductin), (Frand and Kaiser, 1998; Pollard et al., 1998), a protein that sustains the net formation of disulfide bonds. It is now clear that Ero1p re-oxidizes PDI and Mpd2 (Frand and Kaiser, 1999). Additionally, it was shown that deletion of the *GSH1* gene (which encodes γ-glutamylcysteine synthetase, the enzyme catalyzing the first and rate-limiting step in glutathione synthesis) could restore disulfide bond formation activity

in a strain where Ero1 had been mutated (Cuozzo and Kaiser, 1999). This, and the fact that oxidation of RNaseA can be driven by Ero1 and PDI in the absence of a redox buffer (Tu et al., 2000) demonstrates that rather than oxidizing proteins in the ER, glutathione competes for oxidizing equivalents with proteins. Moreover, excretion of glutathione from yeast does not correlate with the number of disulfides of overproduced secreted proteins (Bannister and Wittrup, 2000). This all fits well with the finding that GSH as opposed to GSSG is imported into the ER in a facilitate manner inhibitable with anion transport blockers (Banhegyi et al., 1999). In fact, the ER membrane might be more permeable than originally thought, letting small molecules passively diffuse in and out (Le Gall et al., 2004). Over half of the microsomal glutathione was shown to be associated with proteins (Bass et al., 2004), a finding that also supports the fact that GSH plays an active role in alleviating oxidative stress by providing reducing equivalants in the ER and not just in maintaining the compartment's redox state.

1.5.4 Oxidative Folding in S. cerevisiae

In *S. cerevisiae* oxidative protein folding takes place in the ER, where five thiol-disulfide oxidoreductases are known to reside – Pdi1p, Eug1p, Mpd1p, Mpd2p, Eps1p (see Table 1.1). Pdi1p is the essential and well-studied PDI, which is discussed in further detail in section 1.6.1. The other four are non-essential homologues (Tachibana and Stevens, 1992; Tachikawa et al., 1997; Tachikawa et al., 1995; Wang and Chang, 1999). Please note that there is no ERp57 homologue in *S. cerevisiae*. It seems likely that the different PDIs in yeast have different substrate specificity or can respond to different stress conditions (Norgaard et al., 2001).

Ero1p is a 65 kDa glycosylated lumenal protein that is tethered to the ER membrane and contains non-covalently bound flavin adenine dinucleotide (FAD), (Tu et al., 2000). By reconstituting the pathway for thiol oxidation *in vitro*, it has been conclusively shown that Ero1p shuttles electrons from PDI to the FAD that it is bound to and then to molecular oxygen (Tu et al., 2000; Tu and Weissman, 2002). For this action, two cysteine pairs in Ero1p are essential (Frand and Kaiser, 2000).

Another ER oxidase, Erv2, was identified as a gene that upon overexpression could restore the temperature sensitive mutant *ero1-1* strain in yeast (Sevier et al., 2001). Additional deletion of the biosynthesis gene for glutathione, *GSH1*, in the *ero1*

knock-out strain also resulted in viability, yielding the proposition that Erv2 could pose a bypass mechanism for Ero1 in order to supply PDI with oxidizing equivalents (Sevier et al., 2001). However, loss of *ERV2* in the *ero1-1/gsh1* double knock-out does not affect growth (Tu and Weissman, 2002). Biochemical data clearly support that Erv2p can act as an oxidase for PDI (Sevier et al., 2001), and thus it remains to be investigated if it functions only under special cellular conditions or if it potentially has other preferred target proteins. Erv2p is a 22-kDa membrane-associated ER protein that non-covalently contains FAD (Sevier et al., 2001). The structure of this dimer has been solved and it shows no homology to any other known FAD-binding proteins (Gross et al., 2002).

1.5.5 Oxidative folding in higher eukaryotes

The disulfide bond formation system is least well-studied in higher eukaryotes (see Fig. 1.7). Nevertheless, it is clear that PDI is a universal enzyme capable of performing all three types of redox reactions – oxidation, reduction and isomerization (Freedman et al., 1994). Many other thiol-disulfide oxidoreductases have been identified and partially characterized (see Table 1.1), but it remains to be investigated if they serve different substrate proteins or if they provide separate oxidation/isomerization pathways like in bacteria. So far no thiol-disulfide oxidoreductase in the ER is known to catalyze only one redox reaction *in vivo*.

Two Ero1 genes have been found in mammalian cells, termed *ERO1-Lα* and *ERO1-Lβ* (Cabibbo et al., 2000; Pagani et al., 2000). They lack the C-terminal tail of about 127 amino acids necessary for membrane association of the yeast protein (Pagani et al., 2001). Both gene products were able to rescue *ero1-1* mutant yeast cells in that they allowed growth of these cells at 37°C and alleviated the constitutive unfolded protein response (UPR) that characterizes this strain (Cabibbo et al., 2000; Pagani et al., 2000). However, only the expression of Ero1-Lβ and not Ero1-Lα is induced by UPR. The two genes are also differentially distributed with *ERO1-Lβ* being quite abundant in secretory tissues (Pagani et al., 2000). Mixed disulfides between both Ero1-Lα and Ero1-Lβ and PDI have been found in mammalian cells (Benham et al., 2000; Mezghrani et al., 2001). The reason why mammalian cells have evolved two *ERO1* genes for the transfer of oxidizing equivalents to PDI and subsequently to substrate proteins containing disulfide bonds, while yeast contains

only one *ERO1* gene for this function is at the present not clear. It is conceivable that in mammalian cells this serves for a more subtle control of the ER redox state. A recent report shows that the release of A1 cholera toxin chains via PDI is mediated only by Ero1-Lα and not Ero1-Lβ (Tsai and Rapoport, 2002).

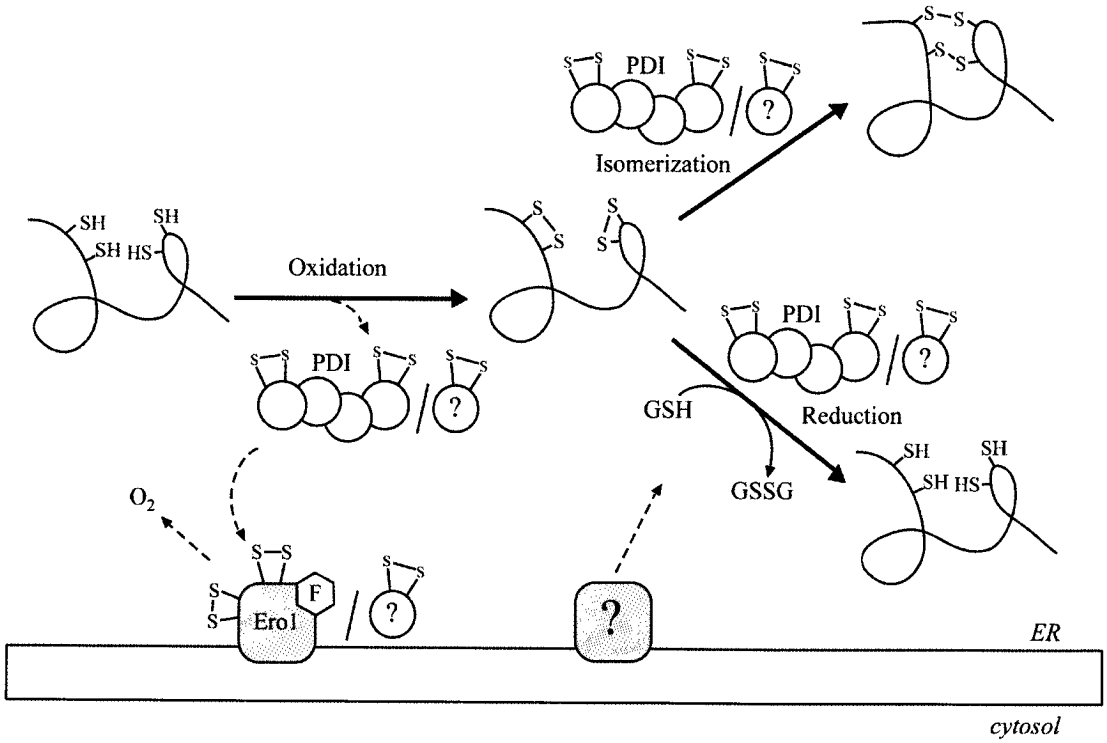

Fig. 1.7 Dithiol oxidation, disulfide reduction and isomerization pathway of higher eukaryotes. Proteins are oxidized in the ER through the action of PDI and other thiol-disulfide oxidoreductases. Ero1, a membrane-associated flavoprotein keeps PDI in the oxidized state and passes the electrons on to the terminal acceptor oxygen. The flow of electrons is shown by the dashed arrows. In yeast, Erv2p has also been shown to be able to oxidize PDI (not depicted). Reduction and isomerization of substrate proteins is mediated by PDI and potentially by other oxidoreductases. No reductases of PDI or related proteins have been identified. The dashed line upwards shows the flow of electrons, which can be taken up by GSSG, PDI or other thiol-disulfide oxidoreductases. GSH competes with substrate proteins for oxidizing equivalents.

1.5 Eukaryotic thiol-disulfide oxidoreductases

1.5.1 Protein disulfide isomerase

Protein disulfide isomerase (PDI) was identified by Anfinsen in 1963 as a component of microsomal extracts that accelerated the folding of RNaseA (Goldberger et al., 1963). This archetypical thiol-disulfide oxidoreductase of the ER is comprised of four thioredoxin-like domains, termed **a**, **b**, **b'**, **a'**, followed by the acidic **c** domain. The **a** and **a'** domains harbor a CGHC motif and are thus catalytically active, while the **b**

and **b'** domains are redox inactive and devoid of CXXC motifs. PDI is a protein of 55 kDa with a C-terminal KDEL ER retrieval sequence. The protein has been isolated as a homodimer (Freedman et al., 1995), a monomer or tetramer (Gilbert, 1998). However, most recently it was found to be a monomer in analytical ultracentrifugation studies (H. F. Gilbert, personal communication). It is highly conserved among species and is found in the micromolar range in the ER (Zapun et al., 1992) with local concentrations approaching millimolar level (Lyles and Gilbert, 1991). This makes it a very abundant protein comprising about 0.4% of the total protein in liver (Hillson et al., 1984). In mammalian cells, PDI is a also a subunit of prolyl 4-hydroxylase (P4H), (Pihlajaniemi et al., 1987) and the microsomal triacylglycerol transfer protein (MTP), (Wetterau et al., 1990).

PDI has been shown to act as an oxidase, reductase and isomerase *in vitro* (Creighton et al., 1980; Darby and Creighton, 1995a), (for reviews see (Freedman et al., 1994; Freedman et al., 2002) and to possesses a peptide-binding site, which has been mapped to its **b'** domain (Klappa et al., 1998). The individual redox-active domains are able to catalyze substrate oxidation, but not isomerization (Darby and Creighton, 1995b; Darby et al., 1998a). Thus, the peptide-binding region and with it the multidomain structure of PDI have probably evolved in order to expand the catalytic repertoire of this thiol-disulfide oxidoreductase. Isomerization by PDI has been shown to be primarily mediated by cycles of reduction and reoxidation (Schwaller et al., 2003; Walker and Gilbert, 1997).

Typically for a thioredoxin fold enzyme, PDI's redox activity is based on the reactivity of the N-terminal cysteine residue in its two CGHC motifs. This cysteine thiol has been shown to have a pK_a of 4.5 (Kortemme et al., 1996) or 6.7 (Hawkins and Freedman, 1991), which is much lower than the pK_a of about 9.5 of a normal cysteine thiol. Partly resulting from this, the PDI **a** and **a'** domains are destabilized in their oxidized form (Alanen et al., 2003b; Darby and Creighton, 1995b), re-enforcing their ability to act as oxidases. Using GSH/GSSG as a reference, the redox potential of PDI has been determined to −175 mV (Lundstrom and Holmgren, 1993), and the equilibrium constants for the PDI **a** domain to 0.7 mM and for the PDI **a'** domain to 1.9 mM (Darby and Creighton, 1995a). This renders PDI among the more oxidizing of the thiol-disulfide oxidoreductases (Fig. 1.8). Along these lines, PDI is able to compensate for DsbA deficiency in *E. coli* (Humphreys et al., 1995; Ostermeier et al., 1996; Stafford and Lund, 2000).

In *S. cerevisiae*, PDI is an essential protein (Farquhar et al., 1991; LaMantia et al., 1991; Scherens et al., 1991). Its predominant function in the cell is still debated. One report has shown that PDI's isomerization function is indispensable, in that the lethal PDI deletion phenotype can be rescued with a CGHS variant of the protein (a shufflease only), but not with a SGHC variant (Laboissiere et al., 1995). Another study demonstrates the importance of PDI's oxidative power *in vivo* by showing marked growth defects in a PDI deletion strain expressing CGHS variants (Holst et al., 1997). These defects can be alleviated upon overexpression of a CXXC variant of the PDI homologue Eug1, which normally harbours a CXXS motif (Holst et al., 1997). On investigation of the redox state of PDI intracellularly, it is found predominantly reduced in mammalian cells (Mezghrani et al., 2001) and mostly oxidized in yeast (Frand and Kaiser, 1999; Tu et al., 2000). This difference might be explained by different cellular conditions, since the redox state of PDI is bound to depend on the load of folding proteins and the activity of its own oxidase, Ero1. *In vitro* data so far do not clearly suggest different functions of the PDI **a** and **a'** domain (Darby and Creighton, 1995b). *In vivo*, carboxypeptidase Y folding is catalyzed by a PDI variant with only the **a** domain in an active form as proficiently as by wild-type PDI, and much slower than wild-type levels by a solely **a'** domain-active version of PDI. That PDI actively and directly promotes the formation of correct disulfides in substrate proteins was shown by the presence of transient mixed disulfide bridges between folding glycoproteins and PDI (Molinari and Helenius, 1999).

PDI has also been implied to function in protein retro-translocation from the ER to the cytosol on the route to degradation. Yeast cells that contained a PDI mutant lacking parts of the peptide-binding **b'** domain showed a defect in the degradation of carboxypeptidase Y and pro-α-factor. Moreover, when retro-translocation was blocked in *sec61* mutants, a high proportion of misfolded pro-α-factor was bound to PDI (Gillece et al., 1999). This substrate lacks cysteine residues, thus suggesting PDI to function not as a thiol-disulfide oxidoreductase, but rather as a linker between the protein to be degraded and the retro-translocation machinery. Other studies have indirectly implied a role for PDI or other oxidoreductases in the reduction of substrate disulfide bridges before their retro-translocation. Ig-μ chains have to be reduced before they are dislocated from the ER to the cytosol (Fagioli et al., 2001) and disruption of the redox environment in the ER inhibits dislocation of T cell receptor α

chain (Tortorella et al., 1998). More direct evidence that PDI acts to reduce and unfold proteins before retrograde transport comes from studies on cholera toxin (Tsai and Rapoport, 2002; Tsai et al., 2001). PDI acts to disassemble and unfold the A1 chain of the toxin in a redox dependent manner, binding to the A chain in its reduced state and releasing the toxin chain in its oxidized state (Tsai et al., 2001). PDI transfers the unfolded A1 chain to the lumenal side of the ER membrane, where Ero1α was shown to oxidize the C-terminal disulfide bond in PDI thereby mediating release of the toxin chain (Tsai and Rapoport, 2002). This lead to the proposition that PDI can act as a redox-dependent chaperone, an idea which has been challenged. Here, PDI was shown to be able to bind to the C-propeptide of procollagen in both its reduced and oxidized state. Moreover, PDI could be induced to dissociate from the α subunit of prolyl 4-hydroxylase (P4H) with equal amounts of GSSG and mastoparan, a non-thiol containing peptide that can bind to PDI (Lumb and Bulleid, 2002).

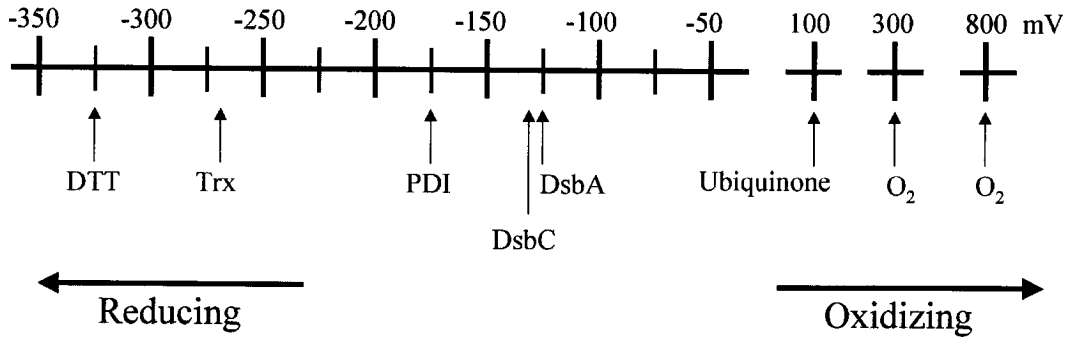

Fig. 1.8 Measured redox potentials of various thiol-disulfide oxidoreductases and small redox molecules. The redox potential is shown in mV from more reducing to more oxidizing potential. The determined values are from (Sevier and Kaiser, 2002) and references therein.

1.5.2 ERp57

ERp57, a member of the thioredoxin enzyme superfamily (Ferrari and Söling, 1999), is the closest known homologue of PDI. Based on sequence similarity with PDI, ERp57 is likely comprised of two thiol-disulfide oxidoreductase active domains denoted **a** and **a'**, as well as two redox inactive domains named **b** and **b'**. The domains are arranged in the order **a-b-b'-a'**. ERp57 lacks PDI's most C-terminal acidic, calcium binding **c** domain. Instead, the c-terminal QDEL endoplasmic reticulum (ER) retrieval signal directly follows the **a'** domain, which even terminates with an unusual amount of basic amino acids. The overall identity to PDI at the amino

acid level is 33% (Ferrari and Söling, 1999). To date, there is no structural information on ERp57 or domains thereof. Nevertheless, it can be assumed that all four domains of ERp57 are of the thioredoxin fold, since the NMR structures of the PDI **a** and **b** domains exhibit this fold (Kemmink et al., 1996; Kemmink et al., 1999).

ERp57 was originally identified as a phospholipase (Bennett et al., 1988), a finding that was later negated (Srivastava et al., 1991; Srivastava et al., 1993). The notion that ERp57 is a protease (Urade et al., 1997) has also been challenged (Bourdi et al., 1995). That ERp57 is a member of the family of protein thiol-disulfide oxidoreductases remains unchallenged (Ferrari and Söling, 1999). It seems clear that ERp57 has reductase and isomerase activity (Bonfils, 1998; Hirano et al., 1995), while its ability to act as an oxidase is uncertain (Blasko et al., 2003; Bonfils, 1998). Recently, the ERp57 *C. elegans* homologue PDI-3 has been found to possess transglutaminase activity (Blasko et al., 2003; Eschenlauer and Page, 2003).

ERp57 functions in the calnexin/calreticulin quality control system in the ER. By associating with calnexin and calreticulin (Oliver et al., 1999; Oliver et al., 1997), ERp57 interacts with folding glycoproteins (see also section 1.4.2). Transient disulfide-linked intermediates between ERp57 and its substrate glycoproteins have been observed *in vivo* (Molinari et al., 2002).

The predominant redox function ERp57 performs in the cell is not clear. In mammalian cells, ERp57 has been observed to be mostly in the reduced state (Mezghrani et al., 2001). This would imply the predominant function of ERp57 to be that of a reductase or isomerase. Ero1, the oxidase of PDI, could not be found in mixed disulfides with ERp57, neither did its overexpression affect the redox state of ERp57 (Mezghrani et al., 2001). This does not, however, rule out the existence of a yet unidentified oxidase for ERp57.

Recently, ERp57 has been shown to be able to reduce partially folded MHC class I heavy chains *in vitro* (Antoniou et al., 2002). When degradation of heavy chains was prevented with a proteasome inhibitor in a mammalian semipermeabilized cell system, ERp57 was found in prolonged association with the heavy chains (Wilson et al., 2000). These findings suggest ERp57 to be able to act as a reductase for proteins destined for retrotranslocation.

1.5.3 Other thioredoxin-like proteins

Other ER thioredoxin domain-containing proteins have been identified in higher eukaryotes (Table 1.1). Whether these proteins serve different redox pathways and/or have different substrate specificity is at present not clear.

Protein	Size (kDa)	Thioredoxin -like domains	Acitve-site number and sequences	ER localization motif	Notes	References
Mammalian homologues						
PDI	55	4	2, CGHC	KDEL	forms mixed disulfides with Ero1	(Pihlajaniemi et al., 1987)
ERp57	54	4	2, CGHC	QEDL	associates with CNX/CRT	(Bennett et al., 1988), (Hirano et al., 1995)
ERp44	44	1	1, C§RFS	RDEL	potential retention factor for Ero1, mixed disulfide observed	(Anelli et al., 2003; Anelli et al., 2002)
ERp46/ EndoPDI	44	3	3, CGHC	KDEL	preferentially expressed in endothelial cells	(Sullivan et al., 2003), (Knoblach et al., 2003)
ERp72	71	5	3, CGHC	KEEL		(Mazzarella et al., 1990)
P5	46	3	2, CGHC	KDEL		(Hayano and Kikuchi, 1995a)
PDIp	56	4	2, CGHC CTHC	KEEL	pancreas-specific expression	(Desilva et al., 1996)
PDIr	57	4	3, CSMC CGHC CPHC	KEEL		(Hayano and Kikuchi, 1995b)
TMX	32	1	1, CPAC	none	transmembrane region	(Matsuo et al., 2001)
TMX2	37	1	1, SNDC	KKEIS	transmembrane region	(Meng et al., 2003)
ERp28	26	1	none	KEEL		(Ferrari et al., 1998)
ERdj5	87	4	4, CSHC CPPC CHPC CGPC	KDEL		(Cunnea et al., 2003)
calsequestrin	42	3	none	none		(Fujii et al., 1990)
ERp19/ ERp18	16	1	1, CGAC	EDEL		(Clark et al., 2003)
Quiescin/sulfhydryl oxidases (QSOX)	50-80	2	1, CGHC	none	contain one ERV/ALR domain with a CXXC and an additional CXXS and CXXC	(Thorpe et al., 2002), (Raje and Thorpe, 2003)

S. cerevisiae homologues						
PDi1	55	2	2, CGHC	HDEL	forms mixed disulfides with Ero1	(Pihlajaniemi et al., 1987)
Eps1	78	1	1, CPHC	KKQD	contains an additional CDKC motif, plus a partial Trx-like domain, and a C-terminal transmembrane region	(Wang and Chang, 1999)
Eug1	56	2	2, CLHS CIHS	HDEL		(Tachibana and Stevens, 1992)
Mpd1	34	1	1, CGHC	HDEL		(Tachikawa et al., 1995)
Mpd2	30	1	1, CQHC	HDEL	forms mixed disulfides with Ero1	(Tachikawa et al., 1997)

Table 1.1 Known eukaryotic thioredoxin-like proteins of the ER.

2 Results

2.1 ERp57 interacts with the calreticulin P-domain (paper I)

2.1.1 Biochemical evidence

In a cross-linking experiment, purified recombinant ERp57 and CRT(189-288) were mixed and treated with the cross-linker disuccinimidyl glutarate (DSG). Fig. 2.1a shows, that in mixtures of CRT(189–288) and ERp57 a band appeared at an approximate molecular weight of 75 kDa. Since the free 12 kDa CRT(189–288) migrates as a protein of approximately 18 kDa, the mobility of this band is compatible with a 1:1 complex of CRT(189–288) and the 54.5 kDa ERp57.

In ELISA experiments, ERp57 showed efficient binding to CRT(189–288), whereas three control proteins (BSA, calmodulin and ubiquitin) did not show appreciable binding. Furthermore, it is noteworthy that PDI, which is the closest known homologue of ERp57, did not interact with CRT(189–288), (Fig. 2.1b). The specific association of the calreticulin P-domain with ERp57 is consistent with *in vivo* (Oliver et al., 1999) and *in vitro* (Zapun et al., 1998) data that demonstrated the presence of functional complexes between CNX or CRT and ERp57, but not between CNX or CRT and PDI.

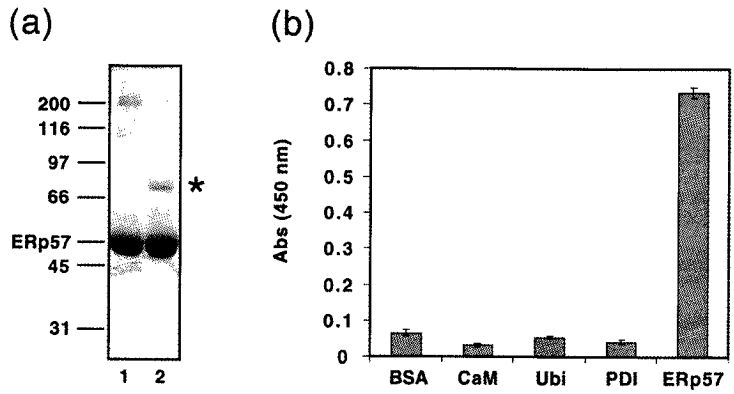

Fig. 2.1 (a) Chemical cross-linking of CRT(189–288) and ERp57. The homobifunctional cross-linker DSG was added to solutions of CRT(189–288) alone (data not shown), ERp57 alone (lane 1) or an equimolar mixture of the two proteins (lane2). After incubation for 30 min on ice, the reaction was quenched with an excess of glycine. Potential protein complexes were analyzed by 12% reducing SDS-PAGE, and the gel was stained with Coomassie blue. Molecular weight standards given in kDa are indicated on the left, along with the position of ERp57. The suggested position of the CRT(189–288)/ERp57 complex (asterisk) is indicated on the right. (b) The interaction of CRT(189–288) and ERp57 studied by ELISA. Potential ligands for CRT(189–288) were coated in microtiter wells and the interaction was probed with biotinylated CRT(189–288), followed by the binding of a primary antibody directed against biotin and a HRP-conjugated secondary antibody.

Development by the addition of BM Blue POD Substrate gives rise to a signal at 450 nm for positive enzymatic reactions. BSA, calmodulin (CaM) and ubiquitin (Ubi) were used as control proteins. The data presented in the graph are mean values of triplicates. The experiment was repeated three times with closely similar results. Standard deviations are given by the vertical bars. Non-specific binding of primary and secondary antibodies to wells coated with protein ligand in the absence of biotinylated CRT(189–288) was subtracted for each well.

2.1.2 *Mapping of the site of interaction of ERp57 on CRT(189-288) by TROSY-NMR*

The NMR structure and the complete sequence-specific NMR assignments of CRT(189–288), (Ellgaard et al., 2001a; Ellgaard et al., 2001b), provided a basis for structural studies of the interactions between CRT(189–288) and ERp57. Since the CRT(189–288)/ERp57 complex was reconstituted *in vitro* from the isolated components, uniform isotope labeling of CRT(189–288) with ^{15}N and ^{2}H enabled selective observation of the ^{15}N–^{1}H fingerprint of this protein in the 66.5 kDa complex with the use of [^{15}N,^{1}H]-TROSY (Pervushin et al., 1997). All NMR analysis was conducted in collaboration with Roland Riek in the group of Kurt Wüthrich, ETH Zürich.

From the amino acid sequence of CRT(189–288) one expects a "fingerprint" containing backbone ^{15}N–^{1}H peaks of 84 residues, of which 81 have previously been assigned in the free protein (Ellgaard et al., 2001a). Under the conditions of the present experiments, the ^{15}N–^{1}H fingerprint of free CRT(189–288) contains 80 of these cross peaks (Fig. 2.2a). With the TROSY experimental scheme used here, the ^{15}N–^{1}H cross peaks of the Gln and Asn side chains, which would appear in the spectral region 112–115 ppm along w_1(^{15}N) and 6.7– 8.7 ppm along w_2(^{1}H), are nearly completely suppressed (Pervushin et al., 2000). In the fingerprint of ^{15}N,^{2}H-labeled CRT(189–288) in a solution containing a 2.7-fold excess of unlabeled ERp57 (Fig. 2.2b), 72 backbone ^{15}N–^{1}H cross peaks and 5 Trp indole peaks could be identified.

Superposition of the [^{15}N,^{1}H]-TROSY spectra of free CRT(189–288) and the CRT(189–288)/ERp57 complex revealed that a large number of peaks in the complex superimposed exactly with peaks in free CRT(189–288). However, Fig. 2.2 also shows that the relative intensities as well as the peak positions of numerous corresponding, well-resolved peaks in free and complexed CRT(189–288) were significantly different. We thus found that for the backbone ^{15}N–^{1}H-moieties of D237,

E238, M240, G242, E245, V248, I249 and N251, and the indole ^{15}N–^{1}H of Trp236 no peaks were observed in the complex, and that for the residues I225, D227, D229, K231, W236, E243 and W244 the peak intensities in the complex were weaker than 3% of the intensities in free CRT(189–288), (Fig. 2.2a and b). In addition, the 6 backbone amide cross peaks of A230, K232, E234, D235, E239, and D241 exhibited chemical shift changes relative to free CRT(189–288) of 0.2 to 1.0 ppm along the ^{15}N dimension, and 0.0 to 0.5 ppm along the ^{1}H dimension in the complex 1:2.7 (Fig. 2.2b). A systematic evaluation of the signal intensities by measurement of the peak heights in the two spectra yielded the data shown in Fig. 2.2c. Whereas the residues near both chain ends of CRT(189–288) had similar intensities in the free and bound protein, there was a continuous loss of peak intensity from the chain ends toward the center of the polypeptide chain. All the 21 residues mentioned above with either a sizeable chemical shift change, complete absence of a cross peak, or very weak cross peak intensity in the bound form are located in the contiguous structural region of residues 225–251, indicating that the ERp57-binding site on CRT(189–288) is at the tip of the hairpin structure of this protein, as illustrated in Fig. 2.3.

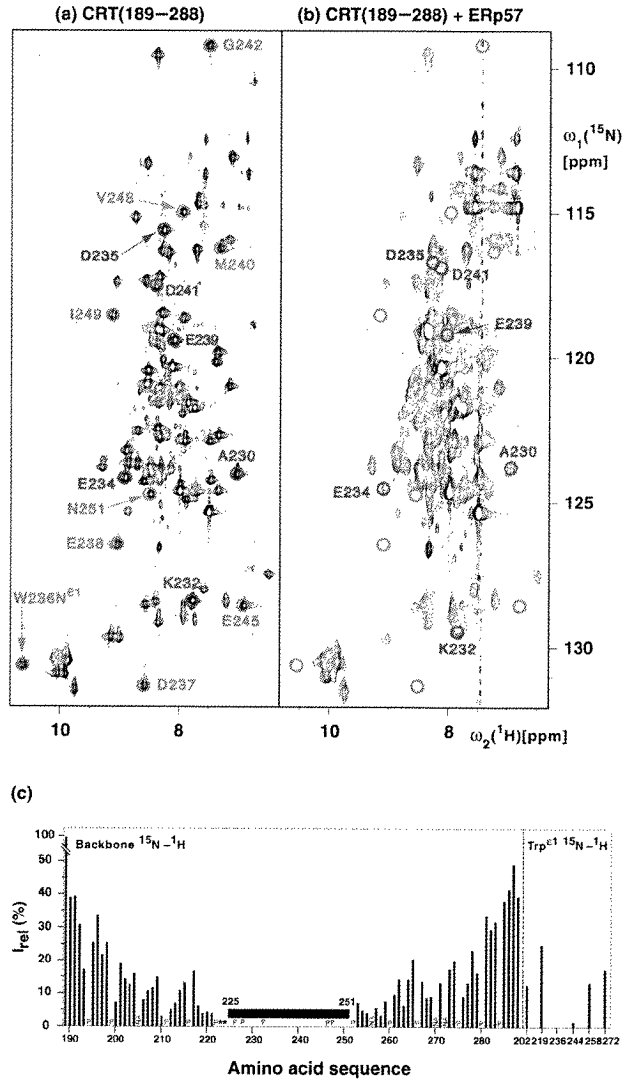

Fig. 2.2 (a) and (b) ^{15}N–^1H correlation NMR spectra used to delineate the surface areas of CRT(189–288) that interact with ERp57. These spectra contain peaks corresponding to backbone amide ^{15}N–^1H groups and, in the lower left, indole ^{15}N–^1H groups of tryptophyl residues. Color-coded peaks indicate outstandingly large effects from ERp57 interactions: Blue circles identify cross peaks with chemical shift differences of more than 0.2 ppm along the ^{15}N dimension between free and ERp57-bound CRT(189–288). Red circles identify cross peak positions in free CRT(189–288) for which no counterpart could be observed in the spectrum of the complex. The color-coded cross peaks are labeled with the sequence-specific resonance assignments. (a) [^{15}N,^1H]-TROSY spectrum of free ^{15}N,^2H-labeled CRT(189–288), (protein concentration = 0.4 mM, polarization transfer time = 5.4 ms, data size 200 × 1024 complex points, zero-filling to 512 × 2048 points, $t_{1,max}$ = 88 ms, $t_{2,max}$ = 98 ms, total measuring time 2 hours). (b) [^{15}N,^1H]-TROSY spectrum of a solution of ^{15}N,^2H-labeled CRT(189–288) and unlabeled ERp57 (protein concentrations of 0.14 mM for ^{15}N,^2H-labeled CRT(189–288) and 0.38 mM for ERp57, polarization transfer time = 3.4 ms, data size 100 × 1024 complex points, zero-filling to 512 × 2048 points, $t_{1,max}$ = 44 ms, $t_{2,max}$ = 98 ms, total measuring time 24 hours). (c) Plot of the relative peak intensities, I_{rel}, of the [^{15}N,^1H]-TROSY cross peaks in the CRT(189–288)/ERp57 complex and free CRT(189–288) versus the amino acid sequence of CRT(189–288). The Trp indole cross peaks are listed separately on the right. The black horizontal bar spanning the polypeptide segment 225–251 indicates that for these residues the cross peaks in the complex have either large chemical shift differences (> 0.2 ppm along the ^{15}N dimension) or very small signal intensities (< 3% of the intensity in free CRT(189–288)), (see text). "P" designates proline residues, "NA" stands for residues for which no resonances could be assigned, and "*" indicates residues for which no reliable data could be measured due to spectral overlap.

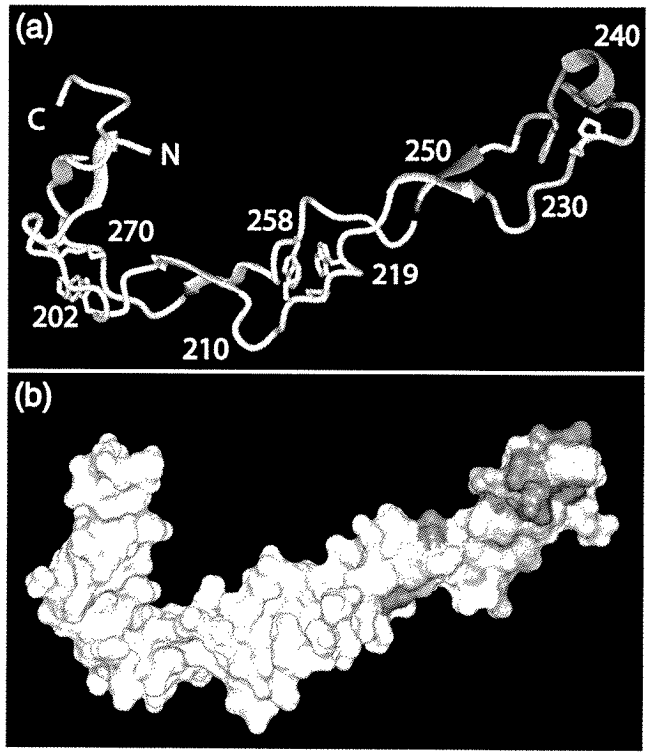

Fig. 2.3 Visual display of the molecular regions of CRT(189–288) that are in direct contact with ERp57. (a) Ribbon representation. (b) Space-filling model displaying the molecular surface of the NMR structure. The residues for which the ^{15}N–^{1}H-moieties show chemical shift changes due to interactions with ERp57 in excess of 0.2 ppm along the ^{15}N dimension are colored blue, those for which no cross peak is observed in the [^{15}N,^{1}H]-TROSY spectrum of the complex are red, and those for which the peak intensity relative to free CRT(189–288) is weaker than 3% are orange. In (a) the positions of selected residues are indicated.

2.1.3 Characterization of thermodynamics and kinetics of the CRT(189-288)/ERp57 interaction

The 1:2.7 CRT(189–288)/ERp57 solution of Fig. 2b was titrated by stepwise addition of unlabeled CRT(189–288), as detailed in Paper I (Table 1). In Fig. 2.4, a - d the change in chemical shift and peak intensity upon titration is shown for four selected residues. When following the chemical shift changes at different titration points we found that for the residues E238, I249 and N251, which showed no peak intensity in the 1:2.7 CRT(189–288)/ERp57 solution, weak cross peaks could be observed in [^{15}N,^{1}H]-TROSY spectra measured at excess molar ratios of CRT(189–288). Specifically, at CRT(189–288):ERp57 molar ratios of 3:1, 2.4:1 and 1.8:1, these cross peaks displayed sizeable chemical shift changes when compared to free CRT(189–288), as illustrated for I249 (Fig. 2.4*c*).

The continuous chemical shift changes (Fig. 2.4, a - d) demonstrated that the exchange rate between bound and free CRT(189–288) was fast on the chemical shift

time scale, with an estimated lower limit for the first order exchange rate constant of $k_{off} > 1000\ s^{-1}$ at 20°C. Using the data for residue K232 (Fig. 2.4b), a fit of the dependence of the chemical shifts on the ERp57:CRT(189–288) molar ratio as described in the caption to Fig. 2.4e yielded a dissociation constant of $K_d = (18\pm5) \times 10^{-6}$ M for the complex of CRT(189–288) and ERp57 (Fig. 2.4e).

In an effort to obtain the K_d of the interaction between CRT(189-288) and ERp57 by a second method, isothermal titration microcalorimetry (ITC) was performed in collaboration with Ilian Jelesarov at the University of Zürich. At 8°C, ITC detected a measurable heat effect upon mixing of the two proteins, which reached saturation with increasing molar ratio of CRT(189–288) to ERp57. The resulting titration curve followed the shape of a typical binding isotherm (Fig. 2.5) with 1:1 stoichiometry. The best fit of the data was obtained with a dissociation constant of $(9.1\pm3.0) \times 10^{-6}$ M.

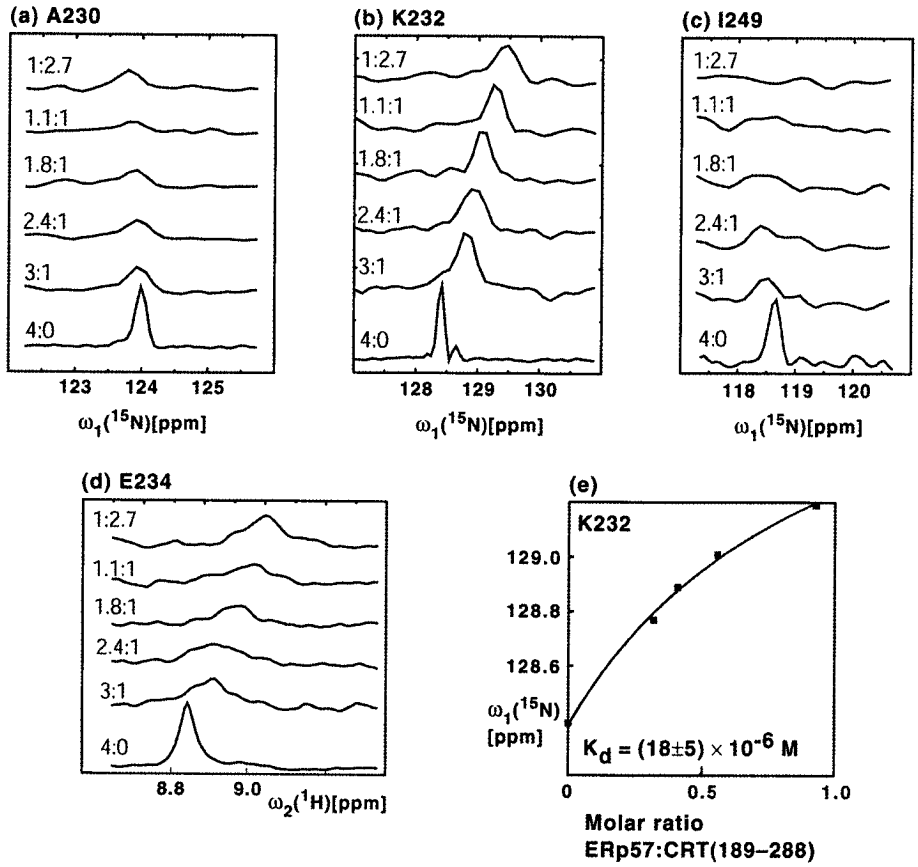

Fig. 2.4 Titration of the $^{15}N,^{2}H$-labeled CRT(189–288)/ERp57 complex with unlabeled CRT(189–288). (a) – (c), Cross sections from [$^{15}N,^{1}H$]-TROSY spectra along the $\omega_1(^{15}N)$ dimension for the residues A230, K232, and I249 of $^{15}N,^{2}H$-labeled CRT(189–288). The numbers on the left of each trace refer to the solution conditions given in Table 1. (d) Cross sections from [$^{15}N,^{1}H$]-TROSY spectra along $\omega_2(^{1}H)$ for residue E234. (e) K_d determination based on the titration data for residue K232. The squares

represent the experimental ^{15}N chemical shifts of K232 at discrete values of the ERp57:CRT(189–288) molar ratio (Table 1). The curve visualizes the fit from which the ^{15}N chemical shift of the CRT(189–288)/ERp57 complex ($\delta(^{15}N_{complex})$) was determined, using the relation $\delta(^{15}N) = \delta(^{15}N_{free}) + (\delta(^{15}N_{complex}) - \delta(^{15}N_{free}))$ ([ERp57]/[CRT(189–288)])/(([ERp57]/[CRT(189–288)]) + K_{ratio}) where δ is the chemical shift, K_{ratio} the K_d expressed as molar ratio, and the brackets indicate molar concentrations of the respective compounds. Subsequently, the K_d value was calculated at each experimental point using the relation K_d = [CRT(189–288)][ERp57]/[CRT(189–288)/ERp57], yielding an average value of $K_d = (18\pm5) \times 10^{-6}$ M.

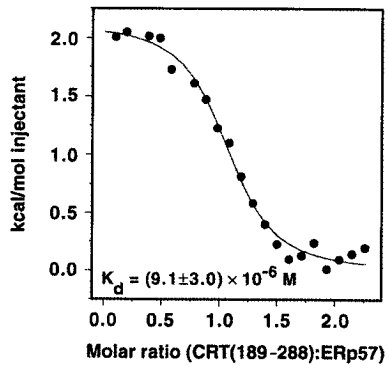

Fig. 2.5 Binding isotherm describing the formation of the CRT(189–288)/ERp57 complex followed by ITC at 8°C. Filled circles represent the integrated heats at each injection after correction for non-specific heat effects and normalization for the molar concentration. The continuous line visualizes a least-squares non-linear fit of the data according to a 1:1 binding model defined by the following parameters: n = 1.04±0.03, $K_d = (9.1\pm3.0) \times 10^{-6}$ M ($K_a = (1.1\pm0.3) \times 10^5$ M^{-1}), and $\Delta H = 2.1\pm0.1$ kcal mol^{-1}.

2.1.4 Molecular mapping of the interaction site for ERp57 on CRT(189-288)

The results shown in the following three sections were generated by Micha Häuptle during the course of his diploma thesis performed under my supervision.

Yeast calnexin Cne1p does not bind to ERp57

In comparing calreticulin and calnexin sequences from different species (Fig. 2.6), one can detect a number of acidic amino acids that are conserved in the region that forms the tip of the hairpin in the structure of canine calnexin and rat calreticulin. The yeast protein Cne1p, which is the calnexin homologue (Parlati et al., 1995), exhibits a noticably changed amino acid sequence in this region (Fig. 2.6). Since yeast does not have an ERp57 homologue, it is tempting to speculate that the tip of the P-domain in Cne1p has retained its hairpin structure, but has not evolved an ERp57 binding site.

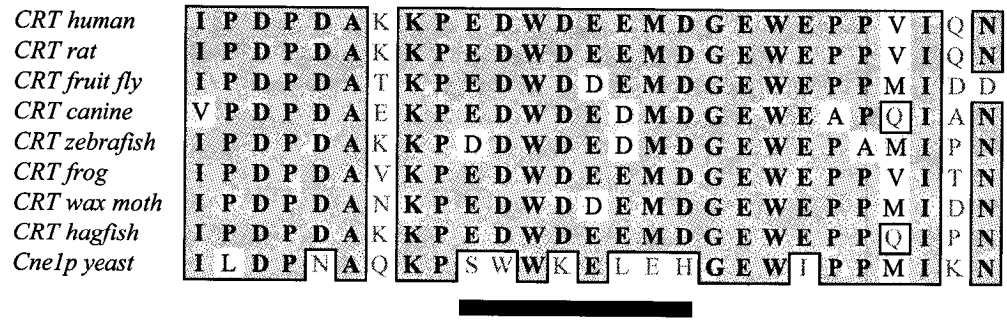

Fig. 2.6 Alignment of CRT and CNX sequences from different species in the region 225-251 of CRT. All amino acid residues are abbreviated in the single letter code. Identical residues are shown with dark gray shading, similar residues with light gray shading. Mismatching amino acids are grey. The tip of the P-domain hairpin structure is indicated by the black bar.

A fragment comprising amino acids 299-331 of Cne1p (Cne1p33), which encompasses 33 residues of the tip of the P-domain of Cne1p (generated by Christiane Schirra and Lars Ellgaard, unpublished) was expressed in *E.coli* as a ubiquitin fusion protein and purified as described for CRT36 (Ellgaard et al., 2002). CRT36 includes the terminal 12 repeat of the CRT P-domain plus a few additional residues on either side. Cne1p33 contains all residues of the sequence shown in Fig. 2.6, with 10 additional residues at the N-terminus and 9 at the C-terminus.

A possible interaction between Cne1p33 and ERp57 was probed by ITC as described in (Frickel et al., 2002). No binding to ERp57 could be detected (Fig. 2.7).

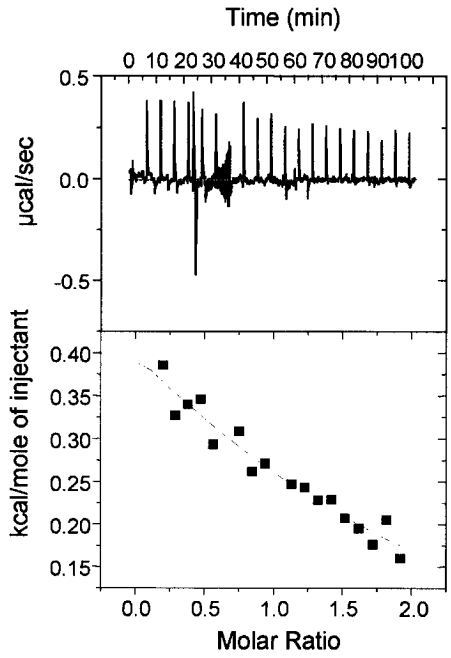

Fig 2.7 Binding isotherm for Cne1p33 and ERp57 followed by ITC at 8°C. Filled squares represent the integrated heats at each injection after correction for non-specific heat effects and normalization for the molar concentration. No binding of Cne1p33 to ERp57 could be detected.

Construction and characterization of a CRT P-domain mutant that lacks ERp57 binding

Five acidic amino acids in the tip region of CRT(189-288) were changed into the corresponding residues of Cne1p by overlap extension (Fig. 2.8), (see Appendix). This created the potential ERp57 binding deficient mutant CRTΔEB that was expressed in *E.coli* and purified essentially like CRT(189-288), (Ellgaard et al., 2001a), with the exception that it was retrieved as a soluble protein after lysis of the cells by french pressing.

Cne1p32(299-331)	Q	K	P	S	W	W	K	**E**	L	**E**	H	G	**E**	W
CRT(189-288)	K	K	P	**E**	**D**	W	**D**	**E**	**E**	M	**D**	G	**E**	W
CRT(189-288)ΔEB	K	K	P	S	W	W	K	**E**	L	M	H	G	**E**	W

Fig. 2.8 Alignment of Cne1p32, CRT(188-289) and CRT(189-288)ΔEB in the region 231-244 of CRT. Shown in bold are the negatively charged amino acids, underlined the mutated residues to eliminate the potential ERp57 binding site.

A possible interaction between CRTΔEB and ERp57 was probed by cross-linking, ELISA and ITC as described before (Frickel et al., 2002). All three methods showed that there was no detectable binding of CRTΔEB to ERp57.

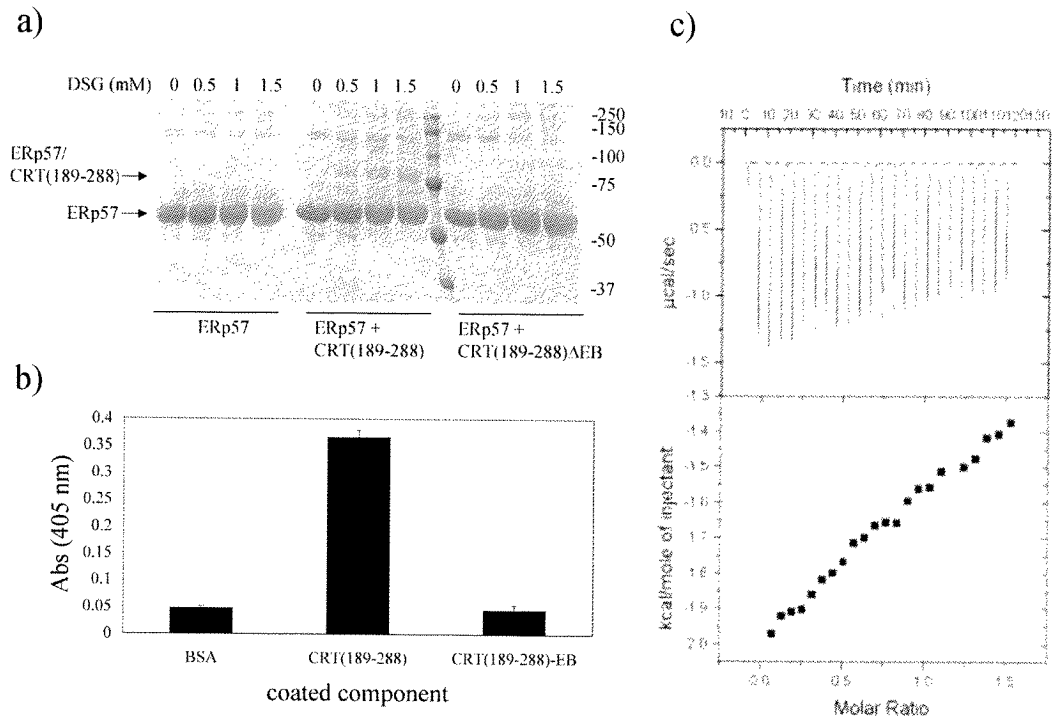

Fig. 2.9 Interaction studies between CRT(189-288)ΔEB and ERp57. (a) Chemical cross-linking visualized on a 15% SDS-PAGE gel. 5 μM ERp57 alone (lanes 1-4), with 5 μM CRT(189-288), (lanes 5-8) or with 5 μM CRT(189-288)ΔEB (lanes 9-12) were incubated with increasing amounts of DSG (lanes 1, 5 and 9 without, lanes 2, 6 and 10 with 0.5 mM, lanes 3, 7 and 11 with 1 mM and lanes 4, 8 and 12 with 1.5 mM DSG). The band suggested to be the 1:1 complex between ERp57 and CRT(189-288) is indicated by an arrow and labelled. No similar complex could be detected in the case of CRT(189-288)ΔEB with ERp57. (b) ELISA study of the interaction. CRT(189-288)ΔEB, CRT(189-288) and BSA as a negative control were coated in microtiter wells, and the interaction was probed with 2.5 μM biotinylated ERp57. The assay was developed for 30 min with alkaline phosphatase yellow after incubation with NeutrAvidin coupled alkaline phosphatase for 1 hour at room temperature. (c) Binding isotherm for CRT(189-288)ΔEB and ERp57 followed by ITC at 8°C. Filled squares represent the integrated heats at each injection after correction for non-specific heat effects and normalization for the molar concentration. No binding of CRT(189-288)ΔEB to ERp57 could be detected.

2.2. ERp57 is a glycoprotein-specific protein disulfide isomerase (paper II)

2.2.1 Experimental determination of the domain boundaries in ERp57

As a first characterization of recombinantly expressed full-length ERp57, we subjected the protein to limited proteolysis. This experimental approach not only gives information about domain boundaries, but also about the relative stability of individual domains towards proteolysis.

For proteolysis of ERp57 at pH 7.0 and 37°C, we used trypsin, chymotrypsin, elastase and thermolysin. Each digestion mixture was resolved by SDS-PAGE (Fig. 2.10), transferred onto a PVDF membrane, and single bands were excised and N-terminally sequenced. Table I in paper II lists the N-terminal sequence obtained for each of the fragments corresponding to the bands indicated in Figure 2.10. Figure 2.11 shows the sequence positions of the ERp57 fragments obtained by partial digestion, as well as the experimentally determined domain structure of PDI.

Cuts were generated at the expected domain boundaries between **b** and **b'**, and between **b'** and **a'** - inferred from a sequence alignment with PDI. All four proteases generated cuts in the sequence region 211-222 between the **b** and **b'** domains (fragments 1, 4, 11 and 16), while trypsin and chymotrypsin cleaved at residues 340 and 341 in a region predicted to connect the **b'** and **a'** domains (fragments 2 and 5). Based on the sequence alignment with PDI and the proposed linker region in PDI deduced from the NMR structures of the PDI **a** and **b** domains (Kemmink et al., 1999), we expected the linker between these two domains in ERp57 to comprise only residues 109-111. The short length of this linker likely explains why no cleavage occured exactly within this region. The closest cut was the one produced by elastase at residue 134 (fragment 7).

The mobility of the proteolytic fragments visible on gels combined with the 12-15 kDa size for a single thioredoxin-like domain, enabled us to predict which single, double and triple domains were present in the different digestion mixtures. The only single domains detected were the **a** (fragments 3, 6, 12, 13, 17 and 18) and **a'** domains (fragments 2 and 5). The only double and triple domains observed were **b'a'** (fragments 1,4 and 16) and **bb'a'** (fragment 7), respectively. However, the **b** domain was rapidly degraded from the N-terminus of this triple domain at higher

concentrations of protease and longer incubation times (Fig. 2.10b, fragments 7-10). At lower concentrations of protease or shorter incubation, **a'** was observed together with **b'** (fragments 1, 4, 11 and 16), indicating that the presence of the **a'** domain stabilized the **b'** domain to a certain extent. Overall, of the four domains, the **a** and **a'** domains appeared to be the most and the **b** domain the least resistant to proteolysis. The **b'** domain could not withstand extended proteolytic cleavage.

For the following experiments performed in this thesis, I used ERp57 **a** and **a'** domain constructs comprising residues 1-112 and 353-473, respectively. For the **a** domain construct the position of the C-terminal boundary was based on a sequence alignment with the PDI **a** domain. The slight C-terminal truncation of the **a'** domain construct was performed to remove the 'QDEL' ER retrieval sequence and a few preceding residues that are likely to constitute a flexible tail. The notion that segment 353-473 corresponds to a properly folded domain is supported by the NMR assignments reported for an **a'** construct comprising residues 349-468 (Silvennoinen et al., 2004). Furthermore, spectroscopic analysis of the **a** and **a'** constructs showed that both display typical features of properly folded proteins (see paper II).

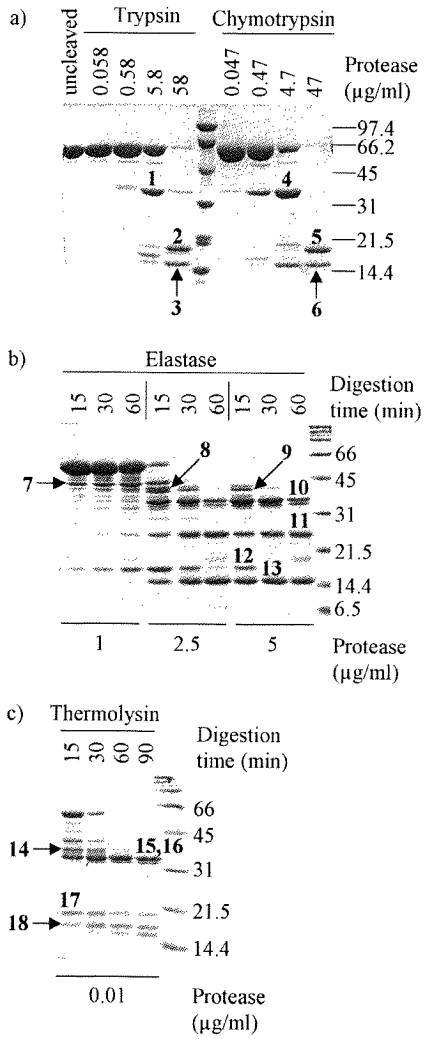

Fig. 2.10 (a)-(c) Limited proteolysis of ERp57. ERp57 (20 µM) was digested at 37°C and pH 7.0 with the indicated concentrations of protease and samples were collected at various time points. The digests were stopped with PMSF or EDTA, and digest mixtures were separated on 15% SDS-PAGE gels and stained with Coomassie Blue.

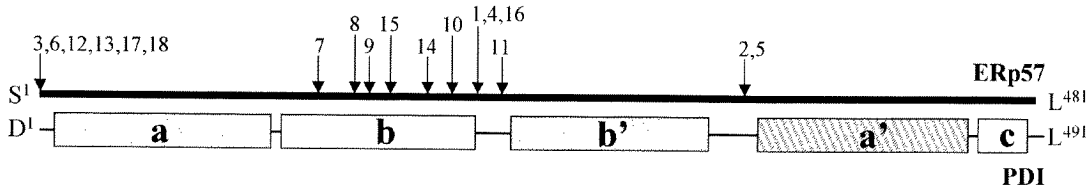

Fig. 2.11 Schematic representation of ERp57 fragments obtained by limited proteolysis. The upper line represents ERp57 and the boxes below depict the experimentally determined domain boundaries in PDI (Darby et al., 1996; Darby et al., 1999; Ferrari and Söling, 1999; Freedman et al., 1998). The arrows pointing to sequence positions within ERp57 indicate the location of the proteolytic fragments. The numbers refer to the bands on the SDS-PAGE gels in Fig. 2.8 for which the experimentally determined N-terminal sequences are listed in paper II, Table 1.

*2.2.2 Determination of the redox potential of the ERp57 **a** and **a'** domain*

As a first means to characterize the redox activity of ERp57, I determined the standard redox potentials for the redox active **a** and **a'** domains. While the redox potential for a given oxidoreductase does not necessarily reveal the redox function of the protein in the living cell, it often provides valuable information about the preferred redox reaction.

Using fluorescence spectroscopy the redox equilibrium of the ERp57 **a** and **a'** domains was analyzed at different GSH/GSSG ratios. The increase in fluorescence emission at 350 nm upon reduction was followed after excitation at 280 nm (Fig. 2.12a and b). Thus, when ERp57 **a** and **a'** were incubated in the presence of 0.1 mM GSSG and varying concentrations of GSH (0.03 - 11 mM) under the exclusion of oxygen, the relative amounts of oxidized and reduced protein at equilibrium could be determined from a fit of the experimental data to equation (1), (see paper II, Materials and Methods), (Fig. 2.13a and b). By this method, the equilibrium constant, K_{eq}, for the ERp57 **a** / glutathione system was found to be 3.3 ± 0.4 mM and 1.5 ± 0.1 mM for the ERp57 **a'** / glutathione system. The standard redox potentials for the ERp57 **a** and **a'** domains were calculated from the Nernst equation using the glutathione standard potential of -0.240 V at pH 7.0 and 25°C (Williams, 1992) and equation (2) in paper II (see Materials and Methods). Like this, the standard redox potential for ERp57 **a** was determined to be -0.167 V and that for ERp57 **a'** to be -0.156 V. These values are comparable to the redox potential of -0.175 V determined for PDI (Lundstrom and Holmgren, 1993).

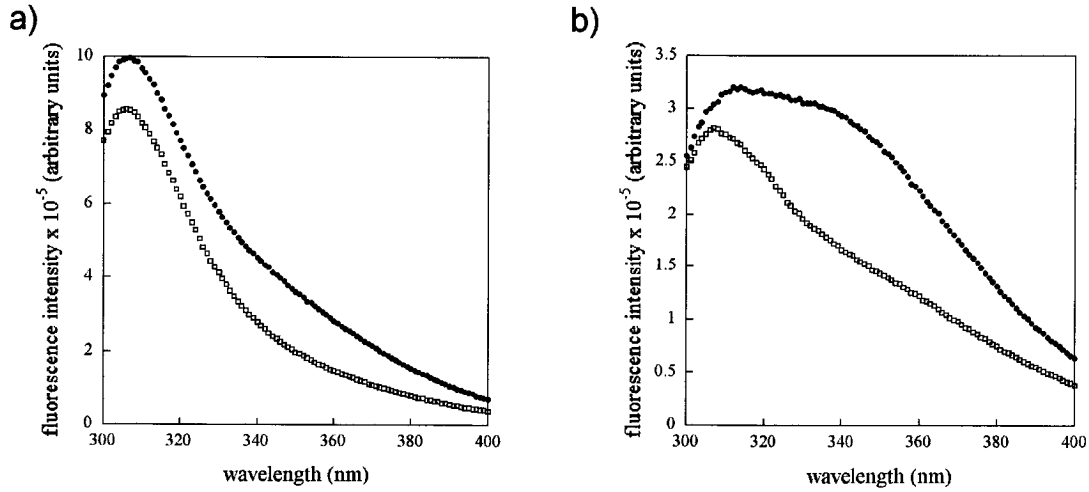

Fig. 2.12 (a) and (b) Spectral analysis of ERp57 at pH 7.0 and 25°C. Fluorescence emission spectra of oxidized and reduced ERp57 a domain (a) and ERp57 a' domain (b) were recorded after excitation at 280 nm. Oxidized domains contained 0.1 mM GSSG (open symbols) and reduced domains 10 mM GSH (closed symbols).

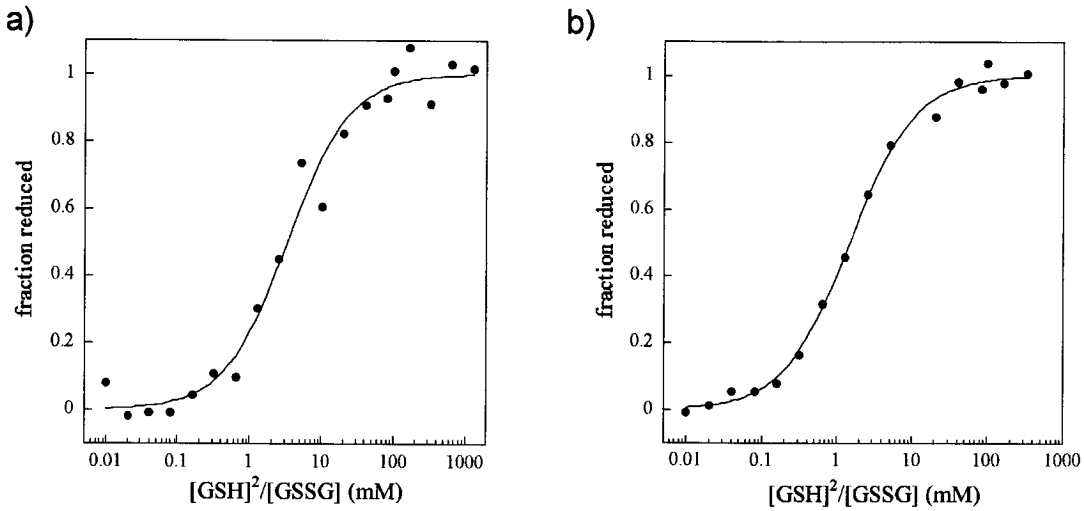

Fig. 2.13 Redox equilibrium of ERp57 a and a' domains with glutathione. The fraction of reduced ERp57 a domain (a) and ERp57 a' domain (b) at pH 7.0 and 25°C was determined by fluorescence spectroscopy after incubation of the proteins for at least 16 hours in a buffer containing 0.1 mM GSSG and varying concentrations of GSH (0.03-11 mM). After excitation at 280 nm, fluorescence emission was recorded at 350 nm, the data were normalized and the fraction of reduced protein was plotted against the $[GSH]^2/[GSSG]$ ratio. The equilibrium constant was determined and the data were normalized by fitting them according to equation 1 (paper II, Materials and Methods). After nonlinear regression, a value of K_{eq} = 3.3 mM was obtained for the ERp57 a domain (correlation coefficient: 0.989) and a value of K_{eq} = 1.5 mM was found for the ERp57 a' domain (correlation coefficient: 0.998).

2.2.3 *In vitro activity studies of ERp57*

Disulfide reductase activity

PDI is a remarkably versatile enzyme exhibiting reductase, isomerase, and oxidase activities. Although not the only determining factor, the similarity in redox potentials between PDI and ERp57 **a** and **a'** could indicate similar redox activities. ERp57's reductase and isomerase activity *in vitro* has been addressed previously (Bonfils, 1998; Bourdi et al., 1995; Eschenlauer and Page, 2003; Hirano et al., 1995). However, a comprehensive quantitative analysis of the catalytic activity of ERp57 in comparison to other thiol-disulfide oxidoreductases is lacking. Therefore, it was decided to investigate whether ERp57 is endowed with the same broad catalytic abilities as PDI by comparing ERp57 to PDI and other well-known thiol-disulfide oxidoreductases. I employed assays to probe disulfide reductase, isomerase, and dithiol oxidase activity.

For the reductase activity, I made use of the fact that insulin aggregates upon reduction by DTT. The resulting turbidity of the protein solution can be measured by detecting the optical density at 650 nm (Holmgren, 1979). To compare the reductase efficiency of ERp57 with that of PDI and other thiol-disulfide oxidoreductases, the onset of aggregation was defined as the time point where OD_{650} exceeded a value of 0.025 (final OD_{650}=1.4-1.8). For the uncatalyzed reaction, this value was reached after 40 minutes.

Wide concentration ranges were tested for each oxidoreductase and plotted against the time for onset of aggregation (Fig. 2.14). By comparing how much catalyst was required to halve the uncatalyzed time of aggregation onset to 20 minutes, a relative measure of the reductase efficiency was obtained (Fig. 2.14, dotted line). Quantified in this way, ERp57 proved to be 20 times less efficient than PDI as a reductase (0.8 μM for ERp57 needed versus 0.04 μM for PDI). However, ERp57 was 5 times more efficient than DsbA, the bacterial oxidase, and only 2 times less efficient than thioredoxin, the bacterial cytosolic reductase.

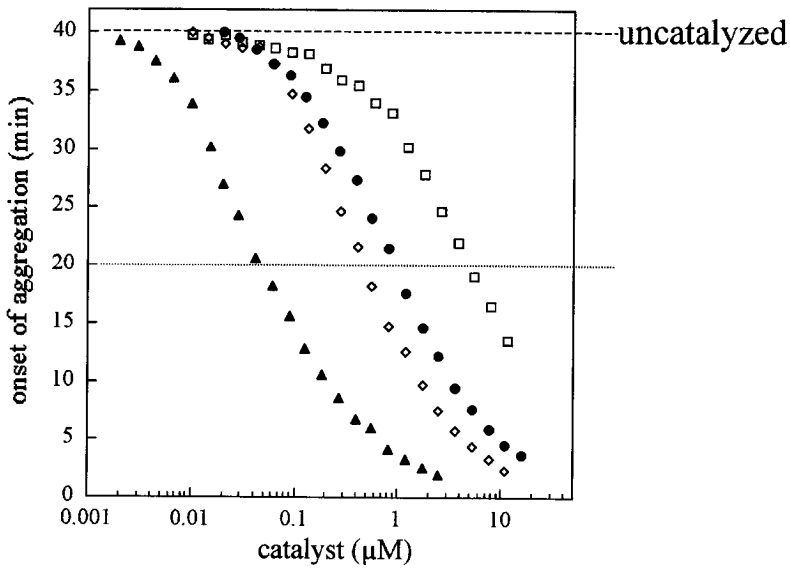

Fig. 2.14 Catalyzed reduction of insulin by DTT. Various concentrations of DsbA (□), ERp57 (●), Trx (◊) and PDI (▲) were tested for their ability to catalyze the reduction of 130 μM insulin by 1 mM DTT at 25°C. The onset of aggregation was defined as the time when the optical density at 650 nm had reached a value of 0.025 and was plotted against the concentration catalyst used.

Disulfide isomerase activity

To characterize the isomerase activity of ERp57, I used a variant of a well-established assay based on the reactivation of disulfide-scrambled RNaseA. The catalyzed isomerization of 40 μM scrambled RNaseA (scRNaseA) to native RNaseA (natRNaseA) was followed over a time period of 8 h in the presence of catalytic amounts of reduced PDI, ERp57 or the ERp57 **a** and **a'** domains. To obtain a measure of isomerase activity, samples were collected at different time points and the rate of cCMP hydrolysis by reactivated RNaseA was determined and expressed as a percentage of the hydrolysis rate obtained with 40 μM natRNaseA (Fig. 2.15).

Reactivation of scRNaseA to the wild-type level was achieved within approximately 3 h using 5 μM PDI. With the same concentration of ERp57, scRNaseA could only be rescued to ~60% of the wild-type level after 8 h. When using 5 μM of each of the ERp57 **a** and **a'** domains, which corresponds to 5 μM full-length ERp57 in active site concentration, the reactivation level reached ~30%. In a control experiment, it was verified that the individual **a** and **a'** domain were both active in our assay (data not shown).

To get a second measure of the disulfide isomerase activity for the different proteins in the assay, I determined the initial rate of catalysis. Hereby, I obtained values for the initial reactivation rate of scRNaseA of greater than or equal to 1.11

μM/min for PDI, 0.16 μM/min for ERp57 and 0.05 μM/min for the ERp57 **a** and **a'** domains, compared to 4.8 x 10^{-3} μM/min for the background reaction (5 μM DTT). Therefore, compared to ERp57, the initial rate of reactivation by PDI is at least 7 times faster, while the rate obtained for the mixture of the **a** and **a'** domains is 3 times slower. The uncatalyzed isomerization reaction is still 33 times slower than the ERp57-catalyzed reaction. Taken together, the results of the isomerase assay indicated that although ERp57 does possess activity, it is by far not as efficient as PDI. When mixed, the two separate redox active domains did not possess the same isomerase activity as the full-length protein.

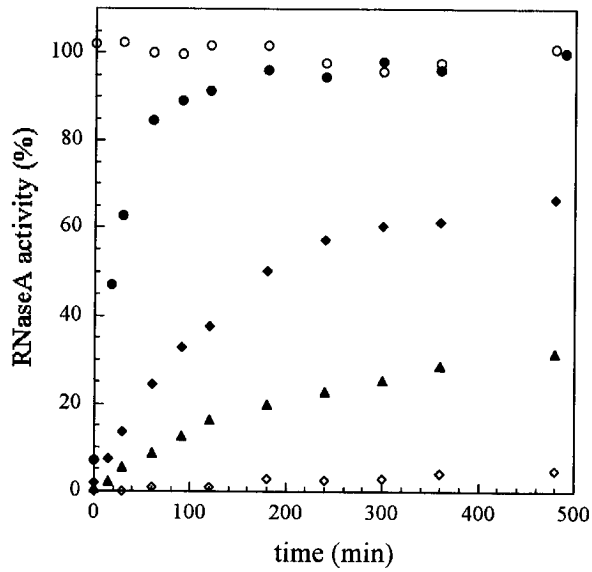

Fig. 2.15 Isomerization and reactivation of scrambled RNaseA. 5 μM PDI (●), 5 μM ERp57 (◆), 5 μM each of the ERp57 a and a' domain (▲) that had been reduced with equimolar amounts (10 μM) of DTT were tested for their ability to reactivate 40 μM scRNaseA at 25°C. At various time points samples were taken from the reaction and the RNaseA activity was followed by the hydrolysis of cCMP for 3 minutes at 296 nm. The initial hydrolysis rate of cCMP for 40 μM natRNaseA (O) was set to 100% RNaseA activity, and all other initial rates were expressed as a percentage of this activity. (◊) 40 μM scRNaseA in the presence of 10 μM DTT (no catalyst added).

Dithiol oxidase activity

To investigate a potential oxidase activity of ERp57, the existence of two distinct and non-interacting pathways for disulfide bond formation in the periplasm of Gram-negative bacteria was exploited.

To test oxidase activity, the ability of periplasmically expressed ERp57, PDI and various domains of both proteins to complement DsbA deficiency in THZ2, an *E. coli* strain that lacks DsbA, was analyzed by two phenotypic characteristics. One assay depends on a test of bacterial motility based on the DsbA-dependent folding of

the P-ring subunits of the flagellar motor (Dailey and Berg, 1993). The other assay involved a blue/white screening that relies on the oxidative inactivation of partially periplasmically located β-galactosidase. This assay probes the DsbA-dependent introduction of inactivating disulfide bonds into a β-galactosidase-MalF fusion protein (Bardwell et al., 1991; Silhavy et al., 1976). Thus, colonies of *E. coli* that lack a periplasmic oxidase turn blue on LB-plates containing X-Gal. As a negative control protein we used a redox inactive DsbC variant in which the two active-site cysteines had been mutated to alanines (DsbC C98A/C101A), and as a positive control DsbA itself was exported to the periplasm. Periplasmic expression of all proteins was ensured by cloning each construct in frame with the DsbA leader peptide and was verified by cell fractionation. The assays were performed in the absence of the inducer IPTG, whereby protein expression results from a leaky promoter. Thus, approximately the same levels of expression are observed for different constructs (Jonda et al., 1999).

The results showed that the ability of bacteria to swarm on top of a soft agar plate and form a bacterial lawn was restored in THZ2 cells transformed with the periplasmic expression plasmids of ERp57, the ERp57 **a** domain and the ERp57 **bb'a'** triple domain (Table 2.1). The latter was used in place of the ERp57 **a'** domain, since we did not observe periplasmic expression of the ERp57 **a'** domain. PDI and the PDI **a** domain, both known to act as oxidases (Jonda et al., 1999; Ostermeier et al., 1996), also restored bacterial swarming. Equivalent results were obtained with the blue/white assay (Table 2.1). In conclusion, ERp57 was able to act as an oxidase in the environment of the bacterial periplasm, and both redox-active domains of ERp57 could compensate for the absence of DsbA.

Construct	Complementation of DsbA (motility screen)	Complementation of DsbA (blue/white screen)
DsbA	+	+
DsbC ko	-	+/-
PDI	+	+
PDI **a**	+	+
ERp57	+	+
ERp57 **a**	+	+
ERp57 **bb'a'**	+	+

Table 2.1 *In vivo* complementation of DsbA by PDI, ERp57 and their redox active domains. Complementation was scored in two different assays - the ability to swarm on soft agar and the ability to oxidatively inactivate a β-galactosidase-MalF fusion protein leading to the formation of white colonies (see text for details). + : complementation; - : no complementation; ± : partial complementation.

3 Discussion

3.1 ERp57 interacts with the tip of the calreticulin P-domain

In the present investigation, the ability to record high-resolution NMR spectra of big structures in solution with the use of TROSY (Pervushin et al., 1997) enabled us to supplement the evidence for CRT(189–288) binding to ERp57 obtained from biochemical experiments with a structural characterization of the complex. Thus, we obtained an identification of the surface residues at the distal end of the calreticulin P-domain that are in or near the contact area with ERp57. Further NMR measurements enabled the determination of the thermodynamic stability of the CRT(189–288)/ERp57 complex. The two K_d-values of $(9.1\pm3.0) \times 10^{-6}$ M at 8°C and $(18\pm5) \times 10^{-6}$ M at 20°C determined by ITC and by TROSY-NMR, respectively, are in good agreement with each other. The relatively low affinity of the CRT/ERp57 complex is comparable to that reported recently for the complex between CRT and the glycoprotein IgG *in vitro*, *i. e.*, $K_d = 1.9 \times 10^{-6}$ M (Patil et al., 2000). However, whereas an exchange rate of $k_{off} = 0.1\ s^{-1}$ was reported for the CRT/glycoprotein complex, the NMR experiment reveals a much faster rate of $k_{off} > 1000\ s^{-1}$ for the CRT(189–288)/ERp57 complex, which is thus very short-lived. The additional presence of a substrate protein might of course result in formation of a more stable ternary complex, which could be further stabilized upon formation of an intermolecular disulfide bond between ERp57 and the glycoprotein (see Fig. 5). The fast off-rate for the binary CRT/ERp57 complex could be of functional significance since it might allow ERp57 to "screen" for pre-existing complexes of CRT and glycoprotein.

The group of David Williams was able to confirm the binding of ERp57 to the P-domain of CRT as well as CNX using fragments of the lectin chaperones in GST-fusion protein pull-down assays (Leach et al., 2002). In this assay, fragments of the P-domain of both lectins that were lacking the first type 1 repeat motif and the last type 2 repeat motif were able to bind to ERp57 (Leach et al., 2002). Furthermore, Lars Ellgaard and collegues showed by NMR that a fragment comprising 36 residues of the tip of the CRT P-domain, which corresponds to the tip type 12 repeat segment, bound to ERp57 (Ellgaard et al., 2002). The affinity of the interaction was the same as for the full-length P-domain as investigated by ITC (Ellgaard et al., 2002).

Based on their close sequence similarity, CRT and CNX are likely not only to possess similar P-domains but also structurally homologous lectin domains. In CNX, the lectin domain contains a single binding site for the oligosaccharide of the substrate glycoprotein and is located close to the site from which the P-domain emerges as an elongated hairpin loop (Schrag et al., 2001). The P-domain forms a slightly curved arm of about 110 Å in CRT (Ellgaard et al., 2001b) and 140 Å in CNX (Schrag et al., 2001). Binding of ERp57 to the distal end of this arm is likely to generate a partially solvent-shielded cavity surrounded by the lectin domain, the P-domain, and ERp57 (see Fig. 3.1). Given the apparent plasticity of the P-domain (Ellgaard et al., 2001b), the size of this cavity might be variable so as to accommodate substrates of different sizes.

The role of CNX and CRT as molecular chaperones seems to rely on three specific features. First, these proteins bind the substrate glycoprotein through the glycan binding site. By binding to the oligosaccharide moiety, they may tether the substrate with minimal constraints on the conformational freedom of the substrate polypeptide chain. Second, they may provide a partially solvent-shielded environment for folding (Fig. 3.1), where access for other ER chaperones and protein folding intermediates is likely to be restricted, so that aggregation and formation of non-native intermolecular disulfides with other newly synthesized proteins is suppressed (Helenius et al., 1997). Third, they provide a strategically placed binding site for ERp57, which supports productive interactions between the thiol-disulfide oxidoreductase and cysteines in the folding glycoprotein. Such interactions have previously been shown to involve the formation of a series of transient mixed disulfides between the substrate glycoprotein and ERp57 (Molinari and Helenius, 1999).

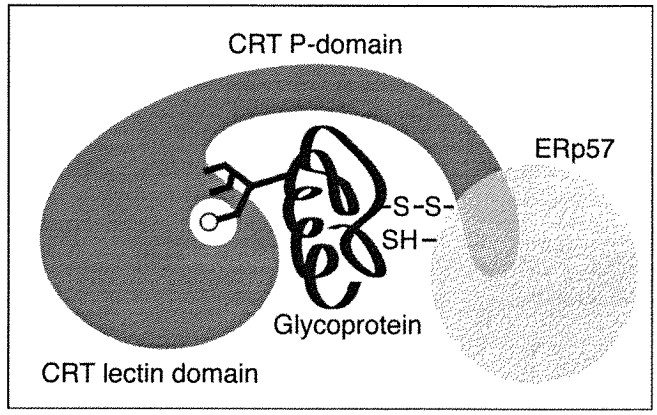

Fig. 3.1 Scheme for a possible mode of cooperative interaction between CRT and ERp57 in assisting the folding of a glycoprotein based on currently available structural, biochemical and cell-biological data (Ellgaard et al., 2001b; Parodi, 2000; Schrag et al., 2001). The substrate glycoprotein (blue) binds to the CRT lectin domain (red) via a branched oligosaccharide. CRT and CNX both interact specifically with the $Glc_1Man_9GlaNAc_2$ form of the oligosaccharide (Hammond et al., 1994; Spiro et al., 1996; Vassilakos et al., 1998). The interaction of the terminal glucose (light blue circle) with the binding site (white circle) would place the glycoprotein polypeptide chain in the partially solvent-shielded cavity bounded by the CRT lectin domain, the P-domain, and ERp57 (orange) bound to the distal end of the protruding P-domain. It is further hypothesized that the CRT-ERp57 interaction places the thiol-disulfide oxidoreductase favorably for the formation of intermolecular disulfide bonds (S-S) with the glycoprotein.

3.2 Characteristics of the ERp57 binding site on calreticulin

The tip of the CRT P-domain is distinctly enriched with acidic amino acids in all organisms that harbour an ERp57 homologue. *S. cerevisiae* lacks ERp57 in its genome, and its CNX homologue is devoid of the cluster of acidic residues. Upon mutating five to these acidic residues in the CRT P-domain to the corresponding amino acids of the CNX homologue of *S. cerevisiae*, Cne1p, the binding to ERp57 was abolished, as shown by ITC, ELISA and crosslinking.

Very recently, S. Pollock and colleagues identified amino acids in the tip region of the CRT homologue CNX that are crucial for ERp57 binding (Pollock et al., 2004). Using NMR, they could solve the structure of a 17-residue fragment of the tip of the CNX P-domain in its free form and when bound to ERp57. Upon addition of ERp57, they singled out the amide backbones and side chains of the amino acids that exhibited the most signal broadening in a ^{1}H-^{15}N HSQC spectra, which is indicative of their participation in the binding. Like this, mostly acidic amino acids in the tip region of CNX were revealed to be affected. Fig. 3.2 shows in bold the residues found in their and our NMR study to be influenced by ERp57 binding. Both sets of residues contain mostly acidic amino acids. A double mutant of CNX, D344A/E352A, showed measurable reduction of binding to ERp57 using a newly devised membrane yeast

two-hybrid system (Pollock et al., 2004). In the same assay, mutating residues D342, D344, D346, D348, E350, E352 to alanines in CNX completely abolished binding to ERp57 (see Fig. 3.2, underlined amino acids), (Pollock et al., 2004).

In conclusion, Pollock et al. identified amino acids in the tip region of CNX that contribute significantly to the binding of the lectin chaperone to ERp57. Most of these residues were acidic (see Fig 3.1). Of the five acidic residues we singled out to be important for ERp57 binding to CRT, four correspond to amino acids found by Pollock et al..

CRT	**A**	K	**K**	P	**E**	**D**	W	**D**	E	**E**	**M**
CNX	A	E	K	P	E	**D**	**W**	**D**	E	**D**	**M**
CRT	**D**	**G**	E	W	**E**	P	P	**V**	**I**	Q	**N**
CNX	**D**	**G**	E	W	**E**	A	P	Q	I	A	N

Fig. 3.2 Sequence alignment of the tip region of CNX and CRT. Amino acids found to be important for CNX binding to ERp57 in NMR studies are shown in bold; residues participating in CNX binding to ERp57 as identified by a membrane yeast two-hybrid screen are underlined (Pollock et al., 2004). Amino acids in CRT identified in this thesis to show outstandingly large effects from ERp57 interactions in NMR are shown in bold (see also Fig. 2.2a); residues that abolished ERp57 binding as judged by ITC, ELISA and crosslinking when collectively mutated are underlined.

3.3 The binding site for calreticulin on ERp57

Detailed knowledge about the three-dimensional structure of CNX, the CRT P-domain and the ERp57 binding site at the tip of the P-domains is now available (Ellgaard et al., 2001b; Frickel et al., 2002; Schrag et al., 2001). It has remained unknown where in ERp57 the P-domains of the two lectin chaperones bind. This was partly due to no available structural data on ERp57.

The tip of the P-domain in both CNX and CRT is enriched with acidic amino acids (see Appendix, Fig. 6.2), leading to the conclusion that a potential binding site in ERp57 may contain basic amino acids. Upon comparison of a sequence alignment between PDIs and ERp57s from different organisms, a region in the **b'** domain that is notably more basic in ERp57 than in PDI can be found (see Appendix, Fig. 6.1). However, this stretch in ERp57 most likely is not the sole mediator of the interaction with CRT. For two proteins to bind to each other generally a region of about 600 to

800 Å to has to present the binding surface (Chothia and Janin, 1975; Lo Conte et al., 1999; Sheinerman et al., 2000).

The notion that PDI has evolved a peptide binding region in its **b'** domain, while ERp57 might have evolved a CRT binding-region was recently evaluated by Stephen High and colleagues (Russell et al., 2004). Using a quantitative pull down assay, they tested which ERp57/PDI chimeras retained binding to CRT, and defined the **b** and **b'** domains as the minimal region sufficient for complex formation. The basic C-terminus in ERp57 was found to further enhance the binding. All but two residues in the ERp57 **b'** domain corresponding to residues important for PDI-substrate binding also had a major effect on ERp57-CRT binding. Another study observed a crosslinking product between the CRT P-domain and the ERp57**abb'**PDI**a'c** chimera, whereas a ERp57**ab**PDI**b'a'c** chimera showed no binding to the CRT P-domain (Silvennoinen et al., 2004). Thus, this study as well indicates a crucial role for the ERp57 **b'** domain in mediating the interaction of the thiol-disulfide oxidoreductase with CRT.

The interaction between ERp57 and CNX was very recently investigated by the group of David Thomas (Pollock et al., 2004). Using a novel membrane yeast two-hybrid system and pull-down assays, they could show that four single-point mutatants in the **b'** and **a'** domain, two double-point mutants, as well as the basic C-terminal stretch in ERp57 affected binding to the CNX P-domain. Truncation of ERp57's basic C-terminus abolished the protein's interaction with CNX, and substitution of the acidic C-terminus in PDI for ERp57's basic region rendered PDI capable of binding the lectin chaperone. From this data it was concluded that the C-terminal tail of ERp57 is involved in the interaction with CNX, but that other regions, likely the **b'** and **a'** domain, play enhancing roles.

In summary, the positively charged region in the **b'** domain shown in Fig. 6.1 by a black bar and the C-terminus of ERp57 are probably crucial for the binding to CRT and CNX. Further investigation into this binding site will undoubtedly require structural information of ERp57.

3.4 Structural and catalytic properties of ERp57

Our investigation of various biophysical and biochemical properties of ERp57 provided new insight into the structure of the molecule, and showed that ERp57 is a

versatile redox enzyme. In many respects, it is similar to its closest homologue, PDI, but significant differences in redox activity were also observed. Our findings gave a better understanding of ERp57 at the molecular level, and have implications for the function of the protein *in vivo*.

The limited proteolysis experiments provided information about domain boundaries and showed that like PDI, ERp57 contains four structural domains. Together with previously published data on domain boundaries in PDI (Darby et al., 1996; Darby et al., 1999; Freedman et al., 1998), and the sequence similarity between the two proteins, our results allow an estimate of the domain boundaries for the four thioredoxin-like domains in ERp57. Based on this analysis, we have recently generated the following ERp57 domain constructs in *E. coli*: **a**, residues 1-112; **b**, residues 108-218; **b'**, residues 219-352 and **a'**, residues 353-473. The domain boundaries are in agreement with those proposed recently by Alanen and coworkers, who based their assignments primarily on sequence alignments between known ER thiol-disulfide oxidoreductases (Alanen et al., 2003a).

For the **b** and **b'** domain constructs, our NMR data show that these proteins give rise to well-dispersed NMR signals indicative of defined three-dimensional structures in solution (R. Riek, V. Wohlgensinger, H. Kovacs, and L. Ellgaard, unpublished data). For the redox active **a** and **a'** domains, it is noteworthy that neither seemed to undergo significant structural changes upon formation of the active site disulfide bond as judged by far UV CD spectroscopy (paper II, Fig. 3b and c). Thus, both domains retained spectra characteristic of folded, globular proteins. This is in contrast to the PDI **a'** domain, where the oxidized form exhibits a far UV CD spectrum much like that of an unfolded protein (Darby and Creighton, 1995b). A destabilization of the oxidized form in comparison to the reduced form has also been observed in other thiol-disulfide oxidoreductases such as DsbA (Wunderlich et al., 1993; Zapun et al., 1993), ERp18 (Alanen et al., 2003b), and the PDI **a** domain (Alanen et al., 2003b).

To obtain insight into the hydrodynamic properties of ERp57, the protein was analyzed by analytical ultracentrifugation. Results from sedimentation velocity measurements showed that ERp57 is an elongated molecule with a length of 16.8 ± 0.5 nm and a diameter of 3.4 ± 0.1 nm and (paper II, Table 2). These dimensions make it unlikely that the four domains pack closely into the shape of a pyramid-like structure. Interestingly, recent ultracentrifugation studies from H. F. Gilbert's lab

indicate that PDI is also likely to be an elongated molecule in solution (H. F. Gilbert, personal communication).

Somewhat surprisingly, the sedimentation equilibrium analysis showed a reversible self-association of ERp57 into trimers and hexamers in solution in the presence of 2 mM DTT. The dissociation constants for the monomer–trimer and the trimer–hexamer equilibria were determined to 1 700 μM^2 and 14 nM, respectively. The high value of the dissociation constant for the monomer-trimer equilibrium suggests that these ERp57-oligomers are unlikely to be physiologically relevant. Moreover, no oligomeric form of the protein has been observed *in vivo* so far.

Sedimentation studies were extended to characterize the interaction between ERp57 and full-length CRT in solution. Analysis of a mixture of ERp57 and CRT revealed that these proteins form a 1:1 molar complex with a K_d in the low micromolar range and are in agreement with results obtained for the ERp57/CRT P-domain system. Using isothermal titration calorimetry, we have previously shown that the CRT P-domain forms a 1:1 complex with ERp57 in solution (Ellgaard et al., 2002; Frickel et al., 2002). The dissociation constants determined between ERp57 and two different recombinant forms of CRT P-domain were found to be 9.1 ± 3.0 μM and 5.1 ± 0.7 μM (Ellgaard et al., 2002; Frickel et al., 2002). Although other contact sites in CRT cannot be ruled out entirely at this point, the studies suggest that the interaction between ERp57 and CRT is mediated exclusively through the CRT P-domain. This is also consistent with the apparent molecular shape of the ERp57:CRT complex as determined by hydrodynamic analysis (paper II, Table 2). That ERp57 and CRT form a 1:1 complex *in vitro* are in agreement with findings showing that a heterodimeric complex of the two proteins isolated from canine pancreatic microsomes runs at ~140 kDa on a native gel and that a complex of similar mobility by SDS-PAGE can be observed after cross-linking of the two proteins in semipermeabilized mammalian cells (Oliver et al., 1999).

Characterization of the redox properties of ERp57 showed that the protein is a versatile redox enzyme. For the **a** and **a'** domains, we determined the equilibrium constants with glutathione to 3.3 mM and 1.5 mM, respectively. This translates into redox potentials of -0.167 V for the **a** domain and -0.156 V for **a'**. In comparison, thioredoxin, the bacterial cytoplasmic reductase, has a redox potential of -0.270 V (Krause et al., 1991) and DsbA, the bacterial oxidase, a value of -0.122 V (Huber-Wunderlich and Glockshuber, 1998). The intermediate values found for the ERp57

redox active domains are thus closer to the redox potential of -0.175 V determined for PDI (Lundstrom and Holmgren, 1993) and the equilibrium constants of 0.7 mM for the PDI **a** domain and of 1.9 mM for PDI **a'** domain (Darby and Creighton, 1995a), all also determined with GSH/GSSG as a reference.

Like PDI, ERp57 was capable of catalyzing reduction, isomerization, and oxidation. The reductase activity of the protein was close to that exhibited by thioredoxin, and clearly higher than that of DsbA (Fig. 2.12). The initial rate of isomerase catalysis by ERp57 was found to be 33 times faster than the DTT-background reaction. However, PDI performed both of these redox functions more efficiently than ERp57. In both cases, the difference is consistent with the finding that PDI, unlike ERp57, has been shown to possess peptide-binding activity, a function that is mediated by its **b'** domain (Klappa et al., 1998). The **b'** domain of PDI has been demonstrated to be essential for binding of scRNaseA, as the replacement of the PDI **b'** domain by the ERp57 **b'** domain abolishes binding (Pirneskoski et al., 2001). Thus, PDI likely catalyzes reduction and isomerization more efficiently than ERp57 by directly interacting with its substrates through the **b'** domain – a function that seems to have been lost in ERp57, perhaps in exchange for the ability to associate with CNX and CRT.

Important insight into the function of ERp57 has come from the observation that acceleration of disulfide-coupled refolding of reduced RNaseB catalysed by ERp57 was shown to be dependent on its interaction with CNX and CRT (Zapun et al., 1998). In this context, it is interesting to note that ERp57, unlike PDI, seemingly does not catalyze refolding of reduced RNaseA or lysozyme (Bonfils, 1998). However, this observation might well be a result of a weaker, as opposed to absent, oxidase and/or isomerase activity of ERp57 compared to PDI. ERp57 probably compensates for its apparent inability to interact directly with substrates through backbone contacts - resulting in a lower redox activity in comparison to PDI when tested *in vitro* on non-glycosated proteins - by depending on CNX and CRT to expose the protein directly to its glycoprotein substrates.

The function of the PDI **b'** domain likely explains to a large extent why the two isolated redox active PDI **a** and **a'** domains do not provide the same efficiency of isomerization as the intact protein (Darby and Creighton, 1995b; Darby et al., 1998a). We observed a similar effect in ERp57 - the combination of the separate **a** and **a'** domains did not isomerize scRNaseA as efficiently as the full-length protein (Fig.

2.13). Features of the protein other than those of the isolated redox active domains are needed for effective isomerization also by ERp57. The molecular characteristics underlying this effect are not clear, but simply the presence of two active sites on the same molecule could provide an explanation for the higher isomerase efficiency observed for the full-length protein. In addition, a weak peptide-binding activity of either ERp57 **b** or **b'** cannot be ruled out.

As an assay for oxidase activity we investigated the ability of ERp57 to complement DsbA deficiency in the periplasm of *E. coli*. Previously, the efficient restoration of the $DsbA^+$ phenotype in the *dsbA*⁻ THZ2 strain has been shown to correlate with the redox potential so that thioredoxin variants with an E_0' higher than -0.221 V showed complementation (Jonda et al., 1999). Our results demonstrated that all three ERp57 constructs tested were able to act as oxidases in this assay. This result is in accordance with the determined redox potentials for the **a** and **a'** domains. Recently, full-length ERp57 from *Caenorhabditis elegans* was also found to complement DsbA deficiency (Blasko et al., 2003). In addition, the ERp57 **a** domain can catalyze the oxidation of a model peptide substrate *in vitro* (Lappi et al., 2004). Our results also indicate that all active sites of ERp57 as well as the PDI **a** domain are substrates of DsbB.

Whereas we have characterized the different redox activities performed by ERp57 *in vitro*, the question of its redox function *in vivo* remains open. The protein has been shown to reduce partially folded MHC class I molecules *in vitro* (Antoniou et al., 2002). Based on this study, it was proposed that ERp57 could play a role in reducing intrachain disulfides in MHC class I molecules targeted for degradation. Since ERp57 is an important component of the peptide loading complex, the protein would be positioned favorably to perform this function. A similar reductase activity has been proposed for PDI in retrotranslocation of the cholera toxin A chain (Tsai et al., 2001).

In addition to its potential reductase function, ERp57 likely catalyzes disulfide-coupled glycoprotein folding directly *in vivo*. The finding that ERp57 forms transient mixed disulfides with productively folding glycoprotein substrates of CNX and CRT argues in favor of this view (Molinari and Helenius, 1999). Furthermore, ERp57 has been implicated in disulfide bond isomerization of the MHC class I heavy chain in the peptide loading complex (Dick et al., 2002).

There is no indication so far that disulfide-exchange reactions with Ero1 regulate the redox function of ERp57, as observed for PDI. Ero1 overexpression seems to have no effect on the redox state of ERp57, and intermolecular disulfides between Ero1 and ERp57 have not been detected (Mezghrani et al., 2001). While this could be due to technical difficulties in trapping and revealing Ero1–ERp57 mixed disulfide complexes, the presence of an Ero1-independent system for ERp57 reoxidation cannot be ruled out. However, two recent studies show that in the ER of mammalian tissue-culture cells ERp57 is found in the reduced state (Antoniou and Powis, 2003; Mezghrani et al., 2001). Although perhaps a cell-type dependent phenomenon, this finding indicates that ERp57 might not react as an oxidase *in vivo* and consequently not depend on a system for its reoxidation. Further studies are needed to clarify this important point.

The analytical ultracentrifugation studies were carried out by Walter Stafford and Marlène Bouvier (see paper II).

3.5 Further mechanistic studies of glycoprotein folding

The extraordinary structure of CRT and CNX raises interesting questions about the functional importance of the shape and plasticity of its P-domain and about the importance of the ERp57 binding site being located at the most distal point from the lectin binding site.

To study the function of the P-domain in glycoprotein folding, we have generated CRT constructs lacking the P-domain or with P-domains of various sizes (see Appendix). CRTΔP is a mutant that lacks the P-domain entirely. Instead, it contains a flexible linker of ten amino acids that connects the two halves of the lectin domain. Constructs of CRT have also been engineered that contain variants of the P-domain with one, two and four 1,2 repeats (instead of the native three) and termed CRTP1, CRTP2 and CRTP4. In CRTP1, the P-domain is made up only of the terminal 1,2 repeat that constitutes the ERp57-binding tip of this domain. CRTP2 is devoid of the middle 1,2 repeat pair, while in CRTP4 this repeat pair is duplicated. Thus, all of the CRT constructs with various P-domain lengths should retain the ability to bind to ERp57. As shown in section 2.1.3, we have also generated a construct of the CRT P-domain (CRTΔEB) with five point mutations at the tip and

shown by isothermal titration calorimetry (ITC), ELISA and crosslinking that ERp57 binding is abolished. The overall fold of the P-domain in this mutant is retained as judged by NMR spectroscopy (Pascal Bettendorf, data not shown). Finally, a CRT clone with three point mutations is available that has been shown by ITC not to bind Glc_1Man_3 (Kapoor et al., 2004).

Using these mutants of CRT, we want to investigate the importance of each of the unique features of the lectin chaperone in glycoprotein folding. We will set up systems to follow CRT- and ERp57-dependent oxidative folding of model glycoproteins in the test tube (*in vitro*) and in mammalian tissue-culture cells (*in vivo*). For the *in vitro* refolding assay we will use scrambled ^{3}H-labelled RNaseB as a glycoprotein substrate, and monitor its folding by native gel electrophoresis. *In vitro*, RNaseB refolding has been used to show that enhanced catalysis of disulfide bond formation by ERp57 is dependent on its interaction with CNX or CRT (Zapun et al., 1998; Zapun et al., 1997). In this assay, the maturation of monoglucosylated ^{3}H-labelled RNaseB to the fully oxidized form was followed by native gel electrophoresis and fluorography. We have already generated the radioactively labelled substrate, and have demonstrated that the scrambled versus the native form of RNaseB exhibits a shift on native gels. We will now monitor the kinetics of ERp57- and CRT-catalyzed refolding of scrambled RNaseB for wild-type CRT and the P-domain mutants. Like this, we will be able to determine the importance of the length of the P-domain in the catalysis of refolding of a small single-domain protein.

For the *in vivo* studies, we will use CRT-deficient mouse fibroblast cells (K42) to make stable cell lines of our CRT mutants and monitor MHC class I surface expression by FACS analysis with a conformation-sensitive monoclonal antibody. One of the best-studied substrates of the CNX/CRT cycle in mammalian tissue-culture cells is the MHC class I complex. The process of MHC class I folding, assembly and peptide loading involves CNX, CRT and ERp57 together with the more specialized proteins TAP (transporter associated with antigen processing) and tapasin. During the early stages of folding the newly synthesized heavy chain interacts with CNX. Upon binding of β_2-microglobulin, CRT replaces CNX (Diedrich et al., 2001) and together with TAP, tapasin and ERp57 forms the so-called peptide loading complex (PLC). In a tapasin-dependent process, the class I molecules are then loaded

with antigenic peptide, the PLC dissociates and the mature MHC class I complex can traffic to the cell surface (Williams et al., 2002).

As a prerequisite for these studies, we can detect by FACS analysis a reduced MHC class I surface expression in K42 versus in the corresponding wild-type cells (K41), as previously published by the group of Elliott (Gao et al., 2002). CNX devoid of its transmembrane segment could not rectify the surface expression of MHC class I in these cells (Gao et al., 2002). In another study, the same construct of CNX performed just as well as CRT in the early biogenesis of heavy chain:β_2-microglobulin heterodimers (Danilczyk et al., 2000). It will be interesting to see if CRTP4 is able to rescue the wild-type situation. This would be an indication that CRT has a distinct function in MHC class I maturation beyond that of its lectin chaperone activity. Moreover, we are planning to investigate the presence of all CRT mutants in the PLC. This will answer questions about the flexibility of the PLC and the order and determinants for CRT recruitment to the complex.

The preliminary results obtained in setting up the *in vitro* RNaseB refolding assay were generated by Karl Bihlmaier during the course of his semester project and ongoing diploma thesis performed under my supervision.

4 References

Alanen, H.I., Salo, K.E., Pekkala, M., Siekkinen, H.M., Pirneskoski, A. and Ruddock, L.W. (2003a) Defining the domain boundaries of the human protein disulfide isomerases. *Antioxid. Redox Signal.*, **5**, 367-374.

Alanen, H.I., Williamson, R.A., Howard, M.J., Lappi, A.K., Jantti, H.P., Rautio, S.M., Kellokumpu, S. and Ruddock, L.W. (2003b) Functional characterization of ERp18, a new endoplasmic reticulum-located thioredoxin superfamily member. *J. Biol. Chem.*, **278**, 28912-28920.

Anelli, T., Alessio, M., Bachi, A., Bergamelli, L., Bertoli, G., Camerini, S., Mezghrani, A., Ruffato, E., Simmen, T. and Sitia, R. (2003) Thiol-mediated protein retention in the endoplasmic reticulum: the role of ERp44. *Embo J*, **22**, 5015-5022.

Anelli, T., Alessio, M., Mezghrani, A., Simmen, T., Talamo, F., Bachi, A. and Sitia, R. (2002) ERp44, a novel endoplasmic reticulum folding assistant of the thioredoxin family. *EMBO J.*, **21**, 835-844.

Anfinsen, C.B., Haber, E., Sela, M. and White, F.H., Jr. (1961) The kinetics of formation of native ribonuclease during oxidation of the reduced polypeptide chain. *Proc Natl Acad Sci U S A*, **47**, 1309-1314.

Antoniou, A.N., Ford, S., Alphey, M., Osborne, A., Elliott, T. and Powis, S.J. (2002) The oxidoreductase ERp57 efficiently reduces partially folded in preference to fully folded MHC class I molecules. *EMBO J.*, **21**, 2655-2663.

Antoniou, A.N. and Powis, S.J. (2003) Characterization of the ERp57-Tapasin complex by rapid cellular acidification and thiol modification. *Antioxid. Redox Signal.*, **5**, 375-379.

Argon, Y. and Simen, B.B. (1999) GRP94, an ER chaperone with protein and peptide binding properties. *Semin Cell Dev Biol*, **10**, 495-505.

Aridor, M. and Balch, W.E. (1999) Integration of endoplasmic reticulum signaling in health and disease. *Nat. Med.*, **5**, 745-751.

Aslund, F., Berndt, K.D. and Holmgren, A. (1997) Redox potentials of glutaredoxins and other thiol-disulfide oxidoreductases of the thioredoxin superfamily determined by direct protein-protein redox equilibria. *J Biol Chem*, **272**, 30780-30786.

Bader, M., Muse, W., Ballou, D.P., Gassner, C. and Bardwell, J.C. (1999) Oxidative protein folding is driven by the electron transport system. *Cell*, **98**, 217-227.

Bader, M.W., Hiniker, A., Regeimbal, J., Goldstone, D., Haebel, P.W., Riemer, J., Metcalf, P. and Bardwell, J.C. (2001) Turning a disulfide isomerase into an oxidase: DsbC mutants that imitate DsbA. *Embo J*, **20**, 1555-1562.

Bader, M.W., Xie, T., Yu, C.A. and Bardwell, J.C. (2000) Disulfide bonds are generated by quinone reduction. *J. Biol. Chem.*, **275**, 26082-26088.

Baksh, S. and Michalak, M. (1991) Expression of calreticulin in Escherichia coli and identification of its Ca2+ binding domains. *J. Biol. Chem.*, **266**, 21458-21465.

Balbach, J., Steegborn, C., Schindler, T. and Schmid, F.X. (1999) A protein folding intermediate of ribonuclease T1 characterized at high resolution by 1D and 2D real-time NMR spectroscopy. *J Mol Biol*, **285**, 829-842.

Banhegyi, G., Lusini, L., Puskas, F., Rossi, R., Fulceri, R., Braun, L., Mile, V., di Simplicio, P., Mandl, J. and Benedetti, A. (1999) Preferential transport of glutathione versus glutathione disulfide in rat liver microsomal vesicles. *J Biol Chem*, **274**, 12213-12216.

Bannister, S.J. and Wittrup, K.D. (2000) Glutathione excretion in response to heterologous protein secretion in Saccharomyces cerevisiae. *Biotechnol Bioeng*, **68**, 389-395.

Bardwell, J.C., McGovern, K. and Beckwith, J. (1991) Identification of a protein required for disulfide bond formation in vivo. *Cell*, **67**, 581-589.

Bass, R., Ruddock, L.W., Klappa, P. and Freedman, R.B. (2004) A major fraction of endoplasmic reticulum-located glutathione is present as mixed disulfides with protein. *J Biol Chem*, **279**, 5257-5262.

Ben-Zvi, A.P. and Goloubinoff, P. (2001) Review: mechanisms of disaggregation and refolding of stable protein aggregates by molecular chaperones. *J Struct Biol*, **135**, 84-93.

Benham, A.M. and Braakman, I. (2000) Glycoprotein folding in the endoplasmic reticulum. *Crit. Rev. Biochem. Mol. Biol.*, **35**, 433-473.

Benham, A.M., Cabibbo, A., Fassio, A., Bulleid, N., Sitia, R. and Braakman, I. (2000) The CXXCXXC motif determines the folding, structure and stability of human Ero1-Lalpha. *EMBO J.*, **19**, 4493-4502.

Bennett, C.F., Balcarek, J.M., Varrichio, A. and Crooke, S.T. (1988) Molecular cloning and complete amino-acid sequence of form-I phosphoinositide-specific phospholipase C. *Nature*, **334**, 268-270.

Blasko, B., Madi, A. and Fesus, L. (2003) Thioredoxin motif of Caenorhabditis elegans PDI-3 provides Cys and His catalytic residues for transglutaminase activity. *Biochem. Biophys. Res. Commun.*, **303**, 1142-1147.

Bonfils, C. (1998) Purification of a 58-kDa protein (ER58) from monkey liver microsomes and comparison with protein-disulfide isomerase. *Eur. J. Biochem.*, **254**, 420-427.

Bourdi, M., Demady, D., Martin, J.L., Jabbour, S.K., Martin, B.M., George, J.W. and Pohl, L.R. (1995) cDNA cloning and baculovirus expression of the human liver endoplasmic reticulum P58: characterization as a protein disulfide isomerase isoform, but not as a protease or a carnitine acyltransferase. *Arch. Biochem. Biophys.*, **323**, 397-403.

Bouvier, M. and Stafford, W.F. (2000) Probing the three-dimensional structure of human calreticulin. *Biochemistry*, **39**, 14950-14959.

Braakman, I. (2001) A novel lectin in the secretory pathway. An elegant mechanism for glycoprotein elimination. *EMBO Rep.*, **2**, 666-668.

Braakman, I., Foellmer, B., Land, A., Helenius, J. and Helenius, A. (in preparation) Obligatory and hierarchical formation of disulfide bonds during influenza hemagglutinin folding in live cells.

Braakman, I., Helenius, J. and Helenius, A. (1992a) Manipulating disulfide bond formation and protein folding in the endoplasmic reticulum. *EMBO J.*, **11**, 1717-1722.

Braakman, I., Helenius, J. and Helenius, A. (1992b) Role of ATP and disulphide bonds during protein folding in the endoplasmic reticulum. *Nature*, **356**, 260-262.

Brightman, S.E., Blatch, G.L. and Zetter, B.R. (1995) Isolation of a mouse cDNA encoding MTJ1, a new murine member of the DnaJ family of proteins. *Gene*, **153**, 249-254.

Bukau, B. and Horwich, A.L. (1998) The Hsp70 and Hsp60 chaperone machines. *Cell*, **92**, 351-366.

Burda, P. and Aebi, M. (1999) The dolichol pathway of N-linked glycosylation. *Biochim. Biophys. Acta*, **1426**, 239-257.

Cabibbo, A., Pagani, M., Fabbri, M., Rocchi, M., Farmery, M.R., Bulleid, N.J. and Sitia, R. (2000) ERO1-L, a human protein that favors disulfide bond formation in the endoplasmic reticulum. *J. Biol. Chem.*, **275**, 4827-4833.

Cannon, K.S., Hebert, D.N. and Helenius, A. (1996) Glycan-dependent and -independent association of vesicular stomatitis virus G protein with calnexin. *J. Biol. Chem.*, **271**, 14280-14284.

Cannon, K.S. and Helenius, A. (1999) Trimming and readdition of glucose to N-linked oligosaccharides determines calnexin association of a substrate glycoprotein in living cells. *J. Biol. Chem.*, **274**, 7537-7544.

Casagrande, R., Stern, P., Diehn, M., Shamu, C., Osario, M., Zuniga, M., Brown, P.O. and Ploegh, H. (2000) Degradation of proteins from the ER of S. cerevisiae requires an intact unfolded protein response pathway. *Mol. Cell*, **5**, 729-735.

Chevet, E., Wong, H.N., Gerber, D., Cochet, C., Fazel, A., Cameron, P.H., Gushue, J.N., Thomas, D.Y. and Bergeron, J.J. (1999) Phosphorylation by CK2 and MAPK enhances calnexin association with ribosomes. *Embo J*, **18**, 3655-3666.

Chothia, C. and Janin, J. (1975) Principles of protein-protein recognition. *Nature*, **256**, 705-708.

Chung, J., Chen, T. and Missiakas, D. (2000) Transfer of electrons across the cytoplasmic membrane by DsbD, a membrane protein involved in thiol-disulphide exchange and protein folding in the bacterial periplasm. *Mol Microbiol*, **35**, 1099-1109.

Chung, K.T., Shen, Y. and Hendershot, L.M. (2002) BAP, a mammalian BiP-associated protein, is a nucleotide exchange factor that regulates the ATPase activity of BiP. *J Biol Chem*, **277**, 47557-47563.

Clark, H.F., Gurney, A.L., Abaya, E., Baker, K., Baldwin, D., Brush, J., Chen, J., Chow, B., Chui, C., Crowley, C., Currell, B., Deuel, B., Dowd, P., Eaton, D., Foster, J., Grimaldi, C., Gu, Q., Hass, P.E., Heldens, S., Huang, A., Kim, H.S., Klimowski, L., Jin, Y., Johnson, S., Lee, J., Lewis, L., Liao, D., Mark, M., Robbie, E., Sanchez, C., Schoenfeld, J., Seshagiri, S., Simmons, L., Singh, J., Smith, V., Stinson, J., Vagts, A., Vandlen, R., Watanabe, C., Wieand, D., Woods, K., Xie, M.H., Yansura, D., Yi, S., Yu, G., Yuan, J., Zhang, M., Zhang, Z., Goddard, A., Wood, W.I., Godowski, P. and Gray, A. (2003) The secreted protein discovery initiative (SPDI), a large-scale effort to identify novel human secreted and transmembrane proteins: a bioinformatics assessment. *Genome Res*, **13**, 2265-2270.

Collet, J.F., Riemer, J., Bader, M.W. and Bardwell, J.C. (2002) Reconstitution of a disulfide isomerization system. *J. Biol. Chem.*, **277**, 26886-26892.

Corbett, E.F. and Michalak, M. (2000) Calcium, a signaling molecule in the endoplasmic reticulum? *Trends Biochem. Sci.*, **25**, 307-311.

Creighton, T.E., Bagley, C.J., Cooper, L., Darby, N.J., Freedman, R.B., Kemmink, J. and Sheikh, A. (1993) On the biosynthesis of bovine pancreatic trypsin inhibitor (BPTI). Structure, processing, folding and disulphide bond formation of the precursor in vitro and in microsomes. *J Mol Biol*, **232**, 1176-1196.

Creighton, T.E., Hillson, D.A. and Freedman, R.B. (1980) Catalysis by protein-disulphide isomerase of the unfolding and refolding of proteins with disulphide bonds. *J Mol Biol*, **142**, 43-62.

Cresswell, P. (2000) Intracellular surveillance: controlling the assembly of MHC class I-peptide complexes. *Traffic*, **1**, 301-305.

Cunnea, P.M., Miranda-Vizuete, A., Bertoli, G., Simmen, T., Damdimopoulos, A.E., Hermann, S., Leinonen, S., Huikko, M.P., Gustafsson, J.A., Sitia, R. and Spyrou, G. (2003) ERdj5, an endoplasmic reticulum (ER)-resident protein containing DnaJ and thioredoxin domains, is expressed in secretory cells or following ER stress. *J. Biol. Chem.*, **278**, 1059-1066.

Cuozzo, J.W. and Kaiser, C.A. (1999) Competition between glutathione and protein thiols for disulphide-bond formation. *Nat. Cell Biol.*, **1**, 130-135.

Daggett, V. and Fersht, A. (2003) The present view of the mechanism of protein folding. *Nat Rev Mol Cell Biol*, **4**, 497-502.

Dailey, F.E. and Berg, H.C. (1993) Mutants in disulfide bond formation that disrupt flagellar assembly in Escherichia coli. *Proc. Natl. Acad. Sci. U S A*, **90**, 1043-1047.

Danilczyk, U.G., Cohen-Doyle, M.F. and Williams, D.B. (2000) Functional relationship between calreticulin, calnexin, and the endoplasmic reticulum luminal domain of calnexin. *J. Biol. Chem.*, **275**, 13089-13097.

Danilczyk, U.G. and Williams, D.B. (2001) The lectin chaperone calnexin utilizes polypeptide-based interactions to associate with many of its substrates in vivo. *J. Biol. Chem.*, **276**, 25532-25540.

Darby, N.J. and Creighton, T.E. (1995a) Characterization of the active site cysteine residues of the thioredoxin-like domains of protein disulfide isomerase. *Biochemistry*, **34**, 16770-16780.

Darby, N.J. and Creighton, T.E. (1995b) Functional properties of the individual thioredoxin-like domains of protein disulfide isomerase. *Biochemistry*, **34**, 11725-11735.

Darby, N.J., Kemmink, J. and Creighton, T.E. (1996) Identifying and characterizing a structural domain of protein disulfide isomerase. *Biochemistry*, **35**, 10517-10528.

Darby, N.J., Penka, E. and Vincentelli, R. (1998a) The multi-domain structure of protein disulfide isomerase is essential for high catalytic efficiency. *J. Mol. Biol.*, **276**, 239-247.

Darby, N.J., Raina, S. and Creighton, T.E. (1998b) Contributions of substrate binding to the catalytic activity of DsbC. *Biochemistry*, **37**, 783-791.

Darby, N.J., van Straaten, M., Penka, E., Vincentelli, R. and Kemmink, J. (1999) Identifying and characterizing a second structural domain of protein disulfide isomerase. *FEBS Lett.*, **448**, 167-172.

Denzel, A., Molinari, M., Trigueros, C., Martin, J.E., Velmurgan, S., Brown, S., Stamp, G. and Owen, M.J. (2002) Early postnatal death and motor disorders in mice congenitally deficient in calnexin expression. *Mol. Cell Biol.*, **22**, 7398-7404.

Desilva, M.G., Lu, J., Donadel, G., Modi, W.S., Xie, H., Notkins, A.L. and Lan, M.S. (1996) Characterization and chromosomal localization of a new protein disulfide isomerase, PDIp, highly expressed in human pancreas. *DNA Cell Biol*, **15**, 9-16.

Deuerling, E., Schulze-Specking, A., Tomoyasu, T., Mogk, A. and Bukau, B. (1999) Trigger factor and DnaK cooperate in folding of newly synthesized proteins. *Nature*, **400**, 693-696.

Di Jeso, B., Ulianich, L., Pacifico, F., Leonardi, A., Vito, P., Consiglio, E., Formisano, S. and Arvan, P. (2003) Folding of thyroglobulin in the calnexin/calreticulin pathway and its alteration by loss of Ca2+ from the endoplasmic reticulum. *Biochem J*, **370**, 449-458.

Dick, T.P., Bangia, N., Peaper, D.R. and Cresswell, P. (2002) Disulfide bond isomerization and the assembly of MHC class I-peptide complexes. *Immunity*, **16**, 87-98.

Diedrich, G., Bangia, N., Pan, M. and Cresswell, P. (2001) A role for calnexin in the assembly of the MHC class I loading complex in the endoplasmic reticulum. *J. Immunol.*, **166**, 1703-1709.

Dinner, A.R., Sali, A., Smith, L.J., Dobson, C.M. and Karplus, M. (2000) Understanding protein folding via free-energy surfaces from theory and experiment. *Trends Biochem Sci*, **25**, 331-339.

Dolinski, K., Muir, S., Cardenas, M. and Heitman, J. (1997) All cyclophilins and FK506 binding proteins are, individually and collectively, dispensable for viability in Saccharomyces cerevisiae. *Proc Natl Acad Sci U S A*, **94**, 13093-13098.

Drickamer, K. and Taylor, M.E. (1998) Evolving views of protein glycosylation. *Trends Biochem. Sci.*, **23**, 321-324.

Dwek, R.A. (1996) Glycobiology: Toward Understanding the Function of Sugars. *Chem. Rev.*, **96**, 683-720.

Ellgaard, L., Bettendorff, P., Braun, D., Herrmann, T., Fiorito, F., Jelesarov, I., Güntert, P., Helenius, A. and Wüthrich, K. (2002) NMR Structures of 36 and 73-residue Fragments of the Calreticulin P- domain. *J. Mol. Biol.*, **322**, 773-784.

Ellgaard, L., Molinari, M. and Helenius, A. (1999) Setting the standards: quality control in the secretory pathway. *Science*, **286**, 1882-1888.

Ellgaard, L., Riek, R., Braun, D., Herrmann, T., Helenius, A. and Wüthrich, K. (2001a) Three-dimensional structure topology of the calreticulin P-domain based on NMR assignment. *FEBS Lett.*, **488**, 69-73.

Ellgaard, L., Riek, R., Herrmann, T., Güntert, P., Braun, D., Helenius, A. and Wüthrich, K. (2001b) NMR structure of the calreticulin P-domain. *Proc. Natl. Acad. Sci. USA*, **98**, 3133-3138.

Elliott, J.G., Oliver, J.D. and High, S. (1997) The thiol-dependent reductase ERp57 interacts specifically with N- glycosylated integral membrane proteins. *J. Biol. Chem.*, **272**, 13849-13855.

Ellis, J. (1987) Proteins as molecular chaperones. *Nature*, **328**, 378-379.

Ellis, R.J. (2001) Macromolecular crowding: an important but neglected aspect of the intracellular environment. *Curr Opin Struct Biol*, **11**, 114-119.

Eschenlauer, S.C. and Page, A.P. (2003) The Caenorhabditis elegans ERp60 homolog protein disulfide isomerase-3 has disulfide isomerase and transglutaminase-like cross-linking activity and is involved in the maintenance of body morphology. *J. Biol. Chem.*, **278**, 4227-4237.

Fagioli, C., Mezghrani, A. and Sitia, R. (2001) Reduction of interchain disulfide bonds precedes the dislocation of Ig-mu chains from the endoplasmic reticulum to the cytosol for proteasomal degradation. *J. Biol. Chem.*, **276**, 40962-40967.

Farquhar, R., Honey, N., Murant, S.J., Bossier, P., Schultz, L., Montgomery, D., Ellis, R.W., Freedman, R.B. and Tuite, M.F. (1991) Protein disulfide isomerase is essential for viability in Saccharomyces cerevisiae. *Gene*, **108**, 81-89.

Ferrari, D.M., Nguyen Van, P., Kratzin, H.D. and Soling, H.D. (1998) ERp28, a human endoplasmic-reticulum-lumenal protein, is a member of the protein disulfide isomerase family but lacks a CXXC thioredoxin-box motif. *Eur J Biochem*, **255**, 570-579.

Ferrari, D.M. and Söling, H.D. (1999) The protein disulphide-isomerase family: unravelling a string of folds. *Biochem. J.*, **339**, 1-10.

Fersht, A. (1999) *Stucture and mechanism in protein science: a guide to enzyme catalysis and protein folding*. W. H. Freeman and Company, New York.

Fewell, S.W., Travers, K.J., Weissman, J.S. and Brodsky, J.L. (2001) The action of molecular chaperones in the early secretory pathway. *Annu. Rev. Genet.*, **35**, 149-191.

Fliegel, L., Burns, K., MacLennan, D.H., Reithmeier, R.A. and Michalak, M. (1989) Molecular cloning of the high affinity calcium-binding protein (calreticulin) of skeletal muscle sarcoplasmic reticulum. *J. Biol. Chem.*, **264**, 21522-21528.

Frand, A.R. and Kaiser, C.A. (1998) The ERO1 gene of yeast is required for oxidation of protein dithiols in the endoplasmic reticulum. *Mol. Cell*, **1**, 161-170.

Frand, A.R. and Kaiser, C.A. (1999) Ero1p oxidizes protein disulfide isomerase in a pathway for disulfide bond formation in the endoplasmic reticulum. *Mol. Cell*, **4**, 469-477.

Frand, A.R. and Kaiser, C.A. (2000) Two pairs of conserved cysteines are required for the oxidative activity of Ero1p in protein disulfide bond formation in the endoplasmic reticulum. *Mol. Biol. Cell*, **11**, 2833-2843.

Freedman, R.B., Gane, P.J., Hawkins, H.C., Hlodan, R., McLaughlin, S.H. and Parry, J.W. (1998) Experimental and theoretical analyses of the domain architecture of mammalian protein disulphide-isomerase. *Biol Chem*, **379**, 321-328.

Freedman, R.B., Hawkins, H.C. and McLaughlin, S.H. (1995) Protein disulfide-isomerase. *Methods Enzymol*, **251**, 397-406.

Freedman, R.B., Hirst, T.R. and Tuite, M.F. (1994) Protein disulphide isomerase: building bridges in protein folding. *Trends Biochem Sci*, **19**, 331-336.

Freedman, R.B., Klappa, P. and Ruddock, L.W. (2002) Protein disulfide isomerases exploit synergy between catalytic and specific binding domains. *EMBO Rep.*, **3**, 136-140.

Frickel, E.-M., Riek, R., Jelesarov, I., Helenius, A., Wüthrich, K. and Ellgaard, L. (2002) TROSY-NMR reveals interaction between ERp57 and the tip of the calreticulin P-domain. *Proc. Natl. Acad. Sci. USA*, **99**, 1954-1959.

Friedlander, R., Jarosch, E., Urban, J., Volkwein, C. and Sommer, T. (2000) A regulatory link between ER-associated protein degradation and the unfolded-protein response. *Nat. Cell Biol.*, **2**, 379-384.

Fujii, J., Willard, H.F. and MacLennan, D.H. (1990) Characterization and localization to human chromosome 1 of human fast-twitch skeletal muscle calsequestrin gene. *Somat Cell Mol Genet*, **16**, 185-189.

Gahmberg, C.G. and Tolvanen, M. (1996) Why mammalian cell surface proteins are glycoproteins. *Trends Biochem. Sci.*, **21**, 308-311.

Gao, B., Adhikari, R., Howarth, M., Nakamura, K., Gold, M.C., Hill, A.B., Knee, R., Michalak, M. and Elliott, T. (2002) Assembly and antigen-presenting function of MHC class I molecules in cells lacking the ER chaperone calreticulin. *Immunity*, **16**, 99-109.

Gavel, Y. and von Heijne, G. (1990) Sequence differences between glycosylated and non-glycosylated Asn-X- Thr/Ser acceptor sites: implications for protein engineering. *Protein Eng.*, **3**, 433-442.

Gilbert, H.F. (1998) Protein disulfide isomerase. *Methods Enzymol*, **290**, 26-50.

Gillece, P., Luz, J.M., Lennarz, W.J., de La Cruz, F.J. and Romisch, K. (1999) Export of a cysteine-free misfolded secretory protein from the endoplasmic reticulum for degradation requires interaction with protein disulfide isomerase. *J Cell Biol*, **147**, 1443-1456.

Golbik, R., Fischer, G. and Fersht, A.R. (1999) Folding of barstar C40A/C82A/P27A and catalysis of the peptidyl-prolyl cis/trans isomerization by human cytosolic cyclophilin (Cyp18). *Protein Sci*, **8**, 1505-1514.

Goldberger, R.F., Epstein, C.J. and Anfinsen, C.B. (1963) Acceleration of reactivation of reduced bovine pancreatic ribonuclease by a microsomal system from rat liver. *J. Biol. Chem.*, **238**, 628-635.

Gordon, E.H., Page, M.D., Willis, A.C. and Ferguson, S.J. (2000) Escherichia coli DipZ: anatomy of a transmembrane protein disulphide reductase in which three pairs of cysteine residues, one in each of three domains, contribute differentially to function. *Mol Microbiol*, **35**, 1360-1374.

Goulding, C.W., Sawaya, M.R., Parseghian, A., Lim, V., Eisenberg, D. and Missiakas, D. (2002) Thiol-disulfide exchange in an immunoglobulin-like fold: structure of the N-terminal domain of DsbD. *Biochemistry*, **41**, 6920-6927.

Grauschopf, U., Fritz, A. and Glockshuber, R. (2003) Mechanism of the electron transfer catalyst DsbB from Escherichia coli. *Embo J.*, **22**, 3503-3513.

Grauschopf, U., Winther, J.R., Korber, P., Zander, T., Dallinger, P. and Bardwell, J.C. (1995) Why is DsbA such an oxidizing disulfide catalyst? *Cell*, **83**, 947-955.

Gross, E., Sevier, C.S., Vala, A., Kaiser, C.A. and Fass, D. (2002) A new FAD-binding fold and intersubunit disulfide shuttle in the thiol oxidase Erv2p. *Nat. Struct. Biol.*, **9**, 61-67.

Guo, L., Nakamura, K., Lynch, J., Opas, M., Olson, E.N., Agellon, L.B. and Michalak, M. (2002) Cardiac-specific expression of calcineurin reverses embryonic lethality in calreticulin-deficient mouse. *J Biol Chem*, **277**, 50776-50779.

Haas, I.G. and Wabl, M. (1983) Immunoglobulin heavy chain binding protein. *Nature*, **306**, 387-389.

Haebel, P.W., Goldstone, D., Katzen, F., Beckwith, J. and Metcalf, P. (2002) The disulfide bond isomerase DsbC is activated by an immunoglobulin-fold thiol oxidoreductase: crystal structure of the DsbC-DsbDalpha complex. *Embo J.*, **21**, 4774-4784.

Hammond, C., Braakman, I. and Helenius, A. (1994) Role of N-linked oligosaccharide recognition, glucose trimming, and calnexin in glycoprotein folding and quality control. *Proc. Natl. Acad. Sci. USA*, **91**, 913-917.

Hammond, C. and Helenius, A. (1994a) Folding of VSV G protein: sequential interaction with BiP and calnexin. *Science*, **266**, 456-458.

Hammond, C. and Helenius, A. (1994b) Quality control in the secretory pathway: retention of a misfolded viral membrane glycoprotein involves cycling between the ER, intermediate compartment, and Golgi apparatus. *J. Cell Biol.*, **126**, 41-52.

Hartl, F.U. and Hayer-Hartl, M. (2002) Molecular chaperones in the cytosol: from nascent chain to folded protein. *Science*, **295**, 1852-1858.

Hauri, H., Appenzeller, C., Kuhn, F. and Nufer, O. (2000) Lectins and traffic in the secretory pathway. *FEBS Lett.*, **476**, 32-37.

Hawkins, H.C. and Freedman, R.B. (1991) The reactivities and ionization properties of the active-site dithiol groups of mammalian protein disulphide-isomerase. *Biochem J*, **275 (Pt 2)**, 335-339.

Hayano, T. and Kikuchi, M. (1995a) Cloning and sequencing of the cDNA encoding human P5. *Gene*, **164**, 377-378.

Hayano, T. and Kikuchi, M. (1995b) Molecular cloning of the cDNA encoding a novel protein disulfide isomerase-related protein (PDIR). *FEBS Lett*, **372**, 210-214.

Hebert, D.N., Foellmer, B. and Helenius, A. (1995) Glucose trimming and reglucosylation determine glycoprotein association with calnexin in the endoplasmic reticulum. *Cell*, **81**, 425-433.

Hebert, D.N., Foellmer, B. and Helenius, A. (1996) Calnexin and calreticulin promote folding, delay oligomerization and suppress degradation of influenza hemagglutinin in microsomes. *EMBO J.*, **15**, 2961-2968.

Hebert, D.N., Zhang, J.X., Chen, W., Foellmer, B. and Helenius, A. (1997) The number and location of glycans on influenza hemagglutinin determine folding and association with calnexin and calreticulin. *J. Cell Biol.*, **139**, 613-623.

Helenius, A. and Aebi, M. (2001) Intracellular functions of N-linked glycans. *Science*, **291**, 2364-2369.

Helenius, A., Trombetta, E.S., Hebert, D.N. and Simons, J.F. (1997) Calnexin, calreticulin and the folding of glycoproteins. *Trends Cell Biol.*, **7**, 193-200.

Hennecke, J., Spleiss, C. and Glockshuber, R. (1997) Influence of acidic residues and the kink in the active-site helix on the properties of the disulfide oxidoreductase DsbA. *J Biol Chem*, **272**, 189-195.

Hesterkamp, T. and Bukau, B. (1996) Identification of the prolyl isomerase domain of Escherichia coli trigger factor. *FEBS Lett*, **385**, 67-71.

High, S., Lecomte, F.J., Russell, S.J., Abell, B.M. and Oliver, J.D. (2000) Glycoprotein folding in the endoplasmic reticulum: a tale of three chaperones? *FEBS Lett.*, **476**, 38-41.

Hillson, D.A., Lambert, N. and Freedman, R.B. (1984) Formation and isomerization of disulfide bonds in proteins: protein disulfide-isomerase. *Methods Enzymol*, **107**, 281-294.

Hiniker, A. and Bardwell, J.C. (2004) In vivo substrate specificity of periplasmic disulfide oxidoreductases. *J Biol Chem*, **279**, 12967-12973.

Hirano, N., Shibasaki, F., Sakai, R., Tanaka, T., Nishida, J., Yazaki, Y., Takenawa, T. and Hirai, H. (1995) Molecular cloning of the human glucose-regulated protein ERp57/GRP58, a thiol-dependent reductase. Identification of its secretory form and inducible expression by the oncogenic transformation. *Eur. J. Biochem.*, **234**, 336-342.

Ho, S.C., Rajagopalan, S., Chaudhuri, S., Shieh, C.C., Brenner, M.B. and Pillai, S. (1999) Membrane anchoring of calnexin facilitates its interaction with its targets. *Mol. Immunol.*, **36**, 1-12.

Ho, S.N., Hunt, H.D., Horton, R.M., Pullen, J.K. and Pease, L.R. (1989) Site-directed mutagenesis by overlap extension using the polymerase chain reaction. *Gene*, **77**, 51-59.

Holmgren, A. (1979) Thioredoxin catalyzes the reduction of insulin disulfides by dithiothreitol and dihydrolipoamide. *J. Biol. Chem.*, **254**, 9627-9632.

Holst, B., Tachibana, C. and Winther, J.R. (1997) Active site mutations in yeast protein disulfide isomerase cause dithiothreitol sensitivity and a reduced rate of protein folding in the endoplasmic reticulum. *J Cell Biol*, **138**, 1229-1238.

Hosokawa, N., Wada, I., Hasegawa, K., Yorihuzi, T., Tremblay, L.O., Herscovics, A. and Nagata, K. (2001) A novel ER alpha-mannosidase-like protein accelerates ER-associated degradation. *EMBO Rep.*, **2**, 415-422.

Houen, G. and Koch, C. (1994) Human placental calreticulin: purification, characterization and association with other proteins. *Acta Chem Scand*, **48**, 905-911.

Huber-Wunderlich, M. and Glockshuber, R. (1998) A single dipeptide sequence modulates the redox properties of a whole enzyme family. *Fold. Des.*, **3**, 161-171.

Humphreys, D.P., Weir, N., Mountain, A. and Lund, P.A. (1995) Human protein disulfide isomerase functionally complements a dsbA mutation and enhances the yield of pectate lyase C in Escherichia coli. *J Biol Chem*, **270**, 28210-28215.

Hurtley, S.M. and Helenius, A. (1989) Protein oligomerization in the endoplasmic reticulum. *Annu. Rev. Cell Biol.*, **5**, 277-307.

Hwang, C., Sinskey, A.J. and Lodish, H.F. (1992) Oxidized redox state of glutathione in the endoplasmic reticulum. *Science*, **257**, 1496-1502.

Ihara, Y., Cohen-Doyle, M.F., Saito, Y. and Williams, D.B. (1999) Calnexin discriminates between protein conformational states and functions as a molecular chaperone in vitro. *Mol. Cell*, **4**, 331-341.

Jackson, M.R., Cohen-Doyle, M.F., Peterson, P.A. and Williams, D.B. (1994) Regulation of MHC class I transport by the molecular chaperone, calnexin (p88, IP90). *Science*, **263**, 384-387.

Jakob, C.A., Bodmer, D., Spirig, U., Battig, P., Marcil, A., Dignard, D., Bergeron, J.J., Thomas, D.Y. and Aebi, M. (2001) Htm1p, a mannosidase-like protein, is involved in glycoprotein degradation in yeast. *EMBO Rep.*, **2**, 423-430.

Joly, J.C. and Swartz, J.R. (1997) In vitro and in vivo redox states of the Escherichia coli periplasmic oxidoreductases DsbA and DsbC. *Biochemistry*, **36**, 10067-10072.

Jonda, S., Huber-Wunderlich, M., Glockshuber, R. and Mossner, E. (1999) Complementation of DsbA deficiency with secreted thioredoxin variants reveals the crucial role of an efficient dithiol oxidant for catalyzed protein folding in the bacterial periplasm. *Embo J.*, **18**, 3271-3281.

Kadokura, H., Tian, H., Zander, T., Bardwell, J.C. and Beckwith, J. (2004) Snapshots of DsbA in Action: Detection of Proteins in the Process of Oxidative Folding. *Science*, **303**, 534-537.

Kang, S.J. and Cresswell, P. (2002) Calnexin, calreticulin and ERp57 cooperate in disulfide bond formation in human CD1d heavy chain. *J. Biol. Chem.*, 44838–44844.

Kapoor, M., Ellgaard, L., Gopalakrishnapai, J., Schirra, C., Gemma, E., Oscarson, S., Helenius, A. and Surolia, A. (2004) Mutational Analysis Provides Molecular Insight into the Carbohydrate-Binding Region of Calreticulin: Pivotal Roles of Tyrosine-109 and Aspartate-135 in Carbohydrate Recognition. *Biochemistry*, **43**, 97-106.

Kapoor, M., Srinivas, H., Kandiah, E., Gemma, E., Ellgaard, L., Oscarson, S., Helenius, A. and Surolia, A. (2003) Interactions of substrate with calreticulin, an endoplasmic reticulum chaperone. *J Biol Chem*, **278**, 6194-6200.

Katti, S.K., LeMaster, D.M. and Eklund, H. (1990) Crystal structure of thioredoxin from Escherichia coli at 1.68 A resolution. *J. Mol. Biol.*, **212**, 167-184.

Kemmink, J., Darby, N.J., Dijkstra, K., Nilges, M. and Creighton, T.E. (1996) Structure determination of the N-terminal thioredoxin-like domain of protein disulfide isomerase using multidimensional heteronuclear 13C/15N NMR spectroscopy. *Biochemistry*, **35**, 7684-7691.

Kemmink, J., Dijkstra, K., Mariani, M., Scheek, R.M., Penka, E., Nilges, M. and Darby, N.J. (1999) The structure in solution of the b domain of protein disulfide isomerase. *J. Biomol. NMR*, **13**, 357-368.

Khanna, N.C., Tokuda, M. and Waisman, D.M. (1986) Conformational changes induced by binding of divalent cations to calregulin. *J. Biol. Chem.*, **261**, 8883-8887.

Kim, J.H., Kim, S.J., Jeong, D.G., Son, J.H. and Ryu, S.E. (2003) Crystal structure of DsbDgamma reveals the mechanism of redox potential shift and substrate specificity(1). *FEBS Lett.*, **543**, 164-169.

Klappa, P., Ruddock, L.W., Darby, N.J. and Freedman, R.B. (1998) The b' domain provides the principal peptide-binding site of protein disulfide isomerase but all domains contribute to binding of misfolded proteins. *EMBO J.*, **17**, 927-935.

Knoblach, B., Keller, B.O., Groenendyk, J., Aldred, S., Zheng, J., Lemire, B.D., Li, L. and Michalak, M. (2003) ERp19 and ERp46, new members of the thioredoxin family of endoplasmic reticulum proteins. *Mol. Cell Proteomics*, **2**, 1104-1119.

Kopito, R.R. and Ron, D. (2000) Conformational disease. *Nat. Cell Biol.*, **2**, E207-209.

Koradi, R., Billeter, M. and Wüthrich, K. (1996) MOLMOL: A program for display and analysis of macromolecular structures. *J. Mol. Graph.*, **14**, 51-55.

Kornfeld, R. and Kornfeld, S. (1985) Assembly of asparagine-linked oligosaccharides. *Annu. Rev. Biochem.*, **54**, 631-664.

Kortemme, T., Darby, N.J. and Creighton, T.E. (1996) Electrostatic interactions in the active site of the N-terminal thioredoxin-like domain of protein disulfide isomerase. *Biochemistry*, **35**, 14503-14511.

Krause, G., Lundstrom, J., Barea, J.L., Pueyo de la Cuesta, C. and Holmgren, A. (1991) Mimicking the active site of protein disulfide-isomerase by substitution of proline 34 in Escherichia coli thioredoxin. *J. Biol. Chem.*, **266**, 9494-9500.

Laboissiere, M.C., Sturley, S.L. and Raines, R.T. (1995) The essential function of protein-disulfide isomerase is to unscramble non-native disulfide bonds. *J Biol Chem*, **270**, 28006-28009.

Labriola, C., Cazzulo, J.J. and Parodi, A.J. (1995) Retention of glucose units added by the UDP-GLC:glycoprotein glucosyltransferase delays exit of glycoproteins from the endoplasmic reticulum. *J. Cell Biol.*, **130**, 771-779.

Labriola, C., Cazzulo, J.J. and Parodi, A.J. (1999) Trypanosoma cruzi calreticulin is a lectin that binds monoglucosylated oligosaccharides but not protein moieties of glycoproteins. *Mol. Biol. Cell*, **10**, 1381-1394.

LaMantia, M., Miura, T., Tachikawa, H., Kaplan, H.A., Lennarz, W.J. and Mizunaga, T. (1991) Glycosylation site binding protein and protein disulfide isomerase are identical and essential for cell viability in yeast. *Proc Natl Acad Sci U S A*, **88**, 4453-4457.

Lappi, A.K., Lensink, M.F., Alanen, H.I., Salo, K.E., Lobell, M., Juffer, A.H. and Ruddock, L.W. (2004) A conserved arginine plays a role in the catalytic cycle of the protein disulphide isomerases. *J. Mol. Biol.*, **335**, 283-295.

Le Gall, S., Neuhof, A. and Rapoport, T. (2004) The endoplasmic reticulum membrane is permeable to small molecules. *Mol Biol Cell*, **15**, 447-455.

Leach, M.R., Cohen-Doyle, M.F., Thomas, D.Y. and Williams, D.B. (2002) Localization of the Lectin, ERp57 Binding, and Polypeptide Binding Sites of Calnexin and Calreticulin. *J. Biol. Chem.*, **277**, 29686-29697.

Levinthal, C. (1968) Are there pathways for protein folding? *J. Chim. Physique*, **65**, 44-45.

Li, J., Puceat, M., Perez-Terzic, C., Mery, A., Nakamura, K., Michalak, M., Krause, K.H. and Jaconi, M.E. (2002) Calreticulin reveals a critical Ca(2+) checkpoint in cardiac myofibrillogenesis. *J. Cell Biol.*, **158**, 103-113.

Liu, Y., Choudhury, P., Cabral, C.M. and Sifers, R.N. (1999) Oligosaccharide modification in the early secretory pathway directs the selection of a misfolded glycoprotein for degradation by the proteasome. *J. Biol. Chem.*, **274**, 5861-5867.

Lo Conte, L., Chothia, C. and Janin, J. (1999) The atomic structure of protein-protein recognition sites. *J Mol Biol*, **285**, 2177-2198.

Lumb, R.A. and Bulleid, N.J. (2002) Is protein disulfide isomerase a redox-dependent molecular chaperone? *Embo J*, **21**, 6763-6770.

Lundstrom, J. and Holmgren, A. (1993) Determination of the reduction-oxidation potential of the thioredoxin-like domains of protein disulfide-isomerase from the equilibrium with glutathione and thioredoxin. *Biochemistry*, **32**, 6649-6655.

Lyles, M.M. and Gilbert, H.F. (1991) Catalysis of the oxidative folding of ribonuclease A by protein disulfide isomerase: pre-steady-state kinetics and the utilization of the oxidizing equivalents of the isomerase. *Biochemistry*, **30**, 619-625.

Lyon, W.R. and Caparon, M.G. (2003) Trigger factor-mediated prolyl isomerization influences maturation of the Streptococcus pyogenes cysteine protease. *J. Bacteriol.*, **185**, 3661-3667.

Ma, Y. and Hendershot, L.M. (2001) The unfolding tale of the unfolded protein response. *Cell*, **107**, 827-830.

Martin, J.L., Bardwell, J.C. and Kuriyan, J. (1993) Crystal structure of the DsbA protein required for disulphide bond formation in vivo. *Nature*, **365**, 464-468.

Matsuo, Y., Akiyama, N., Nakamura, H., Yodoi, J., Noda, M. and Kizaka-Kondoh, S. (2001) Identification of a novel thioredoxin-related transmembrane protein. *J. Biol. Chem.*, **276**, 10032-10038.

Mazzarella, R.A., Srinivasan, M., Haugejorden, S.M. and Green, M. (1990) ERp72, an abundant luminal endoplasmic reticulum protein, contains three copies of the active site sequences of protein disulfide isomerase. *J Biol Chem*, **265**, 1094-1101.

McCarthy, A.A., Haebel, P.W., Torronen, A., Rybin, V., Baker, E.N. and Metcalf, P. (2000) Crystal structure of the protein disulfide bond isomerase, DsbC, from Escherichia coli. *Nat. Struct. Biol.*, **7**, 196-199.

McKay, D.B. (1993) Structure and mechanism of 70-kDa heat-shock-related proteins. *Adv Protein Chem*, **44**, 67-98.

Meng, X., Zhang, C., Chen, J., Peng, S., Cao, Y., Ying, K., Xie, Y. and Mao, Y. (2003) Cloning and identification of a novel cDNA coding thioredoxin-related transmembrane protein 2. *Biochem Genet*, **41**, 99-106.

Mesaeli, N., Nakamura, K., Zvaritch, E., Dickie, P., Dziak, E., Krause, K.H., Opas, M., MacLennan, D.H. and Michalak, M. (1999) Calreticulin is essential for cardiac development. *J. Cell Biol.*, **144**, 857-868.

Mezghrani, A., Fassio, A., Benham, A., Simmen, T., Braakman, I. and Sitia, R. (2001) Manipulation of oxidative protein folding and PDI redox state in mammalian cells. *EMBO J.*, **20**, 6288-6296.

Michalak, M., Corbett, E.F., Mesaeli, N., Nakamura, K. and Opas, M. (1999) Calreticulin: one protein, one gene, many functions. *Biochem. J.*, **344 Pt 2**, 281-292.

Michalak, M., Milner, R.E., Burns, K. and Opas, M. (1992) Calreticulin. *Biochem. J.*, **285**, 681-692.

Michalak, M., Robert Parker, J.M. and Opas, M. (2002) Ca2+ signaling and calcium binding chaperones of the endoplasmic reticulum. *Cell Calcium*, **32**, 269-278.

Missiakas, D., Schwager, F. and Raina, S. (1995) Identification and characterization of a new disulfide isomerase-like protein (DsbD) in Escherichia coli. *Embo J*, **14**, 3415-3424.

Molinari, M., Calanca, V., Galli, C., Lucca, P. and Paganetti, P. (2003) Role of EDEM in the release of misfolded glycoproteins from the calnexin cycle. *Science*, **299**, 1397-1400.

Molinari, M., Eriksson, K.K., Calanca, V., Galli, C., Cresswell, P., Michalak, M. and Helenius, A. (2004) Contrasting functions of calreticulin and calnexin in glycoprotein folding and ER quality control. *Mol Cell*, **13**, 125-135.

Molinari, M., Galli, C., Piccaluga, V., Pieren, M. and Paganetti, P. (2002) Sequential assistance of molecular chaperones and transient formation of covalent complexes during protein degradation from the ER. *J. Cell Biol.*, **158**, 247-257.

Molinari, M. and Helenius, A. (1999) Glycoproteins form mixed disulphides with oxidoreductases during folding in living cells. *Nature*, **402**, 90-93.

Molinari, M. and Helenius, A. (2000) Chaperone selection during glycoprotein translocation into the endoplasmic reticulum. *Science*, **288**, 331-333.

Nakatsukasa, K., Nishikawa, S., Hosokawa, N., Nagata, K. and Endo, T. (2001) Mnl1p, an alpha - mannosidase-like protein in yeast Saccharomyces cerevisiae, is required for endoplasmic reticulum-associated degradation of glycoproteins. *J. Biol. Chem.*, **276**, 8635-8638.

Nelson, J.W. and Creighton, T.E. (1994) Reactivity and ionization of the active site cysteine residues of DsbA, a protein required for disulfide bond formation in vivo. *Biochemistry*, **33**, 5974-5983.

Norgaard, P., Westphal, V., Tachibana, C., Alsoe, L., Holst, B. and Winther, J.R. (2001) Functional differences in yeast protein disulfide isomerases. *J Cell Biol*, **152**, 553-562.

O'Connor, S.E. and Imperiali, B. (1996) Modulation of protein structure and function by asparagine-linked glycosylation. *Chem. Biol.*, **3**, 803-812.

Oda, Y., Hosokawa, N., Wada, I. and Nagata, K. (2003) EDEM as an acceptor of terminally misfolded glycoproteins released from calnexin. *Science*, **299**, 1394-1397.

Oliver, J.D., Roderick, H.L., Llewellyn, D.H. and High, S. (1999) ERp57 functions as a subunit of specific complexes formed with the ER lectins calreticulin and calnexin. *Mol. Biol. Cell*, **10**, 2573-2582.

Oliver, J.D., van der Wal, F.J., Bulleid, N.J. and High, S. (1997) Interaction of the thiol-dependent reductase ERp57 with nascent glycoproteins. *Science*, **275**, 86-88.

Onuchic, J.N., Wolynes, P.G., Luthey-Schulten, Z. and Socci, N.D. (1995) Toward an outline of the topography of a realistic protein-folding funnel. *Proc Natl Acad Sci U S A*, **92**, 3626-3630.

Ora, A. and Helenius, A. (1995) Calnexin fails to associate with substrate proteins in glucosidase-deficient cell lines. *J. Biol. Chem.*, **270**, 26060-26062.

Ostermeier, M., De Sutter, K. and Georgiou, G. (1996) Eukaryotic protein disulfide isomerase complements Escherichia coli dsbA mutants and increases the yield of a heterologous secreted protein with disulfide bonds. *J. Biol. Chem.*, **271**, 10616-10622.

Ostwald, T.J. and MacLennan, D.H. (1974) Isolation of a high affinity calcium-binding protein from sarcoplasmic reticulum. *J. Biol. Chem.*, **249**, 974-979.

Ou, W.J., Bergeron, J.J., Li, Y., Kang, C.Y. and Thomas, D.Y. (1995) Conformational changes induced in the endoplasmic reticulum luminal domain of calnexin by Mg-ATP and Ca2+. *J. Biol. Chem.*, **270**, 18051-18059.

Ou, W.J., Cameron, P.H., Thomas, D.Y. and Bergeron, J.J. (1993) Association of folding intermediates of glycoproteins with calnexin during protein maturation. *Nature*, **364**, 771-776.

Ou, W.J., Thomas, D.Y., Bell, A.W. and Bergeron, J.J. (1992) Casein kinase II phosphorylation of signal sequence receptor alpha and the associated membrane chaperone calnexin. *J. Biol. Chem.*, **267**, 23789-23796.

Pagani, M., Fabbri, M., Benedetti, C., Fassio, A., Pilati, S., Bulleid, N.J., Cabibbo, A. and Sitia, R. (2000) Endoplasmic reticulum oxidoreductin 1-lbeta (ERO1-Lbeta), a human gene induced in the course of the unfolded protein response. *J. Biol. Chem.*, **275**, 23685-23692.

Pagani, M., Pilati, S., Bertoli, G., Valsasina, B. and Sitia, R. (2001) The C-terminal domain of yeast Ero1p mediates membrane localization and is essential for function. *FEBS Lett.*, **508**, 117-120.

Parlati, F., Dignard, D., Bergeron, J.J. and Thomas, D.Y. (1995) The calnexin homologue cnx1+ in Schizosaccharomyces pombe, is an essential gene which can be complemented by its soluble ER domain. *EMBO J.*, **14**, 3064-3072.

Parodi, A.J. (2000) Protein glucosylation and its role in protein folding. *Annu. Rev. Biochem.*, **69**, 69-93.

Patil, A.R., Thomas, C.J. and Surolia, A. (2000) Kinetics and the mechanism of interaction of the endoplasmic reticulum chaperone, calreticulin, with monoglucosylated (Glc1Man9GlcNAc2) substrate. *J. Biol. Chem.*, **275**, 24348-24356.

Pervushin, K., Braun, D., Fernandez, C. and Wüthrich, K. (2000) [^{15}N,^{1}H]/[^{13}C,^{1}H]-TROSY for simultaneous detection of backbone ^{15}N-^{1}H, aromatic ^{13}C-^{1}H and side-chain ^{15}N-^{1}H^{2} correlations in large proteins. *J. Biomol. NMR*, **17**, 195-202.

Pervushin, K., Riek, R., Wider, G. and Wüthrich, K. (1997) Attenuated T2 relaxation by mutual cancellation of dipole-dipole coupling and chemical shift anisotropy indicates an avenue to NMR structures of very large biological macromolecules in solution. *Proc. Natl. Acad. Sci. USA*, **94**, 12366-12371.

Peterson, J.R. and Helenius, A. (1999) In vitro reconstitution of calreticulin-substrate interactions. *J. Cell Sci.*, **112**, 2775-2784.

Peterson, J.R., Ora, A., Van, P.N. and Helenius, A. (1995) Transient, lectin-like association of calreticulin with folding intermediates of cellular and viral glycoproteins. *Mol. Biol. Cell*, **6**, 1173-1184.

Petrescu, A.J., Butters, T.D., Reinkensmeier, G., Petrescu, S., Platt, F.M., Dwek, R.A. and Wormald, M.R. (1997) The solution NMR structure of glucosylated N-glycans involved in the early stages of glycoprotein biosynthesis and folding. *EMBO J.*, **16**, 4302-4310.

Pihlajaniemi, T., Helaakoski, T., Tasanen, K., Myllyla, R., Huhtala, M.L., Koivu, J. and Kivirikko, K.I. (1987) Molecular cloning of the beta-subunit of human prolyl 4-hydroxylase. This subunit and protein disulphide isomerase are products of the same gene. *Embo J*, **6**, 643-649.

Pirneskoski, A., Ruddock, L.W., Klappa, P., Freedman, R.B., Kivirikko, K.I. and Koivunen, P. (2001) Domains b' and a' of protein disulfide isomerase fulfill the minimum requirement for function

as a subunit of prolyl 4-hydroxylase. The N- terminal domains a and b enhances this function and can be substituted in part by those of ERp57. *J. Biol. Chem.*, **276**, 11287-11293.

Pollard, M.G., Travers, K.J. and Weissman, J.S. (1998) Ero1p: a novel and ubiquitous protein with an essential role in oxidative protein folding in the endoplasmic reticulum. *Mol. Cell*, **1**, 171-182.

Pollock, S., Kozlov, G., Pelletier, M.F., Trempe, J.F., Jansen, G., Sitnikov, D., Bergeron, J.J., Gehring, K., Ekiel, I. and Thomas, D.Y. (2004) Specific interaction of ERp57 and calnexin determined by NMR spectroscopy and an ER two-hybrid system. *Embo J*, **23**, 1020-1029.

Radcliffe, C.M., Diedrich, G., Harvey, D.J., Dwek, R.A., Cresswell, P. and Rudd, P.M. (2002) Identification of specific glycoforms of major histocompatibility complex class I heavy chains suggests that class I peptide loading is an adaptation of the quality control pathway involving calreticulin and ERp57. *J Biol Chem*, **277**, 46415-46423.

Raje, S. and Thorpe, C. (2003) Inter-domain redox communication in flavoenzymes of the quiescin/sulfhydryl oxidase family: role of a thioredoxin domain in disulfide bond formation. *Biochemistry*, **42**, 4560-4568.

Rietsch, A., Bessette, P., Georgiou, G. and Beckwith, J. (1997) Reduction of the periplasmic disulfide bond isomerase, DsbC, occurs by passage of electrons from cytoplasmic thioredoxin. *J. Bacteriol.*, **179**, 6602-6608.

Ritter, C. and Helenius, A. (2000) Recognition of local glycoprotein misfolding by the ER folding sensor UDP-glucose:glycoprotein glucosyltransferase. *Nature Struct. Biol.*, **7**, 278-280.

Ritter, C., Quirin, K., Kowarik, M., and Helenius, A. (in preparation).

Rodan, A.R., Simons, J.F., Trombetta, E.S. and Helenius, A. (1996) N-linked oligosaccharides are necessary and sufficient for association of glycosylated forms of bovine RNase with calnexin and calreticulin. *EMBO J.*, **15**, 6921-6930.

Rozhkova, A., Stirnimann, C.U., Frei, P., Grauschopf, U., Brunisholz, R., Grutter, M.G., Capitani, G. and Glockshuber, R. (2004) Structural basis and kinetics of inter- and intramolecular disulfide exchange in the redox catalyst DsbD. *Embo J*, **23**, 1709-1719.

Rudenko, G., Nguyen, T., Chelliah, Y., Sudhof, T.C. and Deisenhofer, J. (1999) The structure of the ligand-binding domain of neurexin Ibeta: regulation of LNS domain function by alternative splicing. *Cell*, **99**, 93-101.

Russell, S.J., Ruddock, L.W., Salo, K.E., Oliver, J.D., Roebuck, Q.P., Llewellyn, D.H., Roderick, H.L., Koivunen, P., Myllyharju, J. and High, S. (2004) The primary substrate binding site in the b' domain of ERp57 is adapted for endoplasmic reticulum lectin association. *J Biol Chem*, **279**, 18861-18869.

Rutishauser, J. and Spiess, M. (2002) Endoplasmic reticulum storage diseases. *Swiss Med. Wkly.*, **132**, 211-222.

Saito, Y., Ihara, Y., Leach, M.R., Cohen-Doyle, M.F. and Williams, D.B. (1999) Calreticulin functions in vitro as a molecular chaperone for both glycosylated and non-glycosylated proteins. *EMBO J.*, **18**, 6718-6729.

Scherens, B., Dubois, E. and Messenguy, F. (1991) Determination of the sequence of the yeast YCL313 gene localized on chromosome III. Homology with the protein disulfide isomerase (PDI gene product) of other organisms. *Yeast*, **7**, 185-193.

Schrag, J.D., Bergeron, J.J., Li, Y., Borisova, S., Hahn, M., Thomas, D.Y. and Cygler, M. (2001) The structure of calnexin, an ER chaperone involved in quality control of protein folding. *Mol. Cell*, **8**, 633-644.

Schwaller, M., Wilkinson, B. and Gilbert, H.F. (2003) Reduction-reoxidation cycles contribute to catalysis of disulfide isomerization by protein-disulfide isomerase. *J Biol Chem*, **278**, 7154-7159.

Sevier, C.S., Cuozzo, J.W., Vala, A., Aslund, F. and Kaiser, C.A. (2001) A flavoprotein oxidase defines a new endoplasmic reticulum pathway for biosynthetic disulphide bond formation. *Nat. Cell Biol.*, **3**, 874-882.

Sevier, C.S. and Kaiser, C.A. (2002) Formation and transfer of disulphide bonds in living cells. *Nat. Rev. Mol. Cell Biol.*, **3**, 836-847.

Shaked, Z., Szajewski, R.P. and Whitesides, G.M. (1980) Rates of thiol-disulfide interchange reactions involving proteins and kinetic measurements of thiol pKa values. *Biochemistry*, **19**, 4156-4166.

Shaw, P.E. (2002) Peptidyl-prolyl isomerases: a new twist to transcription. *EMBO Rep*, **3**, 521-526.

Sheinerman, F.B., Norel, R. and Honig, B. (2000) Electrostatic aspects of protein-protein interactions. *Curr Opin Struct Biol*, **10**, 153-159.

Shen, Y., Meunier, L. and Hendershot, L.M. (2002) Identification and characterization of a novel endoplasmic reticulum (ER) DnaJ homologue, which stimulates ATPase activity of BiP in vitro and is induced by ER stress. *J. Biol. Chem.*, **277**, 15947-15956.

Shou, W., Aghdasi, B., Armstrong, D.L., Guo, Q., Bao, S., Charng, M.J., Mathews, L.M., Schneider, M.D., Hamilton, S.L. and Matzuk, M.M. (1998) Cardiac defects and altered ryanodine receptor function in mice lacking FKBP12. *Nature*, **391**, 489-492.

Silhavy, T.J., Casadaban, M.J., Shuman, H.A. and Beckwith, J.R. (1976) Conversion of beta-galactosidase to a membrane-bound state by gene fusion. *Proc. Natl. Acad. Sci. U S A*, **73**, 3423-3427.

Silvennoinen, L., Myllyharju, J., Ruoppolo, M., Orru, S., Caterino, M., Kivirikko, K.I. and Koivunen, P. (2004) Identification and characterization of structural domains of human ERp57: association with calreticulin requires several domains. *J Biol Chem*, **279**, 13607-13615.

Skowronek, M.H., Rotter, M. and Haas, I.G. (1999) Molecular characterization of a novel mammalian DnaJ-like Sec63p homolog. *Biol Chem*, **380**, 1133-1138.

Smith, M.J. and Koch, G.L. (1989) Multiple zones in the sequence of calreticulin (CRP55, calregulin, HACBP), a major calcium binding ER/SR protein. *EMBO J.*, **8**, 3581-3586.

Sone, M., Akiyama, Y. and Ito, K. (1997) Differential in vivo roles played by DsbA and DsbC in the formation of protein disulfide bonds. *J Biol Chem*, **272**, 10349-10352.

Spiro, R.G., Zhu, Q., Bhoyroo, V. and Soling, H.D. (1996) Definition of the lectin-like properties of the molecular chaperone, calreticulin, and demonstration of its copurification with endomannosidase from rat liver Golgi. *J. Biol. Chem.*, **271**, 11588-11594.

Srivastava, S.P., Chen, N.Q., Liu, Y.X. and Holtzman, J.L. (1991) Purification and characterization of a new isozyme of thiol:protein-disulfide oxidoreductase from rat hepatic microsomes. Relationship of this isozyme to cytosolic phosphatidylinositol-specific phospholipase C form 1A. *J Biol Chem*, **266**, 20337-20344.

Srivastava, S.P., Fuchs, J.A. and Holtzman, J.L. (1993) The reported cDNA sequence for phospholipase C alpha encodes protein disulfide isomerase, isozyme Q-2 and not phospholipase-C. *Biochem Biophys Res Commun*, **193**, 971-978.

Stafford, S.J. and Lund, P.A. (2000) Mutagenic studies on human protein disulfide isomerase by complementation of Escherichia coli dsbA and dsbC mutants. *FEBS Lett*, **466**, 317-322.

Stamnes, M.A., Shieh, B.H., Chuman, L., Harris, G.L. and Zuker, C.S. (1991) The cyclophilin homolog ninaA is a tissue-specific integral membrane protein required for the proper synthesis of a subset of Drosophila rhodopsins. *Cell*, **65**, 219-227.

Stronge, V.S., Saito, Y., Ihara, Y. and Williams, D.B. (2001) Relationship between calnexin and BiP in suppressing aggregation and promoting refolding of protein and glycoprotein substrates. *J. Biol. Chem.*, **276**, 39779-39787.

Sullivan, D.C., Huminiecki, L., Moore, J.W., Boyle, J.J., Poulsom, R., Creamer, D., Barker, J. and Bicknell, R. (2003) EndoPDI, a novel protein disulphide isomerase-like protein that is preferentially expressed in endothelial cells acts as a stress survival factor. *J. Biol. Chem.*, **278**, 47079-47088.

Swanton, E., High, S. and Woodman, P. (2003) Role of calnexin in the glycan-independent quality control of proteolipid protein. *Embo J*, **22**, 2948-2958.

Szajewski, R.P. and Whitesides, G.M. (1980) Rate constants and equilibrium constants for thiol-disulfide interchange reactions involving glutathione. *J. Am. Chem. Soc.*, **102**, 2011-2026.

Tachibana, C. and Stevens, T.H. (1992) The yeast EUG1 gene encodes an endoplasmic reticulum protein that is functionally related to protein disulfide isomerase. *Mol. Cell Biol.*, **12**, 4601-4611.

Tachikawa, H., Funahashi, W., Takeuchi, Y., Nakanishi, H., Nishihara, R., Katoh, S., Gao, X.D., Mizunaga, T. and Fujimoto, D. (1997) Overproduction of Mpd2p suppresses the lethality of protein disulfide isomerase depletion in a CXXC sequence dependent manner. *Biochem Biophys Res Commun*, **239**, 710-714.

Tachikawa, H., Takeuchi, Y., Funahashi, W., Miura, T., Gao, X.D., Fujimoto, D., Mizunaga, T. and Onodera, K. (1995) Isolation and characterization of a yeast gene, MPD1, the overexpression of which suppresses inviability caused by protein disulfide isomerase depletion. *FEBS Lett*, **369**, 212-216.

Thies, M.J., Mayer, J., Augustine, J.G., Frederick, C.A., Lilie, H. and Buchner, J. (1999) Folding and association of the antibody domain CH3: prolyl isomerization preceeds dimerization. *J Mol Biol*, **293**, 67-79.

Thomas, P.J., Qu, B.H. and Pedersen, P.L. (1995) Defective protein folding as a basis of human disease. *Trends Biochem. Sci.*, **20**, 456-459.

Thorpe, C., Hoober, K.L., Raje, S., Glynn, N.M., Burnside, J., Turi, G.K. and Coppock, D.L. (2002) Sulfhydryl oxidases: emerging catalysts of protein disulfide bond formation in eukaryotes. *Arch Biochem Biophys*, **405**, 1-12.

Tjoelker, L.W., Seyfried, C.E., Eddy, R.L., Jr., Byers, M.G., Shows, T.B., Calderon, J., Schreiber, R.B. and Gray, P.W. (1994) Human, mouse, and rat calnexin cDNA cloning: identification of potential calcium binding motifs and gene localization to human chromosome 5. *Biochemistry*, **33**, 3229-3236.

Tortorella, D., Story, C.M., Huppa, J.B., Wiertz, E.J., Jones, T.R., Bacik, I., Bennink, J.R., Yewdell, J.W. and Ploegh, H.L. (1998) Dislocation of type I membrane proteins from the ER to the cytosol is sensitive to changes in redox potential. *J. Cell Biol.*, **142**, 365-376.

Travers, K.J., Patil, C.K., Wodicka, L., Lockhart, D.J., Weissman, J.S. and Walter, P. (2000) Functional and genomic analyses reveal an essential coordination between the unfolded protein response and ER-associated degradation. *Cell*, **101**, 249-258.

Tsai, B. and Rapoport, T.A. (2002) Unfolded cholera toxin is transferred to the ER membrane and released from protein disulfide isomerase upon oxidation by Ero1. *J. Cell Biol.*, **159**, 207-216.

Tsai, B., Rodighiero, C., Lencer, W.I. and Rapoport, T.A. (2001) Protein disulfide isomerase acts as a redox-dependent chaperone to unfold cholera toxin. *Cell*, **104**, 937-948.

Tsai, B., Ye, Y. and Rapoport, T.A. (2002) Retro-translocation of proteins from the endoplasmic reticulum into the cytosol. *Nat. Rev. Mol. Cell Biol.*, **3**, 246-255.

Tu, B.P., Ho-Schleyer, S.C., Travers, K.J. and Weissman, J.S. (2000) Biochemical basis of oxidative protein folding in the endoplasmic reticulum. *Science*, **290**, 1571-1574.

Tu, B.P. and Weissman, J.S. (2002) The FAD- and O(2)-dependent reaction cycle of Ero1-mediated oxidative protein folding in the endoplasmic reticulum. *Mol. Cell*, **10**, 983-994.

Urade, R., Oda, T., Ito, H., Moriyama, T., Utsumi, S. and Kito, M. (1997) Functions of characteristic Cys-Gly-His-Cys (CGHC) and Gln-Glu-Asp-Leu (QEDL) motifs of microsomal ER-60 protease. *J Biochem (Tokyo)*, **122**, 834-842.

Van der Wal, F.J., Oliver, J.D. and High, S. (1998) The transient association of ERp57 with N-glycosylated proteins is regulated by glucose trimming. *Eur. J. Biochem.*, **256**, 51-59.

van Leeuwen, J.E. and Kearse, K.P. (1996) Deglucosylation of N-linked glycans is an important step in the dissociation of calreticulin-class I-TAP complexes. *Proc. Natl. Acad. Sci. USA*, **93**, 13997-14001.

Vassilakos, A., Michalak, M., Lehrman, M.A. and Williams, D.B. (1998) Oligosaccharide binding characteristics of the molecular chaperones calnexin and calreticulin. *Biochemistry*, **37**, 3480-3490.

Wada, I., Imai, S., Kai, M., Sakane, F. and Kanoh, H. (1995) Chaperone function of calreticulin when expressed in the endoplasmic reticulum as the membrane-anchored and soluble forms. *J. Biol. Chem.*, **270**, 20298-20304.

Wada, I., Kai, M., Imai, S., Sakane, F. and Kanoh, H. (1997) Promotion of transferrin folding by cyclic interactions with calnexin and calreticulin. *EMBO J.*, **16**, 5420-5432.

Wada, I., Rindress, D., Cameron, P.H., Ou, W.J., Doherty, J.J., 2nd, Louvard, D., Bell, A.W., Dignard, D., Thomas, D.Y. and Bergeron, J.J. (1991) SSR alpha and associated calnexin are major calcium binding proteins of the endoplasmic reticulum membrane. *J. Biol. Chem.*, **266**, 19599-19610.

Walker, K.W. and Gilbert, H.F. (1997) Scanning and escape during protein-disulfide isomerase-assisted protein folding. *J Biol Chem*, **272**, 8845-8848.

Walter, S. and Buchner, J. (2002) Molecular chaperones--cellular machines for protein folding. *Angew Chem Int Ed Engl*, **41**, 1098-1113.

Wang, Q. and Chang, A. (1999) Eps1, a novel PDI-related protein involved in ER quality control in yeast. *EMBO J.*, **18**, 5972-5982.

Ware, F.E., Vassilakos, A., Peterson, P.A., Jackson, M.R., Lehrman, M.A. and Williams, D.B. (1995) The molecular chaperone calnexin binds Glc1Man9GlcNAc2 oligosaccharide as an initial step in recognizing unfolded glycoproteins. *J. Biol. Chem.*, **270**, 4697-4704.

Weber-Ban, E.U., Reid, B.G., Miranker, A.D. and Horwich, A.L. (1999) Global unfolding of a substrate protein by the Hsp100 chaperone ClpA. *Nature*, **401**, 90-93.

Weichsel, A., Gasdaska, J.R., Powis, G. and Montfort, W.R. (1996) Crystal structures of reduced, oxidized, and mutated human thioredoxins: evidence for a regulatory homodimer. *Structure*, **4**, 735-751.

Wetterau, J.R., Combs, K.A., Spinner, S.N. and Joiner, B.J. (1990) Protein disulfide isomerase is a component of the microsomal triglyceride transfer protein complex. *J Biol Chem*, **265**, 9801-9807.

Williams, A., Peh, C.A. and Elliott, T. (2002) The cell biology of MHC class I antigen presentation. *Tissue Antigens*, **59**, 3-17.

Williams, C.H. (1992) *Chemistry and biochemistry of flavoenzymes*. CRC Press, Boca Raton, FL.

Wilson, C.M., Farmery, M.R. and Bulleid, N.J. (2000) Pivotal role of calnexin and mannose trimming in regulating the endoplasmic reticulum-associated degradation of major histocompatibility complex class I heavy chain. *J Biol Chem*, **275**, 21224-21232.

Wong, H.N., Ward, M.A., Bell, A.W., Chevet, E., Bains, S., Blackstock, W.P., Solari, R., Thomas, D.Y. and Bergeron, J.J. (1998) Conserved in vivo phosphorylation of calnexin at casein kinase II sites as well as a protein kinase C/proline-directed kinase site. *J. Biol. Chem.*, **273**, 17227-17235.

Wormald, M.R. and Dwek, R.A. (1999) Glycoproteins: glycan presentation and protein-fold stability. *Structure Fold. Des.*, **7**, R155-160.

Wormald, M.R., Petrescu, A.J., Pao, Y.L., Glithero, A., Elliott, T. and Dwek, R.A. (2002) Conformational studies of oligosaccharides and glycopeptides: complementarity of NMR, X-ray crystallography, and molecular modelling. *Chem. Rev.*, **102**, 371-386.

Wunderlich, M. and Glockshuber, R. (1993) Redox properties of protein disulfide isomerase (DsbA) from Escherichia coli. *Protein Sci.*, **2**, 717-726.

Wunderlich, M., Jaenicke, R. and Glockshuber, R. (1993) The redox properties of protein disulfide isomerase (DsbA) of Escherichia coli result from a tense conformation of its oxidized form. *J. Mol. Biol.*, **233**, 559-566.

Yamashita, K., Hara-Kuge, S. and Ohkura, T. (1999) Intracellular lectins associated with N-linked glycoprotein traffic. *Biochim. Biophys. Acta.*, **1473**, 147-160.

Yoshida, H., Matsui, T., Hosokawa, N., Kaufman, R.J., Nagata, K. and Mori, K. (2003) A time-dependent phase shift in the mammalian unfolded protein response. *Dev Cell*, **4**, 265-271.

Yu, M., Haslam, R.H. and Haslam, D.B. (2000) HEDJ, an Hsp40 co-chaperone localized to the endoplasmic reticulum of human cells. *J Biol Chem*, **275**, 24984-24992.

Zahn, R., Buckle, A.M., Perrett, S., Johnson, C.M., Corrales, F.J., Golbik, R. and Fersht, A.R. (1996) Chaperone activity and structure of monomeric polypeptide binding domains of GroEL. *Proc. Natl. Acad. Sci. U S A*, **93**, 15024-15029.

Zapun, A., Bardwell, J.C. and Creighton, T.E. (1993) The reactive and destabilizing disulfide bond of DsbA, a protein required for protein disulfide bond formation in vivo. *Biochemistry*, **32**, 5083-5092.

Zapun, A., Creighton, T.E., Rowling, P.J. and Freedman, R.B. (1992) Folding in vitro of bovine pancreatic trypsin inhibitor in the presence of proteins of the endoplasmic reticulum. *Proteins*, **14**, 10-15.

Zapun, A., Darby, N.J., Tessier, D.C., Michalak, M., Bergeron, J.J. and Thomas, D.Y. (1998) Enhanced catalysis of ribonuclease B folding by the interaction of calnexin or calreticulin with ERp57. *J. Biol. Chem.*, **273**, 6009-6012.

Zapun, A., Missiakas, D., Raina, S. and Creighton, T.E. (1995) Structural and functional characterization of DsbC, a protein involved in disulfide bond formation in Escherichia coli. *Biochemistry*, **34**, 5075-5089.

Zapun, A., Petrescu, S.M., Rudd, P.M., Dwek, R.A., Thomas, D.Y. and Bergeron, J.J. (1997) Conformation-independent binding of monoglucosylated ribonuclease B to calnexin. *Cell*, **88**, 29-38.

Appendix

Unpublished Materials and Methods

Construction of CRTΔEB

A mutant of the CRT P-domain that potentially lacks ERp57 binding was generated by PCR overlap extension (Ho et al., 1989) using CRT(189-288), (Ellgaard et al., 2001a), as a template. The two fragments resulted using the primers T7 and EbdelR, 5- CAC TGG TGG TTC CCA CTC TCC ATG CAT CAG TTC TTT CCA CCA CGA AG; and T7rev and EbdelF, 5'- GAC CCT GAT GCT AAG AAG CCT TCG TGG TGG AAA GAA CTG ATG CAT G, respectively. The combined PCR product was digested with BamHI and EcoRI and cloned into a pRSET A- derived *E. coli* expression vector (Zahn et al., 1996) and named CRTΔEB.

Construction of CRT P-domain mutants for E. coli expression

A construct of CRT lacking the internal BamHI site was generated by PCR using the plasmid GST-CRT1-337 (Peterson and Helenius, 1999) as a template and the phosphorylated primers CRT-BamF, 5'- GGACCCTGACGCTGCCAA and CRT-BamR, 5'-TTAATCTTCTTGGGCGGCAGAAAG. The resulting PCR product comprising the entire vector with the *CRT* gene was blunt-end ligated. Next, the vector was digested with BamHI and HindIII and ligated into the same sites of a pRSET A-derived *E. coli* expression vector (Zahn et al., 1996) and named CRT-Bam.

Two mutants of CRT were generated that lack the P-domain and instead contain one of two linkers; CRTΔPL bears the 10 amino acid long linker SEASGTSSTS and CRTΔPH the 10 amino acid long linker GSHHHHHHSG. The vector CRT-Bam was used as a template in a PCR reaction with the phosphorylated primers CRTlinkerF, 5'-ACC ACC AGC ACC AGC CCC GAT GCG AAT ATC TAT G and CRTlinkerR, 5'-GCC GCT GGC TTC GCT GGG CGG CAG AAA GTC CCA; and CRTGSH6SGF, 5'-CAC CAC CAC AGC GGC CCC GAT GCG AAT ATC TAT G and CRTGSH6SGR, 5'-GTG GTG GTG GCT GCC GGG CGG CAG AAA GTC CCA, to yield two PCR fragments respectively. The resulting PCR products were again blunt-end ligated and named CRTΔPL and CRTΔPH.

To generate a CRT construct that consists of a P-domain with only one type 1 repeat followed by one type 2 repeat, the first two type 1 repeats and the last two type

2 repeats were deleted from the wild-type CRT sequence. Thus, a version of CRT results that bears only the terminal type 12 repeat, which is the tip of the hairpin structure of the P-domain and also the region to which ERp57 binds. Using CRT-Bam as a template, two PCR fragments were generated with the phosphorylated primers CRT3.1F, 5'-GAG CAC ATC CCT GAC CCT and CRTStartR, 5'-GGG CGG CAG AAA GTC CCA; and CRT3.2R, 5'-CTT GTA TTC AGG ATT TTG AAT and CRTEndF, 5'-CCC GAT GCG AAT ATC TAT, respectively. Both resulting PCR fragments were blunt-end ligated and yielded one construct in which the two type 1 repeats were deleted and one construct in which the two type 2 repeats were deleted. Both resulting vectors were digested with EcoRV and PstI, and the so-derived fragment comprising parts of the P-domain was isolated and cleaved again with EarI. The respective fragments harbouring the deletions of either the type 1 or the type 2 repeats were isolated and three-way ligated into CRT-Bam that had previously been digested with EcoRV and PstI. The resulting construct was named CRTP1.

In order to obtain a CRT construct that has a P-domain with two type 1 repeats followed by two type 2 repeats, the middle type 1 repeat and the middle type 2 repeat were deleted from a wild-type CRT clone. The resulting CRT P-domain mutant construct thus also retains the tip 12 repeat as well as the 12 repeat that connects to the globular domain. Two PCR fragments were generated by PCR using CRT-Bam as a template and the phosphorylated primers CRT3.1F, 5'-GAG CAC ATC CCT GAC CCT and CRT1.1R, 5'-TCG TTC ATC CCA GTC TTC TGG; and CRT3.2R, 5'-CTT GTA TTC AGG ATT TTG AAT and CRT1.2F, 5'-GGT ACC TGG ATA CAC CCA, respectively. Both resulting PCR fragments were again blunt-end ligated and processed as described above for the generation of CRTP1. This construct was named CRTP2.

To generate a mutant of CRT that contained a P-domain with four type 1 repeats followed by four type two repeats, a type one repeat was inserted after the second type 1 repeat and a type 2 repeat after the first type 2 repeat. This extends the P-domain of CRT by one 12 repeat segment, thus mimicking the length of the CNX P-domain. Using CRT-Bam as a template, two PCR fragments were produced with the phosphorylated primers CRT+m2.1_3.1F, 5'-AGC AAA CCA GAA GAT TGG GAT AAA CCT GAG CAC ATC CCT GAC CCT and CRT+m2.1_2.1R, 5'-GTC GGT TGG ATC GTC GAT TTT AGC TGG CTT GTC CCA GTC CTC; and CRT+m2.2_3.2R, 5'-CTC GCG AGG TTT CCA CTC ACC CTT GTA TTC AGG

ATT TTG AAT C and CRT+m2.2_2.2F, 5'-ATC GAT AAT CCT GAC TAT AAA GGC GAA TGG AAG CCA CGT, respectively. The two resulting PCR fragments were blunt-end ligated and the construct was called CRTP4.

All constructs were verified to be correct by DNA sequencing.

Construction of CRT P-domain mutants for mammalian cell expression

A mammalian expression clone of CRT was generated by amplifying the full-length CRT gene from the template CMV-CRT (Peterson and Helenius, 1999) using the primers D3CRT_HindF, 5'-GCC AAG CTT ATG CTC CTT TCG GTG and D3CRT_XhoIR, 5'-GCC CTC GAG CTA CAG CTC ATC CTT. The resulting PCR fragment was digested with HindIII and XhoI and ligated into the corresponding sites of pcDNA3 (Invitrogen) and named mCRTwt.

To transfer the segments encoding the P-domain of CRTΔPH, CRTΔPL, CRTP1, CRTP2, CRTP4 and CRTΔEB, as well as the segment encoding the three point-mutations of the glycan binding site in CRTΔGB (Kapoor et al., 2004) to the mammalian expression vector mCRTwt, internal restriction sites in the CRT sequence were exploited. The three constructs CRTΔPH, CRTΔPL and CRTP1 were digested with EcoRV and EcoNI and ligated into mCRTwt, which had been treated with the same restriction enzymes. CRTP2 and CRTP4 were transferred using EcoRV and KpnI, CRTΔEB with BstXI and KpnI and CRTΔGB with BstBI and KpnI. The resulting constructs were named mCRTΔPH, mCRTΔPL, mCRTP1, mCRTP2, mCRTP4, mCRTΔEB and mCRTΔGB.

All constructs were verified to be correct by DNA sequencing.

Sequence alignments

ERp57 versus PDI

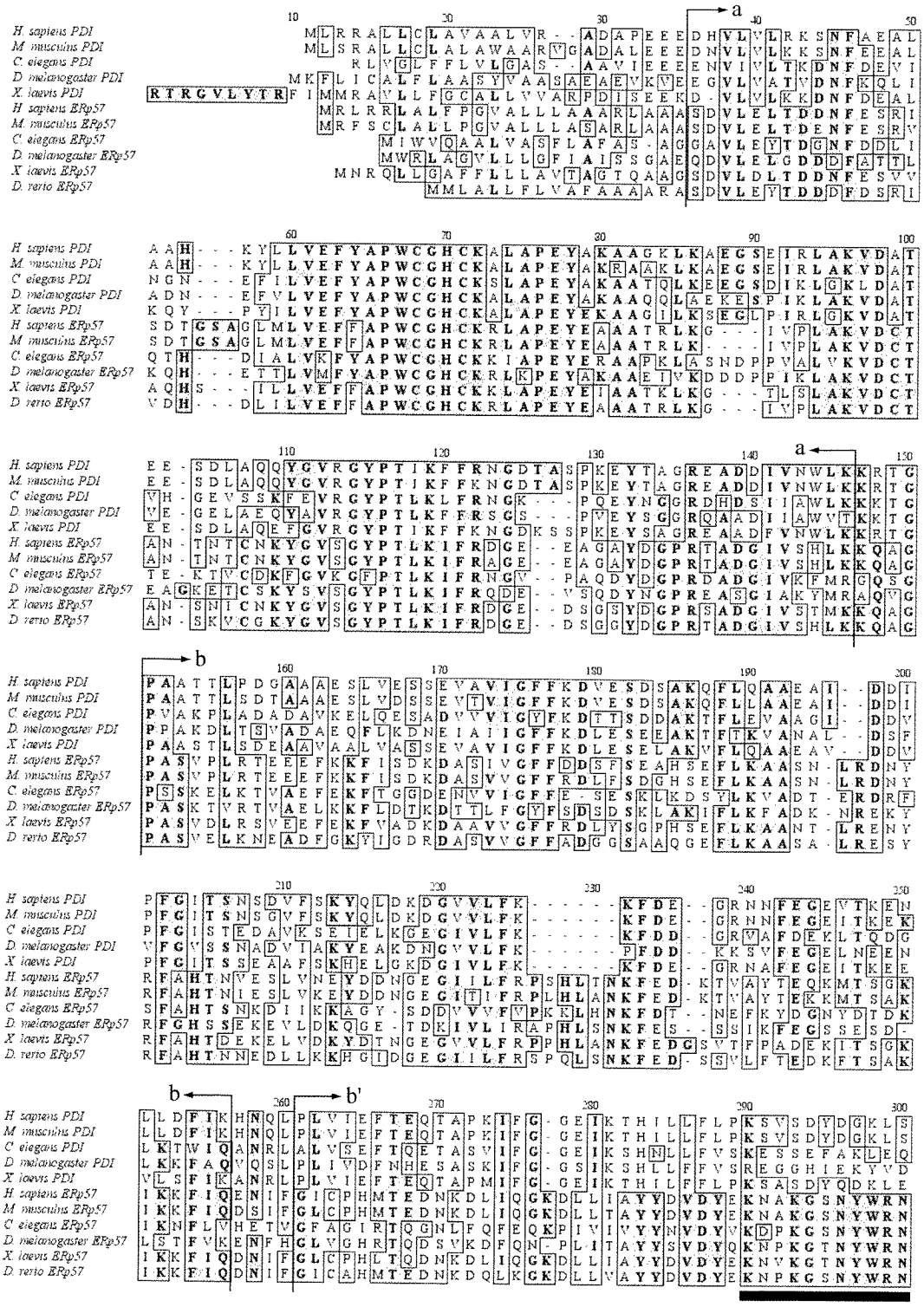

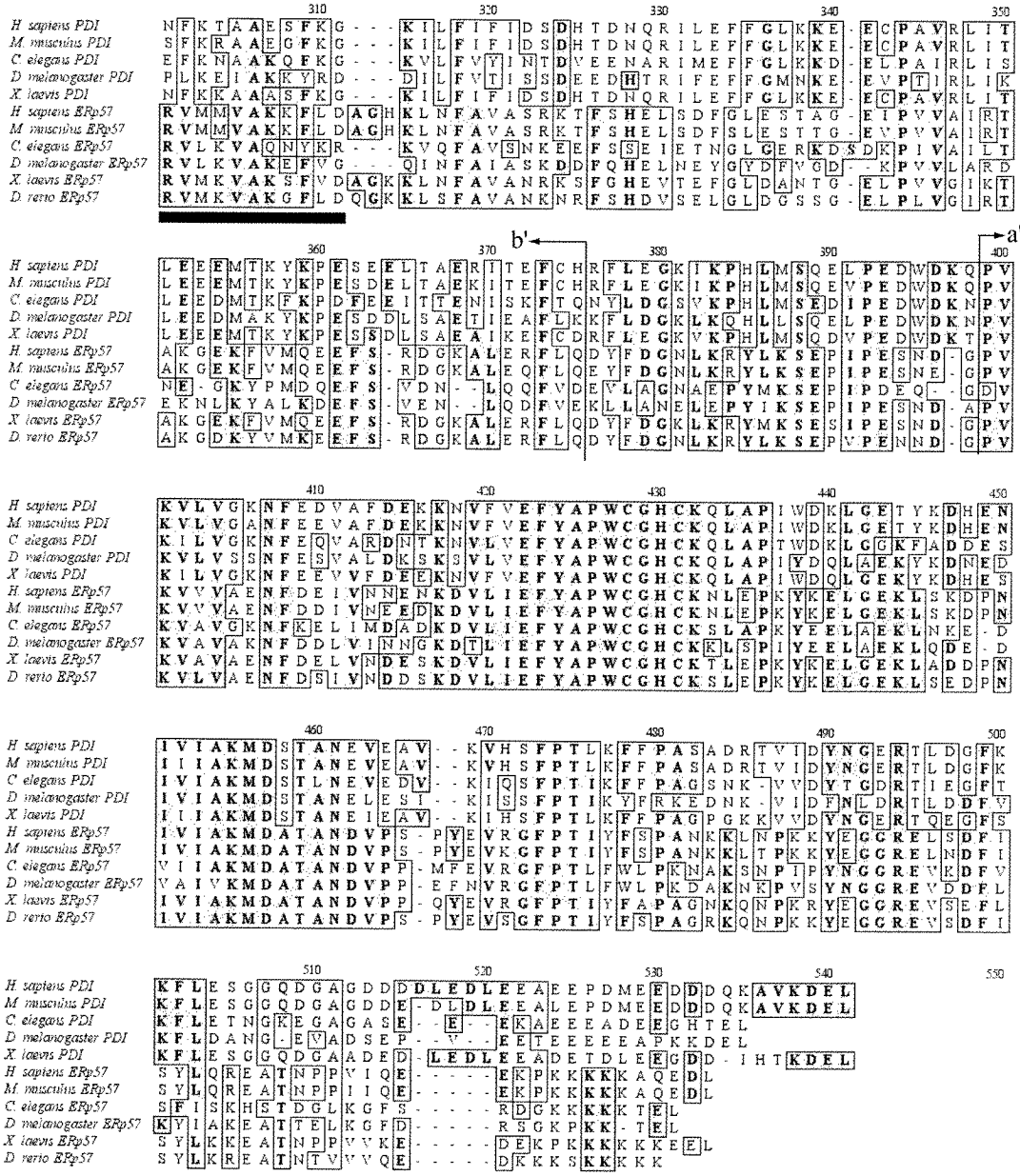

Fig. 6.1 Amino acid sequence alignment of ERp57 and PDI of various species. The domain boundaries as defined by (Ferrari and Söling, 1999) are labeled by arrows. The black bar denotes the area that shows a consensus sequence rich in basic amino acids in ERp57, which is absent in PDI.

Calreticulin versus calnexin

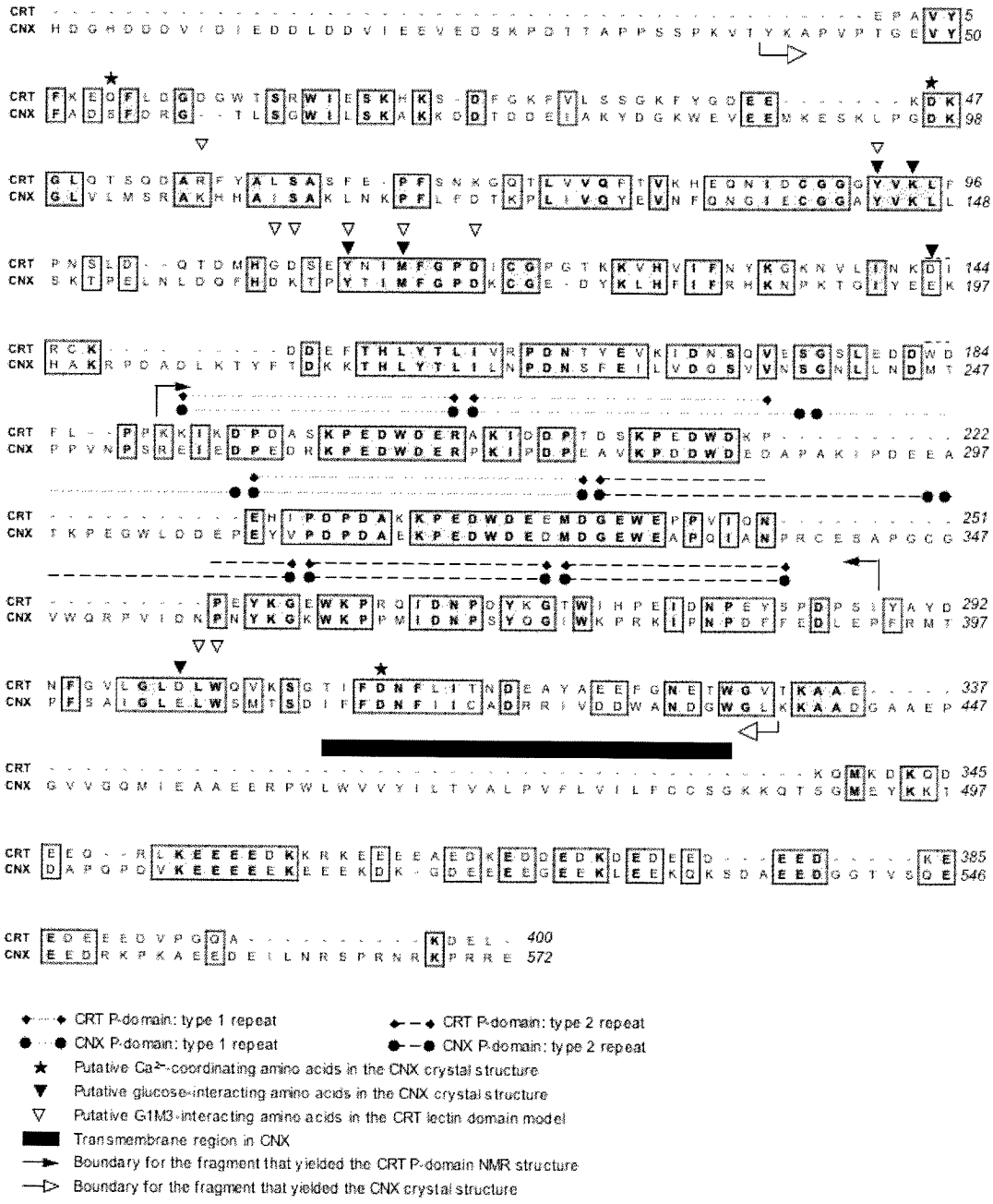

Fig. 6.2 Amino acid sequence alignment of human CNX and human CRT. Both sequences are shown without amino terminal signal sequences and numbered accordingly. Repeat sequences of the P-domain are indicated above the alignment. Amino-acid residues proposed to coordinate Ca^{2+} in the crystal structure of the lumenal domain of CNX are labeled with an asterisk, and amino-acid residues proposed to interact with the glycan are marked with a triangle. The black bar denotes the transmembrane region in CNX. Boundaries for the NMR structure of the CRT P-domain (residues 189–288) and for the crystal structure of the lumenal domain of CNX (residues 40–437) are indicated above and below the respective sequences with arrows.

Curriculum Vitae

Surname	Frickel
First Name	Eva-Maria
Date of Birth	December 6th, 1975
Place of Birth	Frankenthal, Germany
Nationality	German
Address	Nordstr. 182 8037 Zürich Switzerland
Languages	German (native), English, Swedish, School French

Education

1982 – 1989	Grundschule Deidesheim then Käthe-Kollwitz Gymnasium, Neustadt a.d. Weinstr., Germany
1989 – 1992	Briarcliff Middle School then Mountain Lakes High School, Mountain Lakes, NJ, USA
1992 – 1995	Käthe-Kollwitz Gymnasium, Neustadt a.d. Weinstr., Germany
7/1995	German "Abitur"
1995 – 1998	Study of Chemistry at the University of Freiburg, Germany
7/1997	"Vordiplom" in Chemistry
1998 – 2000	Study of Biochemistry at the University of Uppsala, Sweden
1998 – 2000	Master's project and internship at the lab of Prof. Mannervik, University of Uppsala, Sweden (Enzyme Kinetics)
6/2000 – 9/2000	Internship at the lab of Prof. Peter Metcalf, University of Auckland, New Zealand (Protein Crystallography)
8/2000	Magisterexamen (Master of Science), University of Uppsala, Sweden
since 10/2000	Ph.D. student with Prof. Ari Helenius at the Institute of Biochemistry, ETH Zürich, Switzerland

Acknowledgements

Thanks to Ari for giving me the opportunity to pursue this PhD project. I greatly appreciate the scientific freedom and the independence you gave me. Thanks for teaching me scientific openness and letting me put this into practice at many meetings. In choosing my graduate student advisor (which is the most important thing in the life of a scientist, according to Ari), I truly made a good choice.

Thanks to Lars for being my daily advisor, collaborator and even if I hate to admit it, supervisor. This project would not have turned out anyway near to what it is now without your help, ideas and encouragement. It's been invaluable to have you to always be able to discuss with – and fast, if it was necessary!

Thanks to Rudi for making me a better biochemist. Thanks for your ideas, curiosity, and the many discussions. To get your input has really widened my view and sharpened my judgment, I think. *In vitro* veritas?

I am indebted to Yves Barral for having read all this and for being my co-examiner.

I was very fortunate to have been able to share parts of my project with two excellent students, Micha and Karl. Thanks for your efforts with more or less stubborn proteins! I really had fun and couldn't have asked for better daily co-workers.

Thanks to my co-authors. Thanks Roland, for being the first to believe in our complex and for all the work to get it right, and Patrick, for solving many tricky assay details with me; Ilian, Marlène and Walter, thanks for your expertise and Kurt Wüthrich for providing the NMR facilities.

I'd like to thank the former and present members of the Helenius, Martoglio, Ellgaard and Glockshuber lab for all help, discussions and advice. A special thanks goes to the Helenius senior PhDs, who were the true motor of the lab for a long time. Thanks to Marius for your never ending contagious enthusiasm and for having been my partner in many crimes, to Mischael for GT preparation help and lots more, and Anna for cellular advice and also lots more. I am grateful to Katharina and Vondi for german linguistic help. Thanks to Christiane S. for saving me from cloning nightmares many times, and Mauri for excellent, ultra-fast e-mail help and

discussions. Thanks to HC Probst for answering my immunology questions and the gift of antibodies.

Thank you Per, for having taught me so much, but mostly for your drive and speed that I still try to live up to.

Thanks to Ulli, Eilika, Sarah S., and Helena D. for being cool and inspiring women role models in science!

Thanks to Rolf, Toni and Marianne for all the little and big help throughout the years.

I would like to thank my parents for always having supported me, my dreams and my ideas with lots of trust and encouragement. Thanks to my friends for always being there and the many good times. Finally, thank you Lars for putting up with me and for your love.

Paper I

TROSY-NMR reveals interaction between ERp57 and the tip of the calreticulin P-domain

Eva-Maria Frickel, Roland Riek, Ilian Jelasarov, Ari Helenius, Kurt Wüthrich, and Lars Ellgaard

February 19, 2002, PNAS, Volume 99, No. 4, pp. 1954-1959

TROSY-NMR reveals interaction between ERp57 and the tip of the calreticulin P-domain

Eva-Maria Frickel*, Roland Riek†, Ilian Jelesarov‡, Ari Helenius*, Kurt Wüthrich†§, and Lars Ellgaard*§

*Institut für Biochemie, Eidgenössische Technische Hochschule, CH-8092 Zürich, Switzerland; †Institut für Molekularbiologie und Biophysik, Eidgenössische Technische Hochschule, CH-8093 Zürich, Switzerland; and ‡Department of Biochemistry, University of Zürich, CH-8057 Zürich, Switzerland

Contributed by Kurt Wüthrich, December 26, 2001

The lectin chaperone calreticulin (CRT) assists the folding and quality control of newly synthesized glycoproteins in the endoplasmic reticulum (ER). It interacts with ERp57, a thiol-disulfide oxidoreductase that promotes the formation of disulfide bonds in glycoproteins bound by CRT. Here, we investigated the interaction between CRT and ERp57 by using biochemical techniques and NMR spectroscopy. We found that ERp57 binds to the P-domain of calreticulin, an independently folding domain comprising residues 189–288. Isothermal titration calorimetry showed that the dissociation constant of the CRT(189–288)/ERp57 complex is (9.1 ± 3.0) × 10^{-6} M at 8°C. Transverse relaxation-optimized NMR spectroscopy provided data on the thermodynamics and kinetics of the complex formation and on the structure of this 66.5-kDa complex. The NMR measurements yielded a value of (18 ± 5) × 10^{-6} M at 20°C for the dissociation constant and a lower limit for the first-order exchange rate constant of k_{off} > 1,000 s^{-1} at 20°C. Chemical shift mapping showed that interactions with ERp57 occur exclusively through amino acid residues in the polypeptide segment 225–251 of CRT(189–288), which forms the tip of the hairpin structure of this domain. These results are analyzed with regard to the functional mechanism of the CRT/ERp57 chaperone system.

Glycoprotein folding and quality control in the endoplasmic reticulum (ER) are assisted by two homologous molecular chaperones, calreticulin (CRT) and the membrane-bound calnexin (CNX). CRT and CNX are lectins that interact with monoglucosylated trimming intermediates of N-linked core glycans, cooperating with enzymes involved in the trimming and modification of the glycans (1–3). *In vivo*, both proteins also interact with ERp57 (4), a soluble luminal homologue of protein disulfide isomerase (PDI). Like PDI, ERp57 is composed of four thioredoxin-like domains with active site CXXC sequence motifs in the N- and C-terminal domains (5). During the folding of viral glycoproteins in the ER of living cells, ERp57 has been shown to form transient intermolecular disulfide bonds with glycoprotein substrates bound to CNX and CRT (6). When the association of CNX and CRT with glycoproteins is inhibited, the formation of intermolecular disulfide bonds with ERp57 is abrogated. Thus, the interaction between the glycoprotein substrates and either of the lectin chaperones seems to be required for the interaction with ERp57.

The three-dimensional structure of both the CRT P-domain, CRT(189–288) (7) and the CNX ectodomain (including the CNX P-domain) (8) recently have been solved. They show that the P-domain comprises an unusual, extended hairpin fold, which in the crystal structure of the CNX ectodomain protrudes as a long arm from a compact, globular lectin domain. To gain insights into the cooperation of CRT and CNX with ERp57 during glycoprotein folding, we have characterized the interaction between the CRT P-domain and ERp57 by using biochemical methods and transverse relaxation-optimized spectroscopy (TROSY)-NMR.

Materials and Methods

Protein Expression and Purification. CRT(189–288) was prepared as described (9). $^{15}N,^{2}H$ labeling of the protein was obtained by expressing it in 0.5 liters of M9 minimal medium supplemented with 1 g Celtone dN powder (Martek Biosciences, Columbia, MD) and 2 g/liter glucose. Recombinant human PDI was expressed and purified as described (10), except for an additional, final purification step on a Superdex 200 gelfiltration column (Amersham Pharmacia). For the recombinant expression of human ERp57 we used *Escherichia coli* BL21(DE3) cells freshly transformed with the pHisERp57 expression vector, which encodes a N-terminal 22-aa affinity tag containing a deca-histidine sequence and a factor X_a cleavage site. Three liters of LB medium containing ampicillin (100 μg/ml) was inoculated with 30 ml of preculture of pHisERp57-containing *E. coli* BL21(DE3) cells that had been grown at 37°C for 3 h. At OD_{600} = 0.6 expression was induced with 0.4 mM isopropyl L-D-galactopyranoside. The cells were harvested after 4 h, and the pellet was resuspended in 30 ml buffer A (25 mM Tris·HCl, pH 8.0/500 mM NaCl/10 mM β-mercaptoethanol). After sonication, the cell lysate was centrifuged at 20,000 *g* for 30 min, and the supernatant was applied to a Ni^{2+}-charged NTA column (Qiagen, Chatsworth, CA). The fusion protein was eluted with a linear gradient of 0–500 mM imidazole in buffer A. After dialysis against 25 mM Tris·HCl (pH 8.0), 300 mM NaCl, the N-terminal fusion tail was removed by factor X_a cleavage, performed for 20 h at room temperature by using a ratio of 1:200 (wt/wt) of factor X_a to fusion protein. After cleavage, the protein was dialyzed against buffer B (100 mM KH_2PO_4, pH 7.0/25 mM NaCl/10 mM β-mercaptoethanol) and loaded onto a MonoQ 10/10 anion-exchange column (Amersham Pharmacia). ERp57 was eluted with a linear gradient of 0–500 mM NaCl in buffer B. Yields were about 20 mg pure ERp57 per liter of culture medium. The correct molecular weights of all recombinant proteins were verified by matrix-assisted laser desorption ionization–time of flight.

Protein Concentrations. The concentrations of all proteins used in this study were determined from their absorbance at 280 nm by using molar extinction coefficients calculated by the method of Gill and von Hippel (11).

Chemical Cross-Linking. Solutions of CRT(189–288) alone, ERp57 alone, or both proteins together were incubated with 20 μM of the homobifunctional cross-linker disuccinimidyl glutarate (Pierce) for 30 min on ice in a volume of 10 μl. Protein solutions were at 7 μM concentration, containing 100 mM KH_2PO_4, 25 mM NaCl, and 10 mM β-mercaptoethanol at pH 7.0. Excess disuccinimidyl glutarate was quenched with 20 mM glycine. The reactions were supplemented with reducing SDS/PAGE loading buffer and run on a 12% SDS/PAGE gel.

Abbreviations: CNX, calnexin; CRT, calreticulin; ER, endoplasmic reticulum; ITC, isothermal titration microcalorimetry; PDI, protein disulfide isomerase; TROSY, transverse relaxation-optimized spectroscopy.

§To whom reprint requests should be addressed. E-mail: lars.ellgaard@bc.biol.ethz.ch.

The publication costs of this article were defrayed in part by page charge payment. This article must therefore be hereby marked "*advertisement*" in accordance with 18 U.S.C. §1734 solely to indicate this fact.

www.pnas.org/cgi/doi/10.1073/pnas.042699099

Interaction Studies by ELISA. Microtiter wells (Nunc) were coated with 50 μl of either ERp57, PDI, or one of three different negative control proteins at 15 μg/ml in 15 mM Na_2CO_3, 35 mM $NaHCO_3$ by incubating overnight at 4°C. After blocking with 200 μl 5% milk powder in buffer W (PBS/0.05% Tween 20) for 1 h at 37°C in a moist chamber, the wells were washed three times with 200 μl of buffer W. All subsequent incubation steps were performed for 8–16 h at 4°C by using protein or antibody solutions diluted in buffer W. Each incubation step was followed by washing three times with 200 μl of buffer W. The coated protein was incubated with 50 μl of 3.3 μM biotinylated CRT(189–288), followed by the incubation with 50 μl of rabbit-α-biotin antibody (Bethyl Laboratories, Montgomery, TX) (1:2,000 dilution) and 50 μl of horseradish peroxidase-conjugated goat-α-rabbit antibody (Pierce) (1:10,000 dilution). Biotinylation was performed by using EZ-Link Sulfo-NHS-LC-LC-Biotin (Pierce) according to the manufacturer's recommendations. The wells were developed by the addition of 50 μl of BM Blue (3,3′–5,5′–tetramethylbenzidine) (Roche Molecular Biochemicals) for 10 min and the subsequent addition of 30 μl of 10 mM HCl. Finally, the absorbance was recorded at 450 nm versus a reference taken at 655 nm by using an ELISA plate reader.

Isothermal Titration Microcalorimetry (ITC). ITC was performed at 8°C on a MCS instrument (MicroCal, Northampton, MA) calibrated with either electrically generated heat pulses or by measuring the heat of standard chemical reactions. Samples of CRT(189–288) and ERp57 were prepared as described above and gel-filtrated into the same batch of buffer containing 25 mM Tris·HCl, pH 7.0 and 10 mM β-mercaptoethanol. Concentrations were determined after gel filtration. The cell was loaded with 0.2 mM ERp57. The titration protocol consisted of 24 12-μl injections of a 2.0 mM solution of CRT(189–288). Injection duration was 10 s, and equilibration was allowed for 5 min between injections. The stirring rate was 200 rpm. After the experiment, the data were integrated, corrected for nonspecific heat effects, normalized for the concentration, and analyzed according to a 1:1 binding model.

NMR Spectroscopy. The NMR experiments were carried out on a Bruker DRX750 spectrometer at 20°C by using protein solutions that contained 100 mM KH_2PO_4, 25 mM NaCl, and 10 mM β-mercaptoethanol at pH 7.0. A [^{15}N,^{1}H]TROSY spectrum (12) of free ^{15}N,^{2}H-labeled CRT(189–288) was measured at a protein concentration of 0.4 mM, with $t_{1,max}$ = 88 ms, $t_{2,max}$ = 98 ms, a data size of 200 × 1,024 complex points, and an overall recording time of 2 h. For optimal sensitivity a polarization transfer time of 5.4 ms was used. A [^{15}N,^{1}H]TROSY spectrum of the CRT(189–288)/ERp57 complex was measured in a solution containing 0.14 mM ^{15}N,^{2}H-labeled CRT(189–288) and 0.38 mM ERp57, with $t_{1,max}$ = 44 ms, $t_{2,max}$ = 98 ms, a data size of 100 × 1,024 complex points, and an overall recording time of 24 h. For optimal sensitivity a polarization transfer time of 3.4 ms was used (13). The same NMR set-ups as for the CRT(189–288)/ERp57 complex were used in titration experiments performed to investigate the thermodynamic and kinetic stability of the complex (Table 1), except that the overall recording time per experiment was 12 h. The titration experiments were started with the 1:2.7 mixture of CRT(189–288) and ERp57, and unlabeled CRT(189–288) was added stepwise as listed in Table 1. An experiment with a freshly prepared solution containing 0.14 mM ^{15}N,^{2}H-labeled CRT(189–288) and 0.07 mM ERp57 was used as an independent control for this titration protocol.

The NMR data were processed with the program PROSA (14) and analyzed with the program XEASY (15). Drawings of molecular models were performed by using the program MOLMOL (16).

Table 1. Composition of the solutions used in the titration of CRT(189–288) with ERp57

	Concentration, mM		
mol:mol ratio CRT(189–288)/ERp57	^{15}N,^{2}H-labeled CRT(189–288)	Unlabeled CRT(189–288)	Unlabeled ERp57
1:2.7	0.14	0	0.38
1.1:1	0.12	0.24	0.33
1.8:1	0.11	0.41	0.29
2.4:1	0.1	0.54	0.26
3:1	0.09	0.64	0.24
4:0	0.28	0	0
2:1*	0.14	0	0.07

The protein solutions contained 100 mM KH_2PO_4, 25 mM NaCl, and 10 mM β-mercaptoethanol at pH 7.0 and 20°C.

*As an independent control for the titration experiment, spectra were recorded of a freshly prepared solution of unlabeled ERp57 containing a 2-fold excess of labeled CRT(189–288).

Results

The Calreticulin P-Domain Binds ERp57. Evidence for intermolecular interactions between CRT(189–288) and ERp57 was independently obtained from chemical cross-linking (Fig. 1*a*), ELISA experiments (Fig. 1*b*), ITC (Fig. 1*c*), and chemical shift perturbation in TROSY-NMR experiments (Fig. 2).

In the cross-linking experiments, purified recombinant proteins were mixed and treated with the cross-linker disuccinimidyl glutarate (see *Materials and Methods*). Fig. 1*a* shows that in mixtures of CRT(189–288) and ERp57 a band appeared at an approximate molecular mass of 75 kDa. Because the free 12-kDa CRT(189–288) migrates as a protein of approximately 18 kDa, the mobility of this band is compatible with a 1:1 complex of CRT(189–288) and the 54.5-kDa ERp57.

In the ELISA experiments, ERp57 showed efficient binding to CRT(189–288), whereas three control proteins (BSA, calmodulin, and ubiquitin) did not show appreciable binding. Furthermore, it is noteworthy that PDI, which is the closest known homologue of ERp57, did not interact with CRT(189–288) (Fig. 1*b*). The specific association of the calreticulin P-domain with ERp57 is consistent with *in vivo* (4) and *in vitro* (17) data that demonstrated the presence of functional complexes between CNX or CRT and ERp57, but not between CNX or CRT and PDI.

ITC performed at 8°C detected a measurable heat effect on mixing of the two proteins, which reached saturation with increasing molar ratio of CRT(189–288) to ERp57. The resulting titration curve followed the shape of a typical binding isotherm (Fig. 1*c*) with 1:1 stoichiometry. The best fit of the data were obtained with a dissociation constant of (9.1 ± 3.0) × 10^{-6} M.

Chemical Shift Mapping with TROSY-NMR. The NMR structure and the complete sequence-specific NMR assignments of CRT(189–288) (7, 9) provided a basis for structural studies of the interactions between CRT(189–288) and ERp57. Because the CRT(189–288)/ERp57 complex was reconstituted *in vitro* from the isolated components, uniform isotope labeling of CRT(189–288) with ^{15}N and ^{2}H enabled selective observation of the ^{15}N–^{1}H fingerprint of this protein in the 66.5-kDa complex with the use of [^{15}N,^{1}H]TROSY (18).

From the amino acid sequence of CRT(189–288) one expects a "fingerprint" containing backbone ^{15}N–^{1}H peaks of 84 residues, of which 81 have previously been assigned in the free protein (9). Under the conditions of the present experiments, the ^{15}N–^{1}H fingerprint of free CRT(189–288) contains 80 of these cross peaks (Fig. 2*a*). With the TROSY experimental scheme used here, the ^{15}N–^{1}H cross peaks of the Gln and Asn side chains, which would appear in the spectral region 112–115 ppm along

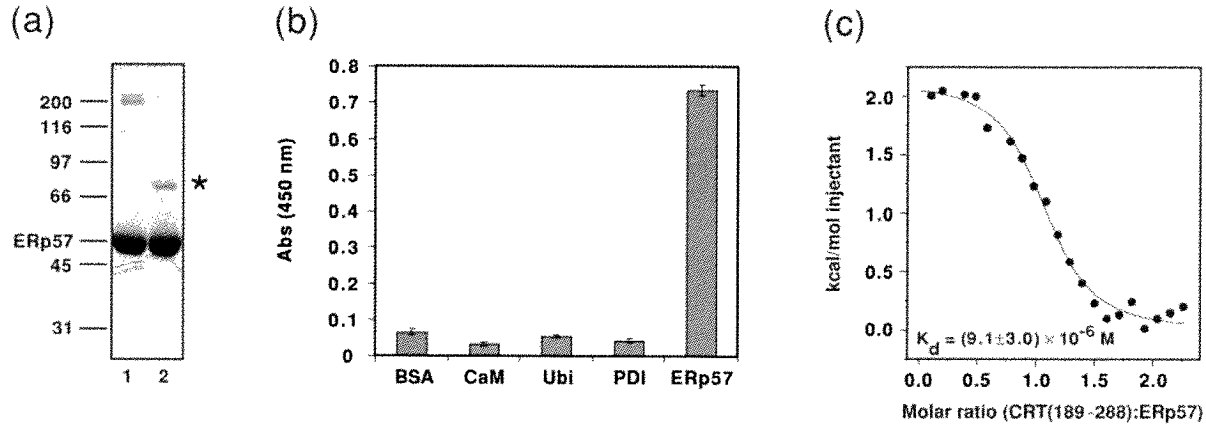

Fig. 1. (*a*) Chemical cross-linking of CRT(189–288) and ERp57. The homobifunctional cross-linker disuccinimidyl glutarate was added to solutions of CRT(189–288) alone (data not shown), ERp57 alone (lane 1), or an equimolar mixture of the two proteins (lane 2). After incubation for 30 min on ice, the reaction was quenched with an excess of glycine. Potential protein complexes were analyzed by 12% reducing SDS/PAGE, and the gel was stained with Coomassie blue. Molecular mass standards given in kDa are indicated on the left, along with the position of ERp57. The suggested position of the CRT(189–288)/ERp57 complex is indicated by *. (*b*) The interaction of CRT(189–288) and ERp57 studied by ELISA. Potential ligands for CRT(189–288) were coated in microtiter wells, and the interaction was probed with biotinylated CRT(189–288), followed by the binding of a primary antibody directed against biotin and a horseradish peroxidase-conjugated secondary antibody. Development by the addition of BM Blue (3,3′–5,5′–tetramethylbenzidine) (Roche Molecular Biochemicals) substrate gives rise to a signal at 450 nm for positive enzymatic reactions. BSA, calmodulin (CaM), and ubiquitin (Ubi) were used as control proteins. The data presented in the graph are mean values of triplicates. The experiment was repeated three times with closely similar results. Standard deviations are given by the vertical bars. Nonspecific binding of primary and secondary antibodies to wells coated with protein ligand in the absence of biotinylated CRT(189–288) was subtracted for each well. (*c*) Binding isotherm describing the formation of the CRT(189–288)/ERp57 complex followed by ITC at 8°C. ● represent the integrated heats at each injection after correction for nonspecific heat effects and normalization for the molar concentration. The continuous line visualizes a least-squares nonlinear fit of the data according to a 1:1 binding model defined by the following parameters: $n = 1.04 \pm 0.03$, $K_d = (9.1 \pm 3.0) \times 10^{-6}$ M [$K_a = (1.1 \pm 0.3) \times 10^5$ M^{-1}], and $\Delta H = 2.1 \pm 0.1$ kcal mol^{-1}.

$\omega_1(^{15}N)$ and 6.7–8.7 ppm along $\omega_2(^1H)$, are nearly completely suppressed (19). In the fingerprint of $^{15}N,^2H$-labeled CRT(189–288) in a solution containing a 2.7-fold excess of unlabeled ERp57 (Fig. 2*b*), 72 backbone ^{15}N–^1H cross peaks and five Trp indole peaks could be identified.

Superposition of the [$^{15}N,^1H$]TROSY spectra of free CRT(189–288) and the CRT(189–288)/ERp57 complex revealed that a large number of peaks in the complex superimposed exactly with peaks in free CRT(189–288). However, Fig. 2 also shows that the relative intensities as well as the peak positions of numerous corresponding, well-resolved peaks in free and complexed CRT(189–288) were significantly different. Titration experiments (see below) enabled transfer of sequence-specific resonance assignments in free CRT(189–288) to $^{15}N,^2H$-labeled CRT(189–288) bound to ERp57. We thus found that for the backbone ^{15}N–^1H-moieties of D237, E238, M240, G242, E245, V248, I249, and N251, and the indole ^{15}N–^1H of Trp-236 no peaks were observed in the complex, and that for the residues I225, D227, D229, K231, W236, E243, and W244 the peak intensities in the complex were weaker than 3% of the intensities in free CRT(189–288) (Fig. 2 *a* and *b*). In addition, the six backbone amide cross peaks of A230, K232, E234, D235, E239, and D241 exhibited chemical shift changes relative to free CRT(189–288) of 0.2 to 1.0 ppm along the ^{15}N dimension and 0.0 to 0.5 ppm along the ^1H dimension in the 1:2.7 complex (Fig. 2). A systematic evaluation of the signal intensities by measurement of the peak heights in the two spectra yielded the data shown in Fig. 2*c*. Whereas the residues near both chain ends of CRT(189–288) had similar intensities in the free and bound protein, there was a continuous loss of peak intensity from the chain ends toward the center of the polypeptide chain. All 21 residues mentioned above with either a sizeable chemical shift change, complete absence of a cross peak, or very weak cross-peak intensity in the bound form are located in the contiguous structural region of residues 225–251, indicating that the ERp57-binding site on CRT(189–288) is at the tip of the hairpin structure of this protein, as illustrated in Fig. 3.

NMR Characterization of Thermodynamics and Kinetics of the CRT(189–288)/ERp57 Interaction. The 1:2.7 CRT(189–288)/ERp57 solution of Fig. 2*b* was titrated by stepwise addition of unlabeled CRT(189–288), as detailed in Table 1. In Fig. 4 *a-d* the change in chemical shift and peak intensity upon titration is shown for four selected residues. When following the chemical shift changes at different titration points we found that for the residues E238, I249, and N251, which showed no peak intensity in the 1:2.7 CRT(189–288)/ERp57 solution, weak cross peaks could be observed in [$^{15}N,^1H$]TROSY spectra measured at excess molar ratios of CRT(189–288). Specifically, at CRT(189–288)/ERp57 molar ratios of 3:1, 2.4:1, and 1.8:1, these cross peaks displayed sizeable chemical shift changes when compared with free CRT(189–288), as illustrated for I249 (Fig. 4*c*).

The continuous chemical shift changes (Fig. 4 *a-d*) demonstrated that the exchange rate between bound and free CRT(189–288) was fast on the chemical shift time scale, with an estimated lower limit for the first-order exchange rate constant of $k_{off} > 1{,}000\ s^{-1}$ at 20°C. Using the data for residue K232 (Fig. 4*b*), a fit of the dependence of the chemical shifts on the ERp57/CRT(189–288) molar ratio as described in the legend to Fig. 4*e* yielded a dissociation constant of $K_d = (18 \pm 5) \times 10^{-6}$ M for the complex of CRT(189–288) and ERp57 (Fig. 4*e*).

Discussion

In the present investigation the ability to record high-resolution NMR spectra of big structures in solution with the use of TROSY (18) enabled us to supplement the evidence for CRT(189–288) binding to ERp57 obtained from biochemical experiments with a structural characterization of the complex. Thus, we obtained an identification of the surface residues in the distal end of the calreticulin P-domain that comprise the contact area with ERp57. Further NMR measurements also enabled the

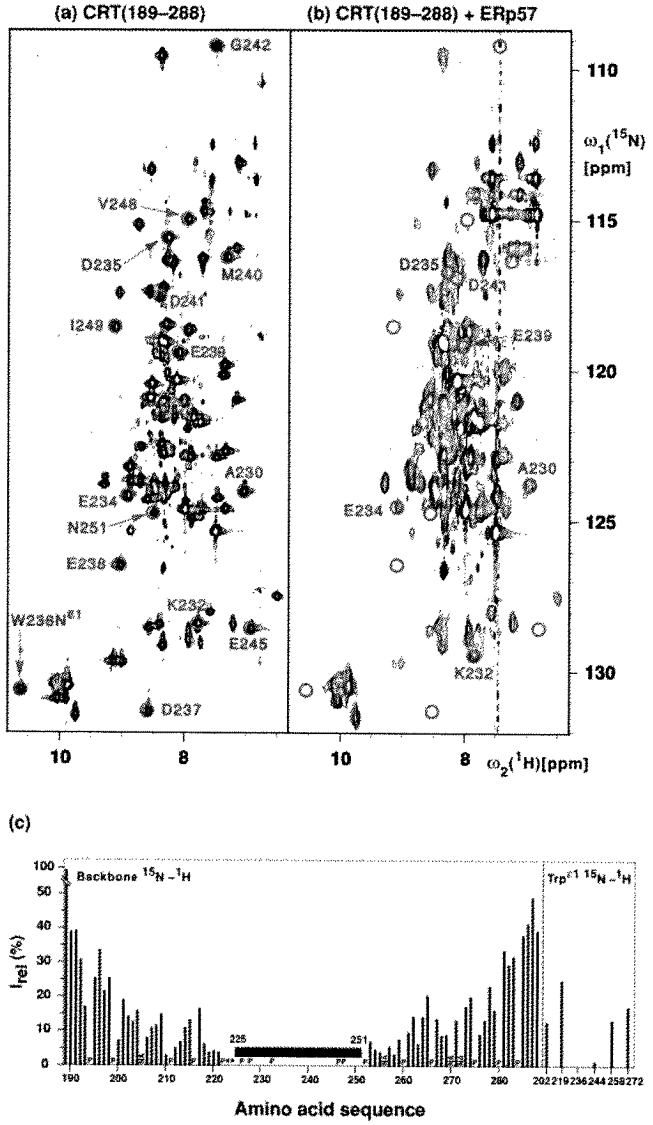

Fig. 2. (*a* and *b*) ^{15}N–^1H correlation NMR spectra used to delineate the surface areas of CRT(189–288) that interact with ERp57. These spectra contain peaks corresponding to backbone amide ^{15}N–^1H groups and, in the lower left, indole ^{15}N–^1H groups of tryptophyl residues. Color-coded peaks indicate outstandingly large effects from ERp57 interactions: Blue circles identify cross peaks with chemical shift differences of more than 0.2 ppm along the ^{15}N dimension between free and ERp57-bound CRT(189–288). Red circles identify cross-peak positions in free CRT(189–288) for which no counterpart could be observed in the spectrum of the complex. The color-coded cross peaks are labeled with the sequence-specific resonance assignments. (*a*) [^{15}N,^1H]TROSY spectrum of free ^{15}N,^2H-labeled CRT(189–288) (protein concentration = 0.4 mM, polarization transfer time = 5.4 ms, data size 200 × 1,024 complex points, zero-filling to 512 × 2,048 points, $t_{1,max}$ = 88 ms, $t_{2,max}$ = 98 ms, total measuring time 2 h). (*b*) [^{15}N,^1H]TROSY spectrum of a solution of ^{15}N,^2H-labeled CRT(189–288) and unlabeled ERp57 [protein concentrations of 0.14 mM for ^{15}N,^2H-labeled CRT(189–288) and 0.38 mM for ERp57, polarization transfer time = 3.4 ms, data size 100 × 1,024 complex points, zero-filling to 512 × 2,048 points, $t_{1,max}$ = 44 ms, $t_{2,max}$ = 98 ms, total measuring time 24 h]. (*c*) Plot of the relative peak intensities, I_{rel}, of the [^{15}N,^1H]TROSY cross peaks in the CRT(189–288)/ERp57 complex and free CRT(189–288) versus the amino acid sequence of CRT(189–288). The Trp indole cross peaks are listed separately on the right. The black horizontal bar spanning the polypeptide segment 225–251 indicates that for these residues the cross peaks in the complex have either large chemical shift differences (> 0.2 ppm along the ^{15}N dimension) or very small signal intensities [< 3% of the intensity in free CRT(189–288)] (see text). P designates proline residues, NA stands for residues for which no resonances could be assigned, and * indicates residues for which no reliable data could be measured because of spectral overlap.

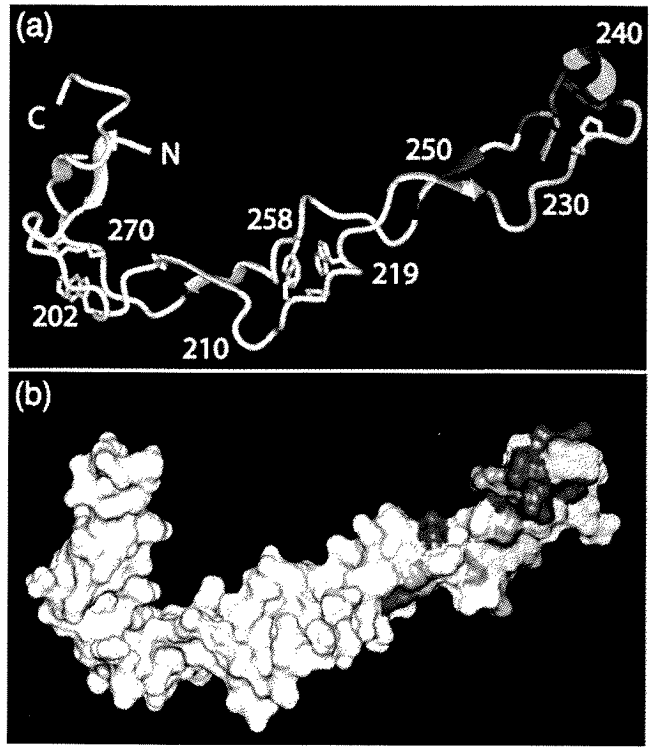

Fig. 3. Visual display of the molecular regions of CRT(189–288) that are in direct contact with ERp57. (*a*) Ribbon representation. (*b*) Space-filling model displaying the molecular surface of the NMR structure. The residues for which the ^{15}N–^1H-moieties show chemical shift changes caused by interactions with ERp57 in excess of 0.2 ppm along the ^{15}N dimension are colored blue, those for which no cross peak is observed in the [^{15}N,^1H]TROSY spectrum of the complex are red, and those for which the peak intensity relative to free CRT(189–288) is weaker than 3% are orange. In *a* the positions of selected residues areindicated.

determination of the thermodynamic stability of the CRT(189–288)/ERp57 complex. The two K_d values of $(9.1 \pm 3.0) \times 10^{-6}$ M at 8°C and $(18 \pm 5) \times 10^{-6}$ M at 20°C determined independently by ITC and TROSY-NMR, respectively, are in good agreement with each other. The relatively low affinity of the CRT/ERp57 complex is comparable to that reported recently for the complex between CRT and the glycoprotein IgG *in vitro*, i.e., $K_d = 1.9 \times 10^{-6}$ M (20). However, whereas an exchange rate of $k_{off} = 0.1\ s^{-1}$ was reported for the CRT/glycoprotein complex, the NMR experiment reveals a much faster rate of $k_{off} > 1{,}000\ s^{-1}$ for the CRT(189–288)/ERp57 complex, which is thus very short-lived. The additional presence of a substrate protein might, of course, result in formation of a more stable ternary complex, which could be further stabilized upon formation of an intermolecular disulfide bond between ERp57 and the glycoprotein (see Fig. 5). The fast off-rate for the binary CRT/ERp57 complex could be of functional significance because it might allow ERp57 to "screen" for pre-existing complexes of CRT and glycoprotein.

Based on their close sequence similarity, CRT and CNX are likely not only to possess similar P-domains but also structurally homologous lectin domains. In CNX, the lectin domain contains a single binding site for the oligosaccharide of the substrate glycoprotein and is located close to the site from which the P-domain emerges as an elongated hairpin loop (8). The P-domain forms a slightly curved arm of about 110 Å in CRT (7) and 140 Å in CNX (8). Binding of ERp57 to the distal end of this arm is likely to generate a partially solvent-shielded cavity surrounded by the lectin domain, the P-domain, and ERp57 (see

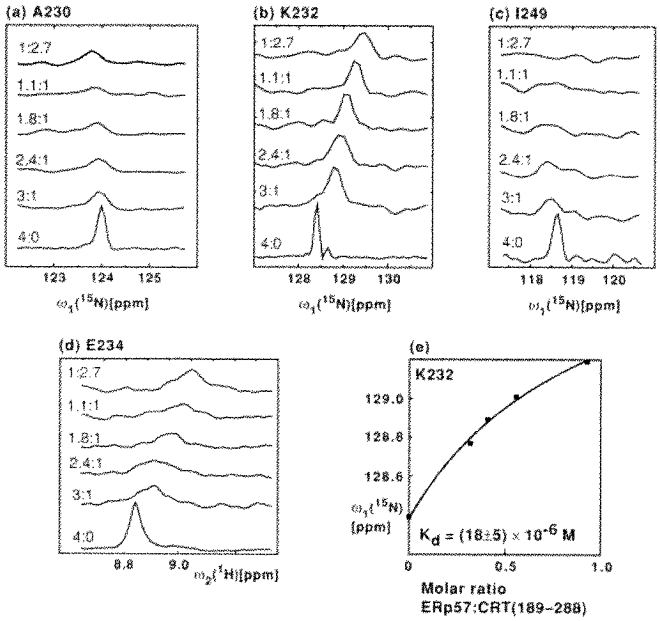

Fig. 4. Titration of the $^{15}N,^2H$-labeled CRT(189–288)/ERp57 complex with unlabeled CRT(189–288). (*a*-*c*), Cross sections from [$^{15}N,^1H$]TROSY spectra along the $\omega_1(^{15}N)$ dimension for the residues A230, K232, and I249 of $^{15}N,^2H$-labeled CRT(189–288). The numbers on the left of each trace refer to the solution conditions given in Table 1. (*d*) Cross sections from [$^{15}N,^1H$]TROSY spectra along $\omega_2(^1H)$ for residue E234. (*e*) K_d determination based on the titration data for residue K232. ■ represent the experimental ^{15}N chemical shifts of K232 at discrete values of the ERp57/CRT(189–288) molar ratio (Table 1). The curve visualizes the fit from which the ^{15}N chemical shift of the CRT(189–288)/ERp57 complex [$\delta(^{15}N_{complex})$] was determined, using the relation $\delta(^{15}N) = \delta(^{15}N_{free}) + [\delta(^{15}N_{complex}) - \delta(^{15}N_{free})]$ ([ERp57]/[CRT(189–288)])/(([ERp57]/[CRT(189–288)]) + K_{ratio}) where δ is the chemical shift and K_{ratio} the K_d expressed as molar ratio, and the brackets indicate molar concentrations of the respective compounds. Subsequently, the K_d value was calculated at each experimental point by using the relation K_d = [CRT(189–288)][ERp57]/[CRT(189–288)/ERp57], yielding an average value of $K_d = (18 \pm 5) \times 10^{-6}$ M.

Fig. 5). Given the apparent plasticity of the P-domain (7), the size of this cavity might be variable so as to accommodate substrates of variable size.

The role of CNX and CRT as molecular chaperones seems to rely on three specific features. First, these proteins bind the substrate glycoprotein through the glycan binding site. By binding to the oligosaccharide moiety, they may tether the substrate with minimal constraints on the conformational freedom of the substrate polypeptide chain. Second, they provide a partially solvent-shielded environment for folding (Fig. 5), where access for other ER chaperones and protein folding intermediates is likely to be restricted, so that aggregation and formation of non-native intermolecular disulfides with other newly synthesized proteins is suppressed (21). Third, they provide a strategically placed binding site for ERp57, which supports productive interactions between the thiol-disulfide oxidoreductase and cysteines in the folding glycoprotein. Such interactions have previously been shown to involve the formation of a series of transient mixed disulfides between the substrate glycoprotein and ERp57 (6).

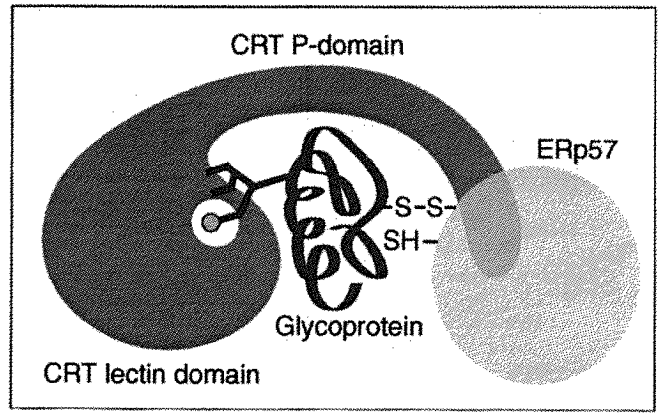

Fig. 5. Scheme for a possible mode of cooperative interaction between CRT and ERp57 in assisting the folding of a glycoprotein based on currently available structural, biochemical, and cell-biological data (2, 7, 8). The substrate glycoprotein (blue) binds to the CRT lectin domain (red) by means of a branched oligosaccharide. CRT and CNX both interact specifically with the $Glc_1Man_9GlaNAc_2$ form of the oligosaccharide (26–28). The interaction of the terminal glucose (light blue circle) with the binding site (white circle) would place the glycoprotein polypeptide chain in the partially solvent-shielded cavity bounded by the CRT lectin domain, the P-domain, and ERp57 (orange) bound to the distal end of the protruding P-domain. It is further hypothesized that the CRT-ERp57 interaction places the thiol-disulfide oxidoreductase favorably for the formation of intermolecular disulfide bonds (S—S) with the glycoprotein.

The presently described insights into the structural basis of the CRT/ERp57 chaperone system emphasize the importance of determining whether ERp57 functions as a thiol oxidase and/or as a disulfide isomerase *in vivo*. It will also be of interest to study in closer detail how the apparent plasticity of the P-domain might affect the function of the bound ERp57 molecule. The accessibility of the glycan to processing enzymes such as glucosidase II and the UDP-glucose:glycoprotein glucosyltransferase will also need further investigation. The available data already indicate, however, that CNX and CRT function by a different mechanism from that of previously analyzed molecular chaperones. Distinctive features are that binding of the substrate molecule occurs by means of oligosaccharide branches (22–24), that there is close structural and functional cooperation between the chaperone and a thiol-disulfide oxidoreductase (4, 25), and that the on-and-off cycle of the glycoprotein substrate is driven by independently acting enzymes that regulate covalent modification of the N-linked glycan (2).

We thank the following for kind gifts of expression vectors and purified protein: S. High, University of Manchester, Manchester, U.K. (pHisERp57), J. Winther, Carlsberg Laboratory, Copenhagen (pET12a-PDI2), and P. Gazzotti, Eidgenössische Technische Hochschule, Zürich (calmodulin). Financial support by the Schweizerischer Nationalfonds [Projects 31.51054.97 (A.H.) and 31.49047.96 (K.W.)] is gratefully acknowledged.

1. Ellgaard, L., Molinari, M. & Helenius, A. (1999) *Science* **286,** 1882–1888.
2. Parodi, A. J. (2000) *Annu. Rev. Biochem.* **69,** 69–93.
3. Chevet, E., Cameron, P. H., Pelletier, M. F., Thomas, D. Y. & Bergeron, J. J. (2001) *Curr. Opin. Struct. Biol.* **11,** 120–124.
4. Oliver, J. D., Roderick, H. L., Llewellyn, D. H. & High, S. (1999) *Mol. Biol. Cell* **10,** 2573–2582.
5. Ferrari, D. M. & Söling, H. D. (1999) *Biochem. J.* **339,** 1–10.
6. Molinari, M. & Helenius, A. (1999) *Nature (London)* **402,** 90–93.
7. Ellgaard, L., Riek, R., Herrmann, T., Güntert, P., Braun, D., Helenius, A. & Wüthrich, K. (2001) *Proc. Natl. Acad. Sci. USA* **98,** 3133–3138.
8. Schrag, J. D., Bergeron, J. J., Li, Y., Borisova, S., Hahn, M., Thomas, D. Y. & Cygler, M. (2001) *Mol. Cell* **8,** 633–644.
9. Ellgaard, L., Riek, R., Braun, D., Herrmann, T., Helenius, A. & Wüthrich, K. (2001) *FEBS Lett.* **488,** 69–73.
10. Westphal, V., Spetzler, J. C., Meldal, M., Christensen, U. & Winther, J. R. (1998) *J. Biol. Chem.* **273,** 24992–24999.
11. Gill, S. C. & von Hippel, P. H. (1989) *Anal. Biochem.* **182,** 319–326.
12. Pervushin, K. V., Wider, G. & Wüthrich, K. (1998) *J. Biomol. NMR* **12,** 345–348.
13. Riek, R., Wider, G., Pervushin, K. & Wüthrich, K. (1999) *Proc. Natl. Acad. Sci. USA* **96,** 4918–4923.

14. Güntert, P., Dötsch, V., Wider, G. & Wüthrich, K. (1992) *J. Biomol. NMR* **2,** 619–629.
15. Bartels, C., Xia, T. H., Billeter, M., Güntert, P. & Wüthrich, K. (1995) *J. Biomol. NMR* **6,** 1–10.
16. Koradi, R., Billeter, M. & Wüthrich, K. (1996) *J. Mol. Graph.* **14,** 51-55.
17. Zapun, A., Darby, N. J., Tessier, D. C., Michalak, M., Bergeron, J. J. & Thomas, D. Y. (1998) *J. Biol. Chem.* **273,** 6009–6012.
18. Pervushin, K., Riek, R., Wider, G. & Wüthrich, K. (1997) *Proc. Natl. Acad. Sci. USA* **94,** 12366–12371.
19. Pervushin, K., Braun, D., Fernandez, C. & Wüthrich, K. (2000) *J. Biomol. NMR* **17,** 195–202.
20. Patil, A. R., Thomas, C. J. & Surolia, A. (2000) *J. Biol. Chem.* **275,** 24348–24356.
21. Helenius, A., Trombetta, E. S., Hebert, D. N. & Simons, J. F. (1997) *Trends Cell Biol.* **7,** 193–200.
22. Ou, W. J., Cameron, P. H., Thomas, D. Y. & Bergeron, J. J. (1993) *Nature (London)* **364,** 771–776.
23. Rodan, A. R., Simons, J. F., Trombetta, E. S. & Helenius, A. (1996) *EMBO J.* **15,** 6921–6930.
24. Zapun, A., Petrescu, S. M., Rudd, P. M., Dwek, R. A., Thomas, D. Y. & Bergeron, J. J. (1997) *Cell* **88,** 29–38.
25. Oliver, J. D., van der Wal, F. J., Bulleid, N. J. & High, S. (1997) *Science* **275,** 86–88.
26. Hammond, C., Braakman, I. & Helenius, A. (1994) *Proc. Natl. Acad. Sci. USA* **91,** 913–917.
27. Spiro, R. G., Zhu, Q., Bhoyroo, V. & Soling, H. D. (1996) *J. Biol. Chem.* **271,** 11588–11594.
28. Vassilakos, A., Michalak, M., Lehrman, M. A. & Williams, D. B. (1998) *Biochemistry* **37,** 3480–3490.

Paper II

ERp57 is a multifunctional thiol-disulfide oxidoreductase

Eva-Maria Frickel, Patrick Frei, Marlène Bouvier, Walter F. Stafford, Ari Helenius, Rudi Glockshuber, and Lars Ellgaard

April 30, 2004, J. Biol. Chem., Volume 279, No. 18, pp. 18277-18287

THE JOURNAL OF BIOLOGICAL CHEMISTRY
Vol. 279, No. 18, Issue of April 30, pp. 18277–18287, 2004
Printed in U.S.A.

ERp57 Is a Multifunctional Thiol-Disulfide Oxidoreductase*

Received for publication, December 23, 2003, and in revised form, February 10, 2004
Published, JBC Papers in Press, February 10, 2004, DOI 10.1074/jbc.M314089200

Eva-Maria Frickel‡, Patrick Frei§, Marlène Bouvier¶, Walter F. Stafford‖, Ari Helenius‡, Rudi Glockshuber§, and Lars Ellgaard‡**

From the ‡Institute of Biochemistry and §Institute of Molecular Biology and Biophysics, ETH Zurich, CH-8093 Zurich, Switzerland, ¶School of Pharmacy, University of Connecticut, Storrs, Connecticut 06269, and ‖Boston Biomedical Research Institute, Watertown, Massachusetts 02472

The thiol-disulfide oxidoreductase ERp57 is a soluble protein of the endoplasmic reticulum and the closest known homologue of protein disulfide isomerase. The protein interacts with the two lectin chaperones calnexin and calreticulin and thereby promotes the oxidative folding of newly synthesized glycoproteins. Here we have characterized several fundamental structural and functional properties of ERp57 *in vitro*, such as the domain organization, shape, redox potential, and the ability to catalyze different thiol-disulfide exchange reactions. Like protein disulfide isomerase, we find ERp57 to be comprised of four structural domains. The protein has an elongated shape of 3.4 ± 0.1 nm in diameter and 16.8 ± 0.5 nm in length. The two redox-active a and a′ domains were determined to have redox potentials of −0.167 and −0.156 V, respectively. Furthermore, ERp57 was shown to efficiently catalyze disulfide reduction, disulfide isomerization, and dithiol oxidation in substrate proteins. The implications of these findings for the function of the protein *in vivo* are discussed.

After translocation into the lumen of the endoplasmic reticulum (ER),[1] newly synthesized proteins fold and oligomerize before they are transported further in the secretory pathway. Covalent modifications, such as *N*-linked glycosylation and signal peptide cleavage, play an important role in protein maturation in the ER. In addition, the formation of disulfide bonds is often essential. By establishing covalent intra- and intermolecular cross-links, disulfide bonds allow a more productive folding of many polypeptides and provide a higher overall stability. The steady production of new proteins in the ER and the continued oxidation of cysteine thiols is supported by a constant supply of oxidizing equivalents.

In recent years, the molecular mechanisms of disulfide bond formation in the periplasm of Gram-negative bacteria and in the ER of *Saccharomyces cerevisiae* have been thoroughly characterized (reviewed in Ref. 1). In the ER of animal cells, disulfide bond formation is less well understood. Still, protein disulfide isomerase (PDI), an essential and well characterized ER resident enzyme, is known to interact with various substrates and to catalyze their oxidation, reduction, and isomerization (reviewed in Ref. 2). Recently, it has become evident that PDI obtains the oxidizing equivalents that it uses for oxidation of cysteine thiols from Ero1, a membrane-associated FAD-binding ER protein that transfers electrons from PDI to molecular oxygen (3, 4). In *S. cerevisiae*, an additional protein, Erv2p, performs a similar function to that of Ero1 (4, 5). Although orthologues of Erv2p do not seem to exist in higher eukaryotes, two human isoforms of Ero1 have been identified, Ero1α and Ero1β (6, 7).

A number of mammalian PDI-like ER proteins are known (8), including ERp57, ERp72, P5, PDIR, PDIp, TMX, ERp44, and the more recently described ERdj5/JPDI (9, 10), ERp18/ERp19 (11, 12), and EndoPDI/ERp46 (11, 13). They all contain one or more domains with sequence homology to thioredoxin, a cytosolic reductase. The redox activity of thioredoxin-like domains is provided by two cysteine residues present in a characteristic C*XX*C sequence motif. For several of the proteins mentioned above, the redox activity has been characterized *in vitro* (12, 14, 15), but in many cases the *in vivo* function is less well studied. Few endogenous substrates have been identified, and it is often not clear whether these PDI homologues serve a role in reduction, oxidation, or disulfide isomerization in the ER.

Cell biological and biochemical studies have revealed ERp57 to be a component of the calnexin/calreticulin chaperone system that promotes the folding and quality control of glycoproteins in the ER (reviewed in Ref. 16). Calnexin (CNX) and calreticulin (CRT) are homologous lectin chaperones that bind to the monoglucosylated glycan present on newly synthesized glycoproteins. Upon association with CNX and CRT (17, 18), ERp57 acts as a thiol-disulfide oxidoreductase for proteins carrying *N*-linked glycans. Transient disulfide-linked intermediates between ERp57 and nascent and newly synthesized glycoproteins have been observed *in vivo* (19). *In vitro*, the ERp57-enhanced oxidative refolding of RNase B, the glycosylated variant of RNase A, is critically dependent on its interaction with CNX and CRT (20). Two well characterized functions of ERp57 are as an important component of the major histocompatibility complex (MHC) class I peptide loading complex (21, 22) and in the folding of influenza hemagglutinin (23).

From the recently solved three-dimensional structures of the CRT P-domain and the luminal domain of CNX (24, 25), it was revealed that both chaperones contain a globular lectin domain with a long, protruding arm-like extension, referred to as the P-domain. The site of interaction with ERp57 has been mapped to the outermost tip of the P-domain in both CNX and CRT

* This work was supported by grants from the Swiss National Research Foundation (to A. H. and L. E.), the ETH Zürich (to A. H. and L. E.), the NCCR structural biology program (to P. F. and R. G.), by NIAID Grant AI45070 from the National Institutes of Health (to M. B.), and in part by National Science Foundation Grant BIR-9513060 (to W. F. S.). The costs of publication of this article were defrayed in part by the payment of page charges. This article must therefore be hereby marked "*advertisement*" in accordance with 18 U.S.C. Section 1734 solely to indicate this fact.

** To whom all correspondence should be addressed. Tel.: 41-1-632-3003; Fax: 41-1-632-1269; E-mail: lars.ellgaard@bc.biol.ethz.ch.

[1] The abbreviations used are: ER, endoplasmic reticulum; CNX, calnexin; CRT, calreticulin; DTT, dithio-1,4-threitol; MHC, major histocompatibility complex; PDI, protein disulfide isomerase; PVDF, polyvinylidene fluoride; Trx, thioredoxin; scRNaseA, scrambled RNase A; natRNaseA, native RNase A; X-gal, 5-bromo-4-chloro-3-indolyl-β-D-galactopyranoside.

(26–28). The exact position of the binding site in ERp57 for the two lectin chaperones remains to be elucidated.

The overall sequence identity at the amino acid level between ERp57 and PDI is 33% (8), making ERp57 the closest known homologue of PDI. The latter protein comprises four thioredoxin-like domains, two of which (denoted **a** and **a′**) are redox-active and contain a CGHC motif, whereas the other two domains (denoted **b** and **b′**) are redox-inactive and are devoid of CXXC motifs. The domains are arranged in the order **a-b-b′-a′**. In addition, PDI has an acidic C-terminal sequence. ERp57 lacks this negatively charged region, and its "QDEL" ER retrieval signal is directly preceded by the region corresponding to the PDI **a′** domain (8). NMR structures of the **a** and **b** domains in PDI show a thioredoxin fold for both (29, 30), and it is thus likely that the **a′** and **b′** domains also exhibit this fold. At present, the spatial organization of the four thioredoxin-like domains in PDI is unknown.

For ERp57, the information regarding the three-dimensional structure is limited to NMR assignments of the **a′** domain (31), and like PDI, ERp57 contains two CGHC active-site sequence motifs. Overall, the protein remains poorly characterized at the molecular level. Here we have investigated the biophysical and enzymatic properties of ERp57 to gain a more detailed understanding of structural and functional aspects of this thiol-disulfide oxidoreductase.

MATERIALS AND METHODS

Protein Expression and Purification—Full-length human ERp57, human PDI, *Escherichia coli* DsbA, *E. coli* thioredoxin (Trx), and human CRT were prepared as described previously (26, 32–34). Bovine insulin was from Sigma. The ERp57 **a** and **a′** domains were expressed and purified like full-length ERp57 (26), except for the absence of reducing agent in all buffers used. The protein sequence for the human ERp57 **a** domain includes residues 1–112 and residues 353–473 for the ERp57 **a′** domain. In this study, all ERp57 residue numbers refer to the human sequence after cleavage of the predicted signal peptide to generate the mature N terminus beginning with the sequence Ser^1-Asp^2-Val^3. Gene products encoding the **a** and **a′** domains were amplified by PCR and cloned into a pRSET A-derived *E. coli* expression vector (35). Protein expression from this vector results in the production of a fusion protein with an N-terminal 17-amino acid affinity tag containing a hexahistidine sequence. The correct sequence of both constructs was verified by DNA sequencing.

Protein Concentration Determination—The concentration of all proteins used in this study was determined from their absorbance at 280 nm by using the molar extinction coefficients calculated by the method of Gill and von Hippel (36). An extinction coefficient of 41,750 M^{-1} cm^{-1} was used for ERp57, 11,050 M^{-1} cm^{-1} for the ERp57 **a** domain, 13,490 M^{-1} cm^{-1} for the ERp57 **a′** domain, 80,630 M^{-1} cm^{-1} for CRT, 21,620 M^{-1} cm^{-1} for DsbA, and 14,060 M^{-1} cm^{-1} for Trx.

Limited Proteolysis of ERp57—Limited proteolysis was carried out in a buffer containing 100 mM KH_2PO_4/KOH, 25 mM NaCl, 10 mM β-mercaptoethanol, pH 7.0, at 37 °C at the concentrations of ERp57 and the specific protease indicated in Fig. 1. For trypsin, chymotrypsin, and elastase (Roche Applied Science), the digestions were stopped by the addition of phenylmethylsulfonide fluoride to 5 mM and in the case of thermolysin (Roche Applied Science) by adding EDTA to 5 mM. After addition of electrophoresis sample buffer, the digests were analyzed on SDS-15% PAGE (w/v), blotted onto a polyvinylidene fluoride (PVDF) membrane, and subjected to N-terminal sequencing.

Circular Dichroism Measurements—CD measurements were performed on a Jasco J-810 spectropolarimeter in a 1-mm path length cell at 25 °C. Spectra were averaged from 10 scans, and the buffer base line was subtracted. All proteins (6–11 μM) were in a buffer containing 100 mM KH_2PO_4/KOH, 25 mM NaCl, pH 7.0. ERp57 was reduced with 10 mM β-mercaptoethanol and oxidized with 2 mM GSSG. The **a** and **a′** domains were reduced with 1 mM DTT and oxidized with 1 mM GSSG. Reduction and oxidation was performed by dialyzing against the respective buffers overnight. The spectra for the ERp57 **a** and **a′** domains were not corrected for the presence of the unstructured N-terminal 17-amino acid affinity tag.

Quantification of Free Thiol Groups—Analysis of free thiol groups in ERp57 by Ellman's reagent 5,5′-dithiobis-2-nitrobenzoic acid was carried out at protein concentrations of 30 μM and 5,5′-dithiobis-2-nitrobenzoic acid concentrations of 0.3 mM in 80 mM sodium phosphate, pH 8.0, 1 mM EDTA, 2% w/v SDS. After incubation for 15 min at room temperature, the absorbance at 412 nm was recorded using an extinction coefficient of 13,600 M^{-1} cm^{-1} per free thiol (37).

Analytical Ultracentrifugation—Sedimentation velocity and equilibrium analysis of ERp57 and sedimentation velocity analysis of a mixture of ERp57 and CRT were performed on a Beckman Instruments Optima XL-I Analytical Ultracentrifuge. The cells were equipped with sapphire windows and 12-mm aluminum-filled Epon double sector centerpieces.

Sedimentation velocity runs for ERp57 were carried out at 20 °C and 50,000 rpm with patterns being acquired every 7 s. Sedimentation boundaries were analyzed using time derivative analysis as described previously (38, 39) and with the recently developed SEDANAL software for the analysis of interacting systems (40). Uncertainties in the fitted parameters were obtained using the bootstrap with replacement method. A stock solution of ERp57 at ~2 mg/ml was dialyzed for at least 16 h against 100 mM KH_2PO_4/KOH, pH 7.0, 25 mM NaCl, containing 2 mM dithio-1,4-threitol (DTT). Solutions of ERp57 in the range 0.1–1.0 mg/ml were prepared using the dialysate as diluent. For this particular buffer, the density and viscosity were calculated with Sednterp to be 1.01141 g/ml and 1.0342 centipoise, respectively. The value of the partial specific volume, $\bar{v}$ = 0.734 cm^3/g, was calculated from the amino acid composition of recombinant human ERp57 using the consensus partial volumes of the amino acids (41). The degree of hydration, δ_1 = 0.418 g of H_2O/g protein, was also calculated from the amino acid composition according to Kuntz and Kauzmann (42). Hydrodynamic modeling of monomeric ERp57 was performed using the equation of Perrin for an equivalent, hydrated prolate ellipsoid of revolution (43).

Sedimentation equilibrium runs for ERp57 were carried out at 4 °C as described previously (44). A stock solution of ERp57 at ~2 mg/ml was dialyzed for at least 24 h immediately prior to analysis in the same buffer as for sedimentation velocity runs. In addition, a series of dilutions of ERp57 in the range 0.1–1.0 mg/ml were prepared using the dialysate as diluent. Six-channel external loading centerpieces (Beckman Coulter part numbers 366755 and 368115) were used. Optical blank runs were performed both before and after the run at the expected and actual speeds, respectively. Sedimentation equilibrium data were analyzed by global fitting, combined data from three loading concentrations, and two speeds, as described previously (44).

Interaction studies between ERp57 and CRT were executed by sedimentation velocity at 20 °C and 50,000 rpm. Separate stock solutions of ERp57 and CRT at ~0.6 mg/ml were simultaneously dialyzed overnight against 100 mM KH_2PO_4, pH 7.0, 25 mM NaCl, and 1 mM DTT. To ensure the absence of any oxidized forms of ERp57 in solution, the protein was treated with 10 mM DTT for 1 h immediately prior to the dialysis step. Values of the partial specific volume and hydration of CRT were 0.698 cm^3/g and 0.502 g of H_2O/g protein as reported previously (34). The sedimentation velocity profiles were analyzed with the program SEDANAL to produce the $g(s^*)$ patterns and also fit to a 1:1 stoichiometry to obtain estimates of the equilibrium constants.

*Redox Equilibrium between the ERp57 **a** and **a′** Domains and Glutathione*—Fluorescence experiments were performed at 25 °C on a PTI Quantamaster QM-7/2003 Spectrofluorometer. All buffers used contained 1 mM EDTA and were filtered, degassed, and flushed with argon. Equilibration of the ERp57 **a** and **a′** domains at different GSH/GSSG ratios in 100 mM KH_2PO_4/KOH, 1 mM EDTA, pH 7.0, was performed for at least 15 h at 25 °C. A protein concentration of 2 μM was used in all experiments. After excitation at 280 nm, the fluorescence intensity at 350 nm, the wavelength at which the maximal difference between the emission of oxidized and reduced protein was observed, was recorded for 20 s and averaged. To determine the equilibrium constant K_{eq} for the ERp57 **a** and **a′** domain/glutathione system, the fluorescence emission at $[GSH]^2/[GSSG]$ ratios from 10^{-5} to 1 M was measured. This was achieved by varying the GSH concentration between 0.03 and 11 mM at a constant GSSG concentration of 0.1 mM. The completely reduced protein was measured at 10 mM GSH and the completely oxidized protein at 0.1 mM GSSG. Ellman's reagent was used as described above to verify that the protein was completely oxidized. The measured fluorescence F was plotted against the $[GSH]^2/[GSSG]$ ratio and fitted according to Equation 1 to obtain F_{ox}, the fluorescence of oxidized and F_{red}, the fluorescence of reduced protein. The relative amount of reduced protein at equilibrium (R), determined with Equation 2, was plotted against the $[GSH]^2/[GSSG]$ ratio, and the data were fitted according to Equation 1 to obtain K_{eq}. The standard redox potentials of the ERp57 **a** and **a′** domains were then calculated with the Nernst Equation 3 using the glutathione standard potential $E'_{0GSH/GSSG}$ of −0.240 V at pH 7.0 and 25 °C (45).

$$F = F_{ox} + (F_{red} - F_{ox})\frac{[GSH]^2/[GSSG]}{K_{eq} + [GSH]^2/[GSSG]} \quad \text{(Eq. 1)}$$

$$R = \frac{F - F_{ox}}{F_{red} - F_{ox}} \quad \text{(Eq. 2)}$$

$$E_0 = E'_{0GSH/GSSG} - (RT/nF) \times \ln K_{eq} \quad \text{(Eq. 3)}$$

Reductase Assay with Insulin—The catalyzed reduction of insulin by DTT was monitored at different concentrations of various thiol-disulfide oxidoreductases as catalysts by measuring the increase in turbidity at 650 nm (46). Each assay was performed at 25 °C and contained 130 μM insulin and different concentrations of catalyst in 100 mM KH_2PO_4/KOH, 1 mM DTT, 2 mM EDTA, pH 7.0. The enzymes were pre-incubated in the DTT-containing buffer for 5 min, and the assay was started by the addition of insulin. The onset of aggregation was defined as the time where OD_{650} had reached the value of 0.025. The enzyme concentration at which this occurred was plotted against the onset of aggregation in order to obtain a concentration-dependent activity curve for the reductase activity of each oxidoreductase.

Preparation of Scrambled RNaseA—Scrambled RNaseA (scRNaseA) was prepared by reducing and denaturing 70 mg of native RNaseA (natRNaseA) (Sigma) overnight at room temperature in 3 ml of 50 mM Tris/HCl, pH 8.0, 6 M guanidinium chloride, and 150 mM DTT. Next, buffer exchange into 100 mM acetic acid/NaOH, pH 4.0, was obtained by gel filtration on a PD-10 column (Amersham Biosciences). The reduced and denatured RNaseA was diluted to 0.25 mg/ml with 50 mM Tris/HCl, pH 8.5, 6 M guanidinium chloride and subjected to air oxidation for 5 days in the dark. Finally, after concentration, RNaseA was gel-filtrated once again on a PD-10 column into 100 mM acetic acid/NaOH, pH 4.0, and stored at −20 °C. Both after reduction and oxidation the number of free thiols was determined by the Ellman's assay. The scRNaseA preparation lacked free thiols, as well as disulfide-linked dimers as shown by non-reducing SDS-PAGE.

Disulfide Isomerase Assay with Scrambled RNaseA—The isomerase function of ERp57 and its redox-active domains was tested by the ability to reactivate scRNaseA. 40 μM scRNaseA was incubated with 10 μM (active-site concentration) of a given thiol-disulfide oxidoreductase previously reduced with an equimolar concentration of DTT. The isomerase reaction was performed in 100 mM KH_2PO_4/KOH, 2 mM EDTA, 10 μM DTT, pH 7.0, at 25 °C. At various time points, 100-μl samples were taken from the reaction and added to 300 μl of 4 mM cCMP, and the hydrolysis of cCMP was followed on a Cary 3E UV-visible spectrophotometer for 3 min at 296 nm. The hydrolysis rate of cCMP catalyzed by 40 μM natRNaseA was set to 100% activity, and all other samples were expressed as a percentage of this value.

Construction of Plasmids for Periplasmic Protein Expression—The plasmid pDsbA3 (47) was used to generate constructs in which the DsbA signal sequence was fused to the respective oxidoreductase. Expression from this plasmid is under the control of the *trc* promoter/lac operator. The cDNA regions encoding ERp57 and PDI were amplified by PCR from the plasmids pHisERp57 (26) and pET12PDI (48), respectively, using the following primers: ERp57OxF, 5′-GGTACTAGTGCGTCCGACGTGCTAGAACTC, and ERp57OxR, 5′-GCAGCCGGATCCTTAGAG; PDIOxF, 5′-AGCGCTAGCGCGGACGCCCCCGAGGAG, and PDIOxR, 5′-TACTAGTGCGGACGCCCCCGAGGAG. The resulting PCR products were digested with SpeI and BamHI and cloned into pDsbA3 where the segment encoding mature DsbA had been removed with NheI and BamHI, thus generating the pDsbAERp57 and pDsbAPDI constructs. The ERp57 **a** domain and **bb′a′** domain constructs were produced by PCR from the plasmid pDsbAERp57 using the phosphorylated primers ERp57aF, 5′-TAAGGATCCCCACGCGCC, and ERp57aR, 5′-CTGCTTCTTCAAGTGGCTG; ERp57bb′a′F, TACTAGTGCGGCAGGACCAGCTTCA, and ERp57bb′a′R, 5′-CCCGGATCCTTAGAGATCCTCCTG. Next, the resulting PCR fragments comprising the entire vector and the desired regions of the *ERp57* gene were blunt-end ligated. The creation of the construct for the secretion of the PDI **a** domain has been described before (49). The DsbC construct used in the assay encodes the redox-inactive C98A/C101A variant as a negative control. The correct sequence of all constructs was verified by DNA sequencing.

In Vivo Complementation Assay—E. coli THZ2 cells (50) lacking the bacterial dithiol oxidase DsbA were transformed with the secretory expression plasmid of the oxidoreductase construct to be tested. Expression, correct localization to the periplasm, and processing of the leader peptide was verified for each construct by cell fractionation. Cytosolic and periplasmic fractions were compared on SDS-PAGE, and in certain cases by transfer to a PVDF membrane followed by N-terminal sequencing or detection by an antibody. To obtain the periplasmic fraction, cells grown at 37 °C in LB medium supplemented with 100 μg/ml ampicillin were induced with 1 mM isopropyl-β-D-thiogalactopyranoside at OD_{600} of 0.6 and grown for 3 h. Next, cells were harvested by centrifugation, and periplasmic proteins were extracted by stirring the cells for 1 h at 4 °C in 50 mM Tris/HCl, pH 7.5, 150 mM NaCl, 1 mg/ml polymyxin B sulfate. Spheroblasts were pelleted by centrifugation, and the periplasmic fraction remained in the supernatant. Because we did not detect expression of the isolated ERp57 **a′** domain in this system, the triple domain construct of ERp57 **bb′a′** was used to test the oxidase activity of the ERp57 **a′** domain.

DsbA complementation was analyzed by the recovery of motility of a single colony (51). 1 μl of LB culture inoculated with a single colony of THZ2 cells transformed with an oxidoreductase secretion construct and adjusted to OD_{600} = 0.7 was placed in the middle of an LB plate containing 0.3% (w/v) agar. After incubation at 37 °C for 24 h, the diameter of the bacterial lawn was compared with that of *E. coli* THZ2 harboring pDsbA3 as a positive control and DsbC C98A/C101A as a negative control. Additionally, DsbA complementation was analyzed by oxidative inactivation of β-galactosidase fused C-terminally to MalF (52). Streak-outs of overnight cultures containing 100 μg/ml ampicillin and transformed with the respective periplasmic expression plasmid were made on LB agar plates supplemented with 0.4% maltose and 40 μg/ml 5-bromo-4-chloro-3-indolyl-β-D-galactopyranoside (X-gal) and incubated for 24 h at 37 °C followed by 6 h at 4 °C. DsbA complementation was classified as follows: white colonies (+), pale blue colonies (+/−), blue colonies (−).

RESULTS

Determination of Domain Boundaries in ERp57—As a first characterization of recombinantly expressed full-length ERp57, we subjected the protein to limited proteolysis. This experimental approach not only gives information about domain boundaries but also about the relative stability of individual domains toward proteolysis.

For proteolysis of ERp57 at pH 7.0 and 37 °C, we used trypsin, chymotrypsin, elastase, and thermolysin. Each digestion mixture was resolved by SDS-PAGE (Fig. 1) and transferred onto a PVDF membrane, and single bands were excised and N-terminally sequenced. Table I lists the N-terminal sequence obtained for each of the fragments corresponding to the bands indicated in Fig. 1. Fig. 2 shows the sequence positions of the ERp57 fragments obtained by partial digestion, as well as the experimentally determined domain structure of PDI.

Cuts were generated at the expected domain boundaries between **b** and **b′** and between **b′** and **a′** inferred from a sequence alignment with PDI. All four proteases generated cuts in the sequence region 211–222 between the **b** and **b′** domains (fragments 1, 4, 11, and 16), whereas trypsin and chymotrypsin cleaved at residues 340 and 341 in a region predicted to connect the **b′** and **a′** domains (fragments 2 and 5). Based on the sequence alignment with PDI and the proposed linker region in PDI deduced from the NMR structures of the PDI **a** and **b** domains (30), we expected the linker between these two domains in ERp57 to comprise only residues 109–111. The short length of this linker likely explains why no cleavage occurred exactly within this region. The closest cut was the one produced by elastase at residue 134 (fragment 7).

The mobility of the proteolytic fragments visible on gels combined with the 12–15-kDa size for a single thioredoxin-like domain enabled us to predict which single, double, and triple domains were present in the different digestion mixtures. The only single domains detected were the **a** (fragments 3, 6, 12, 13, 17, and 18) and **a′** domains (fragments 2 and 5). The only double and triple domains observed were **b′a′** (fragments 1, 4, and 16) and **bb′a′** (fragment 7), respectively. However, the **b** domain was rapidly degraded from the N terminus of this triple domain at higher concentrations of protease and longer incubation times (Fig. 1*b*, *fragments 7–10*). At lower concentrations of protease or shorter incubation, **a′** was observed together with **b′** (fragments 1, 4, 11, and 16), indicating that the pres-

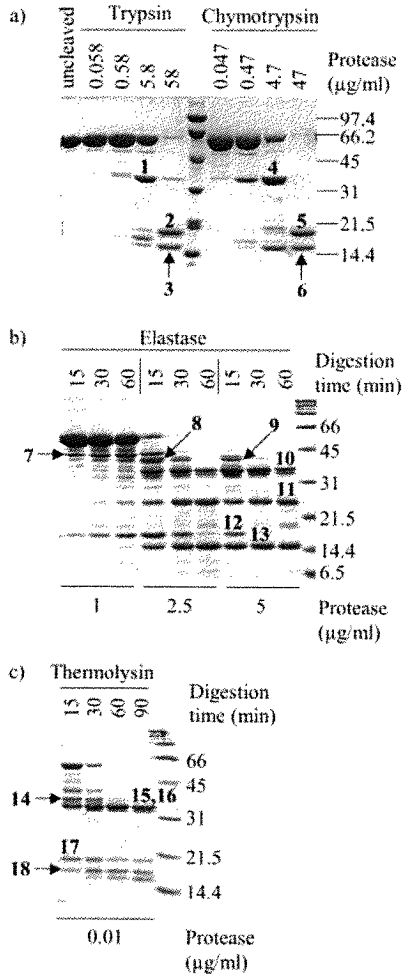

FIG. 1. **Limited proteolysis of ERp57.** ERp57 (20 μM) was digested at 37 °C and pH 7.0 with the indicated concentrations of protease, and samples were collected at various time points. The digests were stopped with phenylmethylsulfonide fluoride or EDTA, and digest mixtures were separated on 15% SDS-PAGE gels and stained with Coomassie Blue.

TABLE I
N-terminally sequenced fragments of ERp57 derived by limited proteolysis

The fragment number listed refers to the numbers shown for the different bands in Fig. 1. Note that recombinant ERp57 contains an "HN" dipeptide sequence at its N terminus.

Fragment	Protease	N-terminal sequence
1	Trypsin	^{211}FIQENI
2		^{340}YLKSEP
3		$^{-2}$HNSDVL
4	Chymotrypsin	^{212}IQENIF
5		^{341}LKSEPI
6		$^{-2}$HNSDVL
7	Elastase	^{134}GFFDD
8		^{152}SNLRD
9		^{159}RFAH
10		^{199}TEQKM
11		^{223}MTEDN
12		$^{-2}$HNSDVL
13		$^{-2}$HNSDVL
14	Thermolysin	^{187}LTNKF
15		^{169}VNE
16		^{212}IQE
17		$^{-2}$HNSDVL
18		$^{-2}$HNSDVL

ence of the **a′** domain stabilized the **b′** domain to a certain extent. Overall, of the four domains, the **a** and **a′** domains appeared to be the most resistant and the **b** domain the least resistant to proteolysis. The **b′** domain could not withstand extended proteolytic cleavage.

For the following experiments performed in this investigation, we used ERp57 **a** and **a′** domain constructs comprising residues 1–112 and 353–473, respectively. For the **a** domain construct the position of the C-terminal boundary was based on a sequence alignment with the PDI **a** domain. The slight C-terminal truncation of the **a′** domain construct was performed to remove the QDEL ER retrieval sequence and a few preceding residues that are likely to constitute a flexible tail. The notion that segment 353–473 corresponds to a properly folded domain is supported by the NMR assignments reported for an **a′** construct comprising residues 349–468 (31). Furthermore, spectroscopic analysis of our **a** and **a′** constructs showed that both display typical features of properly folded proteins (see below).

Spectroscopic Analysis of ERp57—To learn more about structural features of full-length ERp57 and its **a** and **a′** domains, we performed CD and fluorescence spectroscopy under oxidizing and reducing conditions. For all three constructs, the far-UV CD spectrum showed features characteristic of folded proteins of the α-β type (Fig. 3, *a–c*). No noticeable difference in the secondary structure was observed between the oxidized and the reduced states of the full-length protein and the ERp57 **a′** domain (Fig. 3, *a* and *c*), whereas the ERp57 **a** domain showed minor spectral changes (Fig. 3*b*). ERp57 thus differs from PDI in the sense that the oxidized state of the PDI **a′** domain exhibits a far-UV CD spectrum like that of an unfolded protein (48) (see under "Discussion").

The fluorescence emission spectra obtained for the ERp57 **a** and **a′** domains after excitation at 280 nm showed that both proteins displayed a 1.8-fold higher emission at 350 nm for their reduced *versus* their oxidized state (Fig. 3, *d* and *e*). This likely resulted from the quenching of their single trytophan residue, positioned immediately N-terminal to the CGHC sequence motif, upon formation of the active-site disulfide. The spectra of the **a′** domain are dominated by the six tyrosines found in this protein (Fig. 3*e*).

ERp57 Contains a Structural Disulfide—Besides the four active-site cysteines, ERp57 contains three additional cysteines. Of these, two are found in the **a** domain (Cys^{61} and Cys^{68}), and one is located at the beginning of the **b′** domain (Cys^{220}). Because the potential intra- and/or intermolecular disulfide bonding pattern of these three cysteines is not known, we determined the number of free thiol groups in the protein.

When conducting the assay with oxidized ERp57 under denaturing conditions, only one free cysteine could be detected (data not shown). Therefore, two of the additional cysteines in ERp57 form a structural disulfide. Moreover, when repeating the assay with the **a** domain, we detected no free cysteines, indicating that a disulfide bridge must be formed by Cys^{61} and Cys^{68}. This is consistent with the observation that the C^{β} atoms of the two alanines in PDI, corresponding to Cys^{61} and Cys^{68} in ERp57, are positioned 4.85 Å apart in the structure of the human PDI **a** domain (29), a distance compatible with the formation of a disulfide bond.

Analytical Ultracentrifugation Analysis of ERp57 and of Its Complex with CRT—Sedimentation equilibrium and velocity experiments were carried out at pH 7.0 under reducing conditions to determine the oligomeric state of ERp57 in solution. Results revealed that monomeric ERp57 has a sedimentation coefficient, $s^0_{20,w}$, of 3.53 ± 0.4 S. In the presence of 2 mM DTT, ERp57 was determined to self-associate reversibly as indicated by the concentration dependence of the weight average sedimentation coefficient (data not shown). Both the sedimentation equilibrium and sedimentation velocity data could best be fit to a monomer-trimer-hexamer interacting system. The sedimen-

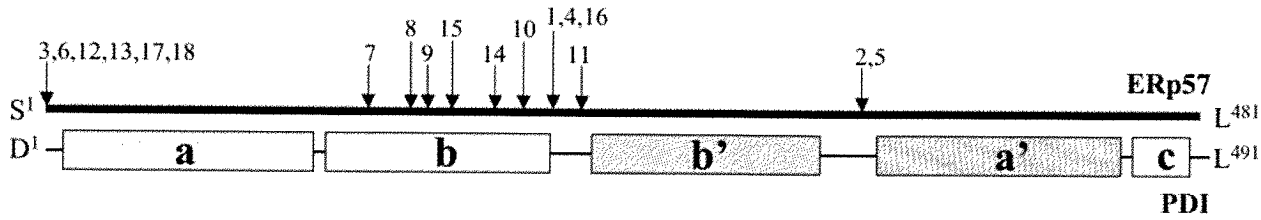

FIG. 2. **Schematic representation of ERp57 fragments obtained by limited proteolysis.** The *upper line* represents ERp57, and the *boxes below* depict the experimentally determined domain boundaries in PDI (8, 61–63). The *arrows* pointing to sequence positions within ERp57 indicate the location of the proteolytic fragments. The *numbers* refer to the bands on the SDS-PAGE in Fig. 1 for which the experimentally determined N-terminal sequences are listed in Table I.

tation velocity data could best be fit with the program SEDANAL to a model with slow re-equilibration kinetic values suggesting the possibility that structural rearrangements are involved in the self-association process. Dissociation constants were calculated to be $K_{d,m-t} = 1700 \pm 400\ \mu M^2$ ($k_f = 5.8 \pm 0.7 \times 10^5\ M^{-1}\ s^{-1}$ and $k_r = 9.7 \pm 1.0 \times 10^{-3}\ s^{-1}$) and a trimer-hexamer dissociation constant to be $K_{d,t-h} = 14 \pm 3$ nM ($k_f = 3.3 \pm 0.3 \times 10^4\ M^{-1}\ s^{-1}$ and $k_r = 4.6 \pm 0.6 \times 10^{-4}\ s^{-1}$). The functional relevance of these high molecular weight oligomeric forms of ERp57 is presently unclear.

Insight into the size and molecular shape of ERp57 was obtained from the frictional ratio, f/f_0, which was determined from the sedimentation coefficient, $s^0_{20,w}$, and the molecular mass = 54.5 kDa (Table II). These calculations yielded an $f/f_0 = 1.24$ using a partial specific volume of 0.734 cm^3/g and a hydration value of 0.418 g of H_2O/g protein (Table II). By using these values for the frictional ratio, partial specific volume, and hydration, monomeric ERp57 could be represented with a hydrodynamically equivalent prolate ellipsoid of revolution having an apparent axial ratio $a/b = 4.9 \pm 0.2$ with a length of 16.8 ± 0.5 nm and a diameter of 3.4 ± 0.1 nm (Table II). Based on this model, the hydrodynamic measurements indicate that the monomeric form of ERp57 is a moderately elongated protein in solution.

We also investigated interactions between ERp57 and full-length CRT by sedimentation velocity experiments (Fig. 4). ERp57 and CRT were mixed in various ratios and analyzed with the program SEDANAL to fit to a heterologous 1:1 stoichiometry of the complex (Fig. 4). A global fit to four data sets over a range of concentrations gave a value of $K_d = 2.56 \pm 0.01$ μM. A value of $s_{20,w} = 4.6 \pm 0.2$ S for the complex of CRT and ERp57 was also obtained from the fits (Table II). By using this value, the ERp57-CRT complex can be represented with a hydrodynamically equivalent prolate ellipsoid of revolution with a length of 32.7 ± 3.0 nm and diameter of 3.4 ± 0.2 nm. Previous studies on free CRT (34) showed that this protein is highly elongated with a length of 29.8 nm and a diameter of 2.4 nm. Thus, shape analysis for the ERp57-CRT system suggests that the complex forms with a partially overlapping geometry, probably involving conformational changes in both proteins.

Determination of Equilibrium Redox Potentials for ERp57 ***a*** *and* ***a'***—As a first means to characterize the redox activity of ERp57, we determined the standard redox potentials for the redox-active **a** and **a'** domains. Although the redox potential for a given oxidoreductase does not necessarily reveal the redox function of the protein in the living cell, it often provides valuable information about the preferred redox reaction.

By using fluorescence spectroscopy, the redox equilibrium of the ERp57 **a** and **a'** domains was analyzed at different GSH/GSSG ratios. The increase in fluorescence emission at 350 nm upon reduction was followed after excitation at 280 nm (Fig. 3, *d* and *e*). Thus, when ERp57 **a** and **a'** were incubated in the presence of 0.1 mM GSSG and varying concentrations of GSH (0.03–11 mM) under the exclusion of oxygen, the relative amounts of oxidized and reduced protein at equilibrium could be determined from a fit of the experimental data to Equation 1 (see "Materials and Methods") (Fig. 5, *a* and *b*). By this method, the equilibrium constant, K_{eq}, for the ERp57 **a**/glutathione system was found to be 3.3 ± 0.4 and 1.5 ± 0.1 mM for the ERp57 **a'**/glutathione system. The standard redox potentials for the ERp57 **a** and **a'** domains were calculated from the Nernst equation by using the glutathione standard potential of −0.240 V at pH 7.0 and 25 °C (45) and Equation 2 (see "Materials and Methods"). Like this, the standard redox potential for ERp57 **a** was determined to be −0.167 V and that for ERp57 **a'** to be −0.156 V. These values are comparable with the redox potential of −0.175 V determined for PDI (53).

Disulfide Reductase Activity of ERp57—PDI is a remarkably versatile enzyme exhibiting reductase, isomerase, and oxidase activities. Although not the only determining factor, the similarity in redox potentials between PDI and ERp57 **a** and **a'** could indicate similar redox activities. The reductase and isomerase activity of ERp57 *in vitro* has been addressed previously (54–57). However, a comprehensive quantitative analysis of the catalytic activity of ERp57 in comparison to other thiol-disulfide oxidoreductase is lacking. Therefore, we decided to investigate whether ERp57 is endowed with the same broad catalytic abilities as PDI by comparing ERp57 to PDI and other well known thiol-disulfide oxidoreductases. We employed assays to probe disulfide reductase, isomerase, and dithiol oxidase activity.

For the reductase activity, we made use of the fact that insulin aggregates upon reduction by DTT. The resulting turbidity of the protein solution can be measured by detecting the optical density at 650 nm (46). To compare the reductase efficiency of ERp57 with that of PDI and other thiol-disulfide oxidoreductases, we defined the onset of aggregation as the time point where OD_{650} exceeded a value of 0.025 (final $OD_{650} = 1.4–1.8$). For the uncatalyzed reaction, this value was reached after 40 min.

Wide concentration ranges were tested for each oxidoreductase and plotted against the time for onset of aggregation (Fig. 6). By comparing how much catalyst was required to halve the uncatalyzed time of aggregation onset to 20 min, a relative measure of the reductase efficiency was obtained (Fig. 6, *dotted line*). Quantified in this way, ERp57 proved to be 20 times less efficient than PDI as a reductase (0.8 μM of ERp57 needed *versus* 0.04 μM of PDI). However, ERp57 was 5 times more efficient than DsbA, the bacterial oxidase, and only 2 times less efficient than thioredoxin, the bacterial cytosolic reductase.

Disulfide Isomerase Activity of ERp57—To characterize the isomerase activity of ERp57, we used a variant of a well established assay based on the reactivation of disulfide-scrambled RNaseA. The catalyzed isomerization of 40 μM scrambled scRNaseA to natRNaseA was followed over a period of 8 h in the presence of catalytic amounts of reduced PDI, ERp57, or the ERp57 **a** and **a'** domains. To obtain a measure of isomerase activity, samples were collected at different time points, and

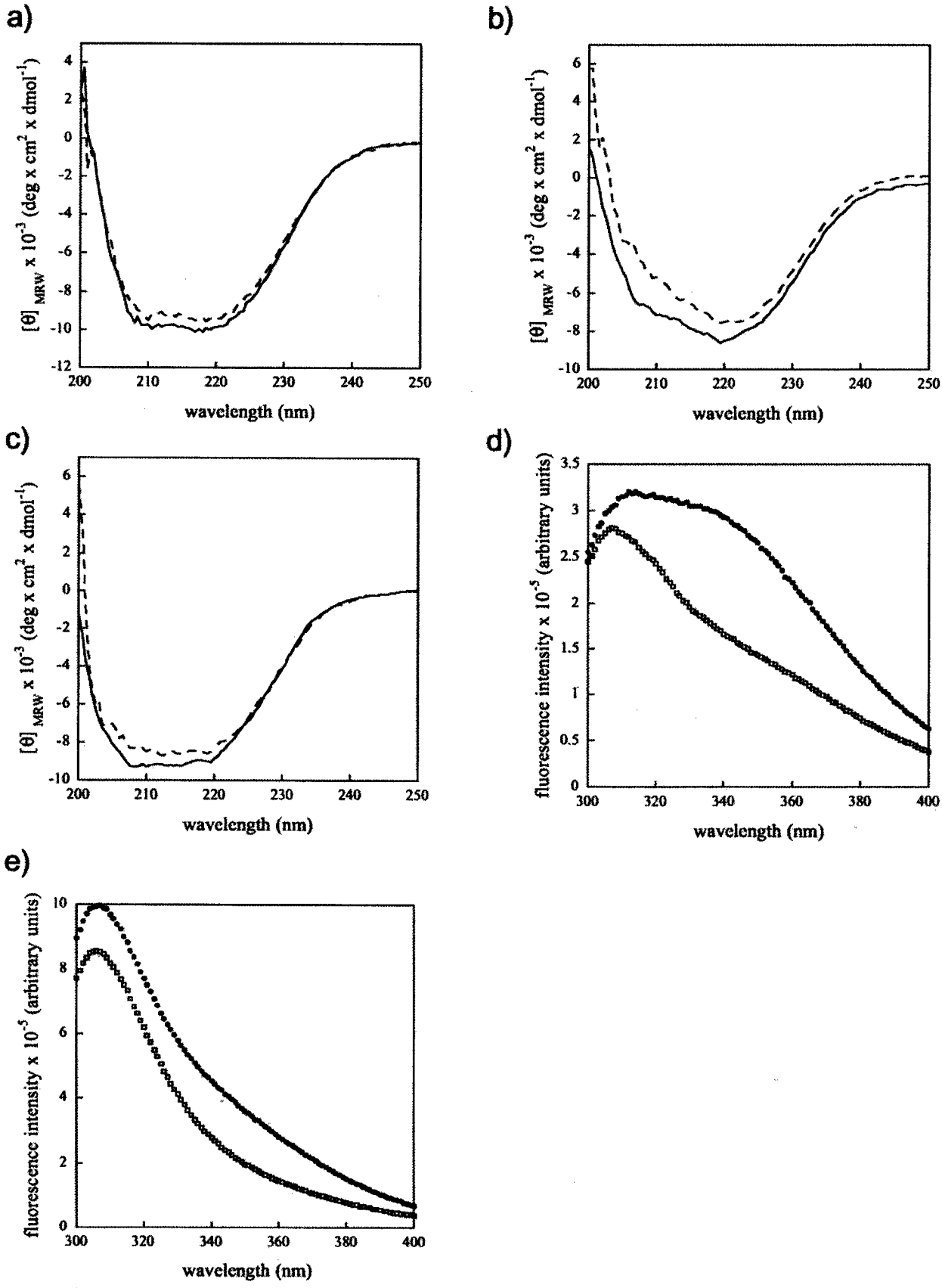

FIG. 3. **Spectral analysis of ERp57 at pH 7.0 and 25 °C.** *a–c*, far-UV circular dichroism spectra of ERp57 (*a*), the ERp57 **a** domain (*b*), and the ERp57 **a′** domain (*c*) in the reduced (*solid lines*) and oxidized (*broken lines*) form. ERp57 was either reduced with 10 mM β-mercaptoethanol or oxidized with 2 mM GSSG. The domains were either reduced with 1 mM DTT or oxidized with 1 mM GSSG. The spectra for the ERp57 **a** and **a′** domains were not corrected for the presence of the unstructured N-terminal 17-amino acid affinity tag. *d* and *e*, fluorescence emission spectra of oxidized and reduced ERp57 **a** domain (*d*) and ERp57 **a′** domain (*e*) were recorded after excitation at 280 nm. Oxidized domains contained 0.1 mM GSSG (*open symbols*) and reduced domains 10 mM GSH (*closed symbols*).

TABLE II
Hydrodynamic properties of monomeric ERp57 and of the ERp57-CRT complex determined by sedimentation analysis

	Monomeric ERp57	ERp57-CRT
Molecular mass[a]	54.5 kDa	101.3 kDa
Sedimentation coefficient ($s^0_{20,w}$)	3.53 ± 0.04S	4.6 ± 0.2S
Stokes radius (R_S)	3.3 nm	5.5 nm
Specific hydration[a] (δ_1)	0.418 g H_2O/g protein	0.475 g H_2O/g protein
Partial specific volume[a] ($\bar{v}$)	0.734 cm^3/g	0.717 cm^3/g
Frictional ratio (f/f_0)	1.24 ± 0.02	1.52 ± 0.07
Axial ratio (a/b)	4.9 ± 0.2	9.6 ± 1.2
Length	16.8 ± 0.5 nm	32.7 ± 3.0 nm
Diameter	3.4 ± 0.1 nm	3.4 ± 0.2 nm

[a] Calculated from the amino acid sequences of recombinant ERp57 and CRT.

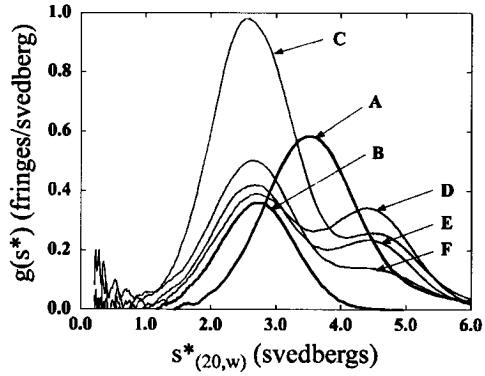

FIG. 4. **Sedimentation velocity analysis of the ERp57-CRT complex.** Sedimentation velocity experiments showing complex formation between ERp57 and full-length CRT. *A*, free ERp57; *B*, free CRT. ERp57 and CRT were mixed in the following molar ratios [ERp57]/[CRT], where concentration units are given in μM. *C*, 1.7:11.3; *D*, 3.2:4.7; *E*, 2.0:4.6; and *F*, 1.1:5.5. CRT was added in excess of ERp57 to drive the equilibrium toward complex formation. These data were fitted with SEDANAL to a heterologous 1:1 association model.

the rate of cCMP hydrolysis by reactivated RNaseA was determined and expressed as a percentage of the hydrolysis rate obtained with 40 μM natRNaseA (Fig. 7).

Reactivation of scRNaseA to the wild-type level was achieved within ~3 h by using 5 μM PDI. With the same concentration of ERp57, scRNaseA could only be rescued to ~60% of the native level after 8 h. When using 5 μM of each of the ERp57 **a** and **a'** domains, which corresponds to 5 μM full-length ERp57 in active-site concentration, the reactivation level reached ~30%. In a control experiment, it was verified that the individual **a** and **a'** domains were both active in our assay (data not shown).

To get a second measure of the disulfide isomerase activity for the different proteins in our assay, we determined the initial rate of catalysis. Here we obtained values for the initial reactivation rate of scRNaseA of greater than or equal to 1.11 μM/min for PDI, 0.16 μM/min for ERp57, and 0.05 μM/min for the ERp57 **a** and **a'** domains, compared with 4.8×10^{-3} μM/min for the background reaction (5 μM DTT). Therefore, compared with ERp57, the initial rate of reactivation by PDI is at least 7 times faster, while the rate obtained for the mixture of the **a** and **a'** domains is 3 times slower. The uncatalyzed isomerization reaction is 33 times slower than the ERp57-catalyzed reaction. Taken together, the results of the isomerase assay indicated that although ERp57 does possess activity, it is by far not as efficient as PDI. When mixed, the two separate redox-active domains did not possess the same isomerase activity as the full-length protein.

Dithiol Oxidase Activity of ERp57—To investigate a potential oxidase activity of ERp57, the existence of two distinct and non-interacting pathways for disulfide bond formation in the periplasm of Gram-negative bacteria was exploited. In *E. coli*, separate enzymes perform different oxidoreductase functions. DsbA functions as the oxidase of protein thiols, itself in turn being reoxidized by DsbB, which obtains oxidizing equivalents from ubiquinone Q_8. On the other hand, DsbC performs reductase and isomerase functions. DsbC is kept in a reduced state by DsbD, which in turn is reduced by thioredoxin (for reviews see Refs. 1 and 58).

To test oxidase activity, the ability of periplasmically expressed ERp57, PDI, and various domains of both proteins to complement DsbA deficiency in THZ2, an *E. coli* strain that lacks DsbA, was analyzed by two phenotypic characteristics. One assay depends on a test of bacterial motility based on the DsbA-dependent folding of the P-ring subunits of the flagellar motor (51). The other assay involved a blue/white screening that relies on the oxidative inactivation of β-galactosidase partially located to the periplasm. This assay probes the DsbA-dependent introduction of inactivating disulfide bonds into a β-galactosidase-MalF fusion protein (52, 59). Thus, colonies of *E. coli* that lack a periplasmic oxidase turn blue on LB-plates containing X-gal. As a negative control protein we used a redox-inactive DsbC variant in which the two active-site cysteines had been mutated to alanines (DsbC C98A/C101A), and as a positive control DsbA itself was exported to the periplasm. Periplasmic expression of all proteins was ensured by cloning each construct in-frame with the DsbA leader peptide and was verified by cell fractionation. The assays were performed in the absence of the inducer isopropyl-β-D-thiogalactopyranoside, whereby protein expression results from a leaky promoter. Thus, approximately the same levels of expression are observed for different constructs (49).

The results showed that the ability of bacteria to swarm on top of a soft agar plate and form a bacterial lawn was restored in THZ2 cells transformed with the periplasmic expression plasmids of ERp57, the ERp57 **a** domain, and the ERp57 **bb'a'** triple domain (Table III). The latter was used in place of the ERp57 **a'** domain, because we did not observe periplasmic expression of the ERp57 **a'** domain. PDI and the PDI **a** domain, both known to act as oxidases (49, 60), also restored bacterial swarming. Equivalent results were obtained with the blue/white assay (Table III). In conclusion, ERp57 was able to act as an oxidase in the environment of the bacterial periplasm, and both redox-active domains of ERp57 could compensate for the absence of DsbA.

DISCUSSION

Our investigation of various biophysical and biochemical properties of ERp57 provides new insight into the structure of the molecule, and we show that ERp57 is a versatile redox enzyme. In many respects, it is similar to its closest homologue, PDI, but significant differences in redox activity were also observed. Our findings give a better understanding of ERp57 at the molecular level, and have implications for the function of the protein *in vivo*.

The limited proteolysis experiments provided information about domain boundaries and showed that like PDI, ERp57 contains four structural domains. Together with previously

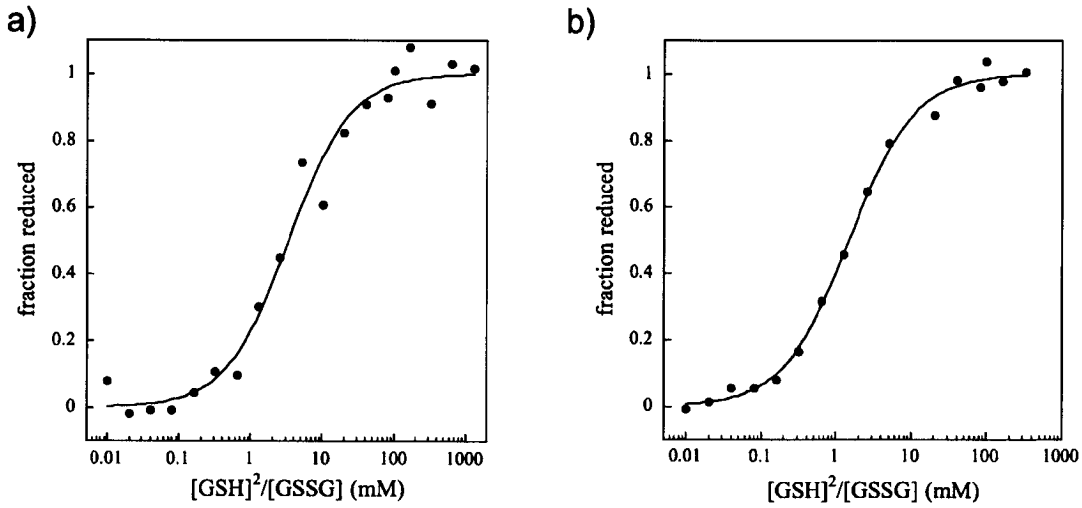

FIG. 5. **Redox equilibrium of ERp57 a and a′ domains with glutathione.** The fraction of reduced ERp57 **a** domain (*a*) and ERp57 **a′** domain (*b*) at pH 7.0 and 25 °C was determined by fluorescence spectroscopy after incubation of the proteins for at least 16 h in a buffer containing 0.1 mM GSSG and varying concentrations of GSH (0.03–11 mM). After excitation at 280 nm, fluorescence emission was recorded at 350 nm, the data were normalized, and the fraction of reduced protein was plotted against the $[GSH]^2/[GSSG]$ ratio. The equilibrium constant was determined, and the data were normalized by fitting them according to Equation 1 (see under "Materials and Methods"). After nonlinear regression, a value of K_{eq} = 3.3 mM was obtained for the ERp57 **a** domain (correlation coefficient, 0.989) and a value of K_{eq} = 1.5 mM was found for the ERp57 **a′** domain (correlation coefficient, 0.998).

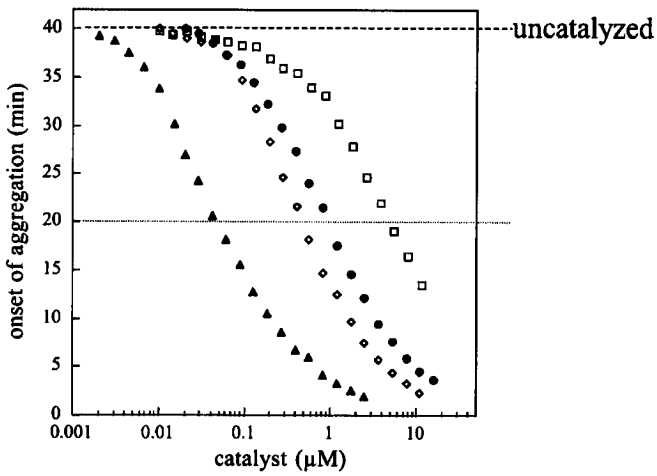

FIG. 6. **Catalyzed reduction of insulin by DTT.** Various concentrations of DsbA (□), ERp57 (●), Trx (◇), and PDI (▲) were tested for their ability to catalyze the reduction of 130 μM insulin by 1 mM DTT at 25 °C. The onset of aggregation was defined as the time when the optical density at 650 nm had reached a value of 0.025 and was plotted against the concentration catalyst used.

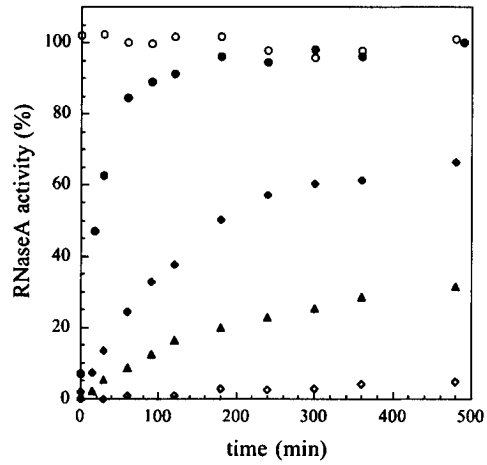

FIG. 7. **Isomerization and reactivation of scrambled RNaseA.** 5 μM PDI (●), 5 μM ERp57 (♦), and 5 μM each of the ERp57 **a** and **a′** domain (▲) that had been reduced with equimolar amounts (10 μM) of DTT were tested for their ability to reactivate 40 μM scRNaseA at 25 °C. At various time points samples were taken from the reaction, and the RNaseA activity was followed by the hydrolysis of cCMP for 3 min at 296 nm. The initial hydrolysis rate of cCMP for 40 μM natRNaseA (○) was set to 100% RNaseA activity, and all other initial rates were expressed as a percentage of this activity. ◇, 40 μM scRNaseA in the presence of 10 μM DTT (no catalyst added).

published data on domain boundaries in PDI (61–63), and the sequence similarity between the two proteins, our results allow an estimate of the domain boundaries for the four thioredoxin-like domains in ERp57. Based on this analysis, we have generated the following ERp57 domain constructs in *E. coli*: **a**, residues 1–112; **b**, residues 108–218; **b′**, residues 219–352; and **a′**, residues 353–473. The domain boundaries are in agreement with those proposed recently by Alanen *et al.* (64), who based their assignments primarily on sequence alignments between known ER thiol-disulfide oxidoreductases.

For the **b** and **b′** domain constructs, our NMR data show that these proteins give rise to well dispersed NMR signals indicative of defined three-dimensional structures in solution.[2] For the redox-active **a** and **a′** domains, it is noteworthy that neither seemed to undergo significant structural changes upon formation of the active-site disulfide bond as judged by far-UV CD spectroscopy (Fig. 3, *b* and *c*). Thus, both domains retained spectra characteristic of folded, globular proteins. This is in contrast to the PDI **a′** domain, where the oxidized form exhibits a far-UV CD spectrum much like that of an unfolded protein (48). A destabilization of the oxidized form in comparison to the reduced form has also been observed in other thiol-disulfide oxidoreductases such as DsbA (20, 65), ERp18 (12), and the PDI **a** domain (12).

To obtain insight into the hydrodynamic properties of ERp57, the protein was analyzed by analytical ultracentrifugation. Results from sedimentation velocity measurements showed that ERp57 is an elongated molecule with a length of 16.8 ± 0.5 nm and a diameter of 3.4 ± 0.1 nm (Table II). These dimensions make it unlikely that the four domains pack closely into the shape of a pyramid-like structure. Most interesting,

[2] R. Riek, V. Wohlgensinger, H. Kovacs, and L. Ellgaard, unpublished data.

TABLE III
In vivo complementation of DsbA by PDI, ERp57, and their redox-active domains

Complementation was scored in two different assays, the ability to swarm on soft agar and the ability to oxidatively inactivate a β-galactosidase-MalF fusion protein leading to the formation of white colonies (see text for details). +, complementation; −, no complementation; ±, partial complementation.

Construct	Complementation of DsbA (motility screen)	Complementation of DsbA (blue/white screen)
DsbA	+	+
DsbC ko	−	±
PDI	+	+
PDI **a**	+	+
ERp57	+	+
ERp57 **a**	+	+
ERp57 **bb'a'**	+	+

recent ultracentrifugation studies from Gilbert's lab indicate that PDI is also likely to be an elongated molecule in solution.[3]

Somewhat surprisingly, the sedimentation equilibrium analysis showed a reversible self-association of ERp57 into trimers and hexamers in solution in the presence of 2 mM DTT. The dissociation constants for the monomer-trimer and the trimer-hexamer equilibria were determined to 1700 μM^2 and 14 nM, respectively. The high value of the dissociation constant for the monomer-trimer equilibrium suggests that these ERp57 oligomers are unlikely to be physiologically relevant. Moreover, no oligomeric form of the protein has been observed *in vivo* so far.

Sedimentation studies were extended to characterize the interaction between ERp57 and full-length CRT in solution. Analysis of a mixture of ERp57 and CRT revealed that these proteins form a 1:1 molar complex with a K_d in the low micromolar range in agreement with results obtained for the ERp57/CRT P-domain system. By using isothermal titration calorimetry, we have shown previously that the CRT P-domain forms a 1:1 complex with ERp57 in solution (26, 27). The dissociation constants determined between ERp57 and two different recombinant forms of CRT P-domain were found to be 9.1 ± 3.0 and 5.1 ± 0.7 μM (26, 27). Although other contact sites in CRT cannot be ruled out entirely at this point, the studies suggest that the interaction between ERp57 and CRT is mediated exclusively through the CRT P-domain. This is also consistent with the apparent molecular shape of the ERp57-CRT complex as determined by hydrodynamic analysis (Table II). That ERp57 and CRT form a 1:1 complex *in vitro* is in agreement with findings showing that a heterodimeric complex of the two proteins isolated from canine pancreatic microsomes runs at ~140 kDa on a native gel and that a complex of similar mobility by SDS-PAGE can be observed after cross-linking of the two proteins in semi-permeabilized mammalian cells (18).

Characterization of the redox properties of ERp57 showed that the protein is a versatile redox enzyme. For the **a** and **a'** domains, we determined the equilibrium constants with glutathione to 3.3 and 1.5 mM, respectively. This translates into redox potentials of −0.167 V for the **a** domain and −0.156 V for **a'**. In comparison, thioredoxin, the bacterial cytoplasmic reductase, has a redox potential of −0.270 V (66), and DsbA, the bacterial oxidase, has a value of −0.122 V (67). The intermediate values found for the ERp57 redox-active domains are thus closer to the redox potential of −0.175 V determined for PDI (53) and the equilibrium constants of 0.7 mM for the PDI **a** domain and of 1.9 mM for PDI **a'** domain (68), all determined with GSH/GSSG as a reference.

[3] H. F. Gilbert, personal communication.

Like PDI, ERp57 was capable of catalyzing reduction, isomerization, and oxidation. The reductase activity of the protein was close to that exhibited by thioredoxin and was clearly higher than that of DsbA (Fig. 6). The initial rate of isomerase catalysis by ERp57 was found to be 33 times faster than the DTT background reaction. However, PDI performed both of these redox functions more efficiently than ERp57. In both cases, the difference is consistent with the finding that PDI, unlike ERp57, has been shown to possess peptide binding activity, a function that is mediated by its **b'** domain (69). The **b'** domain of PDI has been demonstrated to be essential for binding of scRNaseA, as the replacement of the PDI **b'** domain by the ERp57 **b'** domain abolishes binding (70). Thus, PDI likely catalyzes reduction and isomerization more efficiently than ERp57 by directly interacting with its substrates through the **b'** domain, a function that seems to have been lost in ERp57, perhaps in exchange for the ability to associate with CNX and CRT.

Important insight into the function of ERp57 has come from the observation that acceleration of disulfide-coupled refolding of reduced RNaseB catalyzed by ERp57 was shown to be dependent on its interaction with CNX and CRT (71). In this context, it is interesting to note that ERp57, unlike PDI, seemingly does not catalyze refolding of reduced RNaseA or lysozyme (56). However, this observation might well be a result of a weaker, as opposed to absent, oxidase and/or isomerase activity of ERp57 compared with PDI. ERp57 probably compensates for its apparent inability to interact directly with substrates through backbone contacts (resulting in a lower redox activity in comparison to PDI when tested *in vitro* on non-glycosylated proteins) by depending on CNX and CRT to expose the protein directly to its glycoprotein substrates.

The function of the PDI **b'** domain likely explains to a large extent why the two isolated redox-active PDI **a** and **a'** domains do not provide the same efficiency of isomerization as the intact protein (48, 72). We observed a similar effect in ERp57, where the combination of the separate **a** and **a'** domains did not isomerize scRNaseA as efficiently as the full-length protein (Fig. 7). Features of the protein other than those of the isolated redox-active domains are needed for effective isomerization also by ERp57. The molecular characteristics underlying this effect are not clear, but simply the presence of two active sites on the same molecule could provide an explanation for the higher isomerase efficiency observed for the full-length protein. In addition, a weak peptide-binding activity of either ERp57 **b** or **b'** cannot be ruled out.

As an assay for oxidase activity, we investigated the ability of ERp57 to complement DsbA deficiency in the periplasm of *E. coli*. Previously, the efficient restoration of the $DsbA^+$ phenotype in the *dsbA*$^-$ THZ2 strain has been shown to correlate with the redox potential so that thioredoxin variants with an E_0' higher than −0.221 V showed complementation (49). Our results demonstrated that all three ERp57 constructs tested were able to act as oxidases in this assay. This result is in accordance with the determined redox potentials for the **a** and **a'** domains. Recently, full-length ERp57 from *Caenorhabditis elegans* was also found to complement DsbA deficiency (73). In addition, the ERp57 **a** domain can catalyze the oxidation of a model peptide substrate *in vitro* (74). Our results also indicate that all active sites of ERp57 as well as the PDI **a** domain are substrates of DsbB.

Although we have characterized the different redox activities performed by ERp57 *in vitro*, the question of its redox function *in vivo* remains open. The protein has been shown to reduce partially folded MHC class I molecules *in vitro* (75). Based on this study, it was proposed that ERp57 could play a role in

reducing intrachain disulfides in MHC class I molecules targeted for degradation. Because ERp57 is an important component of the peptide loading complex, the protein would be positioned favorably to perform this function. A similar reductase activity has been proposed for PDI in retrotranslocation of the cholera toxin A chain (76).

In addition to its potential reductase function, ERp57 likely catalyzes disulfide-coupled glycoprotein folding directly *in vivo*. The finding that ERp57 forms transient mixed disulfides with productively folding glycoprotein substrates of CNX and CRT argues in favor of this view (77). Furthermore, ERp57 has been implicated in disulfide bond isomerization of the MHC class I heavy chain in the peptide loading complex (78).

There is no indication so far that disulfide-exchange reactions with Ero1 regulate the redox function of ERp57, as observed for PDI. Ero1 overexpression seems to have no effect on the redox state of ERp57, and intermolecular disulfides between Ero1 and ERp57 have not been detected (79). Although this could be due to technical difficulties in trapping and revealing Ero1-ERp57 mixed disulfide complexes, the presence of an Ero1-independent system for ERp57 reoxidation cannot be ruled out. However, two recent studies (79, 80) show that in the ER of mammalian tissue-culture cells ERp57 is found in the reduced state. Although perhaps a cell type-dependent phenomenon, this finding indicates that ERp57 might not react as an oxidase *in vivo* and consequently not depend on a system for its reoxidation. Further studies are needed to clarify this important point.

Acknowledgments—We thank Ulla Grauschopf and Eva Zobely for helpful discussions, Christiane Schirra for help with cloning work, Kenneth Woycechowsky for critical reading of the manuscript, and René Brunisholz from the Protein Service Laboratory for performing N-terminal protein sequencing. M. B. thanks Shu Wang for excellent technical assistance.

Note Added in Proof—During the revision of this manuscript, articles by Pollock *et al.* and Russell *et al.* (Pollock, S., Kozlov, G., Pelletier, M.-F., Trempe, J.-F., Jansen, G., Sitnikov, D., Bergeron, J. J. M., Gehring, K., Ekiel, I., and Thomas, D. Y. (2004) *EMBO J.* **23,** 1020–1029 and Russell, S., Ruddock, L. W., Salo, E. E. H., Oliver, J. D., Roebuck, Q. P., Llewellyn, D. H., Roderick, H. L., Koivunen, P., Myllyharju, J., and High, S. (February 10, 2004) *J. Biol. Chem.* 10.1074/jbc.M400575200) have mapped the binding site for calreticulin and calnexin in ERp57, whereas an article by Silvennoinen *et al.* (Silvennoinen, L., Myllyharju, J., Ruoppolo, M., Orru, S., Caterino, M., Kivrikko, K. I., and Koivunen, P. (2004) *J. Biol. Chem.* **279,** 13607–13615) has also identified four thioredoxin-like domains in ERp57.

REFERENCES

1. Sevier, C. S., and Kaiser, C. A. (2002) *Nat. Rev. Mol. Cell Biol.* **3,** 836–847
2. Freedman, R. B., Klappa, P., and Ruddock, L. W. (2002) *EMBO Rep.* **3,** 136–140
3. Tu, B. P., Ho-Schleyer, S. C., Travers, K. J., and Weissman, J. S. (2000) *Science* **290,** 1571–1574
4. Tu, B. P., and Weissman, J. S. (2002) *Mol. Cell* **10,** 983–994
5. Sevier, C. S., Cuozzo, J. W., Vala, A., Aslund, F., and Kaiser, C. A. (2001) *Nat. Cell Biol.* **3,** 874–882
6. Pagani, M., Fabbri, M., Benedetti, C., Fassio, A., Pilati, S., Bulleid, N. J., Cabibbo, A., and Sitia, R. (2000) *J. Biol. Chem.* **275,** 23685–23692
7. Cabibbo, A., Pagani, M., Fabbri, M., Rocchi, M., Farmery, M. R., Bulleid, N. J., and Sitia, R. (2000) *J. Biol. Chem.* **275,** 4827–4833
8. Ferrari, D. M., and Söling, H. D. (1999) *Biochem. J.* **339,** 1–10
9. Cunnea, P. M., Miranda-Vizuete, A., Bertoli, G., Simmen, T., Damdimopoulos, A. E., Hermann, S., Leinonen, S., Huikko, M. P., Gustafsson, J. A., Sitia, R., and Spyrou, G. (2003) *J. Biol. Chem.* **278,** 1059–1066
10. Hosoda, A., Kimata, Y., Tsuru, A., and Kohno, K. (2003) *J. Biol. Chem.* **278,** 2669–2676
11. Knoblach, B., Keller, B. O., Groenendyk, J., Aldred, S., Zheng, J., Lemire, B. D., Li, L., and Michalak, M. (2003) *Mol. Cell Proteomics* **2,** 1104–1119
12. Alanen, H. I., Williamson, R. A., Howard, M. J., Lappi, A. K., Jantti, H. P., Rautio, S. M., Kellokumpu, S., and Ruddock, L. W. (2003) *J. Biol. Chem.* **278,** 28912–28920
13. Sullivan, D. C., Huminiecki, L., Moore, J. W., Boyle, J. J., Poulsom, R., Creamer, D., Barker, J., and Bicknell, R. (2003) *J. Biol. Chem.* **278,** 47079–47088
14. Kramer, B., Ferrari, D. M., Klappa, P., Pohlmann, N., and Soling, H. D. (2001) *Biochem. J.* **357,** 83–95
15. Matsuo, Y., Akiyama, N., Nakamura, H., Yodoi, J., Noda, M., and Kizaka-Kondoh, S. (2001) *J. Biol. Chem.* **276,** 10032–10038
16. Ellgaard, L., and Frickel, E.-M. (2003) *Cell Biochem. Biophys.* **39,** 223–248
17. Oliver, J. D., van der Wal, F. J., Bulleid, N. J., and High, S. (1997) *Science* **275,** 86–88
18. Oliver, J. D., Roderick, H. L., Llewellyn, D. H., and High, S. (1999) *Mol. Biol. Cell* **10,** 2573–2582
19. Molinari, M., Galli, C., Piccaluga, V., Pieren, M., and Paganetti, P. (2002) *J. Cell Biol.* **158,** 247–257
20. Zapun, A., Bardwell, J. C., and Creighton, T. E. (1993) *Biochemistry* **32,** 5083–5092
21. Bouvier, M. (2003) *Mol. Immunol.* **39,** 697–706
22. Antoniou, A. N., Powis, S. J., and Elliott, T. (2003) *Curr. Opin. Immunol.* **15,** 75–81
23. Daniels, R., Kurowski, B., Johnson, A. E., and Hebert, D. N. (2003) *Mol. Cell* **11,** 79–90
24. Ellgaard, L., Riek, R., Herrmann, T., Güntert, P., Braun, D., Helenius, A., and Wüthrich, K. (2001) *Proc. Natl. Acad. Sci. U. S. A.* **98,** 3133–3138
25. Schrag, J. D., Bergeron, J. J., Li, Y., Borisova, S., Hahn, M., Thomas, D. Y., and Cygler, M. (2001) *Mol. Cell* **8,** 633–644
26. Frickel, E.-M., Riek, R., Jelesarov, I., Helenius, A., Wüthrich, K., and Ellgaard, L. (2002) *Proc. Natl. Acad. Sci. U. S. A.* **99,** 1954–1959
27. Ellgaard, L., Bettendorff, P., Braun, D., Herrmann, T., Fiorito, F., Jelesarov, I., Güntert, P., Helenius, A., and Wüthrich, K. (2002) *J. Mol. Biol.* **322,** 773–784
28. Leach, M. R., Cohen-Doyle, M. F., Thomas, D. Y., and Williams, D. B. (2002) *J. Biol. Chem.* **277,** 29686–29697
29. Kemmink, J., Darby, N. J., Dijkstra, K., Nilges, M., and Creighton, T. E. (1996) *Biochemistry* **35,** 7684–7691
30. Kemmink, J., Dijkstra, K., Mariani, M., Scheek, R. M., Penka, E., Nilges, M., and Darby, N. J. (1999) *J. Biomol. NMR* **13,** 357–368
31. Silvennoinen, L., Karvonen, P., Koivunen, P., Myllyharju, J., Kivirikko, K., and Kilpelainen, I. (2001) *J. Biomol. NMR* **20,** 385–386
32. Wunderlich, M., and Glockshuber, R. (1993) *Protein Sci.* **2,** 717–726
33. Mossner, E., Huber-Wunderlich, M., and Glockshuber, R. (1998) *Protein Sci.* **7,** 1233–1244
34. Bouvier, M., and Stafford, W. F. (2000) *Biochemistry* **39,** 14950–14959
35. Zahn, R., Buckle, A. M., Perrett, S., Johnson, C. M., Corrales, F. J., Golbik, R., and Fersht, A. R. (1996) *Proc. Natl. Acad. Sci. U. S. A.* **93,** 15024–15029
36. Gill, S. C., and von Hippel, P. H. (1989) *Anal. Biochem.* **182,** 319–326
37. Ellman, G. L. (1958) *Arch. Biochem. Biophys.* **74,** 443–450
38. Stafford, W. F., III (1992) *Anal. Biochem.* **203,** 295–301
39. Stafford, W. F., III (1994) *Methods Enzymol.* **240,** 478–501
40. Stafford, W. F., and Sherwood, P. J. (2004) *Biophys. Chem.* **108,** 231–243
41. Perkins, S. J., and Sim, R. B. (1986) *Eur. J. Biochem.* **157,** 155–168
42. Kuntz, I. D., Jr., and Kauzmann, W. (1974) *Adv. Protein Chem.* **28,** 239–345
43. Stafford, W. F., and Schuster, T. M. (1995) in *Hydrodynamic Transport Methods. An Introduction to Physical Methods for Protein and Nucleic Acid Research* (Glaser, J. A., and Deutscher, M. P., eds) pp. 111–145, Academic Press Inc., Orlando, FL
44. Brenner, S. L., Zlotnick, A., and Stafford, W. F., III (1990) *J. Mol. Biol.* **216,** 949–964
45. Williams, C. H. (1992) *Chemistry and Biochemistry of Flavoenzymes* (Muller, F., ed) pp. 121–211, CRC Press, Inc., Boca Raton, FL
46. Holmgren, A. (1979) *J. Biol. Chem.* **254,** 9627–9632
47. Hennecke, J., Sebbel, P., and Glockshuber, R. (1999) *J. Mol. Biol.* **286,** 1197–1215
48. Darby, N. J., and Creighton, T. E. (1995) *Biochemistry* **34,** 11725–11735
49. Jonda, S., Huber-Wunderlich, M., Glockshuber, R., and Mossner, E. (1999) *EMBO J.* **18,** 3271–3281
50. Jacobi, A., Huber-Wunderlich, M., Hennecke, J., and Glockshuber, R. (1997) *J. Biol. Chem.* **272,** 21692–21699
51. Dailey, F. E., and Berg, H. C. (1993) *Proc. Natl. Acad. Sci. U. S. A.* **90,** 1043–1047
52. Bardwell, J. C., McGovern, K., and Beckwith, J. (1991) *Cell* **67,** 581–589
53. Lundstrom, J., and Holmgren, A. (1993) *Biochemistry* **32,** 6649–6655
54. Hirano, N., Shibasaki, F., Sakai, R., Tanaka, T., Nishida, J., Yazaki, Y., Takenawa, T., and Hirai, H. (1995) *Eur. J. Biochem.* **234,** 336–342
55. Bourdi, M., Demady, D., Martin, J. L., Jabbour, S. K., Martin, B. M., George, J. W., and Pohl, L. R. (1995) *Arch. Biochem. Biophys.* **323,** 397–403
56. Bonfils, C. (1998) *Eur. J. Biochem.* **254,** 420–427
57. Eschenlauer, S. C., and Page, A. P. (2003) *J. Biol. Chem.* **278,** 4227–4237
58. Collet, J. F., and Bardwell, J. C. (2002) *Mol. Microbiol.* **44,** 1–8
59. Silhavy, T. J., Casadaban, M. J., Shuman, H. A., and Beckwith, J. R. (1976) *Proc. Natl. Acad. Sci. U. S. A.* **73,** 3423–3427
60. Ostermeier, M., De Sutter, K., and Georgiou, G. (1996) *J. Biol. Chem.* **271,** 10616–10622
61. Darby, N. J., Kemmink, J., and Creighton, T. E. (1996) *Biochemistry* **35,** 10517–10528
62. Freedman, R. B., Gane, P. J., Hawkins, H. C., Hlodan, R., McLaughlin, S. H., and Parry, J. W. (1998) *Biol. Chem. Hoppe-Seyler* **379,** 321–328
63. Darby, N. J., van Straaten, M., Penka, E., Vincentelli, R., and Kemmink, J. (1999) *FEBS Lett.* **448,** 167–172
64. Alanen, H. I., Salo, K. E., Pekkala, M., Siekkinen, H. M., Pirneskoski, A., and Ruddock, L. W. (2003) *Antioxid. Redox Signal.* **5,** 367–374
65. Wunderlich, M., Jaenicke, R., and Glockshuber, R. (1993) *J. Mol. Biol.* **233,** 559–566
66. Krause, G., Lundstrom, J., Barea, J. L., Pueyo de la Cuesta, C., and Holmgren, A. (1991) *J. Biol. Chem.* **266,** 9494–9500
67. Huber-Wunderlich, M., and Glockshuber, R. (1998) *Folding Des.* **3,** 161–171
68. Darby, N. J., and Creighton, T. E. (1995) *Biochemistry* **34,** 16770–16780
69. Klappa, P., Ruddock, L. W., Darby, N. J., and Freedman, R. B. (1998) *EMBO J.* **17,** 927–935
70. Pirneskoski, A., Ruddock, L. W., Klappa, P., Freedman, R. B., Kivirikko, K. I.,

and Koivunen, P. (2001) *J. Biol. Chem.* **276,** 11287–11293
71. Zapun, A., Darby, N. J., Tessier, D. C., Michalak, M., Bergeron, J. J., and Thomas, D. Y. (1998) *J. Biol. Chem.* **273,** 6009–6012
72. Darby, N. J., Penka, E., and Vincentelli, R. (1998) *J. Mol. Biol.* **276,** 239–247
73. Blasko, B., Madi, A., and Fesus, L. (2003) *Biochem. Biophys. Res. Commun.* **303,** 1142–1147
74. Lappi, A. K., Lensink, M. F., Alanen, H. I., Salo, K. E., Lobell, M., Juffer, A. H., and Ruddock, L. W. (2004) *J. Mol. Biol.* **335,** 283–295
75. Antoniou, A. N., Ford, S., Alphey, M., Osborne, A., Elliott, T., and Powis, S. J. (2002) *EMBO J.* **21,** 2655–2663
76. Tsai, B., Rodighiero, C., Lencer, W. I., and Rapoport, T. A. (2001) *Cell* **104,** 937–948
77. Molinari, M., and Helenius, A. (1999) *Nature* **402,** 90–93
78. Dick, T. P., Bangia, N., Peaper, D. R., and Cresswell, P. (2002) *Immunity* **16,** 87–98
79. Mezghrani, A., Fassio, A., Benham, A., Simmen, T., Braakman, I., and Sitia, R. (2001) *EMBO J.* **20,** 6288–6296
80. Antoniou, A. N., and Powis, S. J. (2003) *Antioxid. Redox Signal.* **5,** 375–379

Paper III

Calnexin, Calreticulin, and ERp57

Teammates in Glycoprotein Folding

Lars Ellgaard and Eva-Maria Frickel

December 2003, Cell Biochem. Biophys., Volume 39, No. 3, pp. 223-247

1085-9195/03/39/223–247/$25.00

REVIEW ARTICLE

Calnexin, Calreticulin, and ERp57

Teammates in Glycoprotein Folding

Lars Ellgaard* and Eva-Maria Frickel

Institute of Biochemistry, ETH Zurich, CH-8093 Zurich, Switzerland

Abstract

In eukaryotic cells, the endoplasmic reticulum (ER) plays an essential role in the synthesis and maturation of a variety of important secretory and membrane proteins. For glycoproteins, the ER possesses a dedicated maturation system, which assists folding and ensures the quality of final products before ER release. Essential components of this system include the lectin chaperones calnexin (CNX) and calreticulin (CRT) and their associated co-chaperone ERp57, a glycoprotein specific thiol-disulfide oxidoreductase. The significance of this system is underscored by the fact that CNX and CRT interact with practically all glycoproteins investigated to date, and by the debilitating phenotypes revealed in knockout mice deficient in either gene. Compared to other important chaperone systems, such as the Hsp70s, Hsp90s and GroEL/GroES, the principles whereby this system works at the molecular level are relatively poorly understood. However, recent structural and biochemical data have provided important new insights into this chaperone system and present a solid basis for further mechanistic studies.

Index Entries: Calnexin; calreticulin; endoplasmic reticulum; ERp57; lectin; molecular chaperone; oxidoreductase.

INTRODUCTION

The addition of N-linked glycans to newly synthesized polypeptide chains occurs in the endoplasmic reticulum (ER). Here the 14-saccharide core glycan (Fig. 1), $Glc_3Man_9GlcNAc_2$, is added to the growing nascent polypeptide chain from a dolicholpyrophosphate-linked precursor in a reaction catalyzed by the oligosaccharyl transferase complex *(1,2)*. The modified asparagine side chain occurs within the Asn-Xxx-Ser/Thr consensus sequence, where Xxx denotes any amino acid except proline *(3)*. Although only relatively few of the soluble ER-resident proteins seem to be glycosylated, the majority of extracellular proteins produced in mammalian cells carry N-linked glycans *(4)*. The large number of different glycoproteins that traffic through the ER are involved in many fundamental intra- and intercellular processes. Consequently, mutations in

*Author to whom all correspondence and reprint requests should be addressed. E-mail: lars.ellgaard@bc.biol.ethz.ch

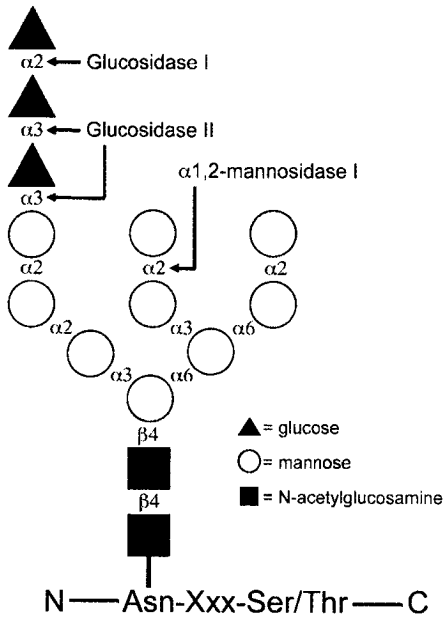

Fig. 1. Schematic representation of the N-linked core oligosaccharide attached to an asparagine side chain in an Asn-Xxx-Ser/Thr amino acid consensus sequence. The linkage for each individual glycosyl residue is indicated along with cleavage sites for various ER enzymes that modify the sugar structure.

proteins of the N-glycosylation pathway are known to cause severe disease phenotypes, and a number of congenital disorders of glycosylation are known *(5,6)*.

The sugar itself can directly modulate protein structure and function, e.g., by increasing properties such as stability and solubility *(7–11)*. In addition, N-linked glycans act as tags in intracellular trafficking *(12)*, and accordingly different lectins act as sorting receptors in the secretory pathway *(13–15)*. Despite the many different and widely recognized functions of *N*-linked glycans, the role of the N-linked glycan in protein folding in the ER has only become fully appreciated within the past 10 yr. Specifically, it has been found that modifications of the core glycan to generate a monoglucosylated ($Glc_1Man_9GlcNAc_2$) form determine the interaction with two homologous lectin chaperones, calnexin (CNX) and calreticulin (CRT).

Studies in tissue culture cells and ER-derived microsomes have demonstrated that the interaction with CNX and CRT protects glycoproteins from aggregation and premature degradation *(16–20)*. Repeated cycles of binding to and release from CNX and CRT, controlled by enzymes that modify the core oligosaccharide, ensure the retention of substrate glycoproteins in the favorable folding environment of the ER until correctly folded. If permanently misfolded, these substrate proteins are degraded. At least for certain glycoproteins, the removal of a mannose residue in the middle branch of the glycan is a signal for degradation *(21)*. A recently discovered mannose-binding lectin, EDEM, specifically accelerates the degradation of glycoproteins and could well be directly involved in targeting $Man_8GlcNAc_2$-containing proteins for degradation *(22–28)*. Overall, the oligosaccharide and the different enzymes that modify it play important roles in glycoprotein folding and degradation. These aspects have been covered in great detail in other reviews *(29–33)*.

Cell biological studies have provided most of our current knowledge about the CNX/CRT chaperone system. However, more recent work has revealed structural information at atomic resolution for both CNX and CRT, along with details about their interaction with the co-chaperone ERp57. Moreover, other studies have explored the possibility that protein–protein interactions, in addition to the glycan-mediated interaction, contribute to the function of CNX and CRT as molecular chaperones. Taken together, these investigations have considerably increased our understanding of the molecular basis for glycoprotein folding and have also raised interesting new questions. This review describes the function of the CNX/CRT chaperone system. In particular, we emphasize the role of molecular properties of CNX, CRT, and ERp57 in determining the mechanism of chaperone function in the living cell.

ER QUALITY CONTROL

The endoplasmic reticulum (ER) plays a fundamental role in the synthesis, folding, and assembly of numerous important proteins, such as cell-surface receptors, membrane channels, extracellular matrix components, serum proteins, and antibodies. The environment in the ER is optimal for the correct folding and maturation of such proteins. For many proteins the maturation process involves co- and posttranslational modifications, such as signal-peptide cleavage, glycophosphatidylinositol (GPI)-anchor addition and N-linked glycosylation. Furthermore, the oxidizing milieu of the ER supports the formation of disulfide bonds. This stabilization of protein conformation is likely to help proteins maintain their structure in the extracellular environment. Finally, the ER is rich in chaperones and enzymes, which are crucial in assisting the process of correct protein folding *(34,35)*.

Still, incorrectly folded or incompletely assembled proteins are common side products during protein synthesis in the ER. Such products, which could be harmful to the cell if allowed to proceed along the secretory pathway to the cell surface or another cellular location, are subject to a stringent quality control (QC) system *(36,37)*. A number of general chaperones, including BiP, a member of the Hsp70 family of chaperones, and protein disulfide isomerase (PDI), a thiol-disulfide oxidoreductase, recognize and retain proteins that expose non-native features. This system ensures that misfolded and incorrectly assembled proteins are retained in the ER and eventually degraded. Many so-called ER storage diseases are known, which arise from the ER retention of mutant alleles of certain proteins. Such diseases include cystic fibrosis and emphysema (for reviews, *see* refs. *38–41*).

Defective ER-retained proteins are typically degraded by the proteasome after selective retrotranslocation to the cytosol and ubiquitination *(42)*. This process is referred to as ER-associated degradation (ERAD). Moreover, the cell responds to increased misfolding of proteins in the ER by the unfolded protein response (UPR) (reviewed in ref. *43*). Signaling from the ER to the nucleus leads to increased transcription of genes encoding ER chaperones to help alleviate the folding problem. In addition, another signaling pathway involving phosphorylation of the translation initiation factor eIF2α leads to attenuation of protein translation to further reduce the load on the ER folding machinery. Lastly, yet other genes involved in degradation are upregulated, as recently shown in the case of EDEM *(28)*. Several investigations show that the processes of ERAD and UPR are closely coordinated *(44–46)*.

THE CALNEXIN/CALRETICULIN CYCLE

The QC system described above applies to all proteins that encounter the lumen of the ER or are inserted into the ER membrane. CNX, CRT, and ERp57 are important factors of this general ER QC system *(47)*.

CNX and CRT cooperate with a number of enzymes in the process of assisting glycoprotein folding. The first step of this so-called CNX/CRT cycle (*see* Fig. 2) involves binding to either chaperone through the monoglucosylated glycan, $Glc_1Man_9GlcNAc_2$, present on nascent chains and on newly synthesized glycoproteins. This form of the sugar appears either as a trimmed intermediate of the triglucosylated core oligosaccharide or by readdition of a glucose residue to the fully deglucosylated glycan (*see* below). Sequential trimming of the two outermost glucose residues on the core oligosaccharide is executed by glucosidases I and II. The importance of monoglucosylation for CNX and CRT binding has been shown in living cells, in microsomes and in vitro for a number of different proteins (*see* for instance refs. *48–56*). Many such studies have used inhibitors of glucosidase II, such as castanospermine and deoxynojirimycin, to prevent the formation of the monoglucosylated, trimmed intermediate of the original core oligosaccharide. Under these experimental conditions, access to CNX and CRT is prevented and proteins are retained in the ER where they often form high molecular weight complexes

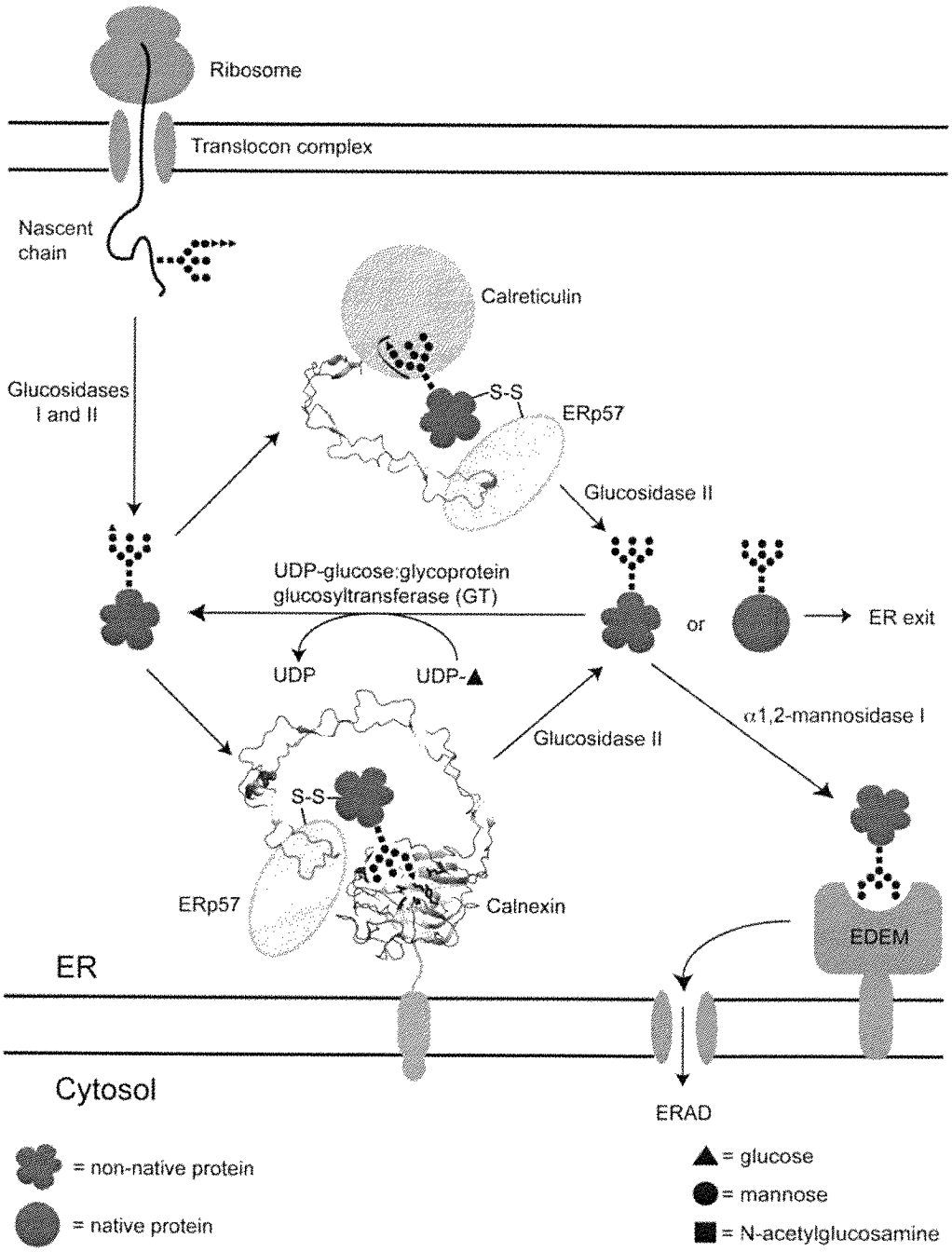

and eventually are targeted for degradation. In addition to the initial binding through the monoglucosylated glycan, protein–protein interactions of CNX and CRT with their substrates could well contribute to the chaperone function of both proteins (*see* below) *(57,58)*.

The process of disulfide bond formation in glycoprotein substrates of CNX and CRT is assisted by the thiol-disulfide oxidoreductase ERp57, which is found noncovalently associated with both proteins in vivo *(47,59,60)*. The importance of ERp57 in the CNX/CRT cycle has

Fig. 2. The calnexin/calreticulin cycle. The folding of newly synthesized glycoproteins in the ER is assisted by calnexin (CNX) and calreticulin (CRT). Both proteins bind to the monoglucosylated form of the glycoprotein generated after the initial removal of two glucoses by glucosidases I and II. Here, we have used the available three-dimensional structures of CNX (the lumenal domain) and CRT (the P-domain) to depict parts of the two molecules (*see also* Fig. 4). The glycan binds to the lectin domain of both chaperones—in CRT the glycan binding site is represented by the curved black line. Other interactions can occur through protein-protein contacts (not depicted). Disulfide bond formation in glycoprotein substrates of CNX and CRT is catalyzed by the associated thiol-disulfide oxidoreductase ERp57, with which substrates form transient mixed disulfide intermediates. In both CNX and CRT, the tip region of the P-domain mediates the interaction with ERp57. Removal of the remaining glucose, in a reaction catalyzed by glucosidase II, prevents interaction with CNX and CRT. Upon release, one of three possible fates awaits the glycoprotein. First, if the protein has reached its native conformation it is not longer retained in the ER and is free to travel along the secretory pathway. Second, if the protein is still not correctly folded, it can be recognized by the UDP-glucose:glycoprotein glucosyltransferase (GT). This enzyme uses UDP-glucose as a sugar donor to reglucosylate non-native glycoproteins carrying high-mannose glycans. Consequently, it acts as a folding sensor in CNX/CRT cycle. The readdition of a glucose residue to the N-linked glycan promotes reassociation with CNX and CRT. An important role of CNX and CRT is to retain glycoproteins in the ER, where the conditions for folding are favorable. Finally, prolonged ER-retention increases the chances of encountering the ER α1,2-mannosidase I. This enzyme removes a mannose residue in the middle branch of the glycan to generate a form with eight mannoses (*see also* Fig. 1). A novel ER lectin, EDEM, is likely to recognize this form of the glycan and thereby extract the glycoprotein from the CNX/CRT cycle. Moreover, EDEM directs the glycoprotein for degradation by the ERAD pathway.

become apparent from studies showing that the protein interacts with soluble secretory proteins, as well as integral membrane proteins, carrying N-linked glycans (*59,61*). As observed for substrates of CNX and CRT, both the association and release of substrates from ERp57 are modulated by glucose trimming (*61–63*). That the addition of glucosidase inhibitors can result in impaired disulfide bond formation was recently shown in the case of CD1d heavy chain, which interacts with CNX and CRT during folding (*64*). Furthermore, the direct involvement of ERp57 in the oxidative folding of glycoproteins is evident from the finding that the protein forms transient mixed disulfides with CNX- and CRT-associated glycoproteins during folding in living cells (*63*). Thus, by interacting with CNX and CRT, ERp57 functions as a specialized thiol-disulfide oxidoreductase for glycoproteins.

Glycoproteins are released from CNX and CRT by the action of glucosidase II, which removes the terminal glucose of the glycan (*49,54*). This step most likely occurs irrespective of the folding state of the glycoprotein, and prevents its renewed association with CNX and CRT. If not correctly folded at this stage, the glycoprotein is recognized by UDP-glucose:glycoprotein glucosyltransferase (GT). This enzyme works as a folding sensor and only re-adds a glucose residue to the oligosaccharide on non-native glycoproteins (*29*). In this way, the action of GT ensures that proteins in a misfolded conformation can reassociate with CNX and CRT (*52,54,65*). GT has been shown to detect misfolding on a domain level (*66*), and even local folding defects in one domain can be distinguished so that only glycans in structurally destabilized regions are reglucosylated (C. Ritter, K. Quirin and A. Helenius, personal communication). Therefore, surveillance can take place on a domain-by-domain basis and it can be hypothesized that glycosylation sites in

domains with a tendency for misfolding have been maintained throughout evolution in order to optimize the folding efficiency of glycoproteins carrying such domains.

Overall, cycles of binding and release slow down the rate of folding but increase its efficiency for many glycoproteins by keeping them exposed to the ER QC system *(20)*. Like other protein QC systems in the cell, the detection of non-native glycoproteins in the ER by GT relies on features of the polypeptide chain that distinguish it from proteins in a native conformation. The benefit of using sugars as "reporter molecules" for the protein folding status likely relates to the fact that the modifications of the core oligosaccharide that control the fate of glycoproteins in the ER are independent of the specific protein. Thereby the glycan, which is present in a large number of molecules, works as a highly versatile tag that can be modified and recognized by a relatively small number of ER-resident enzymes and lectins.

SUBSTRATE INTERACTIONS OF CALNEXIN AND CALRETICULIN

A wide variety of important cellular and viral glycoproteins are known substrates of CNX and CRT. These include HIV gp120 and gp160 *(67–70)*, class I major histocompatibility complex (MHC) heavy chain *(17,71–77)*, T-cell receptor subunits *(71,78)*, α_1-antitrypsin *(50,79,80)*, tyrosinase *(81–83)*, the prion protein *(84,85)*, and the cystic fibrosis transmembrane conductance regulator (CFTR) *(86,87)*. Although many glycoproteins associate with both CNX and CRT, and despite having the same glycan specificity, these two lectins can have distinct roles in glycoprotein maturation. For instance, they can bind to the same protein at different stages of the folding process as seen for both the MHC class I heavy chain *(88,89)* and influenza hemagglutinin (HA) *(18)*. For the latter, association has been shown to depend on the position of the sugar within the molecule. Whereas CRT associates preferentially with the glycans of the HA top domain, CNX associates more efficiently with those glycans present in the membrane-proximal stem domain *(90)*.

The set of substrates bound by the two proteins is largely, but not completely, overlapping *(51,91)*. In line with the results obtained for HA, the difference in substrate recognition pattern has been shown to depend on the presence of the membrane anchor in CNX *(92,93)*. However, the finding that the lumenal domain of CNX cannot complement the function of CRT in MHC class I assembly when expressed in CRT-deficient cells indicates that the two proteins possess protein specific functions despite their many similarities *(76)*.

As mentioned previously, the exact mode of interaction by CNX and CRT with their glycoprotein substrates is not entirely clear. Studies performed in vitro using RNaseB as a model glycoprotein and studies of glycoprotein folding in the protozoan parasite *Trypanosoma cruzi* suggest that the function of CNX and CRT as molecular chaperones can be attributed solely to their lectin activity *(53,55,94)*. However, assays of aggregation and refolding using purified proteins as substrates show that CNX and CRT could have an additional function as classical chaperones, characterized by protein–protein contacts with hydrophobic regions exposed by non-native polypeptide chains *(57,58)*. As observed for classical chaperones, CNX and CRT can suppress aggregation and preserve proteins in a folding competent state, independent of their glycosylation status (monoglucosylated or nonglycosylated) *(57,58)*. However, the efficiency of suppressing aggregation was enhanced for monoglucosylated proteins, potentially indicating an avidity effect of two binding sites, one for the glycan and one for the polypeptide chain of the substrate *(95)*. Whereas native conformers were shown not to interact with CNX and CRT, complexes were formed with misfolded conformers.

The effects of cofactors, such as Zn^{2+}, adenosine triphosphate (ATP) and the monoglucosylated glycan on this bonafide chaperone function of CNX and CRT, have also been investigated in vitro. These cofactors are known to modulate structural properties of

CNX and CRT (*see* below). Although ATP was shown to enhance the ability to suppress protein aggregation, addition of the monoglucosylated glycan inhibited this function *(57,58)*. The latter result indicated that occupation of the oligosaccharide binding site is capable of influencing the protein–protein interactions proposed to mediate the chaperone function.

Overall, these experiments support the notion that protein–protein based contacts of CNX and CRT with their substrates, in addition to an initial glycan based interaction, play an important role during folding *(57,58)*. Moreover, ATP binding by CNX and CRT, and potentially Zn^{2+} binding in the case of CRT, could promote substrate interaction by leading to the exposure of hydrophobic surface. Substrate release would then occur by ATP hydrolysis or dissociation, both processes possibly mediated by a co-chaperone.

MOLECULAR PROPERTIES OF CALNEXIN AND CALRETICULIN

Besides its well-established role as a molecular chaperone, CRT is a major Ca^{2+} storage protein and plays an important role in Ca^{2+} homeostasis in the ER *(96,97)*. Thus, the embryonic lethal phenotype observed in CRT-deficient mice is connected to the function of the protein in Ca^{2+} signaling during cardiac development *(99,100)*. Although CNX also binds Ca^{2+} *(101,102)*, the protein does not seem to play a significant role in Ca^{2+} homeostasis and its major function is that of a molecular chaperone. CNX gene-deficient mice do not show as serious defects as CRT knockout mice. However, 50% die within 2 d of birth, whereas the rest display severe motor disorders, a selective loss of large myelinated fibers and die within 3 mo *(103)*.

Biochemical studies of CNX and CRT are abundant, and below the most important biochemical properties of the two proteins are summarized. Together with structural data, these molecular characteristics constitute the basis for understanding the mechanism of chaperone function of CNX and CRT in detail.

Primary Structure

The molecular cloning of CRT (46.5 kDa, 400 residues) *(104,105)* and CNX (65.4 kDa, 572 residues) *(101,102)* has revealed that the two proteins are highly similar (Fig. 3). The main differences are found in their carboxyl terminal regions. Whereas CRT is a soluble luminal protein with a carboxyl terminal KDEL retrieval sequence, CNX is a type I transmembrane protein with a predicted transmembrane region spanning residues 463–485, followed by a 87-residue carboxyl terminal cytosolic tail. However, the luminal domain of CNX is highly similar to CRT. Based on sequence analysis, both proteins have been suggested to consist of three regions, the N-, P-, and C-domains (Fig. 4) *(104–107)*. The N-domain (CRT residues 1–188, CNX residues 1–253) was originally predicted to comprise a β-sheet rich globular structure *(104,105)*. The unique P-domain (CRT residues 189–283, CNX residues 254–388) constitutes the signature sequence for this family of proteins, and has obtained its name due to the many prolines present in this region. It consists in its entire length of two short sequence repeats, the type 1 and type 2 repeats. Each type of repeat is present in three and four copies in CRT and CNX, respectively. In both proteins, the arrangement of the repeat sequences is such that all type 1 repeats are clustered together, followed by a cluster of type 2 repeats (Figs. 3 and 4). The distinguishing feature of the CRT C-domain (residues 284–400) is the enrichment of acidic amino-acid residues in the approx 60 carboxyl terminal residues. This region is known to play a role in low-affinity Ca^{2+} binding *(106,108,109)*. In contrast, the C-domain of CNX, residues 389–462, does not display noticeable traits. Here, the membrane-proximal region of approx 20 residues is likely to represent a linker sequence between the membrane anchor and a globular lectin domain (*see* below).

The sequences of both CNX and CRT encode cysteine residues that form intrachain disulfide bonds. In CNX the four cysteines pair to form

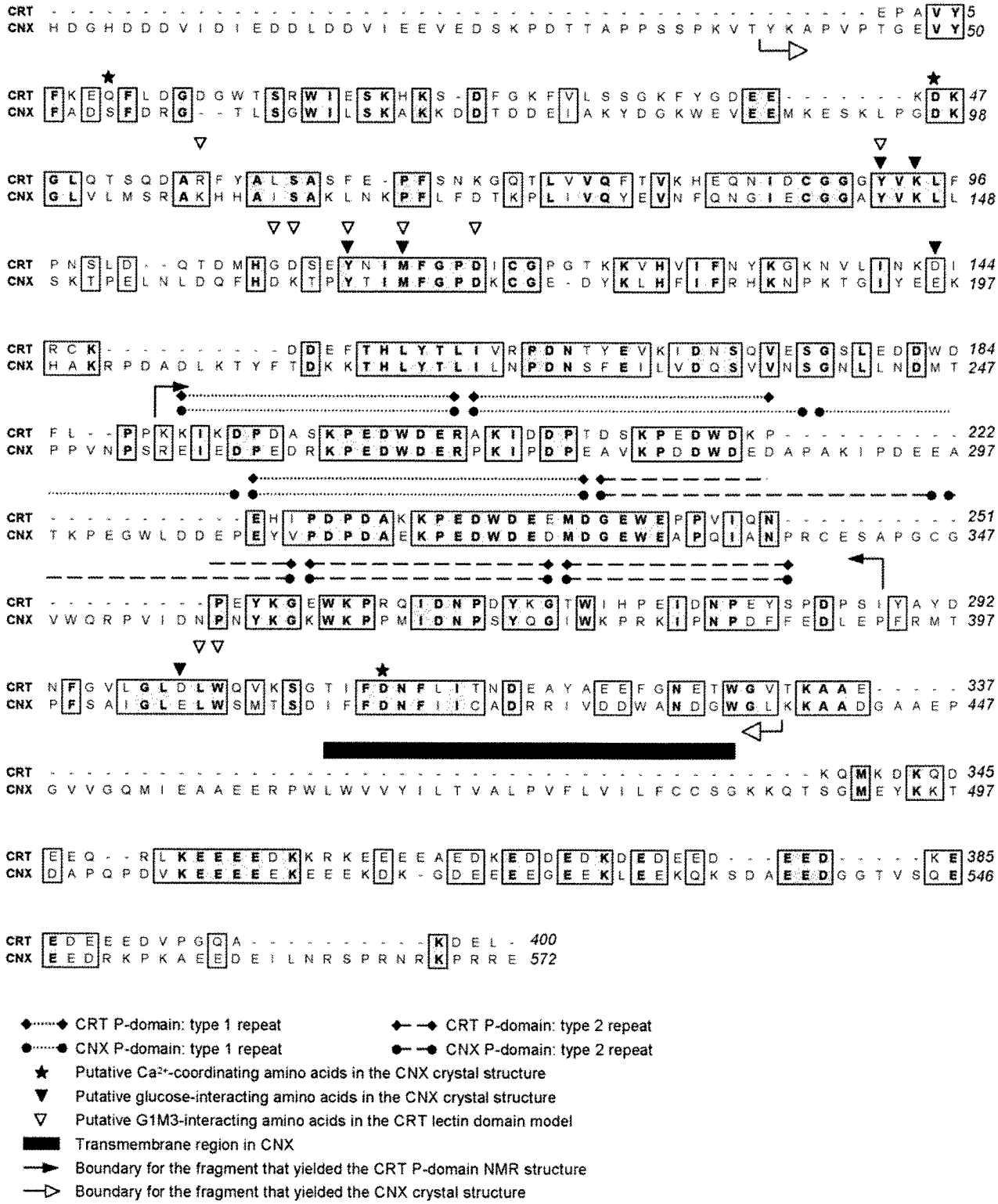
CRT
CNX
CRT P-domain: type 1 repeat
CRT P-domain: type 2 repeat
CNX P-domain: type 1 repeat
CNX P-domain: type 2 repeat
Putative Ca2+-coordinating amino acids in the CNX crystal structure
Putative glucose-interacting amino acids in the CNX crystal structure
Putative G1M3-interacting amino acids in the CRT lectin domain model
Transmembrane region in CNX
Boundary for the fragment that yielded the CRT P-domain NMR structure
Boundary for the fragment that yielded the CNX crystal structure

Fig. 3. Amino-acid sequence alignment of human CNX and human CRT. Both sequences are shown without amino terminal signal sequences and numbered accordingly. Repeat sequences of the P-domain are indicated above the alignment. Amino-acid residues proposed to coordinate Ca^{2+} in the crystal structure of the lumenal domain of CNX are labeled with an asterisk, and amino-acid residues proposed to interact with the glycan are marked with a triangle. The black bar denotes the transmembrane region in CNX. Boundaries for the NMR structure of the CRT P-domain (residues 189–288) and for the crystal structure of the lumenal domain of CNX (residues 40–437) are indicated above and below the respective sequences with arrows.

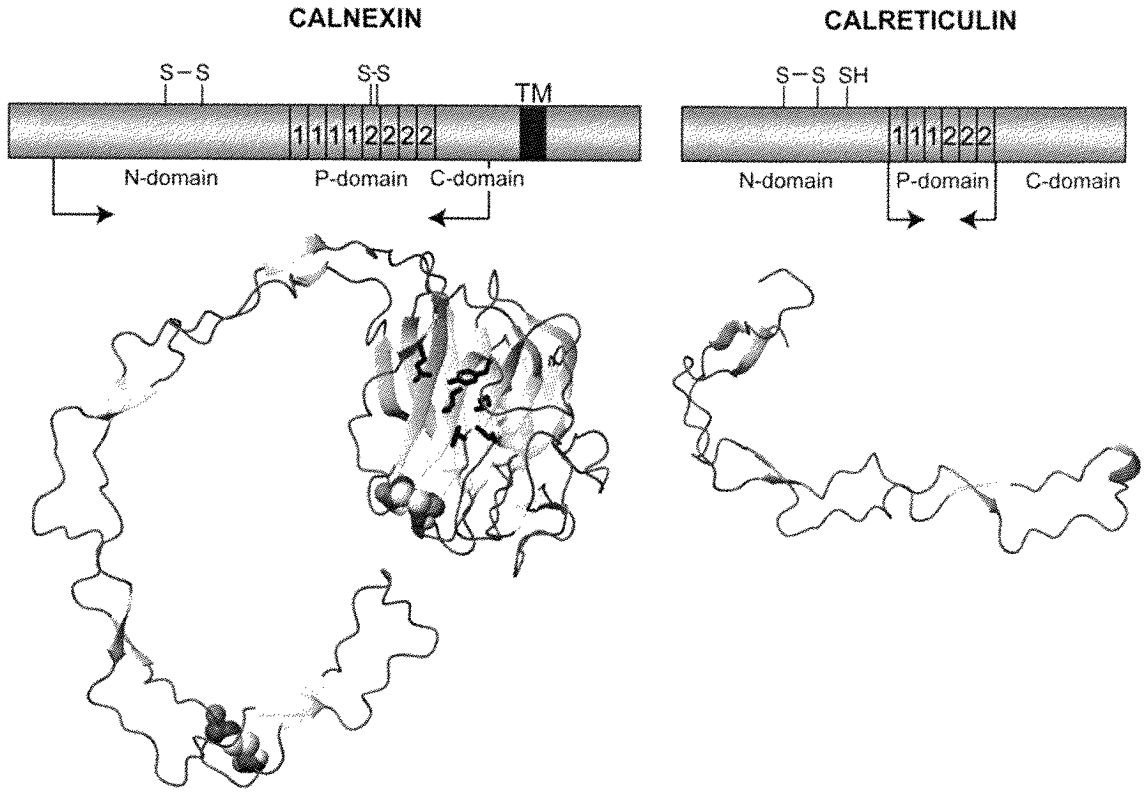

Fig. 4. Overview of the primary amino-acid sequence of CNX and CRT, and the three-dimensional structures solved for the two proteins. In the schematic representation, the position of type 1 and type 2 repeats of the P-domain is indicated along with the position of free and disulfide-bonded cysteine residues. 'TM' denotes the transmembrane region in CNX. The arrows indicate the boundaries of the fragments for which the three-dimensional structures are shown below. In the representation of the three-dimensional structure of the lumenal domain of CNX, residues involved in the binding of the glucose are shown as black stick models and the cysteines forming the two disulfide bonds are shown as CPK models. This figure was prepared using the program MOLMOL.

the Cys140–Cys174 and Cys340–Cys346 disulfides *(110)*. In CRT a free cysteine is present at position 146, whereas the Cys89–Cys120 disulfide is equivalent to the Cys140–Cys174 disulfide in CNX *(111)*. Although certain animal CRT sequences contain a conserved N-glycosylation site at residue 326, human placental CRT has been shown not to be glycosylated *(111)*. Animal CNXs do not contain potential sites for N-linked glycosylation. A unique feature of the carboxyl terminal cytosolic tail of CNX is the presence of sites for phosphorylation by casein kinase II at Ser534 and Ser544 and by extracellular-signal regulated kinase-1 at Ser563 *(112,113)*. Phosphorylation at these positions has been shown to regulate the association of CNX with ribosomes *(114)*.

Both CNX and CRT have a tissue-specific isoform in testis. The CNX isoform, calmegin, interacts with nascent chains of glycoproteins and is required for male fertility in mice *(115,116)*, whereas the function of the recently discovered CRT isoform, CRT2, has not yet been investigated *(117)*. The sequence similarity of both testis isoforms with the respective ubiquitously expressed forms is high (>60%), and it is very likely that the isoforms also function as lectin chaperones *(117–119)*.

Ca^{2+} Binding

Different cofactors have been found to interact with CNX and CRT in vitro and thereby modulate the structural properties of both proteins. The effects of metal binding by CRT have been thoroughly characterized by a variety of methods, such as circular dichroism, intrinsic fluorescence, 8-anilino-1-naphtalenesulfonate (ANS) binding and equilibrium dialysis. Of twelve different divalent cations tested for binding to CRT, only Ca^{2+} and Zn^{2+} were shown to bind specifically *(109)*. CNX binds Ca^{2+} *(101,102,120,121)*, whereas there is little evidence that the protein binds other metals.

Owing to its role in Ca^{2+} homeostasis, the Ca^{2+}-binding properties of CRT have been particularly well investigated (*see* for instance, refs. *106,108,109,122–125*). The protein has two distinct classes of binding sites: one high-affinity binding site that complexes 1 mol Ca^{2+}/mol protein with a K_d of 0.05–11 μ*M*, and several low-affinity sites, located in the acidic C-terminal domain, that bind approx 20 mol Ca^{2+}/mol protein with a K_d of 2 m*M* *(106,108,109)*. As pointed out earlier *(107)*, the rather broad range of K_d values determined for high-affinity Ca^{2+} binding by CRT is likely a result of the different experimental conditions employed in these studies.

Ca^{2+} binding by CRT seems to have only little effect on the content of regular secondary structure elements and on the global structure of the protein *(109,123,125,126)*. However, upon occupancy of the high-affinity Ca^{2+} binding site, local structural effects are observed that indicate a more compact conformation with increased thermal stability *(109,125)*. These results can be rationalized based on the crystal structure of the lumenal domain of CNX, which coordinates one Ca^{2+} ion with a proposed role of structural stabilization *(110)*. In addition, CRT shows increased resistance toward proteolytic digestion by a variety of proteases at high Ca^{2+} concentrations *(124,125)*. A similar result has been reported for CNX *(121)*.

Zn^{2+} Binding

CRT contains one high-affinity binding site for Zn^{2+} (apparent K_d of 0.05 μ*M*) and 14 low-affinity binding sites (apparent K_d of 310 μ*M*) *(109)*. Zn^{2+} binding by CRT has been mapped to the N-domain *(127)* and has been shown to induce a considerable conformational change in the protein resulting in the exposure of hydrophobic surface *(57,109)*. In accordance with these results, CRT is found to aggregate at concentrations of Zn^{2+} above 600 μ*M* *(109,127)*, whereas CNX aggregates already in the presence of 100 μ*M* Zn^{2+} *(128)*. In CRT the observed conformational change is accompanied by an increased susceptibility toward proteolytic digestion by trypsin and chymotrypsin and a decreased thermal stability *(125)*.

As proposed by several authors, the exposure of hydrophobic surface by CRT observed

in vitro in the presence of concentrations as low as 50 μ*M* $ZnCl_2$ could potentially be important for the ability of the protein to suppress aggregation through protein–protein interactions with its substrates *(57,124,125)*. Unfortunately, although Zn^{2+} is present in the ER lumen, little is known about its concentration and all the mammalian zinc transporters described to date are localized to cellular compartments other than the ER. However, recent studies show that the ER of *Schizosaccharomyces pombe* harbors a zinc transporter thought to regulate ER zinc homeostasis in this organism *(129,130)*.

ATP Binding

Another potentially important cofactor of CNX and CRT is ATP. Both proteins bind ATP in vitro *(57,58,121,131)*. Although a weak ATPase activity has been reported for both proteins *(57,58)*, others have been unable to detect any such activity *(121,124)*. For both proteins, the binding of ATP is accompanied by a decrease in intrinsic fluorescence emission and enhanced binding of ANS, indicating exposure of hydrophobic surface *(57,58)*. Whereas the presence of ATP protects the carboxyl terminal region of CRT from proteolysis *(124)*, both destabilizing and stabilizing effects of ATP binding by CNX have been reported *(121,131)*.

Currently, the physiological significance of ATP binding by CNX and CRT remains unclear. Classical chaperones such as those belonging to the Hsp70 family, including the ER-resident protein BiP, are ATPases. Cycles of ATP binding, hydrolysis and nucleotide exchange control substrate binding and release, and are, in turn, regulated by cofactors that either influence ATPase activity or act as nucleotide exchange factors. The reported ATPase activity of <0.1 pmol/min/μg for CNX and CRT is very low *(57,58)*. In comparison, BiP, which is considered a weak ATPase, has an activity of 5.2 pmol/min/μg *(132)*. Thus, if ATP hydrolysis plays a role for the chaperone function of CNX and CRT, positive regulators of ATPase activity and nucleotide exchange are likely to exist.

Glycan Binding

A number of studies performed in vitro have characterized the direct interaction of CNX and CRT with isolated glycans using biochemical methods. All support the notion that both proteins are lectins that specifically interact with the monoglucosylated form of the core glycan (Fig. 1) *(50,131,133–135)*. These studies also show that CNX and CRT interact with glycans with increasing affinity when comparing oligosaccharides of different lengths as follows: Glc(G1) << Glcα1-3Man(G1M1) << Glcα1-3Manα1-2Man(G1M2) < Glcα1-3Manα1-2Manα1-2Man(G1M3). Therefore, the glycan interaction is likely to involve the entire α1-3 branch of the oligosaccharide, which forms a continuous molecular surface in the NMR structure of $Glc_1Man_9GlcNAc_2$ *(136)*. Direct affinity measurements have shown that the G1M3 tetrasaccharide binds CRT with comparable affinity to an IgG molecule carrying the entire monoglucosylated glycan *(135)*. However, glycan binding by CNX and CRT could potentially also involve contacts to the mannose residues on the α1-6 branch of the glycan *(50,133)*.

Detailed biophysical analysis of the binding of IgG carrying a single monoglucosylated glycan to CRT demonstrated a K_d of approx 2 μ*M* *(137)*. Furthermore, this study showed that—at least under these experimental conditions using a native monoglucosylated protein—no contribution to the binding reaction was observed from protein–protein interactions. As proposed by Surolia and coworkers *(137)*, the relatively low affinity of CRT for the glycan could be advantageous to allow for rounds of glycoprotein association and dissociation. This feature would permit trimming of the remaining glucose of the glycan by glucosidase II to occur on the nonbound substrate. Such a model is supported by the finding that RNaseB bound by the lumenal domain of CNX is protected effectively from glucosidase II and PNGaseF digestion *(53)*.

In vitro, the binding of the oligosaccharide by either CNX or CRT depends critically on the

presence of Ca^{2+} *(131,137)*. Thus, it is possible that the deleterious effect of Ca^{2+} depletion from the ER, observed for the folding of glycoproteins known to interact with CNX and CRT, directly reflects structural changes in the lectin domain, which render both proteins incapable of ligand interaction *(138)*.

STRUCTURAL STUDIES OF CALNEXIN AND CALRETICULIN

The biochemically determined properties of CNX and CRT have been put into new perspective by recent structural studies on both molecules. For CNX, the crystal structure of a fragment comprising residues 40–437, encompassing most of the lumenal domain, has been reported to a resolution of 2.9 Å (Fig. 4) *(110)*. This highly unusual structure contains two separate entities: a globular β-sandwich domain homologous to legume lectins and an extended hairpin fold of approx 140 Å in length, corresponding to the P-domain. The globular domain comprises a concave and a convex β-sheet with six and seven β-strands, respectively. In this part of the molecule, the CNX model also shows a putative Ca^{2+} binding site, with the Ca^{2+} ion proposed to play a role in structural stabilization rather than ligand interaction. The only regular secondary structure elements in the P-domain are four short, anti-parallel β-sheets where each β-strand contains three residues. The disulfide bond connecting the cysteine residues 340 and 346 is found close to the tip of the P-domain.

By soaking the crystal in glucose and determining its location in the electron density, it was found that the concave β-sheet of the globular domain harbors a monovalent glycan binding site. Modeling the binding of the G1M3 tetrasaccharide indicated that steric hindrance is likely to prevent the access of glucosidase II to its sugar substrate. This finding supports the idea that the glycoprotein must dissociate from the lectin for cleavage by glucosidase II to occur. The disulfide bond connecting the cysteine residues 140 and 174 is present in the globular domain where it connects two β-strands in the vicinity of the proposed glycan-binding site. This feature can account for the observed sensitivity of oligosaccharide binding by CNX toward reduction *(121,131)*.

Interestingly, legume lectins, galectins and neurexin 1β possess a fold closely related to the globular domain of CNX *(110)*. The laminin G-like domain of neurexin 1β contains alternative splice sites in loops connecting the β-strands and the absence or presence of inserted sequences at these sites determines ligand interactions *(139)*. Similarly, the P-domain of CNX is introduced at the same topological position as one of the splice sites in neurexin 1β and also establishes a protein–protein interaction (*see* below).

For CRT, the NMR structure of the P-domain, residues 189–288, has been solved (Fig. 4) *(140,141)*. Like the CNX P-domain it shows an extended hairpin fold, in the case of CRT with a length of approx 110 Å. Three short antiparallel β-sheets and three small hydrophobic clusters stabilize the structure. This threefold repetition of structural elements and the four-fold repetition of similar structural features in the CNX P-domain closely reflects the repetitive nature of the P-domain sequence in the two molecules (Figs. 3 and 4). Roughly, each type 1 repeat sequence pairs up with a type 2 repeat sequence in the structure of both P-domains by forming interactions across the hairpin. In addition, it has recently been shown that a short fragment corresponding to one type 1 repeat and one type 2 repeat, and comprising the β-sheet and the hydrophobic cluster at the tip of CRT P-domain, constitutes an independently folding structure *(142)*. It is tempting to speculate that the unique sequence of the P-domain has evolved by the sequential insertion of such "12" units into a loop region of the globular lectin domain.

Currently, the structure corresponding to the CNX lectin domain is not known for CRT. However, the crystal structure of the lumenal domain of CNX and the sequence similarity between the two proteins (Figs. 3 and 4) strongly indicate that the CRT N-domain and

residues 284–337 of the C-domain will form a globular domain with structural similarity to the CNX lectin domain. Indeed, this is exactly what the recently modeled structure of the CRT lectin domain also suggests *(135)*. Furthermore, biochemical and biophysical analysis of full-length CRT has shown that the molecule is asymmetric and elongated *(126)*. Based on this information, the known structural data for both proteins and the overall high conservation of sequence and function between the two proteins, it can be assumed that both CNX and CRT show a two domain structure comprising a globular lectin domain and a long protruding P-domain. In addition, the residues of CNX proposed to be involved in the binding of glucose and Ca^{2+} are largely conserved in CRT. Likewise, residues in CRT proposed to bind the G1M3 tetrasaccharide are well conserved in CNX (Fig. 3).

Whereas the crystal structure of the lumenal domain of CNX revealed the lectin function of the globular domain, the function of the P-domain remained unclear despite detailed structural analysis obtained by both X-ray crystallography and NMR spectroscopy. However, it has now been shown that the P-domain of both CNX and CRT binds to ERp57 *(128,142,143)*. Using NMR spectroscopy and deletion mutants of both CNX and CRT, these studies have mapped the site of interaction with ERp57 to the distal end of the P-domain. Furthermore, the K_d of the interaction between ERp57 and the CRT P-domain was determined to approx 9 μ*M (142,143)*. Although this affinity is quite weak, it is likely that a more stable tertiary complex results in the presence of a cysteine-containing glycoprotein substrate through the formation of transient mixed disulfide bonds between the glycoprotein and ERp57.

THE ROLE OF ERP57

The growing family of ER thiol-disulfide oxidoreductases, most of which contain one or more thioredoxin-like domains, promotes the proper oxidation, isomerization and reduction of disulfide bonds *(144)*. The reactions involving these proteins proceed through intermolecular disulfide-bonded intermediates and both ERp57 and PDI form mixed disulfides with viral glycoproteins during folding in living cells *(63)*. Therefore, rather than regulating the redox state of other factors in the ER, these proteins directly catalyze the oxidative folding of proteins.

Molecular Studies of ERp57

The best characterized of the redox-active proteins in the ER is PDI. It comprises four thioredoxin-like domains—termed a, b, b′, and a′—followed by an acidic carboxyl terminal c-domain, which also harbors the KDEL ER-retention motif. Thioredoxin is a small 12 kDa protein, which functions as a disulfide reductase in the cytosol. The three-dimensional structures of thioredoxin and related domains show a typical α/β fold with a five-stranded β-sheet surrounded by four α-helices (for a review, *see* ref. *145*). In PDI, the a and a′ domains are catalytically active and both contain two cysteine residues in a characteristic 'CXXC' sequence motif. Within the thioredoxin superfamily these cysteines are redox-active and switch between the dithiol and disulfide forms.

ERp57 is the closest known homolog of PDI, with which it shares the same domain composition except for the absence of the acidic c-domain. Consequently, the QDEL ER-retention motif in ERp57 is located directly at the carboxyl terminal end of the a′ domain *(146)*. PDI and ERp57 show an overall amino acid identity of 29%, with the a and a′ domains being most closely related, whereas the b′ domains are the most divergent. In PDI, the b′ domain has been shown to bind peptides, a feature that is likely to be related to its function as a bonafide chaperone. Since the ERp57 b′ domain does not possess a similar function, it is tempting to speculate that this domain in ERp57 could have evolved to constitute a binding site for CNX and CRT, as proposed recently by Freedman and colleagues *(145)*. Currently, no structural data are available for ERp57. However, NMR structures of the PDI a and b domains show

that they both comprise typical thioredoxin-like folds *(149,150)*. Preliminary NMR data and assignments have been reported for the a' domain of ERp57 *(151)*.

Using in vitro assays for redox activity, ERp57 has been shown to have disulfide reductase and isomerase activity *(152–155)*. Only one in vitro study has investigated the catalytic activity of ERp57 using an endogenous substrate of the protein, namely partially folded MHC class I heavy chain molecules *(156)*. Toward this substrate, ERp57 was shown to exhibit reductase activity, and it was proposed that this activity might be involved in reducing heavy chain molecules prior to retrotranslocation and degradation *(156)*. However, it remains to been seen exactly which type(s) of disulfide exchange reaction(s) ERp57 performs in vivo.

PDI and Glycoprotein Folding

As mentioned previously, ERp57 acts as a glycoprotein specific redox-active enzyme through its cooperative interaction with CNX and CRT. The finding that ERp57-enhanced disulfide bond formation in vitro is dependent on CNX and CRT stresses the functional cooperation of both lectin chaperones with ERp57 *(157)*. No positive effects on glycoprotein refolding by PDI were observed upon addition of CNX and CRT. Although PDI has been shown to be involved in glycoprotein folding *(63)*, substrate interaction of PDI in vivo is not regulated by glucose trimming *(59–61,63,158)*. These studies all indicate that PDI functions independently of CNX and CRT, which is in agreement with findings that were unable to detect complexes of either lectin with PDI *(60,143)*. However, other data have shown that PDI interacts with CRT *(123,159)*. It is possible that this apparent discrepancy is a result of the different experimental conditions used because the interaction is strongly influenced by changes in Ca^{2+} concentrations *(123)*. Thus, fluctuations in the free concentration of Ca^{2+} in the ER could affect protein folding, either directly by inducing conformational changes in CNX and CRT resulting in altered substrate interactions or indirectly by modulating the binding of co-chaperones *(97,123)*.

ERp57 in MHC Class I Assembly

Recently, several investigations have focused on the interaction of ERp57 with glycoproteins during CNX- and CRT-dependent folding (*see*, for instance, refs. *64,160–162*). To date, the best-studied glycoprotein substrate of ERp57 in vivo is the MHC class I complex. This heterodimer is comprised of the glycosylated heavy chain and the associated protein, β_2-microglobulin. The MHC class I complex plays a critical role in the immune response by delivering for instance virus- and tumor-derived antigenic peptides to the cell surface for presentation to receptors on cytotoxic T-cells. The process of MHC class I folding, assembly and peptide loading takes place in the ER, and has been shown to involve CNX, CRT and ERp57 together with the more specialized proteins transporter associated with antigen processing (TAP) and tapasin. During the early stages of folding the newly synthesized heavy chain interacts with CNX. Upon binding of β_2-microglobulin, CRT replaces CNX and together with TAP, tapasin and ERp57 form the so-called peptide loading complex (PLC). In a tapasin-dependent process, the class I molecules are then loaded with peptide, the PLC dissociates and the mature MHC class I complex can traffic to the cell surface (for recent reviews, *see* refs. *77,163,164*).

ERp57 is involved at various stages of MHC class I assembly. The heavy chain contains two disulfide bonds and folds and oxidizes while associated with CNX, but prior to incorporation into the PLC *(165–167)*. Because a ternary complex of heavy chain, CNX and ERp57 has been observed already at this early stage of maturation, it is possible that ERp57 is involved in catalyzing disulfide bond formation in the heavy chain *(167)*. Moreover, ERp57 is an important component of the PLC *(167)*. The association of ERp57 with the PLC has been shown to be tapasin dependent and correlate with CRT association *(169,171)*. The latter finding suggests that a preformed complex of CRT and

ERp57 could enter into the PLC *(171)*. The functional cooperation between ERp57 and tapasin is stressed by the finding that the two proteins form an intermolecular disulfide bond in the PLC *(172)*. Analysis of cysteine-lacking mutants of ERp57 and tapasin has led to the conclusion that the two proteins in concert mediate the isomerization and/or re-oxidation of the disulfide bond in the peptide-binding groove of MHC class I heavy chain *(172)*. Although it is presently not known exactly how this process occurs, it has been shown to be important for the correct loading of the MHC class I β_2-microglobulin heterodimer with high affinity peptides *(172)*.

FROM MOLECULAR PROPERTIES TO IN VIVO FUNCTION

The insight gained from the many biochemical and cell biological studies of CNX, CRT and ERp57 is providing a more and more detailed picture of the processes involving these three chaperones. Our understanding is now so advanced that many functional features observed in vivo can be rationalized based on known biochemical and structural properties. As described previously, the present data strongly indicate that CNX and CRT show a similar overall structural organization. Functionally, the lectin domain is responsible for binding the glycan attached to substrate glycoproteins, whereas the P-domain binds ERp57 at its tip. These features, in combination with the properties of both chaperones determined in vivo, have led us to present a basic model for the cooperative interaction of either chaperone and ERp57 with the nascent chain or non-native conformers of newly synthesized glycoproteins in the ER *(143,173)*.

We propose that substrate binding occurs through the interaction of the monoglucosylated glycan with the lectin domain of either CNX or CRT. This feature allows the polypeptide chain a certain degree of conformational freedom in the process of folding. The structural arrangement of the lectin domain and the elongated P-domain with ERp57 bound at the tip sequesters the polypeptide chain of the substrate in a partially protected space during folding. This partial shielding of the bound glycoprotein substrate should help to suppress intermolecular aggregation that could result from interactions with other ER folding intermediates. The role of the P-domain is likely to involve positioning of ERp57 for the formation of intermolecular disulfide bonds with a variety of bound substrate proteins. The conformational plasticity observed in the NMR structure of the CRT P-domain could allow both chaperones to adapt to substrates of varying size and shape *(140)*. This complements the idea that the overall molecular flexibility of CRT characterized biophysically by Bouvier and colleagues is advantageous for the protein in its function as a molecular chaperone by allowing transient and dynamic interactions with a number of substrates *(109,123,125,126)*. An additional function of the P-domain could be to constrain diffusion of the substrate after dissociation from CNX and CRT. This would allow for a more rapid reassociation, provided that the remaining glucose on the glycoprotein substrate has meanwhile not been trimmed by glucosidase II. Taken together, the function of CNX and CRT is likely to be dictated by their distinctive structural features and the close cooperation with ERp57, which leads to the productive oxidative folding of glycoprotein substrates.

This basic model supports the view that CNX and CRT function as molecular chaperones by keeping their substrates "out of trouble" rather than by actively promoting folding. However, it leaves room for the incorporation of additional features of both proteins relating to the binding of cofactors and protein–protein contacts with substrate glycoproteins. The prediction of protein–protein interactions during CNX- and CRT-assisted glycoprotein folding is appealing because it provides explanations for results otherwise not easy to rationalize. For instance, when performing immunoprecipitation experiments to identify glycoprotein substrates of CNX in vivo, it has been observed

that certain complexes persist even after removal of the glycan by glycosidase treatment with Endo H or PNGase F *(50,78,174,175)*. Therefore, it could be that the initial binding of CNX and CRT to the glycoprotein substrate occurs as a result of the lectin activity, but that subsequent protein-protein contacts stabilize the complexes. Polypeptide-based contacts could also help explain the rather high efficiency observed for coimmunoprecipitation of substrate proteins with CNX and CRT in spite of the relatively low affinity measured for the interaction between CRT and monoglucosylated IgG *(137)*.

Currently, however, the data relating to the function of CNX and CRT as bona fide molecular chaperones are not easy to assess definitively. For instance, the physiologic role of potentially important cofactors implicated in this function, such as Zn^{2+} and ATP, is presently not evident. It has also been argued that immunoprecipitation is not the method of choice to study interactions that involve nonnative conformers or nascent chains owing to their hydrophobic nature *(29)*. For example, overexpression of protein or addition of tunicamycin, which inhibits glycosylation and turns on the UPR, often results in protein misfolding and aggregation. Potentially, complexes of CNX and nonglycosylated proteins immunoisolated under such conditions that perturb the folding environment in the ER lumen are nonphysiologic in nature. Besides, interactions of membrane proteins with CNX could possibly be preserved if caught in the same detergent micelle *(20)*.

The fact that the experimental conditions employed in immunoprecipitation experiments can influence results considerably contributes an additional difficulty. When performing immunoprecipitations under mild detergent conditions *(176)*, interaction of nonglycosylated proteins or proteins carrying di- or triglucosylated glycans with CNX and CRT can be observed. In contrast, when performing similar experiments under more stringent detergent conditions, no binding to CNX was observed *(177)*. No matter which experimental conditions are employed, any substrate interaction observed with CNX and CRT should be critically assessed to ensure that it is transient and that it results in the formation of a fully mature and correctly folded substrate protein. Only such interactions are expected to occur as a result of the chaperone function of CNX and CRT. In contrast, long-lasting interactions with substrate proteins are likely to be nonproductive and of nonspecific nature.

PERSPECTIVES

Since 1989 when Suh and colleagues observed that a misfolded variant of the vesicular stomatitis virus G-protein was retained in the ER in a monoglucosylated form *(178)*, our understanding of the processes involved in glycoprotein folding in the ER has increased tremendously. In particular, the roles of the different proteins in the CNX/CRT cycle have become much more evident. The publication of three-dimensional structures of CNX and CRT has provided substantial new insight into the molecular mechanism of the chaperone function of these proteins and has significantly changed the way we think about these two lectin chaperones.

The next goals for the field should involve the determination of a high-resolution structure of the CRT lectin domain, if possible in complex with the G1M3 glycan. More detailed information about the interaction of CNX and CRT with ERp57, as well as structure determination of ERp57, or individual domains thereof, will be important. Additional experiments will be needed to clarify the exact role of the P-domain in glycoprotein folding. Despite being structurally similar, the P-domains in CNX and CRT differ with a "12" repeat unit in size. Whether this difference also conveys functional distinctions is presently unclear. Addressing such questions relating to the P-domain should also promote a better understanding of how the cooperation of CNX and CRT with ERp57 assists disulfide bond formation in substrate glycoproteins.

The direct mapping of specific residues in CNX and CRT that decide the interaction with ATP, Zn^{2+} and polypeptide regions of substrate proteins will also be essential. Such information could for instance be obtained by structure determination in the presence of these co-factors, which might also provide direct information on the local and global conformational changes that occur upon cofactor binding. These results should in turn allow the design of mutations that specifically remove the co-factor interactions individually. Provided that such mutants can be shown to retain structural and functional properties of the wild-type protein, they will become valuable tools for the characterization of functions related to cofactor binding both in vivo and in vitro. Application of this experimental strategy will be particularly important to investigate functions such as ATP binding, which can otherwise not easily be targeted in vivo without perturbing the cellular environment. To fully appreciate the role of ATP binding by CNX and CRT the identification of potential co-chaperones for ATP hydrolysis, nucleotide exchange or dissociation will be critical. Taken together, the results of such experiments should provide us with a more detailed understanding of how the CNX/CRT chaperone system functions at the molecular level.

ACKNOWLEDGMENTS

We would like to thank M. Molinari and R. Mancini for critical reading of the manuscript and helpful comments. The continued support by Ari Helenius is much appreciated. Financial support by the Swiss National Science Foundation (to L. E.) is gratefully acknowledged.

REFERENCES

1. Kornfeld, R. and Kornfeld, S. (1985) Assembly of asparagine-linked oligosaccharides. *Annu. Rev. Biochem.* **54,** 631–664.
2. Burda, P. and Aebi, M. (1999) The dolichol pathway of N-linked glycosylation. *Biochim. Biophys. Acta* **1426,** 239–257.
3. Gavel, Y. and von Heijne, G. (1990) Sequence differences between glycosylated and non-glycosylated Asn-X- Thr/Ser acceptor sites: implications for protein engineering. *Protein Eng.* **3,** 433–442.
4. Gahmberg, C. G. and Tolvanen, M. (1996) Why mammalian cell surface proteins are glycoproteins. *Trends Biochem. Sci.* **21,** 308–311.
5. Stanley, P. and Ioffe, E. (1995) Glycosyltransferase mutants: key to new insights in glycobiology. *FASEB J.* **9,** 1436–1444.
6. Aebi, M. and Hennet, T. (2001) Congenital disorders of glycosylation: genetic model systems lead the way. *Trends Cell. Biol.* **11,** 136–141.
7. O'Connor, S. E. and Imperiali, B. (1996) Modulation of protein structure and function by asparagine-linked glycosylation. *Chem. Biol.* **3,** 803–812.
8. Dwek, R. A. (1996) Glycobiology: Toward understanding the function of sugars. *Chem. Rev.* **96,** 683–720.
9. Drickamer, K. and Taylor, M. E. (1998) Evolving views of protein glycosylation. *Trends Biochem. Sci.* **23,** 321–324.
10. Wormald, M. R. and Dwek, R. A. (1999) Glycoproteins: glycan presentation and protein-fold stability. *Structure Fold. Des.* **7,** R155–160.
11. Wormald, M. R., Petrescu, A. J., Pao, Y. L., Glithero, A., Elliott, T., and Dwek, R. A. (2002) Conformational studies of oligosaccharides and glycopeptides: complementarity of NMR, X-ray crystallography, and molecular modelling. *Chem. Rev.* **102,** 371–386.
12. Helenius, A., and Aebi, M. (2001) Intracellular functions of N-linked glycans. *Science* **291,** 2364–2369.
13. Yamashita, K., Hara-Kuge, S., and Ohkura, T. (1999) Intracellular lectins associated with N-linked glycoprotein traffic. *Biochim. Biophys. Acta.* **1473,** 147–160.
14. Hauri, H., Appenzeller, C., Kuhn, F., and Nufer, O. (2000) Lectins and traffic in the secretory pathway. *FEBS Lett.* **476,** 32–37.
15. Schrag, J. D., Procopio, D. O., Cygler, M., Thomas, D. Y., and Bergeron, J. J. (2003) Lectin control of protein folding and sorting in the secretory pathway. *Trends Biochem. Sci.* **28,** 49–57.
16. Ou, W. J., Cameron, P. H., Thomas, D. Y., and Bergeron, J. J. (1993) Association of folding intermediates of glycoproteins with calnexin during protein maturation. *Nature* **364,** 771–776.

17. Jackson, M. R., Cohen-Doyle, M. F., Peterson, P. A., and Williams, D. B. (1994) Regulation of MHC class I transport by the molecular chaperone, calnexin (p88, IP90). *Science* **263,** 384–387.
18. Hebert, D. N., Foellmer, B., and Helenius, A. (1996) Calnexin and calreticulin promote folding, delay oligomerization and suppress degradation of influenza hemagglutinin in microsomes. *EMBO J.* **15,** 2961–2968.
19. Labriola, C., Cazzulo, J. J., and Parodi, A. J. (1995) Retention of glucose units added by the UDP-GLC:glycoprotein glucosyltransferase delays exit of glycoproteins from the endoplasmic reticulum. *J. Cell Biol.* **130,** 771–779.
20. Helenius, A., Trombetta, E. S., Hebert, D. N., and Simons, J. F. (1997) Calnexin, calreticulin and the folding of glycoproteins. *Trends Cell Biol.* **7,** 193–200.
21. Liu, Y., Choudhury, P., Cabral, C. M., and Sifers, R. N. (1999) Oligosaccharide modification in the early secretory pathway directs the selection of a misfolded glycoprotein for degradation by the proteasome. *J. Biol. Chem.* **274,** 5861–5867.
22. Nakatsukasa, K., Nishikawa, S., Hosokawa, N., Nagata, K., and Endo, T. (2001) Mnl1p, an alpha -mannosidase-like protein in yeast Saccharomyces cerevisiae, is required for endoplasmic reticulum-associated degradation of glycoproteins. *J. Biol. Chem.* **276,** 8635–8638.
23. Hosokawa, N., Wada, I., Hasegawa, K., Yorihuzi, T., Tremblay, L. O., Herscovics, A., et al. (2001) A novel ER alpha-mannosidase-like protein accelerates ER-associated degradation. *EMBO Rep.* **2,** 415–422.
24. Jakob, C. A., Bodmer, D., Spirig, U., Battig, P., Marcil, A., Dignard, D., et al. (2001) Htm1p, a mannosidase-like protein, is involved in glycoprotein degradation in yeast. *EMBO Rep.* **2,** 423–430.
25. Braakman, I. (2001) A novel lectin in the secretory pathway. An elegant mechanism for glycoprotein elimination. *EMBO Rep.* **2,** 666–668.
26. Molinari, M., Calanca, V., Galli, C., Lucca, P., and Paganetti, P. (2003) Role of EDEM in the release of misfolded glycoproteins from the calnexin cycle. *Science* **299,** 1397–1400.
27. Oda, Y., Hosokawa, N., Wada, I., and Nagata, K. (2003) EDEM as an acceptor of terminally misfolded glycoproteins released from calnexin. *Science* **299,** 1394–1397.
28. Yoshida, H., Matsui, T., Hosokawa, N., Kaufman, R. J., Nagata, K., and Mori, K. (2003) A time-dependent phase shift in the mammalian unfolded protein response. *Dev. Cell* **4,** 265–271.
29. Parodi, A. J. (2000) Protein glucosylation and its role in protein folding. *Annu. Rev. Biochem.* **69,** 69–93.
30. Parodi, A. J. (2000) Role of N-oligosaccharide endoplasmic reticulum processing reactions in glycoprotein folding and degradation. *Biochem. J.* **348,** 1–13.
31. Trombetta, E. S., and Parodi, A. J. (2001) N-glycan processing and glycoprotein folding. *Adv. Protein. Chem.* **59,** 303–344.
32. Roth, J. (2002) Protein N-glycosylation along the secretory pathway: relationship to organelle topography and function, protein quality control, and cell interactions. *Chem. Rev.* **102,** 285–303.
33. Roth, J., Zuber, C., Guhl, B., Fan, J. Y., and Ziak, M. (2002) The importance of trimming reactions on asparagine-linked oligosaccharides for protein quality control. Histochem. *Cell Biol.* **117,** 159–169.
34. Benham, A. M., and Braakman, I. (2000) Glycoprotein folding in the endoplasmic reticulum. *Crit. Rev. Biochem. Mol. Biol.* **35,** 433–473.
35. Fewell, S. W., Travers, K. J., Weissman, J. S., and Brodsky, J. L. (2001) The action of molecular chaperones in the early secretory pathway. *Annu. Rev. Genet.* **35,** 149–191.
36. Hurtley, S. M. and Helenius, A. (1989) Protein oligomerization in the endoplasmic reticulum. *Annu. Rev. Cell Biol.* **5,** 277–307.
37. Ellgaard, L., Molinari, M., and Helenius, A. (1999) Setting the standards: quality control in the secretory pathway. *Science* **286,** 1882–1888.
38. Thomas, P. J., Qu, B. H., and Pedersen, P. L. (1995) Defective protein folding as a basis of human disease. *Trends Biochem. Sci.* **20,** 456–459.
39. Aridor, M. and Balch, W. E. (1999) Integration of endoplasmic reticulum signaling in health and disease. *Nat. Med.* **5,** 745–751.
40. Kopito, R. R. and Ron, D. (2000) Conformational disease. *Nat. Cell Biol.* **2,** E207–209.
41. Rutishauser, J. and Spiess, M. (2002) Endoplasmic reticulum storage diseases. *Swiss Med. Wkly.* **132,** 211–222.
42. Tsai, B., Ye, Y., and Rapoport, T. A. (2002) Retro-translocation of proteins from the endo-

plasmic reticulum into the cytosol. *Nat. Rev. Mol. Cell Biol.* **3,** 246–255.
43. Ma, Y. and Hendershot, L. M. (2001) The unfolding tale of the unfolded protein response. *Cell* **107,** 827–830.
44. Casagrande, R., Stern, P., Diehn, M., Shamu, C., Osario, M., Zuniga, M., et al. (2000) Degradation of proteins from the ER of S. cerevisiae requires an intact unfolded protein response pathway. *Mol. Cell* **5,** 729–735.
45. Travers, K. J., Patil, C. K., Wodicka, L., Lockhart, D. J., Weissman, J. S., and Walter, P. (2000) Functional and genomic analyses reveal an essential coordination between the unfolded protein response and ER-associated degradation. *Cell* **101,** 249–258.
46. Friedlander, R., Jarosch, E., Urban, J., Volkwein, C., and Sommer, T. (2000) A regulatory link between ER-associated protein degradation and the unfolded-protein response. *Nat. Cell Biol.* **2,** 379–384.
47. High, S., Lecomte, F. J., Russell, S. J., Abell, B. M., and Oliver, J. D. (2000) Glycoprotein folding in the endoplasmic reticulum: a tale of three chaperones? *FEBS Lett.* **476,** 38–41.
48. Hammond, C. and Helenius, A. (1994) Quality control in the secretory pathway: retention of a misfolded viral membrane glycoprotein involves cycling between the ER, intermediate compartment, and Golgi apparatus. *J. Cell Biol.* **126,** 41–52.
49. Hebert, D. N., Foellmer, B., and Helenius, A. (1995) Glucose trimming and reglucosylation determine glycoprotein association with calnexin in the endoplasmic reticulum. *Cell* **81,** 425–433.
50. Ware, F. E., Vassilakos, A., Peterson, P. A., Jackson, M. R., Lehrman, M. A., and Williams, D. B. (1995) The molecular chaperone calnexin binds Glc1Man9GlcNAc2 oligosaccharide as an initial step in recognizing unfolded glycoproteins. *J. Biol. Chem.* **270,** 4697–4704.
51. Peterson, J. R., Ora, A., Van, P. N., and Helenius, A. (1995) Transient, lectin-like association of calreticulin with folding intermediates of cellular and viral glycoproteins. *Mol. Biol. Cell* **6,** 1173–1184.
52. Wada, I., Kai, M., Imai, S., Sakane, F., and Kanoh, H. (1997) Promotion of transferrin folding by cyclic interactions with calnexin and calreticulin. *EMBO J.* **16,** 5420–5432.
53. Zapun, A., Petrescu, S. M., Rudd, P. M., Dwek, R. A., Thomas, D. Y., and Bergeron, J. J. (1997) Conformation-independent binding of monoglucosylated ribonuclease B to calnexin. *Cell* **88,** 29–38.
54. Cannon, K. S. and Helenius, A. (1999) Trimming and readdition of glucose to N-linked oligosaccharides determines calnexin association of a substrate glycoprotein in living cells. *J. Biol. Chem.* **274,** 7537–7544.
55. Labriola, C., Cazzulo, J. J., and Parodi, A. J. (1999) Trypanosoma cruzi calreticulin is a lectin that binds monoglucosylated oligosaccharides but not protein moieties of glycoproteins. *Mol. Biol. Cell* **10,** 1381–1394.
56. Radcliffe, C. M., Diedrich, G., Harvey, D. J., Dwek, R. A., Cresswell, P., and Rudd, P. M. (2002) Identification of specific glycoforms of major histocompatibility complex class I heavy chains suggests that class I peptide loading is an adaptation of the quality control pathway involving calreticulin and ERp57. *J. Biol. Chem.* **277,** 46415–46423.
57. Saito, Y., Ihara, Y., Leach, M. R., Cohen-Doyle, M. F., and Williams, D. B. (1999) Calreticulin functions in vitro as a molecular chaperone for both glycosylated and non-glycosylated proteins. *EMBO J.* **18,** 6718–6729.
58. Ihara, Y., Cohen-Doyle, M. F., Saito, Y., and Williams, D. B. (1999) Calnexin discriminates between protein conformational states and functions as a molecular chaperone in vitro. *Mol. Cell* **4,** 331–341.
59. Oliver, J. D., van der Wal, F. J., Bulleid, N. J., and High, S. (1997) Interaction of the thiol-dependent reductase ERp57 with nascent glycoproteins. *Science* **275,** 86–88.
60. Oliver, J. D., Roderick, H. L., Llewellyn, D. H., and High, S. (1999) ERp57 functions as a subunit of specific complexes formed with the ER lectins calreticulin and calnexin. *Mol. Biol. Cell* **10,** 2573–2582.
61. Elliott, J. G., Oliver, J. D., and High, S. (1997) The thiol-dependent reductase ERp57 interacts specifically with N- glycosylated integral membrane proteins. *J. Biol. Chem.* **272,** 13849–13855.
62. Van der Wal, F. J., Oliver, J. D., and High, S. (1998) The transient association of ERp57 with N-glycosylated proteins is regulated by glucose trimming. *Eur. J. Biochem.* **256,** 51–59.
63. Molinari, M. and Helenius, A. (1999) Glycoproteins form mixed disulphides with oxidoreductases during folding in living cells. *Nature* **402,** 90–93.

64. Kang, S. J. and Cresswell, P. (2002) Calnexin, calreticulin and ERp57 cooperate in disulfide bond formation in human CD1d heavy chain. *J. Biol. Chem.* **277,** 44838-44844.
65. Van Leeuwen, J. E., and Kearse, K. P. (1997) Reglucosylation of N-linked glycans is critical for calnexin assembly with T cell receptor (TCR) alpha proteins but not TCRbeta proteins. *J. Biol. Chem.* **272,** 4179–4186.
66. Ritter, C. and Helenius, A. (2000) Recognition of local glycoprotein misfolding by the ER folding sensor UDP-glucose:glycoprotein glucosyltransferase. *Nature Struct. Biol.* **7,** 278–280.
67. Otteken, A. and Moss, B. (1996) Calreticulin interacts with newly synthesized human immunodeficiency virus type 1 envelope glycoprotein, suggesting a chaperone function similar to that of calnexin. *J. Biol. Chem.* **271,** 97–103.
68. Li, Y., Bergeron, J. J., Luo, L., Ou, W. J., Thomas, D. Y., and Kang, C. Y. (1996) Effects of inefficient cleavage of the signal sequence of HIV-1 gp 120 on its association with calnexin, folding, and intracellular transport. *Proc. Natl. Acad. Sci. USA* **93,** 9606–9611.
69. Li, Y., Luo, L., Thomas, D. Y., and Kang, C. Y. (2000) The HIV-1 Env protein signal sequence retards its cleavage and down-regulates the glycoprotein folding. *Virology* **272,** 417–428.
70. Land, A., and Braakman, I. (2001) Folding of the human immunodeficiency virus type 1 envelope glycoprotein in the endoplasmic reticulum. *Biochimie* **83,** 783–790.
71. Hochstenbach, F., David, V., Watkins, S., and Brenner, M. B. (1992) Endoplasmic reticulum resident protein of 90 kilodaltons associates with the T- and B-cell antigen receptors and major histocompatibility complex antigens during their assembly. *Proc. Natl. Acad. Sci. USA* **89,** 4734–4738.
72. Ortmann, B., Androlewicz, M. J., and Cresswell, P. (1994) MHC class I/beta 2-microglobulin complexes associate with TAP transporters before peptide binding. *Nature* **368,** 864–867.
73. Sadasivan, B., Lehner, P. J., Ortmann, B., Spies, T., and Cresswell, P. (1996) Roles for calreticulin and a novel glycoprotein, tapasin, in the interaction of MHC class I molecules with TAP. *Immunity* **5,** 103–114.
74. van Leeuwen, J. E. and Kearse, K. P. (1996) Deglucosylation of N-linked glycans is an important step in the dissociation of calreticulin-class I-TAP complexes. *Proc. Natl. Acad. Sci. USA* **93,** 13997–14001.
75. Vassilakos, A., Cohen-Doyle, M. F., Peterson, P. A., Jackson, M. R., and Williams, D. B. (1996) The molecular chaperone calnexin facilitates folding and assembly of class I histocompatibility molecules. *EMBO J.* **15,** 1495–1506.
76. Gao, B., Adhikari, R., Howarth, M., Nakamura, K., Gold, M. C., Hill, A. B., et al. (2002) Assembly and antigen-presenting function of MHC class I molecules in cells lacking the ER chaperone calreticulin. *Immunity* **16,** 99–109.
77. Williams, A., Peh, C. A., and Elliott, T. (2002) The cell biology of MHC class I antigen presentation. *Tissue Antigens* **59,** 3–17.
78. van Leeuwen, J. E. and Kearse, K. P. (1996) Calnexin associates exclusively with individual CD3 delta and T cell antigen receptor (TCR) alpha proteins containing incompletely trimmed glycans that are not assembled into multisubunit TCR complexes. *J. Biol. Chem.* **271,** 9660–9665.
79. Le, A., Steiner, J. L., Ferrell, G. A., Shaker, J. C., and Sifers, R. N. (1994) Association between calnexin and a secretion-incompetent variant of human alpha 1-antitrypsin. *J. Biol. Chem.* **269,** 7514–7519.
80. Liu, Y., Choudhury, P., Cabral, C. M., and Sifers, R. N. (1997) Intracellular disposal of incompletely folded human alpha1-antitrypsin involves release from calnexin and post-translational trimming of asparagine-linked oligosaccharides. *J. Biol. Chem.* **272,** 7946–7951.
81. Halaban, R., Cheng, E., Zhang, Y., Moellmann, G., Hanlon, D., Michalak, M., et al. (1997) Aberrant retention of tyrosinase in the endoplasmic reticulum mediates accelerated degradation of the enzyme and contributes to the dedifferentiated phenotype of amelanotic melanoma cells. *Proc. Natl. Acad. Sci. USA* **94,** 6210–6215.
82. Halaban, R., Svedine, S., Cheng, E., Smicun, Y., Aron, R., and Hebert, D. N. (2000) Endoplasmic reticulum retention is a common defect associated with tyrosinase-negative albinism. *Proc. Natl. Acad. Sci. USA* **97,** 5889–5894.
83. Branza-Nichita, N., Negroiu, G., Petrescu, A. J., Garman, E. F., Platt, F. M., Wormald, M. R., et al. (2000) Mutations at critical N-glycosylation sites reduce tyrosinase activity by altering

folding and quality control. *J. Biol. Chem.* **275,** 8169–8175.
84. Capellari, S., Zaidi, S. I., Urig, C. B., Perry, G., Smith, M. A., and Petersen, R. B. (1999) Prion protein glycosylation is sensitive to redox change. *J. Biol. Chem.* **274,** 34846–34850.
85. Rudd, P. M., Wormald, M. R., Wing, D. R., Prusiner, S. B., and Dwek, R. A. (2001) Prion glycoprotein: structure, dynamics, and roles for the sugars. *Biochemistry* **40,** 3759–3766.
86. Pind, S., Riordan, J. R., and Williams, D. B. (1994) Participation of the endoplasmic reticulum chaperone calnexin (p88, IP90) in the biogenesis of the cystic fibrosis transmembrane conductance regulator. *J. Biol. Chem.* **269,** 12784–12788.
87. Loo, M. A., Jensen, T. J., Cui, L., Hou, Y., Chang, X. B., and Riordan, J. R. (1998) Perturbation of Hsp90 interaction with nascent CFTR prevents its maturation and accelerates its degradation by the proteasome. *EMBO J.* **17,** 6879–6887.
88. Cresswell, P. (2000) Intracellular surveillance: controlling the assembly of MHC class I-peptide complexes. *Traffic* **1,** 301–305.
89. Diedrich, G., Bangia, N., Pan, M., and Cresswell, P. (2001) A role for calnexin in the assembly of the MHC class I loading complex in the endoplasmic reticulum. *J. Immunol.* **166,** 1703–1709.
90. Hebert, D. N., Zhang, J. X., Chen, W., Foellmer, B., and Helenius, A. (1997) The number and location of glycans on influenza hemagglutinin determine folding and association with calnexin and calreticulin. *J. Cell Biol.* **139,** 613–623.
91. Wada, I., Imai, S., Kai, M., Sakane, F., and Kanoh, H. (1995) Chaperone function of calreticulin when expressed in the endoplasmic reticulum as the membrane-anchored and soluble forms. *J. Biol. Chem.* **270,** 20298–20304.
92. Ho, S. C., Rajagopalan, S., Chaudhuri, S., Shieh, C. C., Brenner, M. B., and Pillai, S. (1999) Membrane anchoring of calnexin facilitates its interaction with its targets. *Mol. Immunol.* **36,** 1–12.
93. Danilczyk, U. G., Cohen-Doyle, M. F., and Williams, D. B. (2000) Functional relationship between calreticulin, calnexin, and the endoplasmic reticulum luminal domain of calnexin. *J. Biol. Chem.* **275,** 13089–13097.
94. Rodan, A. R., Simons, J. F., Trombetta, E. S., and Helenius, A. (1996) N-linked oligosaccharides are necessary and sufficient for association of glycosylated forms of bovine RNase with calnexin and calreticulin. *EMBO J.* **15,** 6921–6930.
95. Stronge, V. S., Saito, Y., Ihara, Y., and Williams, D. B. (2001) Relationship between calnexin and BiP in suppressing aggregation and promoting refolding of protein and glycoprotein substrates. *J. Biol. Chem.* **276,** 39779–39787.
96. Michalak, M., Corbett, E. F., Mesaeli, N., Nakamura, K., and Opas, M. (1999) Calreticulin: one protein, one gene, many functions. *Biochem. J.* **344 Pt 2,** 281–292.
97. Corbett, E. F. and Michalak, M. (2000) Calcium, a signaling molecule in the endoplasmic reticulum? *Trends Biochem. Sci.* **25,** 307–311.
98. Mesaeli, N., Nakamura, K., Zvaritch, E., Dickie, P., Dziak, E., Krause, K. H., et al. (1999) Calreticulin is essential for cardiac development. *J. Cell Biol.* **144,** 857–868.
99. Li, J., Puceat, M., Perez-Terzic, C., Mery, A., Nakamura, K., Michalak, M., et al. (2002) Calreticulin reveals a critical Ca(2+) checkpoint in cardiac myofibrillogenesis. *J. Cell Biol.* **158,** 103–113.
100. Guo, L., Nakamura, K., Lynch, J., Opas, M., Olson, E. N., Agellona, L. B., et al. (2002) Cardiac specific expression of calcineurin reverses embryonic lethality in calreticulin-deficient mouse. *J. Biol. Chem.* **277,** 50776–50779.
101. Wada, I., Rindress, D., Cameron, P. H., Ou, W. J., Doherty, J. J., 2nd, Louvard, D., et al. (1991) SSR alpha and associated calnexin are major calcium binding proteins of the endoplasmic reticulum membrane. *J. Biol. Chem.* **266,** 19599–19610.
102. Tjoelker, L. W., Seyfried, C. E., Eddy, R. L., Jr., Byers, M. G., Shows, T. B., Calderon, J., et al. (1994) Human, mouse, and rat calnexin cDNA cloning: identification of potential calcium binding motifs and gene localization to human chromosome 5. *Biochemistry* **33,** 3229–3236.
103. Denzel, A., Molinari, M., Trigueros, C., Martin, J. E., Velmurgan, S., Brown, S., et al. (2002) Early postnatal death and motor disorders in mice congenitally deficient in calnexin expression. *Mol. Cell Biol.* **22,** 7398–7404.
104. Fliegel, L., Burns, K., MacLennan, D. H., Reithmeier, R. A., and Michalak, M. (1989) Molecular cloning of the high affinity calcium-binding protein (calreticulin) of skeletal muscle sarcoplasmic reticulum. *J. Biol. Chem.* **264,** 21522–21528.

105. Smith, M. J. and Koch, G. L. (1989) Multiple zones in the sequence of calreticulin (CRP55, calregulin, HACBP), a major calcium binding ER/SR protein. *EMBO J.* **8,** 3581–3586.
106. Baksh, S., and Michalak, M. (1991) Expression of calreticulin in Escherichia coli and identification of its Ca2+ binding domains. *J. Biol. Chem.* **266,** 21458–21465.
107. Michalak, M., Milner, R. E., Burns, K., and Opas, M. (1992) Calreticulin. *Biochem. J.* **285,** 681–692.
108. Ostwald, T. J., and MacLennan, D. H. (1974) Isolation of a high affinity calcium-binding protein from sarcoplasmic reticulum. *J. Biol. Chem.* **249,** 974–979.
109. Khanna, N. C., Tokuda, M., and Waisman, D. M. (1986) Conformational changes induced by binding of divalent cations to calregulin. *J. Biol. Chem.* **261,** 8883–8887.
110. Schrag, J. D., Bergeron, J. J., Li, Y., Borisova, S., Hahn, M., Thomas, D. Y., et al. (2001) The structure of calnexin, an ER chaperone involved in quality control of protein folding. *Mol. Cell* **8,** 633–644.
111. Houen, G. and Koch, C. (1994) Human placental calreticulin: purification, characterization and association with other proteins. *Acta. Chem. Scand.* **48,** 905–911.
112. Ou, W. J., Thomas, D. Y., Bell, A. W., and Bergeron, J. J. (1992) Casein kinase II phosphorylation of signal sequence receptor alpha and the associated membrane chaperone calnexin. *J. Biol. Chem.* **267,** 23789–23796.
113. Wong, H. N., Ward, M. A., Bell, A. W., Chevet, E., Bains, S., Blackstock, W. P., et al. (1998) Conserved in vivo phosphorylation of calnexin at casein kinase II sites as well as a protein kinase C/proline-directed kinase site. *J. Biol. Chem.* **273,** 17227–17235.
114. Chevet, E., Wong, H. N., Gerber, D., Cochet, C., Fazel, A., Cameron, P. H., et al. (1999) Phosphorylation by CK2 and MAPK enhances calnexin association with ribosomes. *EMBO J.* **18,** 3655–3666.
115. Ikawa, M., Wada, I., Kominami, K., Watanabe, D., Toshimori, K., Nishimune, Y., et al. (1997) The putative chaperone calmegin is required for sperm fertility. *Nature* **387,** 607–611.
116. Ikawa, M., Nakanishi, T., Yamada, S., Wada, I., Kominami, K., Tanaka, H., et al. (2001) Calmegin is required for fertilin alpha/beta heterodimerization and sperm fertility. *Dev. Biol.* **240,** 254–261.
117. Persson, S., Rosenquist, M., and Sommarin, M. (2002) Identification of a novel calreticulin isoform (Crt2) in human and mouse. *Gene* **297,** 151–158.
118. Ohsako, S., Hayashi, Y., and Bunick, D. (1994) Molecular cloning and sequencing of calnexin-t. An abundant male germ cell-specific calcium-binding protein of the endoplasmic reticulum. *J. Biol. Chem.* **269,** 14140–14148.
119. Watanabe, D., Yamada, K., Nishina, Y., Tajima, Y., Koshimizu, U., Nagata, A., et al. (1994) Molecular cloning of a novel Ca(2+)-binding protein (calmegin) specifically expressed during male meiotic germ cell development. *J. Biol. Chem.* **269,** 7744–7749.
120. Cala, S. E., Ulbright, C., Kelley, J. S., and Jones, L. R. (1993) Purification of a 90-kDa protein (Band VII) from cardiac sarcoplasmic reticulum. Identification as calnexin and localization of casein kinase II phosphorylation sites. *J. Biol. Chem.* **268,** 2969–2975.
121. Ou, W. J., Bergeron, J. J., Li, Y., Kang, C. Y., and Thomas, D. Y. (1995) Conformational changes induced in the endoplasmic reticulum luminal domain of calnexin by Mg-ATP and Ca2+. *J. Biol. Chem.* **270,** 18051–18059.
122. Waisman, D. M., Salimath, B. P., and Anderson, M. J. (1985) Isolation and characterization of CAB-63, a novel calcium-binding protein. *J. Biol. Chem.* **260,** 1652–1660.
123. Corbett, E. F., Oikawa, K., Francois, P., Tessier, D. C., Kay, C., Bergeron, J. J., et al. (1999) Ca2+ regulation of interactions between endoplasmic reticulum chaperones. *J. Biol. Chem.* **274,** 6203–6211.
124. Corbett, E. F., Michalak, K. M., Oikawa, K., Johnson, S., Campbell, I. D., Eggleton, P., et al. (2000) The conformation of calreticulin is influenced by the endoplasmic reticulum luminal environment. *J. Biol. Chem.* **275,** 27177–27185.
125. Li, Z., Stafford, W. F., and Bouvier, M. (2001) The metal ion binding properties of calreticulin modulate its conformational flexibility and thermal stability. *Biochemistry* **40,** 11193–11201.
126. Bouvier, M., and Stafford, W. F. (2000) Probing the three-dimensional structure of human calreticulin. *Biochemistry* **39,** 14950–14959.
127. Baksh, S., Spamer, C., Heilmann, C., and Michalak, M. (1995) Identification of the Zn2+ binding region in calreticulin. *FEBS Lett.* **376,** 53–57.
128. Leach, M. R., Cohen-Doyle, M. F., Thomas, D. Y., and Williams, D. B. (2002) Localization of

the Lectin, ERp57 Binding, and Polypeptide Binding Sites of Calnexin and Calreticulin. *J. Biol. Chem.* **277,** 29686–29697.
129. Borrelly, G. P., Harrison, M. D., Robinson, A. K., Cox, S. G., Robinson, N. J., and Whitehall, S. K. (2002) Surplus zinc is handled by Zym1 metallothionein and Zhf endoplasmic reticulum transporter in Schizosaccharomyces pombe. *J. Biol. Chem.* **277,** 30394–30400.
130. Clemens, S., Bloss, T., Vess, C., Neumann, D., Nies, D. H., and Zur Nieden, U. (2002) A transporter in the endoplasmic reticulum of Schizosaccharomyces pombe cells mediates zinc storage and differentially affects transition metal tolerance. *J. Biol. Chem.* **277,** 18215–18221.
131. Vassilakos, A., Michalak, M., Lehrman, M. A., and Williams, D. B. (1998) Oligosaccharide binding characteristics of the molecular chaperones calnexin and calreticulin. *Biochemistry* **37,** 3480–3490.
132. Wei, J., and Hendershot, L. M. (1995) Characterization of the nucleotide binding properties and ATPase activity of recombinant hamster BiP purified from bacteria. *J. Biol. Chem.* **270,** 26670–26676.
133. Spiro, R. G., Zhu, Q., Bhoyroo, V., and Soling, H. D. (1996) Definition of the lectin-like properties of the molecular chaperone, calreticulin, and demonstration of its copurification with endomannosidase from rat liver Golgi. *J. Biol. Chem.* **271,** 11588–11594.
134. Peterson, J. R., and Helenius, A. (1999) In vitro reconstitution of calreticulin-substrate interactions. *J. Cell Sci.* **112,** 2775–2784.
135. Kapoor, M., Srinivas, H., Kandiah, E., Gemma, E., Ellgaard, L., Oscarson, S., et al. (2003) Interactions of substrate with calreticulin, an endoplasmic reticulum chaperone. *J. Biol. Chem.* **278,** 6194–6200.
136. Petrescu, A. J., Butters, T. D., Reinkensmeier, G., Petrescu, S., Platt, F. M., Dwek, R. A., et al. (1997) The solution NMR structure of glucosylated N-glycans involved in the early stages of glycoprotein biosynthesis and folding. *EMBO J.* **16,** 4302–4310.
137. Patil, A. R., Thomas, C. J., and Surolia, A. (2000) Kinetics and the mechanism of interaction of the endoplasmic reticulum chaperone, calreticulin, with monoglucosylated (Glc1Man9GlcNAc2) substrate. *J. Biol. Chem.* **275,** 24348–24356.
138. Di Jeso, B., Ulianich, L., Pacifico, F., Leonardi, A., Vito, P., Consiglio, E., et al. (2002) The folding of thyroglobulin in the calnexin/calreticulin pathway and its alteration by a loss of Ca 2+ from the endoplasmic reticulum. *Biochem. J.* **370,** 449–458.
139. Rudenko, G., Nguyen, T., Chelliah, Y., Sudhof, T. C., and Deisenhofer, J. (1999) The structure of the ligand-binding domain of neurexin Ibeta: regulation of LNS domain function by alternative splicing. *Cell* **99,** 93–101.
140. Ellgaard, L., Riek, R., Herrmann, T., Güntert, P., Braun, D., Helenius, A., et al. (2001) NMR structure of the calreticulin P-domain. *Proc. Natl. Acad. Sci. USA* **98,** 3133–3138.
141. Ellgaard, L., Riek, R., Braun, D., Herrmann, T., Helenius, A., and Wüthrich, K. (2001) Three-dimensional structure topology of the calreticulin P-domain based on NMR assignment. *FEBS Lett.* **488,** 69–73.
142. Ellgaard, L., Bettendorff, P., Braun, D., Herrmann, T., Fiorito, F., Jelesarov, I., et al. (2002) NMR Structures of 36 and 73-residue Fragments of the Calreticulin P- domain. *J. Mol. Biol.* **322,** 773–784.
143. Frickel, E.-M., Riek, R., Jelesarov, I., Helenius, A., Wüthrich, K., and Ellgaard, L. (2002) TROSY-NMR reveals interaction between ERp57 and the tip of the calreticulin P-domain. *Proc. Natl. Acad. Sci. USA* **99,** 1954–1959.
144. Fassio, A. and Sitia, R. (2002) Formation, isomerisation and reduction of disulphide bonds during protein quality control in the endoplasmic reticulum. *Histochem. Cell Biol.* **117,** 151–157.
145. Freedman, R. B., Klappa, P., and Ruddock, L. W. (2002) Protein disulfide isomerases exploit synergy between catalytic and specific binding domains. *EMBO Rep.* **3,** 136–140.
146. Bennett, C. F., Balcarek, J. M., Varrichio, A., and Crooke, S. T. (1988) Molecular cloning and complete amino-acid sequence of form-I phosphoinositide-specific phospholipase C. *Nature* **334,** 268–270.
147. Klappa, P., Ruddock, L. W., Darby, N. J., and Freedman, R. B. (1998) The b′ domain provides the principal peptide-binding site of protein disulfide isomerase but all domains contribute to binding of misfolded proteins. *EMBO J.* **17,** 927–935.
148. Pirneskoski, A., Ruddock, L. W., Klappa, P., Freedman, R. B., Kivirikko, K. I., and Koivunen, P. (2001) Domains b′ and a′ of protein disulfide isomerase fulfill the minimum requirement for function as a subunit of prolyl 4-hydroxylase. The N- terminal domains a and

b enhances this function and can be substituted in part by those of ERp57. *J. Biol. Chem.* **276,** 11287–11293.
149. Kemmink, J., Darby, N. J., Dijkstra, K., Nilges, M., and Creighton, T. E. (1996) Structure determination of the N-terminal thioredoxin-like domain of protein disulfide isomerase using multidimensional heteronuclear 13C/15N NMR spectroscopy. *Biochemistry* **35,** 7684–7691.
150. Kemmink, J., Dijkstra, K., Mariani, M., Scheek, R. M., Penka, E., Nilges, M., et al. (1999) The structure in solution of the b domain of protein disulfide isomerase. *J. Biomol. NMR* **13,** 357–368.
151. Silvennoinen, L., Karvonen, P., Koivunen, P., Myllyharju, J., Kivirikko, K., and Kilpelainen, I. (2001) Assignment of 1H, 13C and 15N resonances of the a' domain of ERp57. *J. Biomol. NMR* **20,** 385–386.
152. Srivastava, S. P., Fuchs, J. A., and Holtzman, J. L. (1993) The reported cDNA sequence for phospholipase C alpha encodes protein disulfide isomerase, isozyme Q-2 and not phospholipase-C. *Biochem. Biophys. Res. Commun.* **193,** 971–978.
153. Hirano, N., Shibasaki, F., Sakai, R., Tanaka, T., Nishida, J., Yazaki, Y., et al. (1995) Molecular cloning of the human glucose-regulated protein ERp57/GRP58, a thiol-dependent reductase. Identification of its secretory form and inducible expression by the oncogenic transformation. *Eur. J. Biochem.* **234,** 336–342.
154. Bonfils, C. (1998) Purification of a 58-kDa protein (ER58) from monkey liver microsomes and comparison with protein-disulfide isomerase. *Eur. J. Biochem.* **254,** 420–427.
155. Bourdi, M., Demady, D., Martin, J. L., Jabbour, S. K., Martin, B. M., George, J. W., et al. (1995) cDNA cloning and baculovirus expression of the human liver endoplasmic reticulum P58: characterization as a protein disulfide isomerase isoform, but not as a protease or a carnitine acyltransferase. *Arch. Biochem. Biophys.* **323,** 397–403.
156. Antoniou, A. N., Ford, S., Alphey, M., Osborne, A., Elliott, T., and Powis, S. J. (2002) The oxidoreductase ERp57 efficiently reduces partially folded in preference to fully folded MHC class I molecules. *EMBO J.* **21,** 2655–2663.
157. Zapun, A., Darby, N. J., Tessier, D. C., Michalak, M., Bergeron, J. J., and Thomas, D. Y. (1998) Enhanced catalysis of ribonuclease B folding by the interaction of calnexin or calreticulin with ERp57. *J. Biol. Chem.* **273,** 6009–6012.
158. Elliott, J. G., Oliver, J. D., Volkmer, J., Zimmermann, R., and High, S. (1998) In vitro characterisation of the interaction between newly synthesised proteins and a pancreatic isoform of protein disulphide isomerase. *Eur. J. Biochem.* **252,** 372–377.
159. Baksh, S., Burns, K., Andrin, C., and Michalak, M. (1995) Interaction of calreticulin with protein disulfide isomerase. *J. Biol. Chem.* **270,** 31338–31344.
160. Keller, S. H., Lindstrom, J., and Taylor, P. (1998) Inhibition of glucose trimming with castanospermine reduces calnexin association and promotes proteasome degradation of the alpha-subunit of the nicotinic acetylcholine receptor. *J. Biol. Chem.* **273,** 17064–17072.
161. Allen, S., Goodeve, A. C., Peake, I. R., and Daly, M. E. (2001) Endoplasmic reticulum retention and prolonged association of a von Willebrand's disease-causing von Willebrand factor variant with ERp57 and calnexin. *Biochem. Biophys. Res. Commun.* **280,** 448–453.
162. Tamura, T., Yamashita, T., Segawa, H., and Taira, H. (2002) N-linked oligosaccharide chains of Sendai virus fusion protein determine the interaction with endoplasmic reticulum molecular chaperones. *FEBS Lett.* **513,** 153–158.
163. Van Kaer, L. (2002) Major histocompatibility complex classI-restricted antigen processing and presentation. *Tissue Antigens* **60,** 1–9.
164. Bouvier, M. (2003) Accessory proteins and the assembly of human class I MHC molecules: a molecular and structural perspective. *Mol. Immunol.* **39,** 697–706.
165. Smith, J. D., Solheim, J. C., Carreno, B. M., and Hansen, T. H. (1995) Characterization of class I MHC folding intermediates and their disparate interactions with peptide and beta 2-microglobulin. *Mol. Immunol.* **32,** 531–540.
166. Tector, M., Zhang, Q., and Salter, R. D. (1997) Beta 2-microglobulin and calnexin can independently promote folding and disulfide bond formation in class I histocompatibility proteins. *Mol. Immunol.* **34,** 401–408.
167. Farmery, M. R., Allen, S., Allen, A. J., and Bulleid, N. J. (2000) The role of ERp57 in disulfide bond formation during the assembly of major histocompatibility complex class I in a synchronized semipermeabilized cell translation system. *J. Biol. Chem.* **275,** 14933–14938.
168. Morrice, N. A. and Powis, S. J. (1998) A role for the thiol-dependent reductase ERp57 in the

assembly of MHC class I molecules. *Curr. Biol.* **8,** 713–716.
169. Hughes, E. A. and Cresswell, P. (1998) The thiol oxidoreductase ERp57 is a component of the MHC class I peptide-loading complex. *Curr. Biol.* **8,** 709–712.
170. Lindquist, J. A., Jensen, O. N., Mann, M., and Hammerling, G. J. (1998) ER-60, a chaperone with thiol-dependent reductase activity involved in MHC class I assembly. *EMBO J.* **17,** 2186–2195.
171. Harris, M. R., Lybarger, L., Yu, Y. Y., Myers, N. B., and Hansen, T. H. (2001) Association of ERp57 with mouse MHC class I molecules is tapasin dependent and mimics that of calreticulin and not calnexin. *J. Immunol.* **166,** 6686–6692.
172. Dick, T. P., Bangia, N., Peaper, D. R., and Cresswell, P. (2002) Disulfide bond isomerization and the assembly of MHC class I-peptide complexes. *Immunity* **16,** 87–98.
173. Ellgaard, L., and Helenius, A. (2001) ER quality control: towards an understanding at the molecular level. *Curr. Opin. Cell Biol.* **13,** 431–437.
174. Zhang, Q., Tector, M., and Salter, R. D. (1995) Calnexin recognizes carbohydrate and protein determinants of class I major histocompatibility complex molecules. *J. Biol. Chem.* **270,** 3944–3948.
175. Bennett, M. J., Van Leeuwen, J. E., and Kearse, K. P. (1998) Calnexin association is not sufficient to protect T cell receptor alpha proteins from rapid degradation in CD4+CD8+ thymocytes. *J. Biol. Chem.* **273,** 23674–23680.
176. Danilczyk, U. G. and Williams, D. B. (2001) The lectin chaperone calnexin utilizes polypeptide-based interactions to associate with many of its substrates in vivo. *J. Biol. Chem.* **276,** 25532–25540.
177. Ora, A., and Helenius, A. (1995) Calnexin fails to associate with substrate proteins in glucosidase-deficient cell lines. *J. Biol. Chem.* **270,** 26060–26062.
178. Suh, K., Bergmann, J. E., and Gabel, C. A. (1989) Selective retention of monoglucosylated high mannose oligosaccharides by a class of mutant vesicular stomatitis virus G proteins. *J. Cell Biol.* **108,** 811–819.
179. Koradi, R., Billeter, M., and Wüthrich, K. (1996) MOLMOL: A program for display and analysis of macromolecular structures. *J. Mol. Graph.* **14,** 51–55.